DISSERTATION

COUPLING AN URBAN PARAMETERIZATION TO AN ATMOSPHERIC MODEL USING AN OPERATIONAL CONFIGURATION

Submitted by

Timothy E. Nobis

Department of Atmospheric Science

In partial fulfillment of the requirements

For the Degree of Doctor of Philosophy

Colorado State University

Fort Collins, Colorado

Summer 2010

COLORADO STATE UNIVERSITY

June 25, 2010

WE HEREBY RECOMMEND THAT THE DISSERTATION PREPARED UNDER OUR SUPERVISION BY TIMOTHY E. NOBIS ENTITLED COUPLING AN URBAN PARAMETERIZATION TO AN ATMOSPHERIC MODEL USING AN OPERATIONAL CONFIGURATION BE ACCEPTED AS FULFILLING IN PART REQUIREMENTS FOR THE DEGREE OF DOCTOR OF PHILOSOPHY.

Committee on Graduate Work

_____
Jeffrey L. Collett Jr.

_____
Richard H. Johnson

_____
Robert N. Meroney

_____
Advisor: Roger A. Pielke Sr.

_____
Department Head: Richard H. Johnson

ABSTRACT OF DISSERTATION

COUPLING AN URBAN PARAMETERIZATION TO AN ATMOSPHERIC MODEL USING AN OPERATIONAL CONFIGURATION

Operational weather centers use numerical weather prediction (NWP) models to provide forecast weather guidance. Output from these models are then used to drive non-weather decision aids such as air quality forecast or dispersion models which are sensitive to near surface weather and very important in urban areas. While NWP models are usually run at resolutions fine enough to allow them to account for mesoscale flow systems (e.g. sea breeze), they are not designed to explicitly model an urban heat island (UHI) response. Other studies have shown that the UHI can interact with and alter local mesoscale flow systems in and around urban areas. This study examines the ability of an urban parameterization to improve operational NWP characterization of the sensible weather in Washington, DC on three separate days. The urban parameterization does seemly function in a subjective fashion to create many of the typical UHI features in spite of being run at a much coarser resolution than typically used with urban parameterization studies. When compared to actual near surface temperature data, while the parameterization was found to significantly underestimate the strength of the UHI (likely a product of the resolution), it does act to reduce the forecast temperature error in the

District, especially when compared against an available vertical temperature profile. The parameterization did perform more ambiguously in the transition area between the suburban and rural regions where it seems the resolution was not high enough to model the often observed sharp transition between urban and rural environment. Overall, the presence of an urban parameterization seemed to improve the model's characterization of the near surface environment around Washington, DC.

Timothy E. Nobis
Department of Atmospheric Science
Colorado State University
Fort Collins, CO 80523
Summer 2010

ACKNOWLEDGEMENTS

I wish to thank my advisor, Dr. Roger Pielke Sr, for his guidance and support, especially as this task ran much longer than I ever envisioned it going. I also thank my committee members Drs Jeffrey Collett, Richard Johnson, and Robert Meroney for their willingness to hang with me and for their advice both relating to this document and professionally.

I also wish to acknowledge Dr. Masson for providing the urban parameterization used in this study.

A very special thanks to my family; especially my wife who hung with this effort as we moved first from Colorado to Nebraska, then to New York before finally seeing this completed.

Finally, the views expressed in this document are mine and do not express the views of the Department of the Air Force, Department of Defense or the US Government.

CONTENTS

Chapter 1: Coupling an Urban Parameterization to an Atmospheric Model Using an Operational Configuration I: Subjective Results and Sensitivity

1. Introduction

A basic review of Planetary Boundary Layer (PBL) theory (e.g. Stull 1988) demonstrates that the structure of the PBL and its sensible weather (temperatures, winds, moisture, and stability) is driven largely by the underlying surface. Therefore, it is not surprising that a growing body of literature over the past few decades has demonstrated that urban landscapes have different boundary layer structures than the landscapes that surround them. [Oke (1988) offers a representative review of the energy balance over an urban area.]

While the urban land surface does not make up much of the land surface (less than 2% of the land cover in the US according to Dabberdt et al. 2000), it does hold an increasing percentage of population. Cohen (2003) states that in 2000 nearly 50% of the human population lived in urban areas, and of the 2.2 billion people expected to be added to the global population over the next 30 years, 2.1 billion of them will likely reside in urban areas. So while the urban area is small, the environment in and around it is experienced by a disproportionate amount of the earth's population. This fact is driving an increasing interest in the day-to-day impacts of air pollution and dispersion of hazardous materials (whether accidentally or purposely released), both of which have a disproportional impact

in urban areas. Also, Military personnel need to predict the performance of precision weapons, night vision goggles, and even acoustical propagation accurately in urban areas. Pollution, dispersion, and many military applications are all very sensitive to the accuracy of the simulated boundary layer features. The makes the differences of the Urban Boundary Layer (UBL) important to characterize.

This difference in UBL development is commonly referred to as the Urban Heat Island (UHI) due to the noticeable influence on temperature in the urban area relative to the surrounding rural area. The 3-dimensional nature of the urban morphology coupled with the thermal characteristics of the artificial urban materials and the presence of significant anthropogenic sources of heat is generally recognized as the primary factors driving the UHI, though which factor dominates varies from urban area to area (e.g. Carlson and Borland 1978; Oke et al. 1991; Offerle et al. 2005; Tomita et al. 2007; Coutts et al. 2007; Basara et al. 2008). Based on a number of field and model studies the climatology of a 'typical' UHI has been constructed. Oke (1987) offers one such view, and it is temping to approach the UHI as a one-fits-all climatology adjustment in the vicinity of an urban area. However, extensive studies and reviews (e.g. Torok et al. 2001; Arnfield 2003; Roth 2007) have demonstrated that each urban area has a unique UHI signature due to the unique character of each urban area and unique aspects of the surrounding landscape the urban area is imbedded within. In addition, the signature of the UHI will vary daily due to synoptic forcing (e.g. Grimmond and Oke 1995; Basara et al. 2008; Rosenzweig et al. 2009).

While the UHI is identified with temperature, it is not the only aspect of the UBL influenced. Several sources including Oke (1988), Hunter et al. (1990/1991), Roth

(2000), Rotach et al. (2001), and Arnfield (2003) offer comprehensive reviews of the UBL demonstrating that effects include winds, moisture, and boundary layer height and stability. Further, when differences between adjacent boundary layers become great enough, mesoscale flow systems (e.g. sea breeze) can be generated (e.g. Pielke et al. 1991). Studies have demonstrated that UHI induced flow systems are possible (e.g. Bornstein and Lin 2000; Baik et al. 2001; Lemonsu and Masson 2002; Rozoff 2002) and will interact with other local mesoscale flow systems in non-linear ways producing new, more complex area flow patterns (e.g. Yoshiado 1992; Biak 2001; Ohashi and Kida 2002, 2004; Brazel et al. 2005; Lo et al. 2007). These altered flow systems can than alter local patterns of sensible weather such as convection (e.g. Craig 2002; Rozoff 2003; Niyogi et al. 2006; Mote et al. 2007; Lei et al. 2008; Han and Baik 2008; Farias et al. 2009; Shepherd et al. 2010; Gauthier et al. 2010; Carrió et al. 2010). Thus, failure to properly account for an evolution of the UBL could influence the characterization, evolution, and sensible weather impact of mesoscale flow systems.

Mesoscale models are routinely used by operational meteorological centers to simulate boundary layer properties such as temperature, moisture, and wind along with the non-linear interactions they drive. The models used to make operational weather forecasts for civilian and military customers routinely use grid dimensions of 4-12 km, permitting them to simulate not just the synoptic scale effects on boundary layer properties, but the mesoscale flow effects as well (e.g. sea breeze, valley breeze). These operational models have been coupled to a land surface model (LSM) in an effort to properly drive the atmospheric boundary layer. LSMs have tended to concentrate on the processing of energy by vegetative, water, and soil surfaces, as these land class types

represent the vast majority of land cover. As a result, urban land class tends to be treated as a modified vegetation type given a higher roughness and different thermal properties that are a mix of concrete and vegetation. Given the lack of 3D effects and anthropogenic influence, it should come as no surprise if the current operational mesoscale models struggle to re-create a typical UHI signature. This failure would be expected to have impacts on the capability of operational meteorological centers to model the mesoscale flow systems (and subsequent sensible weather) in and around urban areas.

Researchers have recognized the deficiency of the current LSM to handle the unique aspects of urban surface flux generation and have developed a suite of urban land surface parameterizations (reference Craig 2002 for a review) of varying levels of sophistication from relatively simplistic bulk approaches (e.g. Seaman et al. 1989; Taha 1999; Shem and Shepherd 2009; Lynn et al. 2009) to single layer models (e.g. Masson, 2000; Kusaka et al. 2001; Jin et al. 2007) to the most sophisticated multi-layer schemes (e.g. Brown and Williams 1998; Martilli 2002). However, the vast majority of work done with these has been research oriented to model specific events at generally fine scales (<4 km) (e.g. Lemonsu and Masson 2002; Rozoff et al. 2003; Grossman-Clarke et al. 2005; Lo et al. 2007; Holt and Pullen 2007; Zhang et al. 2008; Lemonsu et al. 2009; Rozenzweig et al. 2009; Miao et al. 2009; Ching et al. 2009; Carrió et al. 2010; Shepherd et al. 2010). To date, neither the National Centers for Environmental Prediction (NCEP) nor military weather centers have incorporated an urban parameterization into their operational models (although urban parameterization options are now available in the Weather Research and Forecast (WRF) model used by both NCEP and the Air Force); yet output from these models are used as input to user applications in urban areas (e.g. Community

Multiscale Air Quality (CMAQ) modeling system for air quality predictions, Byun and Schere 2006)

This chapter will assess the impact of an urban parameterization on a mesoscale model in a configuration closely matching an operational configuration. The primary question addressed is the ability of the urban parameterization to function at this relatively 'coarse' resolution; thus assessing its potential readiness for use by the operational centers. To do this, simulations with and without the urban parameterization are evaluated over Washington DC for a summer day in 1984 expected to have a measurable UHI. Results from the simulations are compared to the structure of a 'typical' UHI response in a subjective fashion. In addition, a number of sensitivity tests are evaluated to assess how sensitive the urban parameterization is to other model aspects in order to provide an assessment of critical dependencies for the operational center to consider.

Chapter 2 will assesses whether the inclusion of the parameterization objectively improved the simulated sensible weather elements observed at various points in and around Washington DC using meteorological observations from three days in 1984 with distinctly different weather regimes. A more detailed literature review and motivation discussion for this work can be found in Appendix A.

2. Models

a. The Regional Atmospheric Modeling System (RAMS) and Land Ecosystem-Atmospheric Feedback-2 (LEAF-2).

The RAMS Version 4.3 is the mesoscale model being used for the current study and is fully described in Cotton et al. (2003). RAMS is a fully non-hydrostatic numerical model

with several well known physics parameterizations available for radiation, convection, microphysics, and PBL. The model has been used extensively to simulate atmospheric fields at the mesoscale (2-2000 km) and features a multi-nesting capability allowing stable simulation at varying resolutions.

RAMS has been fully coupled to the LEAF-2 (Walko et al. 2000) model for the calculation of surface fluxes. LEAF-2 has the ability to offer multiple surface patches such that given grid cell can have multiple sub-patches each with its own vegetation, soil and snowcover (one patch is always reserved for any percentage of open water). The total flux for the grid cell is an area weighted average from the multiple patches. This allows effective utilization of land surface data at a higher resolution than what is being modeled in the parent mesoscale model. LEAF-2 uses the Biosphere-Atmosphere Transfer Scheme (BATS) vegetation classes to define many of its land surface type parameters. BATS was originally developed for the NCAR community climate model and is described in Dickinson et al. (1986) and uses 18 specific classes of vegetation. In addition, another 12 classes were defined from the NASA/NOAA Land Data Assimilation System (LDAS) [ldas.gsfc.nasa.gov] bringing the total number of classes available in RAMS to 30. The model uses Leaf Area Index (LAI), fractional coverage, displacement height, roughness height, albedo, and emissivity for its calculations. One of the 30 assigned land classes is urban; however, LEAF-2 treats this as simply another type of vegetation. By using LAI to simulate the urban canopy, LEAF-2 will process incoming energy and transpire as vegetation and not as artificial, non-porous surface. The roughness length assigned to urban is 0.8, which is likely exceeded by many urban areas. The displacement height is likewise significantly lower than most urban areas

would see. Also, there is no ability to alter either the roughness length or displacement height from city to city although the morphology changes greatly between them. There is no accounting for the difference in thermal capacity of the urban material, no capability to allow for LW or SW energy trapping within the urban canopy, and no capacity for including output from anthropogenic sources.

b. The Town Energy Balance (TEB) Model.

The TEB model is an urban parameterization described in Masson (2000). The model is designed to replace the parent land surface scheme for urban grid cells. It treats the urban area as a 3D volume with each grid cell containing a local street canyon system of roofs, walls, and roads. This allows the 3D geometry of the canyon to be simulated and its dynamic/thermodynamic impacts on the fluxes to be accounted for. TEB utilizes a user provided set of morphology characteristics that describe the urban environment to perform its calculations (see section 3.a.). The scheme tracks separate energy balance evolutions for roofs, walls, and roads that it aggregates to calculate the final fluxes. All fluxes calculated in this 3D volume are provided as surface inputs, even if the actual morphology of the urban area extends into the lower layers of the model. (This limitation is not expected to be an issue for this study since the model set-up is such that the first atmospheric layer is above the average height of the city morphology and no grid cell in the model has more than one layer in the morphology.) The scheme also permits the addition of anthropogenic fluxes, which it adds to the calculated urban fluxes. Finally the scheme has an internal building temperature model that permits climate controlled internal temperatures to interact with the natural climate outdoors. Masson et al. (2002)

describes minor modifications to the original model and it is this version of the model used for this work. TEB was selected in part because it is a single layer model in the middle of the spectrum in terms of complexity. In addition, work has already been done to couple TEB to LEAF-2/RAMS (Rozoff 2002). Finally, Masson states that the parameterization is usable with horizontal grid increments up to 'several kilometers' and work presented in Trusilova et al. (2009) using grid increments of 10 km support Masson's claim.

c. Coupling RAMS and TEB

The coupling employed by Rozoff (2002) formed the initial starting point for this work. TEB is coupled via the LEAF-2. LEAF-2 will use TEB whenever the land surface patch is identified as 'urban'. Several modifications were made to Rozoff's original effort to improve the robustness of the coupling. First, as mentioned, the newer 2002 version of TEB was used. The most significant change allowed the system to read and retain an array of morphology data, thus allowing morphology information to vary from grid point to grid point as opposed to assigning a city wide average morphology to each urban patch. The system is robust enough to use a user provided default set of morphology wherever detailed data was unavailable. In addition, TEB was formally incorporated into the surface radiation scheme ensuring consistent values of surface albedo and longwave radiation were used by the radiation parameterization when called for. Finally, some software engineering was accomplished to add TEB configuration options to the RAMSIN file allowing users the ability to manipulate the use of TEB without the need to re-compile the model.

3. Data

a. Morphology Data.

TEB requires morphology information in order perform its calculations. Table 1 details the values TEB expects. To take advantage of the newly developed variable morphology capability, a morphology database of Washington DC was needed. A suitable database was not available that would be representative of the time period in question (mid-1980's), thus a unique database was developed for this study.

TABLE 1: List of morphology related variables that TEB requires to execute.

Morphology Element	Description
Building Height (h)*	Average building height within a grid cell in Meters. Information varies by grid cell.
Fractional area of buildings (bld) *	Identifies the fraction of urban fabric occupied by roof area. The remaining fraction is classified as road. Information varies by grid cell.
Building Aspect Ratio (h/l) *	Identifies the shape of the urban canyons and is the ratio of the height of the building to the distance between buildings. This is critical to determine dynamic flow category and to determine the sky view for radiation calculations. Information varies by grid cell.
Dynamic Roughness (Zo) *	Used to determine the amount of dynamic drag induced by the urban fabric. For this study, Zo=h/10. Information varies by grid cell.
Albedo / emissivity Roads (aroad, eroad) *	Albedo and Emissivity values for roads. Area of concrete vs. asphalt was estimated. Resultant value is an area weighted average of characteristics from concrete and asphalt. Information varies by grid cell.
Albedo / emissivity Roofs (aroof, eroof) *	Albedo and Emissivity values for roofs. All roofs categorized as housing, non-housing light, or non-housing dark. Resultant value is an area weighted average of the categories. Information varies by grid cell.
Albedo / emissivity Walls (awall, ewall)	Albedo and Emissivity values for walls. Value drawn from Rozoff (2002). Information fixed for all grid cells.
Building material characteristics	Includes number and thickness of road, roof, and wall layers with thermal conductivity and heat capacity of each layer. All values were drawn from Rozoff (2002) and information remained fixed for all grid cells.
Internal Building Temperature (tbld)	Set at 293.16K. Used along with building material characteristics to calculate the temperature wave. Fixed for all grid cells.
Sensible and Latent heat from traffic (sh_traffic, le_traffic) *	Values of sensible and latent heat generated from traffic. Three categories of traffic use identified: housing, downtown, and interstate and given different values. Grid cell total is an area weighted average and therefore varies.
Sensible and Latent heat from industry (sh_industry, le_industry) *	Values of sensible and latent heat generated from industry. Value set to 10 and 5 W/M^2 respectively for any grid cell identified with industry present, zero otherwise. Value varies by grid cell as a binary value.

The database was constructed for a 36X32 km area centered on the Mall in downtown DC and was constructed at 1 km resolution. Three sources were used to construct the database. The USGS 1:24,000 map series (dated 1979-1984) for the counties

surrounding Washington DC provided the 1km grid, details on land use, and place names. A series of high resolution photography (from Apr 1981 and Mar 1983) provided details on the urban fabric. Finally, the book "Above Washington DC" (Camaron 2000) provided detailed photography of various neighborhoods to provide additional morphology details. The resulting morphology is estimated to be a good representation of the Washington DC area for the early 1980's time period. Using these sources, values for a number of TEB variables could be estimated and thus were allowed to vary by grid cell (indicated with a '*' in Table 1). Those that could not be estimated using this procedure were set to default values from Rozoff (2002). Appendix B contains a detailed description of how the morphology was constructed as well as providing the resultant morphology for all 1152 grid cells.

b. Land Surface Data

One of the primary advantages to using a scheme like TEB with variable morphology is that there is no need for many different types of urban land class categories (e.g. 'industrial', 'residential', or 'commercial') in order to model the land surface variations within the city. Instead, one 'urban' land class can be used and the TEB model will naturally model different subsets of urban land use based on the provided morphology data. This is important since LEAF-2 only distinguishes one type of urban landcover.

Even with this relative simplicity, there is still the matter of what source to use for land surface information. There are a number of land surface data sources available varying both in method of obtaining and also in resolution. The RAMS model comes with a standard 30 second (approximately 1 km) land class data set derived from

Advanced Very High Resolution Radiometer (AVHRR) data in 1992-1993 and made available from the United States Geological Survey (USGS) Earth Resources Observation System (EROS). In addition, a land use/land class (LULC) data set collected at a resolution of 30 meters was obtained for a seventy-five square kilometer area around Washington DC. These data were collected by a joint effort of the USGS and the U.S. Environmental Protection Agency. In this case, a number of sources were used, including the Landsat Thermatic Mapper, high resolution terrain databases, Bureau of Census, USGS land use and land cover, plus the National Wetlands Inventory. The end result is collectively known as the National Land Cover Data (NLCD). This database is also representative of land cover in the 1990's. Finally, one of the fallouts of creating a morphology database was an independent estimate of urban, water, vegetation estimation for the 36X32 km area over Washington DC. Because of the sources, this estimate should be more representative of land cover in the early 1980's. It also accounts for the fact that even the most urban areas (shopping malls, business districts etc) are not pure artificial surface, but contain at least some vegetation. This effort was able to separate out that percentage of vegetation leaving the urban land class as purely artificial. The other two land surface datasets explicitly assume vegetation is part of urban land class grid cells. Thus this morphology effort derived urban estimate should be much lower then either the AVHRR or LULC databases. It is worth noting that this is the type of information TEB expects as it deals only with impervious surface leaving all vegetation to the parent land surface model.

In the end, for the area immediately around Washington DC, three land surface data sets were available. One consisted of just the RAMS 1 km dataset. The second

supplanted the RAMS 1 km data with the LULC data for the 75 km X 75 km area around Washington, DC. The third further supplanted the LULC database with the independent one created within the 36 km X 32 km urban center of DC. All three datasets were then aggregated to 5 km to match the inner most resolution of the model. LEAF-2 was then configured to use three land patches and one water patch. Once scaled up to 5 km, the datasets overlapped on the 35 km X 30 km area centered on Washington, DC. The RAMS provided land surface identified this region as 72% urban, the LULC was 60% urban while the LULC-modified dropped the urban percentage to just 37%. The large drop-off from LULC to LULC-modified is a reflection of separating the vegetation percentage out of the urban grid cells. Most of this comes from the residential neighborhoods where the land surface data files identify all of the area as 'urban', but examination showed that the area consists of significant amounts of vegetation (lawns, trees, medians, parks, etc.).

The third data base (LULC-modified) was selected as the primary land surface data set used in the simulations as it was the only one to truly attempt to estimate the percentage of impervious surface (which is the only portion of the land surface that TEB really wants to simulate) and is most representative of land surface in the early 1980's. The other two depictions were used to conduct sensitivity tests. More details on the land surface data files and a table of land surface values for all 1152 grid cells are found in Appendix B.

c. Meteorological Data

During 1984, the city of Washington DC conducted a year-long campaign to collect data on dispersion of trace gases in the greater DC area, known as the Metropolitan

Tracer Experiment (METREX) (Draxler 1985). The value of the campaign was the availability of supplemental meteorological data that would be helpful to an objective validation of a meteorological model attempting to model the UHI of Washington DC (See chapter 2 for details). For this reason, 1984 was selected as the candidate year to simulate. The national weather daily summary maps were examined for 1984 to determine candidate days to select for simulations. For this initial simulation, 26 Jun 1984 represented high pressure moving overhead with building southwesterly flow and increasing temperatures and humidity. This regime was thought to provide generally good conditions for the formation of an urban heat island and was the date selected to perform the subjective evaluation and sensitivity tests against.

4. Model Simulation and Subjective Results.

a. RAMS Set-Up.

The primary goal of this study is to examine the operational viability of an urban parameterization. As a result, the set up of the model was designed to mimic what an operational center might run. Table 2 contains the specifics of how RAMS was configured for the run. The set-up included three nests centered on the Mall area in Washington DC. Figure 1 shows the layout of the three grids. Note that the inner nest is running at a grid spacing of 5 km, typical of Air Force operational settings, yet much coarser than typically used for an urban study. Each run was initialized at 12 UTC (early morning in Washington DC) on the day of interest and run through the following afternoon, 36 hours in all. Output was captured every hour. The runs were initialized

using data from the NCEP Re-analysis fields (Kalnay et al. 1996), and utilized climatological Sea Surface Temperatures (SST) from the standard RAMS SST files.

TABLE 2: List of select model configuration options.

Description	Option
Grid Structure	Arakawa C Grid; 3 fixed nested (80, 20, 5 km)
PBL Parameterization	Mellor-Yamada
Radiation Parameterization	Chen, both LW and SW
Lower Boundary	LEAF-2 with Town Energy Balance
Lateral Boundary	Klemp/Wilhelmson
Level of First Model Layer	23 Meters (11m for those written to center)

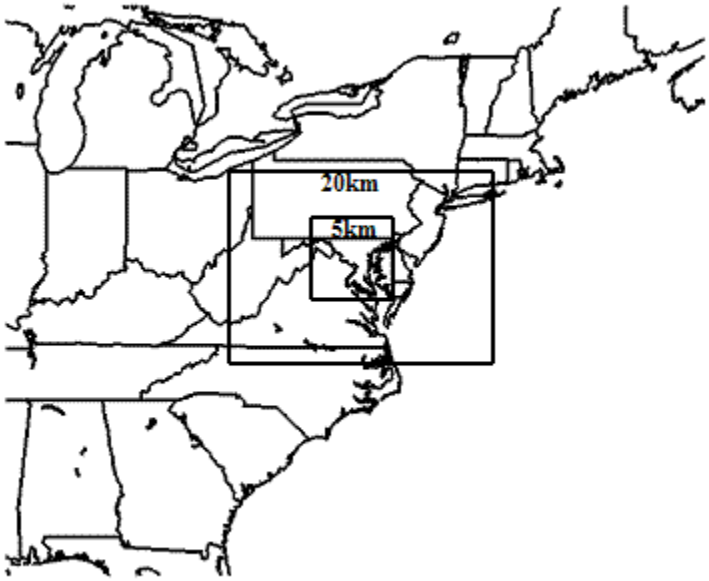

Figure 1: Grid domain layout and spacing

For the surface, a method was needed to determine an appropriate way to initialize soil moisture. The Crop Bulletin (Vol 71, no 25) for the week prior to 26 June and the weekly weather charts from NOAA were used to assess moisture availability. The drought index indicated that conditions had been moist with no long-term precipitation deficit. Closer to the week in question, the crop bulletin had dry crop moisture indices to

the higher terrain west of the city, with near neutral values over the city itself. The NOAA summary bulletin indicated there had been some scattered convective precipitation in the area each day 23-25 Jun, but no wide spread precipitation for the area. Combining this data suggests the overall soil moisture for the area immediately around the city was neither too moist nor too dry. RAMS allows the user to set the soil moisture using a value between .01 and .99. LEAF-2 documentation indicates that the model reaches a wilting point below .20 and saturation above .70. Therefore soil moisture in the model was initialized at .45, a value right in between and most representative of conditions neither too moist or too dry.

b. Simulation Results

The goal is to examine how the addition of the urban parameterization changed the structure of the boundary layer and, subjectively, whether the TEB scheme was able to create many of the features typically associated with UHI behavior in spite of being run at 5 km. The simulations were from 1200 UTC 26 June to 0000 UTC 28 June. Difference fields between the TEB and No TEB simulations and selected individual fields were examined to find evidence of modeled UHI behavior.

1) TEMPERATURE

As late afternoon approached (1700 LT 26 June) difference fields show that the TEB simulation begins to form an urban heat island which continues intensifying into the night. Figure 2 shows the difference field (in °C) at 2300 LT and represents the time of maximum difference between the models. It shows a more than 3.5 °C perturbation over

and just north of the city center. The shape largely conforms to the shape of the urban area except that the center of the heat island is displaced to the NNE (likely by the SSW winds present over the city at this time).

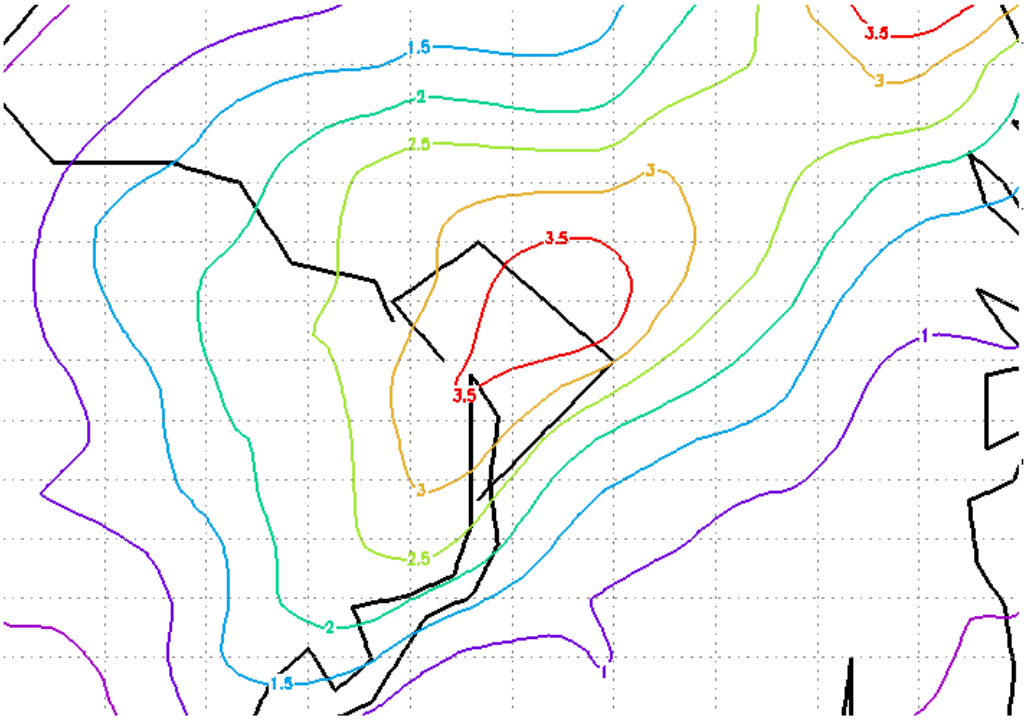

Fig 2: Difference of the 2m temperature fields TEB – No TEB (°C) at 2300 LT 26 June 1984.

The intensity of the heat island decreases to just over 1 °C by 0300 LT, then intensifies to nearly 3 degrees again briefly prior to sunrise (not shown). Within one hour of sunrise the difference between the models erodes and a negative TEB – No TEB develops. Figure 3 is an example of this at 1000 LT. This is likely a reflection of the morphology shadowing effect impacting morning heating rates. This effect has been observed in other cities (e.g. Cleugh and Oke 1986; Rosenzweig et al. 2009). By early afternoon, the temperature difference between the simulations differences reduce to near

zero, although by this point it may have as much to do with boundary condition contamination as it does the land surface modeling. Overall, results for temperature are encouraging that the TEB model can simulate the formation of a UHI even at this relatively 'coarse' resolution.

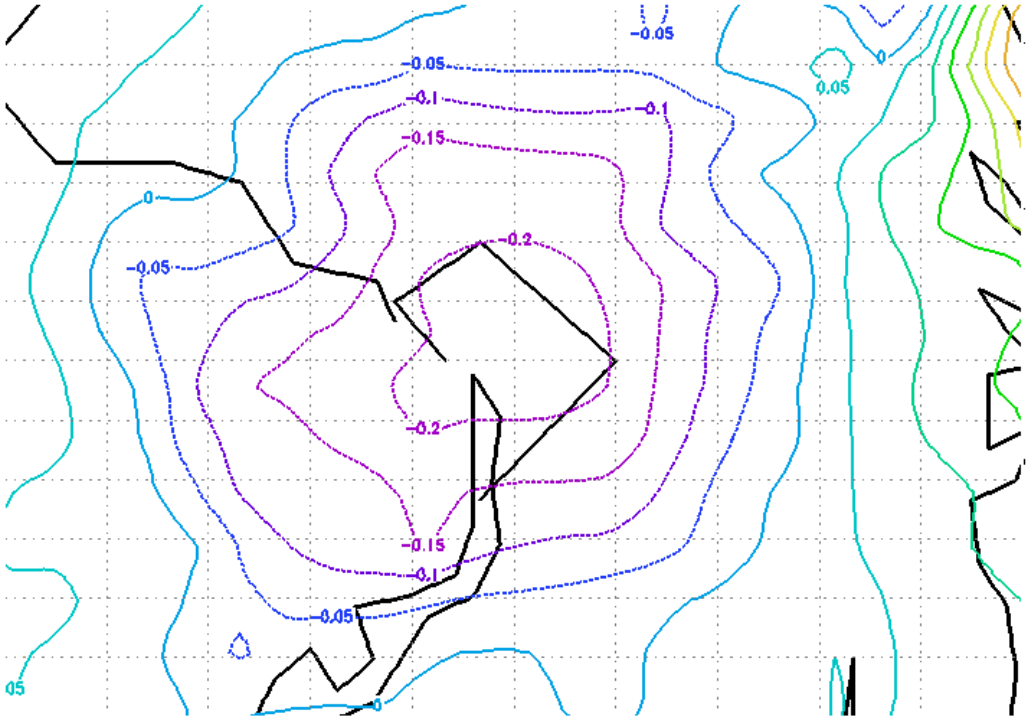

Fig 3: Difference of the 2 m temperature fields TEB – No TEB (° C) at 1000 LT 27 June 1984.

2) WINDS AND CIRCULATION

Another area of encouraging results is with the wind behavior. Figure 4 shows the difference in the wind speeds between TEB and no TEB simulation at 1300 LT. The run with TEB reduces the wind speeds over the city, likely due to the greater roughness

lengths obtained when utilizing the urban morphology. In contrast, Figure 5 shows the difference in wind speeds at 2300 LT 26 June where the TEB run has stronger winds by

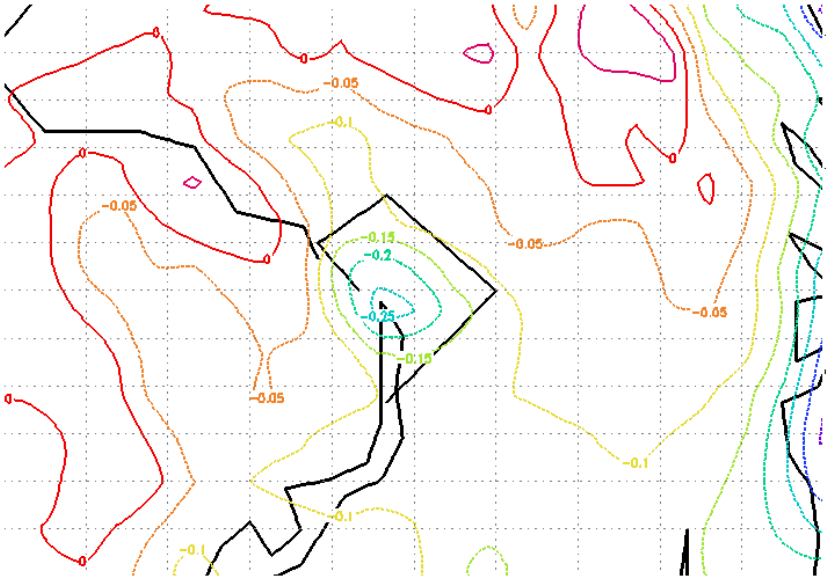

Fig 4: Difference of the first model layer winds field TEB – No TEB (m s^{-1}) at 1300 LT 26 June 1984.

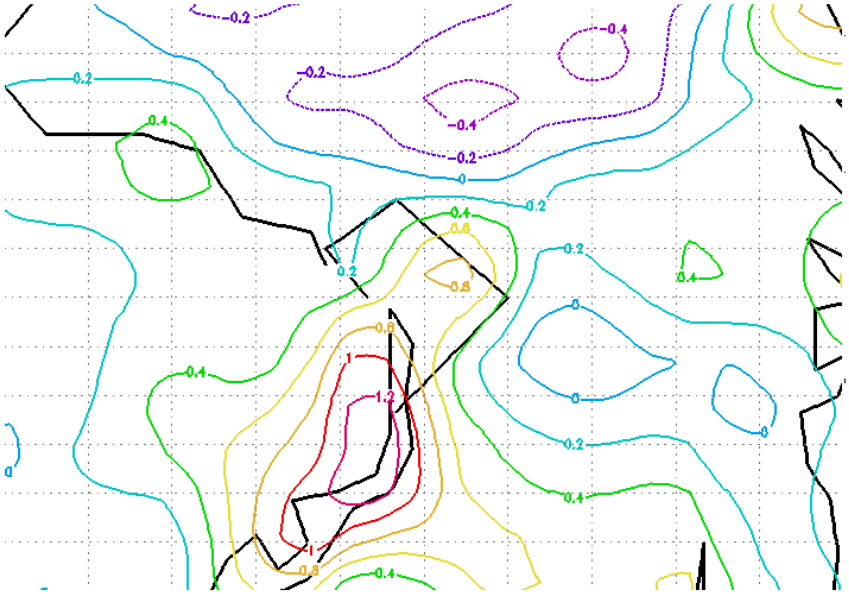

Fig 5: Difference of the first model layer winds field TEB – No TEB (m s^{-1}) at 2300 LT 26 June 1984.

over 1.2 m s^{-1} in places. The stronger winds are likely due to the lack of stabilization over the city in the TEB run at night allowing the winds to remain active. Note how there also seems to be some influence from the urban area to the winds over the water to the south. Perhaps the lack of stabilization over the urban area promoted a similar lack of stabilization over the water. Again both of these wind features (decreased during the day, increase at night) are typical of UHI behavior (e.g. Soriano et al. 2001).

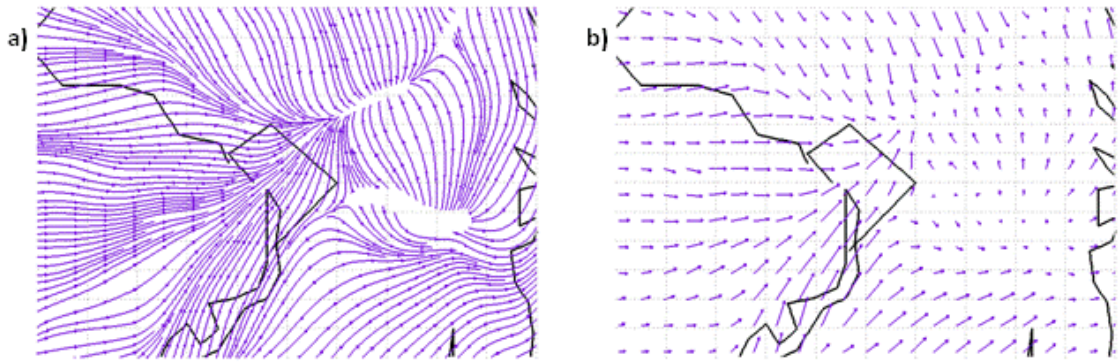

Fig 6: a) Streamlines and b) wind vectors for the difference TEB-No TEB at 2300 LT 26 Jun 1984

Looking at the streamlines and wind vectors confirms that the TEB run produces fundamental changes to the flow over Washington, DC. Figure 6 shows the streamlines (6a) and wind vectors (6b) of the difference between the TEB and no-TEB simulation at 2300 LT. The presence of the temperature perturbation leads to an organized mesoscale circulation. This is usually referred to as the UHI circulation pattern and has been modeled in other studies (e.g. Rozoff 2002; Lemonsu and Masson 2002; Lei et al. 2008). This mesoscale circulation integrates into the background synoptic and mesoscale flow pattern and creates a new flow pattern with changes in direction and location of convergence zones (e.g. Yoshiado 1992) and demonstrates one of the critical motivations

for the need to account for urban areas in operational models. Changes like this would be expected to impact air pollution and dispersion modeling results.

3) VERTICAL STRUCTURE AND STABILITY

The impacts of the UHI are not confined to the surface. Often, urban areas are observed to maintain sensible heat fluxes throughout the night, and as a result, can maintain neutral or even unstable boundary layers while surrounding rural areas may stabilize (Hilderbrand and Ackerman 1984; Basara et al. 2008). Oke (1987) discusses how the fluxes and mechanical turbulence often 'bump up' the height of the UBL by several hundred meters by day and then helps to maintain an active boundary layer well into the night.

Figure 7 shows a vertical cross section of temperature difference between the simulations at 38.9° latitude from west to east through the heart of the city at 2300 LT. TEB introduces a positive temperature perturbation extending up over 1.5 km, although the majority of the 'bubble' is below 200 m. Figure 8 shows the difference in Total Kinetic Energy (TKE) produced by the model and the model derived difference in PBL height at 2300 LT. Thanks to positive sensible heat flux at the surface, figure 8 demonstrates that the model drives an active PBL well after sunset. Thus TEB's influence is being carried into the evolution of the model PBL in ways consistent with climatological expectations. Further, sustainment of an active PBL into the night is another feature that would be expected to have an effect on air pollution and dispersion modeling.

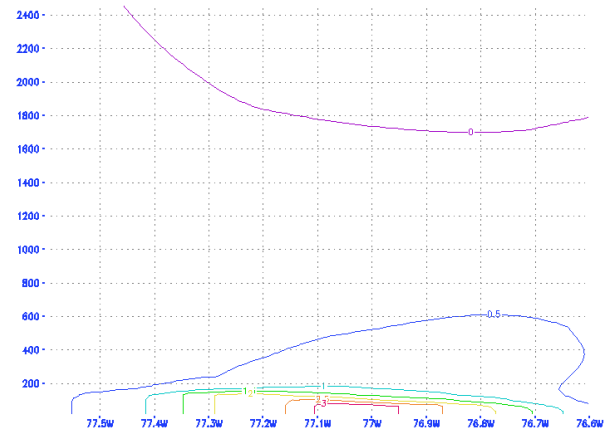

Fig 7: Vertical cross section of temperature difference TEB-no TEB at 38.9 latitude west to east through the city at 2300L

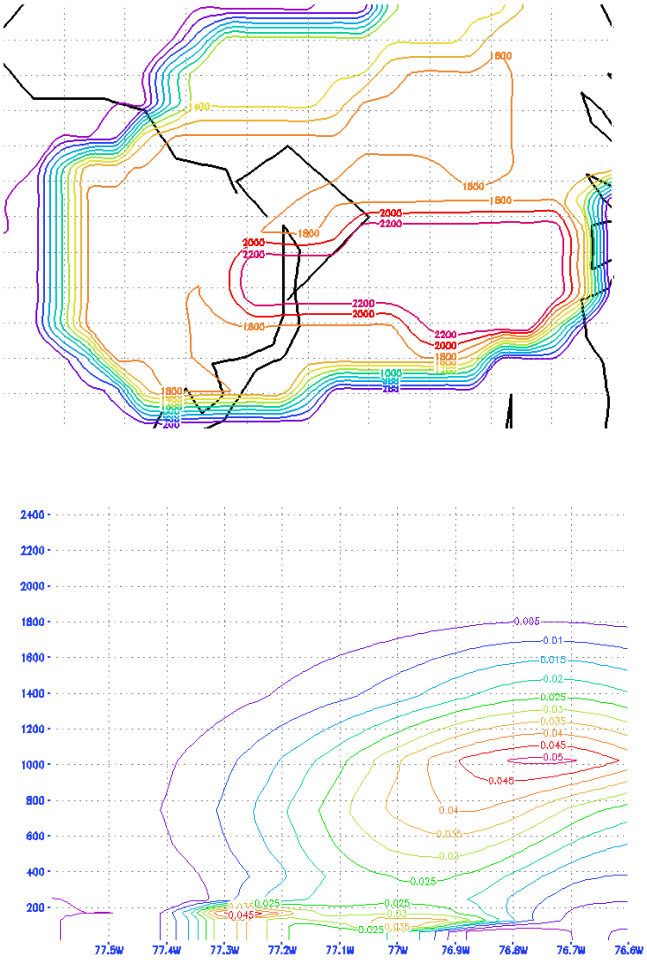

Fig 8: Difference of model calculated a) TKE and b) PBL height (m) for TEB – No TEB at 2200L on 26 Jun 1984.

4) SUMMARY

Taken as a whole, the behavior of the simulation with TEB active suggests that the urban parameterization is producing a nocturnal UHI and that this UHI is interacting with the larger mesoscale environment producing fundamental alterations to the sensible weather observed both within and around the urban core of Washington, DC. The types of changes seen would be expected to influence the modeling in follow-on applications such as air pollution or dispersion. Chapter 2 examines whether the available observations suggest that the TEB simulations are producing a more representative boundary layer over Washington, DC.

5. Sensitivity Studies

The subjective results above are encouraging in suggesting that an operationally configured model may be capable of utilizing an urban parameterization to better represent the urban mesoscale environment. Another important aspect to consider with an eye towards operational utilization of the parameterization is the relative sensitivity of the parameterization to various aspects of the model. This section will examine results from several sensitivity experiments.

a. Land Surface Sensitivity

Current operational models generally use 1 km land surface data, which is relatively coarse compared to the widely available LULC 30 m sets. Additionally, these land surface datasets (1 km or 30 m) define their urban land surface as assuming to have some amount of vegetation and not purely artificial surface. However, the TEB

parameterization was designed to model only that percentage of the land surface made up of truly impervious, artificial surface. How sensitive is TEB to both the resolution and composition of the data sets? To test this, TEB was run with the RAMS provided 1 km dataset, the 30 m LULC dataset, and the morphology derived LULC-modified dataset and the results compared. Recall that the RAMS land surface dataset 'sees' Washington, DC as 72% urban, the 30 m LULC 'sees' Washington DC as 60% urban, while the LULC-Modified 'sees' Washington, DC as only 37% urban.

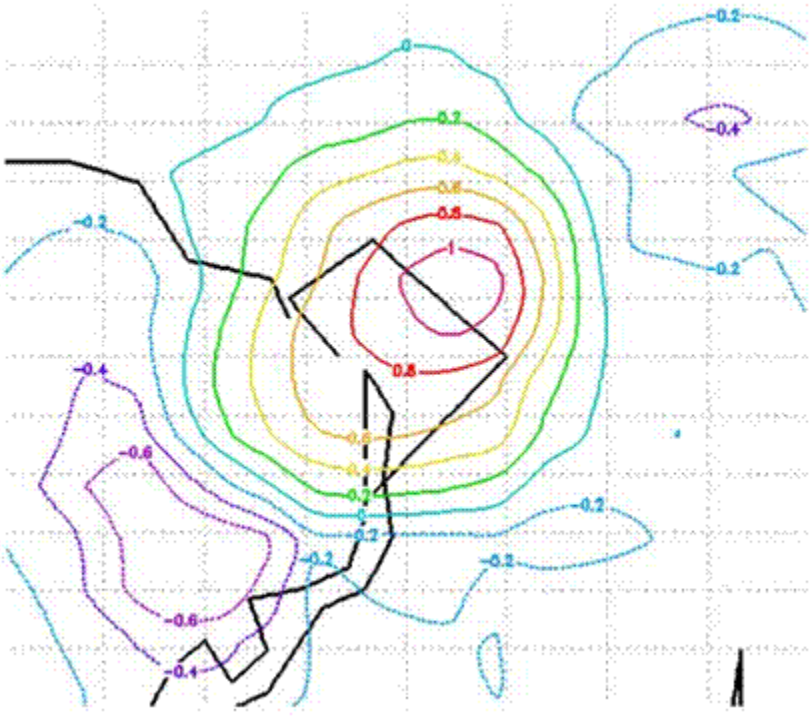

Fig 9: Difference of the 2m temperature fields RAMS 1km land surface - LULC-modified land surface in °C at 2300 LT 26 Jun 1984.

Figure 9 shows the difference between TEB with RAMS 1 km land surface vs. LULC-modified at the time of maximum UHI strength. Perhaps not surprisingly, the model shows significant sensitivity to the different land surfaces with the RAMS land surface driving a UHI more than 33% (>1 °C) stronger. The difference between the RAMS and

LULC datasets (not shown) was very much smaller (<.1 °C) and considered non-significant. This small sensitivity is, perhaps, not that surprising since the difference in urban percentage between them was only on the order of 12%. What it does suggest is that land surface differences between 1 km and 30 m don't matter much at this modeling resolution. However, the sensitivity shown in the 1 km vs. modified set is worth further examination. This difference arises from two factors. First, the morphology derived land use was created using photography from the early 1980's while the 1 km dataset used data from the early 1990's so some of the difference is due to growth in the urban area over the decade. A study by Johnston and Watters (1996) used Landsat imagery and estimated that the amount of urban fabric in Washington DC increased 7% between 1982 and 1993, growth they termed 'explosive'. Second, the morphology derived landcover is a closer estimation of the actual artificial surface percentage where the l km set assumes some aggregate between urban and vegetation coverage. Based on the results from the RAMS 1km and LULC sensitivity and the finding of Johnston and Watters (1996), most of this sensitivity is probably a result of separating the vegetation out of the urban land class.

b. Morphology Sensitivity

With the relatively coarse resolution of operational models, a logical set of questions would center around the demands of the morphology database required by TEB. At this resolution do you need a detailed morphology which varies by gridpoint or can you get away with using average morphology representative of the city as a whole? Further, do you need to worry about inter-city differences or can you use a set of default values for

the whole country? To begin examining this a few experiments were carried out. First, TEB was run using the fully resolved grid cell variable morphology and then again with each cell using the city wide average value.

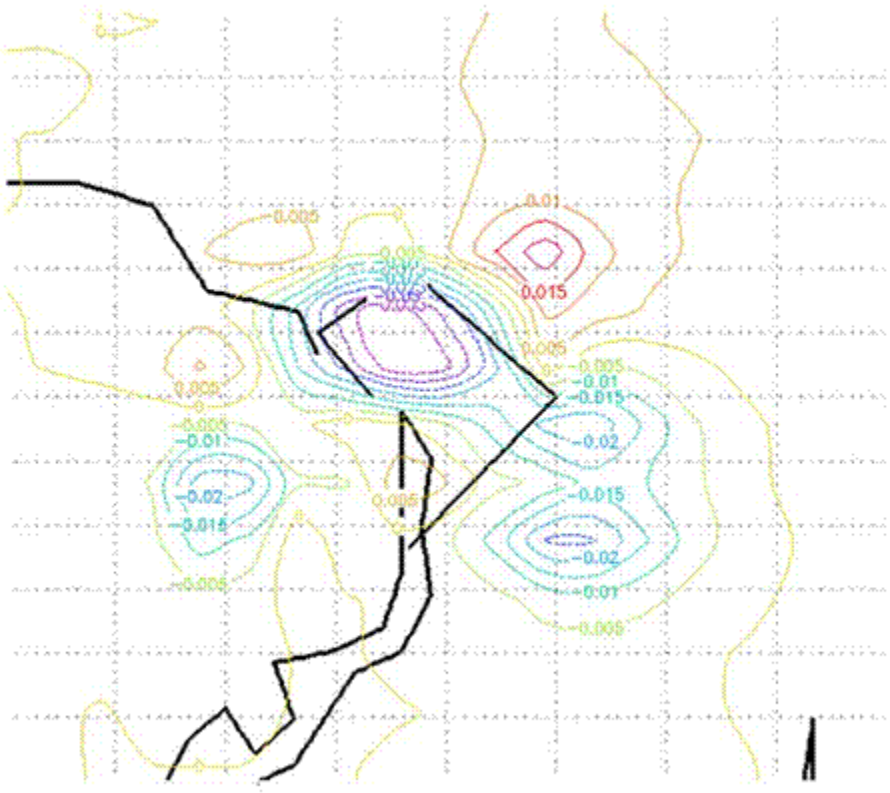

Fig 10: Difference of 2m temperature (°C) at 2300 LT 26 June between the simulation with morphology variable by grid point minus the simulation with a city wide average morphology at each grid point.

Figure 10 shows that the runs were relatively insensitive to fully resolved morphology suggesting that at 5 km using a city wide average morphology may suffice. However, it should be pointed out that Washington DC does not have the most severe morphology and this should likely be carried out in a city with more intense variations in morphology. Next, the morphology of Washington DC was arbitrarily changed to examine how sensitive TEB is to specific variables.

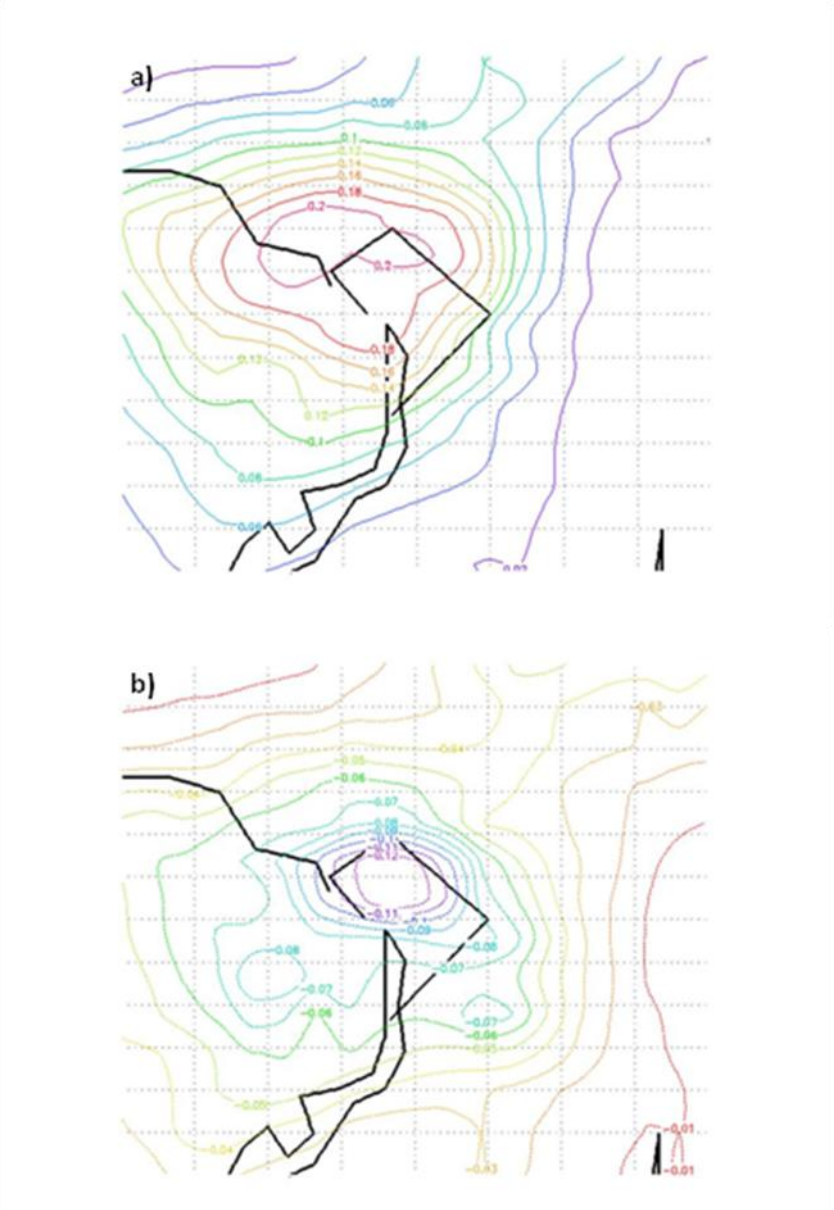

Fig 11: Difference of UHI temperature signature at 2300 LT (°C) between a) average morphology height of 16 vs. 8 meters and b) average roofs/roads albedo of 0.18/0.13 vs. 0.09/0.07.

Figure 11 shows the results of doubling the average height of the city from 8 to 16 m (10a) and the result of decreasing the city average albedo of roofs from 0.18 to 0.09 and roads from 0.13 to 0.07 (10b). The simulation did show significant sensitivity to the change in height but not albedo. However, the height results alone do suggest that differences between cities would likely be great enough to warrant using different default

morphology values. So while it appears that one average set of morphology values may suffice for a given city this does suggest different cities should utilize different averages. Also it would be worth exploring whether changing multiple parameters simultaneously drives larger changes.

c. Soil Moisture Sensitivity

Mesoscale model simulations are usually quite sensitive to soil moisture; however, given the dynamics of the UHI, there is also reason to believe that the UHI formation may also be sensitive to soil moisture. Basically if the surrounding vegetation is very moist or dry, the relative difference between the imperious urban center and surrounding landscape may cause UHI formation to proceed in a different way. Figure 12 shows the maximum UHI strength simulated by TEB with soil moisture set to a saturation value (12a) vs. one with soil moisture set at the wilting point (12b). It is clear that the moisture of the surrounding landscape does play a role in the model towards modulating the strength of the UHI formed over Washington DC. The moist simulation drives a stronger response than the dry. Considering just radiation concepts this may be a bit surprising as one might expect the drier rural landscape better conditioned to radiatively cool at night thus perhaps allowing a stronger UHI response in the dry. Further examination suggests that the dry simulation drives a stronger BL response which in turn produces higher nighttime winds in the UHI as seen in Figure 13. It is believed that this more energetic UHIC is more effective at venting the temperature heat island leading to lower absolute

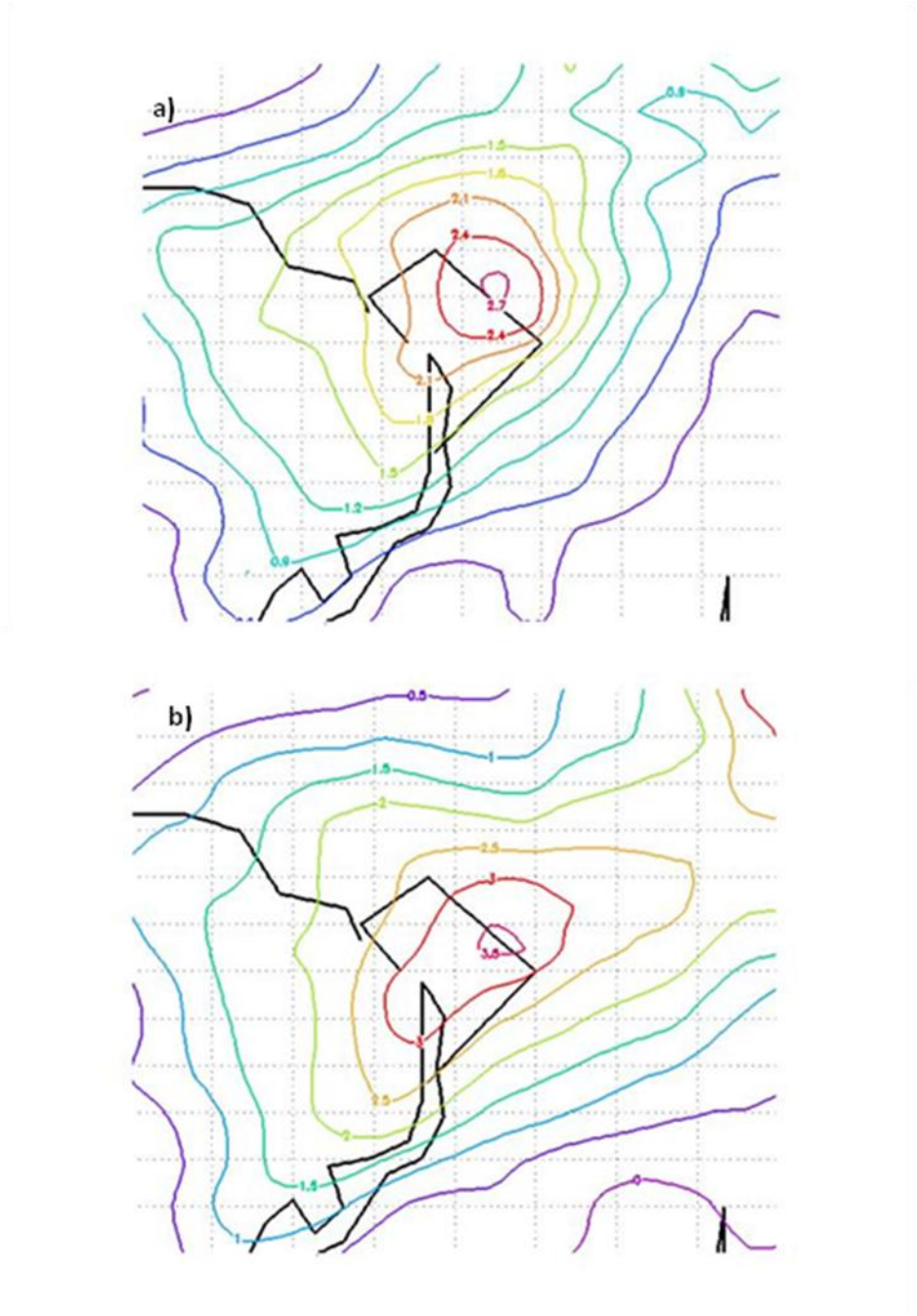

Fig 12: UHI strength (°C) at 2300L 26 June for a) simulation with soil moisture set to wilting and b) simulation with soil moisture saturated.

temperature differences. Thus the dry scenario did seeming drive a stronger response, but the energy of the response did not go preferentially into temperature. Overall, these

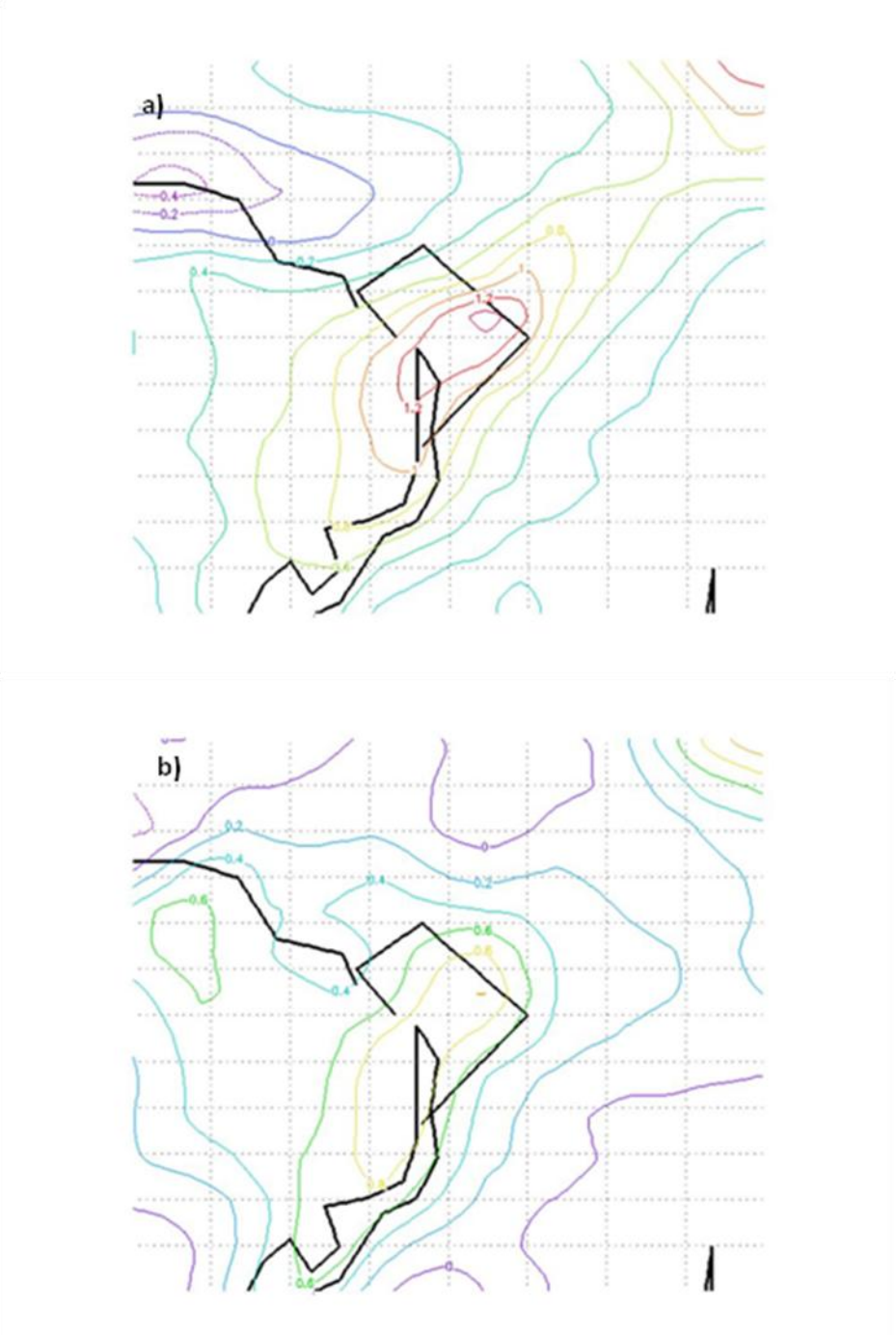

Fig 13: First model level wind speed differences TEB-No TEB at 2300L, 26 June for a) simulation with soil moisture set to wilting b) simulation with soil moisture set to saturation.

results suggest that the urban parameterization is changing the characteristics of the UHI due to the relative soil moisture availability.

d. Sensitivity to the presence of Baltimore

Analysis of the temporal evolution of the UHI within Washington, DC suggested that the presence of the Baltimore UHI to the NE may be interacting with and re-enforcing the Washington, DC UHI in the early morning hours. To test this, the city of Baltimore was removed and replaced with vegetation.

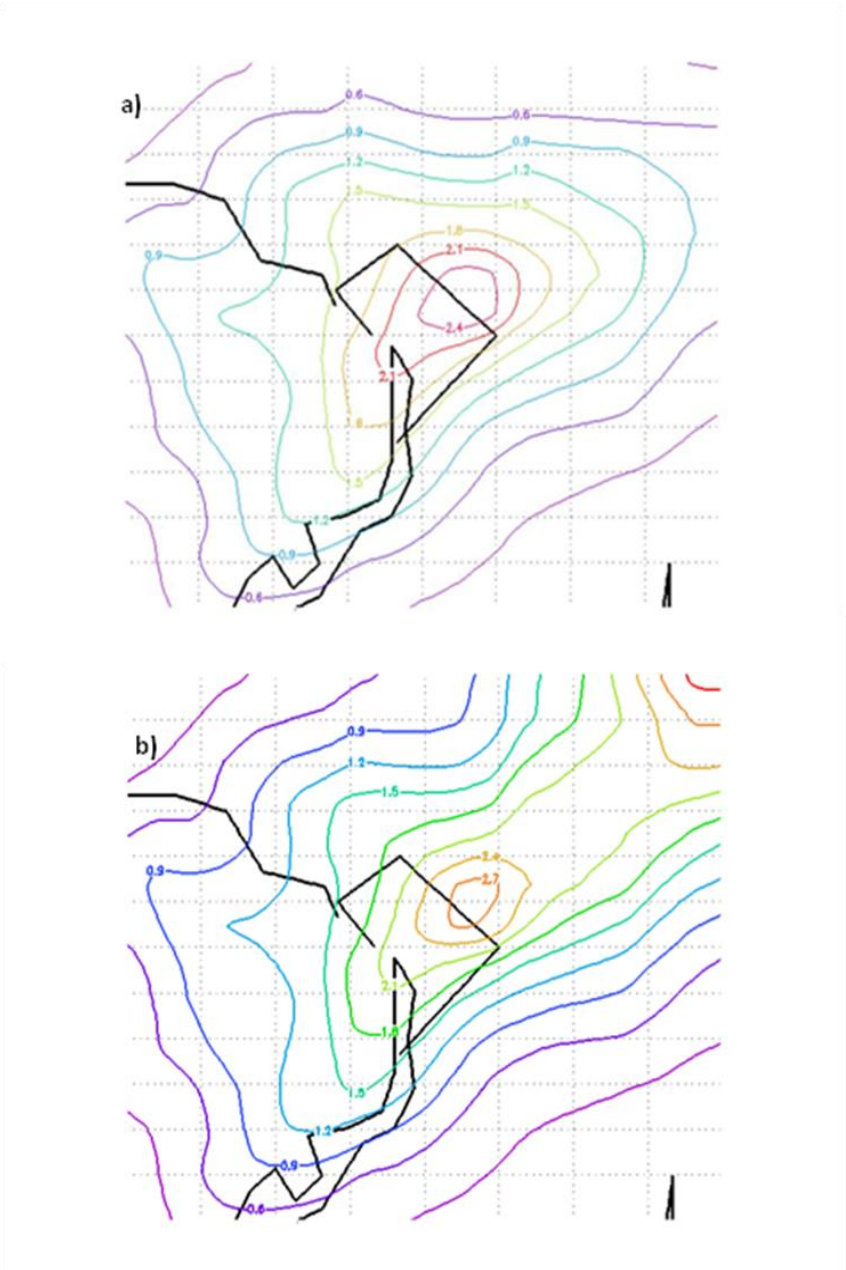

Fig 14: 2m Temperature difference (°C) TEB-no TEB at 0700 LT 27 June for a) simulation without Baltimore b) simulation with Baltimore.

Figure 14 shows a comparison between the strength of the Washington DC UHI with and without Baltimore present at 0700 LT. While the differences are only on the order of .3 °C, it does suggest that the model is simulating interaction between the two cities. It is beyond the scope of this paper to address the observational reality of the effect or to attempt to address the mechanisms involved in the interaction. Instead, it is enough to note the effect as an area that warrants further study, especially given the proximity of many large urban areas on the east coast.

6. Conclusions

Simulations were conducted for a summer night in Washington DC to examine whether an urban parameterization would be capable of generating a UHI response over the city with a relatively coarse model configuration typical of those run by operational meteorological agencies. In addition, several sensitivity experiments were conducted to determine what aspects of the model configuration would have to be managed most closely if an urban parameterization were to be adopted by an operational agency.

Results indicated the presence of the urban parameterization did allow the model to develop a nocturnal UHI. In addition to temperature, changes typical of other observed and model UHI's were seen in the simulations, including changes in winds, mesoscale circulations, and stability. Sensitivity experiments conducted suggest that detailed morphologies may not be necessary at these resolutions; instead, modelers may be able to use a single set of representative values for the city as a whole. However, sensitivity to building height suggests that having variability between cities may be warranted. In addition, the studies suggested that while the resolution of the land surface data fields

may not have much impact, the ability to derive the actual percent of impervious surface and the need to update the land surface datasets to account for growth of cities may be necessary to properly utilize an urban parameterization. The urban parameterization also showed sensitivity to the soil moisture above and beyond the typical model response suggesting that the use of an urban parameterization will further re-enforce the need for quality soil moisture information. Finally, the removal of Baltimore suggests that cities in close proximity to each other may see some level of UHI interaction, a item worthy of further study.

Chapter 2 will examine the performance of the urban parameterization against objectively collected field data over three different synoptic driven situations to attempt to comment on the parameterizations ability to simulate a 'better' BL response over the city.

Chapter 2: Coupling an Urban Parameterization to an Atmospheric Model Using an Operational Configuration II: Objective Results

1. Introduction

Mesoscale models are employed by operational forecast centers in both the civilian and military sectors to provide numerical guidance on the current and expected evolution of the atmosphere. The inner nests of these models are generally run with a grid spacing of 4-12 km enabling them to capture and simulate many of the mesoscale atmospheric systems of interest such as sea breezes, valley flow effects, and even larger organized convective structures and gust fronts. However, this resolution is not sufficient to model many of the smallest scale features so models rely on parameterizations to handle these features and feedback to the resolvable scales. One feature which is largely parameterized is the land surface interaction. Land surface parameterizations are designed to provide the surface fluxes necessary to drive the overlying atmospheric boundary layer (also parameterized). These parameterizations allow the model to produce different boundary layers over different land surface types which in turn allows the model to drive appropriate responses to near surface sensible weather parameters (temperature, moisture, etc) and even allow for the development of mesoscale atmospheric flow responses such as a sea breeze. These land surface schemes model a number of different surface types including different types of vegetation and soils, plus water.

Chapter 1 and Appendix A develop motivation concerning the potential need to devote more attention to the handling of urban land surface within operationally run mesoscale models. To summarize, urban environments drive a specific boundary layer response (commonly called the Urban Heat Island, UHI) that operational land surface parameterizations are not well positioned to model. Further, a disproportionate number of people experience the sensible weather of this urban boundary layer due to the population of the urban environment relative to the rural. Finally, output from operational mesoscale models are often used to drive simulations of effects (e.g. air pollution and dispersion) that are both sensitive to boundary layer inputs and important to the population in urban areas.

A number of urban parameterizations have been developed to account for the short comings of the land surface parameterizations; however, the vast majority of work with these urban parameterizations has been applied to very high resolution runs (2 km or less) for specific urban cases studies. This study was motivated by the desire to evaluate the performance of an urban parameterization with a model running in a configuration more typical of operational meteorological centers to see if these parameterizations could improve sensible weather performance in urban areas.

For this effort, the city of Washington DC was selected. It was selected to perform this evaluation in for a number of reasons. First, the city is situated in a relatively flat location far enough inland to be free of sea breeze influences thus the secondary mesoscale circulation environment is relatively benign, but it is a large metropolitan area with a documented UHI (DeMarrias 1975; Hicks et al. 2010). Additionally, the city is an interesting study area due to the political importance of the city and thus higher risk of

effects based incidents (e.g. terrorism). Finally, in 1984 the city hosted a yearlong field campaign aimed at obtaining a dataset for the improvement of dispersion modeling. This provided the potential for validation data under a variety of weather scenarios and not just 'golden days' often selected for urban based modeling studies. One aspect of operational models is that they run everyday under every type of forcing, so ideally one would want to look at the performance of the parameterization under a variety of weather days.

Chapter 1 started this examination by looking at the ability of the parameterization to function subjectively. A summer night with clear skies and light winds was selected for this portion of the study. Results showed that the model, when running with the urban parameterization active, did seem to produce many of the expected features of an urban heat island, including expected responses in temperature, winds, stability, and the local wind flows.

This chapter will now address the performance of the urban parameterization against observed data to see if the presence of the urban parameterization is creating a better characterization of the sensible weather in an urban environment. The focus will be on temperature, both in the horizontal and vertical, as this is the standard variable that defines a UHI. As mentioned above, it is important to examine the behavior of the urban parameterization under a variety of synoptic weather conditions to assess it performance for operational use. First, the same summer night used for the subjective runs will be assessed. In addition, two other days from different seasons and different synoptic regimes were selected in an effort to examine the performance of the parameterization under more varied conditions. This effort is not designed to be a complete assessment of

urban parameterizations for operational use; instead it is intended to motivate operational centers to examine the potential usefulness of an urban parameterization in their models.

2. Models and Data

a. The Model System

The Regional Atmospheric Modeling System (RAMS) Version 4.3 and its associated land surface model, the Land Ecosystem-Atmospheric Feedback-2 (LEAF-2) model are the base model system selected for this study. Details on these models can be found in Cotton et al. (2003) and Walko et al. (2000) respectively. Additional details on LEAF-2 can also be found in Appendix A. This model system was then linked to the Town Energy Balance (TEB) urban parameterization (Masson 2000) via LEAF-2 and the RAMS radiation parameterization. TEB accounts for the 3D effects of the urban land surface as well as permitting anthropogenic heat sources; key features missing in the LEAF-2 approach to urban land surface modeling. The coupling was accomplished such that LEAF-2 will hand over the land surface flux calculations to TEB whenever the land surface data type is identified as 'urban'. Details on the coupling of TEB and LEAF-2 were presented in Chapter 1.

b. The non-Meteorological Datasets

As detailed in Chapter 1, two critical non-meteorological datasets were needed to conduct this study; a land surface dataset of Washington DC and detailed morphology database. Some of Chapter 1 was spent examining the sensitivity of the model simulations to these datasets in order to understand what was needed.

Three different land surface datasets were examined in Chapter 1. TEB is designed to handle only the actual artificial surface of the urban area, while land surface datasets classify urban areas as a mix of artificial and other (vegetation, soil) type surfaces. In addition, census data and a study by Johnston and Watters (1996) demonstrate that the Washington DC area has been experiencing explosive growth. Based on the results of the sensitivity studies described in Chapter 1, the simulations described in this chapter were run using the 30 m LULC dataset modified to account for both the actual amount of artificial surface and the decade of urban growth that occurred between the simulation year (1984) and year that the LULC dataset represents (1992). In terms of the morphology database, even though sensitivity studies suggested that at 5 km grid spacing an average morphology would suffice, these simulations were executed using the fully resolved morphology since the effort to create it had been undertaken. Additional details on the creation of both the modified land surface and morphology datasets is detailed in Chapter 1 and Appendix B.

c. Meteorology Data

The national weather daily summary maps were examined for the year of 1984 to determine candidate days to select for simulations. The decision was made to stay away from days with precipitation as this aspect of TEB has not been examined well in the reviewed literature. However, a variety of weather types were wanted. In the end three days from different seasons were selected to examine against objective weather: 26 June, 1984 represented building southwesterly flow with increasing summer like temperatures and humidity. Based on typical UHI climatology, it was suspected that this regime would

provide generally good conditions for the formation of an urban heat island. This was the day selected for the subjective examination and sensitivity experiments discussed in Chapter 1. 7 November, 1984 saw a building polar continental surface high-pressure system with generally clear skies and NW winds. This could be viewed as a 'typical' pleasant fall day for the Mid-Atlantic States. Finally, January 7, 1984 was a day that featured cloudy periods and an abrupt shift in winds from NW to S; however, the day was free of precipitation. This day was representative of a more synoptically complex winter situation and climatologically less favorable for a strong UHI response.

From November 1983 through December 1984 the city of Washington DC conducted a transport and diffusion campaign known as the Metropolitan Tracer Experiment (METREX) (Draxler 1985). The campaign featured tracer releases every 36hrs throughout the year from different parts of the city. In addition, they conducted a number of intensive field campaign days scattered throughout the year in which additional data were collected. During this experiment, a number of sites around the city were instrumented to measure basic meteorological variables and this data set provided the back bone of data available for comparison against the model simulations. Two of the three days selected (26 June and 7 November) were intensive field campaign days.

Figure 15 shows the location and types of meteorological data available in and around Washington DC against a background depicting the boundary of the District and the 1 km land use with urban as yellow, vegetation as green and water as blue. Surface observations were collected at the standard airports (Reagan, Dulles [located to the west of the mapped area], Andrews AFB, and Fort Belvoir) and consisted of information found in the standard METAR reports. In addition, during the intensive field campaign

periods, supplemental data were collected hourly during the night from two tethersonde sites. One was set up on the campus of Gallaudet College in the NE sector of Washington, DC while the other was set up on the grounds of Woodward High School (since closed) located in North Bethesda, MD. The tethersondes were able to sample temperature in the lowest 300 m of the atmosphere providing a fantastic source of data in the vertical. Details on the instrument packages for the tethersondes can be found in Draxler (1985). Although the current 'DC Net' (dcnet.atdd.noaa.gov) contains more surface data sites, the availability of the tethersonde data made this 1984 dataset more interesting for use than the more current 'DC Net'.

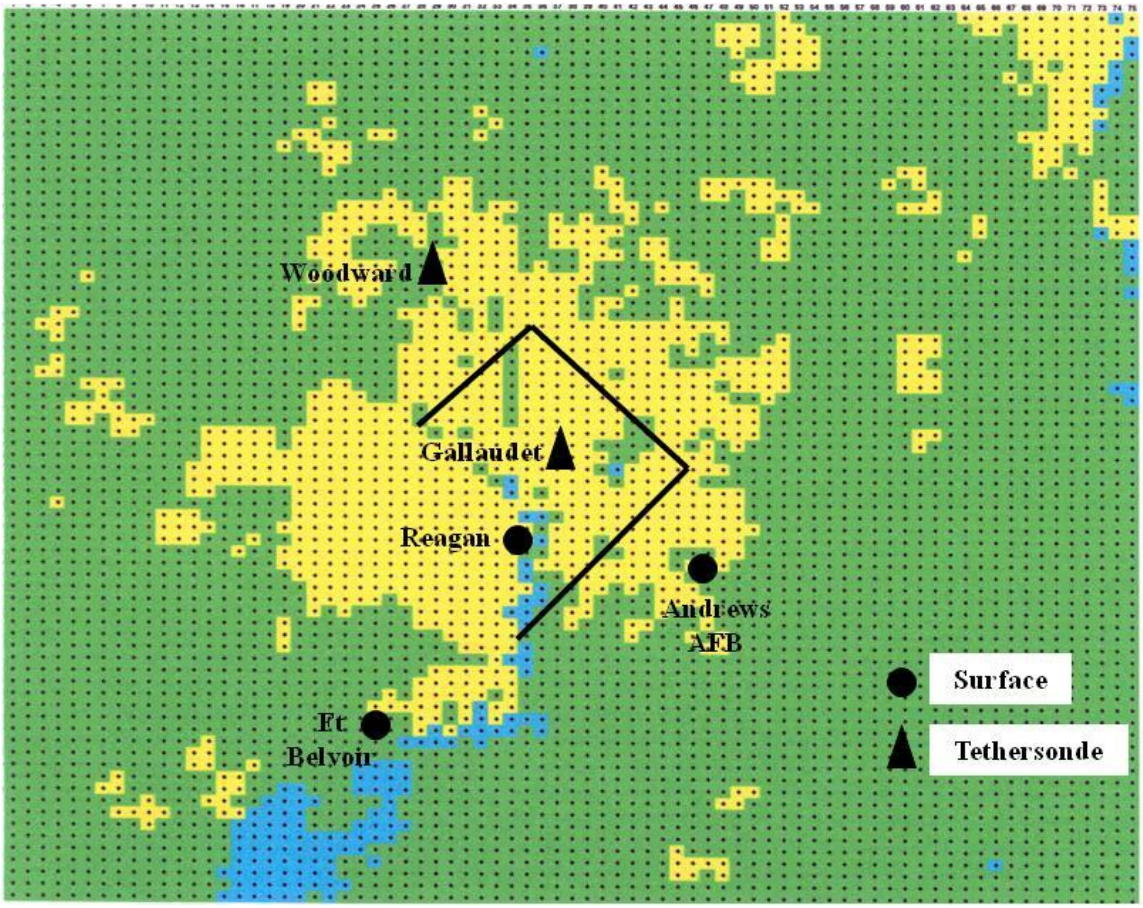

Fig 15: Map of Washington DC show names, types, and locations of available meteorological data against a backdrop of 1km land surface data with yellow as urban, green as vegetation, and blue as water.

Observational studies of UHI's often compare surface stations located within the urban area with those located in nearby rural station to gauge the intensity and behavior of the heat island. For example, DeMarrais (1975) used a comparison between Reagan and Dulles airports to characterize the heat island of Washington DC. This study will also use Dulles to represent a 'rural' measurement against which to compare other measurements made in and around the District. It should be noted that the elevation difference between Dulles and Reagan is approximately 90 m. Using a standard atmosphere, one would expect a difference of 0.5-1.0 °C in surface temperature just due to elevation. The data presented in the study were not corrected for this; however, this fact was taken into account for the analysis of results.

3. Model Set-Up

One of the primary goals of this study is to examine the operational viability of an urban parameterization. As a result, the set up of the model was designed to mimic what an operational center might run. Table 2 in Chapter 1 contains the specifics of how RAMS was configured for the simulations. The set-up included three nested grids centered on Washington DC. Figure 1 from Chapter 1 shows the layout of the three grids. Note that the inner nest is running at a grid spacing of 5 km, typical of Air Force operational settings, yet much coarser than typically used for an urban study. To maximize the value of the 30 m land surface dataset, the LEAF-2 model was set up to run four land surface patches for each RAMS grid cell. One cell is reserved for any water content and the other three cells represent the three most common non-water land surface types found in that grid cell. If there are more than 3 types in a particular cell, the

relative weights of the 3 most prevalent are adjusted to sum to 100%. The output of LEAF-2 is simply the area weighted average of the four surface types. There is only one surface type assigned to 'urban' in LEAF-2. Two simulations were performed for each day, one with TEB active and one with all surface fluxes calculated by LEAF-2. Each simulation was initialized at 12 UTC (early morning in Washington DC) on the day of interest and run through the following afternoon, 36 hours in all. Output was captured every hour on 26-27 June and 7-8 November, and every half hour on 7-8 January. All three simulation days were initialized using data from the NCEP Re-analysis fields (Kalnay et al. 1996), and utilized climatological Sea Surface Temperatures (SST) from the standard RAMS SST files.

4. Results:

a. 26-27 June 1984

1) GENERAL OBSERVED CONDITIONS

The large scale synoptic condition aloft featured a long wave trough centered over eastern Canada with a short wave ridge building into New England and the Mid Atlantic states. At the surface, high pressure was centered over the Mid-Atlantic States on the morning of 26 June and moved off shore over the next 24-hours. Sensible weather in the Washington DC area featured mostly clear skies throughout the period with a high temperature in the low 20's °C. Overnight temperatures varied more as discussed in later in the section. Winds in the DC area were out of the NW around 5-6 m s^{-1} for the morning of the 26th, but swung to SSW during the afternoon, evening and overnight slackening to 2.5-5 m s^{-1} as the high moved overhead and then to the east. The 27th

featured highs in lower 30's °C with stronger SSW winds of 5-6 m s^{-1} for locations both within and outside of the city.

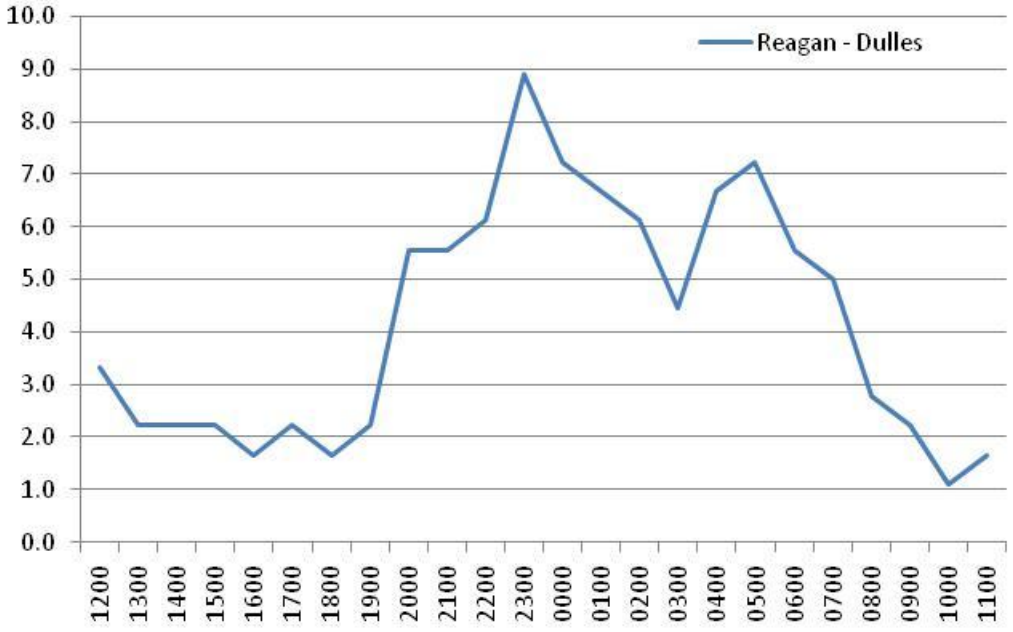

Fig 16: Plot of the temperature difference (in °C) of Reagan – Dulles from 1200 LT 26 June to 1100 LT 27 June.

Figure 16 shows the temperature difference between Reagan and Dulles for 24-hrs starting at 1200 LT on the 26th. The graph shows a weak UHI of around 2 °C through the daylight hours with a much stronger nighttime response approaching 9 °C at 2300 LT. The values then vary through the night and quickly diminish as the sun rises the following morning. During the middle of the night (2200-0200 LT), surface observations were available for five sites around the city. The differences between these five sites and Dulles are plotted in Fig 17. They show a strong UHI near the urban center (Reagan/Gallaudet) at times greater than 10 °C falling off to 4-5 °C near the Beltway (Woodward High School to the NW and Andrews AFB to the SE) dropping to 2-3 °C further south at Ft. Belvoir. Interestingly, all locations peak at 2300 LT.

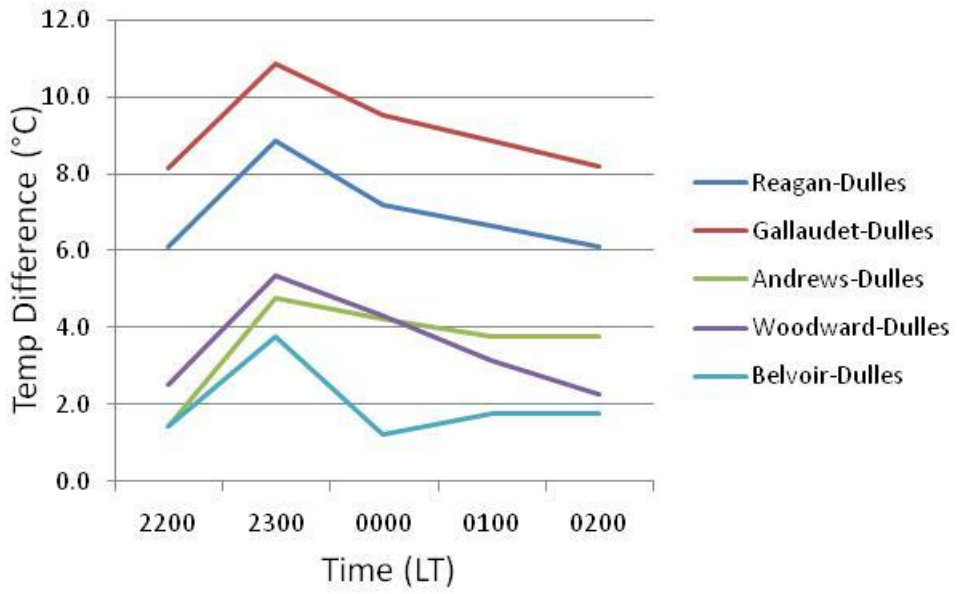

Fig 17: Plot of the temperature difference (in °C) between five sites with Dulles during the night of 26-27 June.

On this night, the two tethersonde locations operated from 2200L to 0200L capturing vertical temperature profiles every hour with data missing from some hours at each site. Figure 18 shows the observed vertical temperature profiles from the two tethersonde sites at 2200 and 0100 LT, two times in which complete sets were available for both locations. The vertical profiles at Gallaudet inside the heart of the UHI show warmer air near the ground (positive lapse rate) becoming near zero as the night progresses. The Woodward site shows a weak inversion (negative lapse rate) becoming stronger with time. The behavior at Woodward is slightly surprising given that temperature data suggests a healthy 4-5 °C UHI at the surface. However, even today the NW sector of the Washington, DC area is not the most urbanized sector of the city and it is possible that although there is a measureable UHI response when compared to Dulles, the local near surface conditions still permitted cooling (just not as quickly as out at Dulles), thus allowing the development of an inversion. Regardless, the ability to properly characterize the environmental lapse rate is important because of implications it has

towards local stability, which is an important driver in applications like air pollution and dispersion.

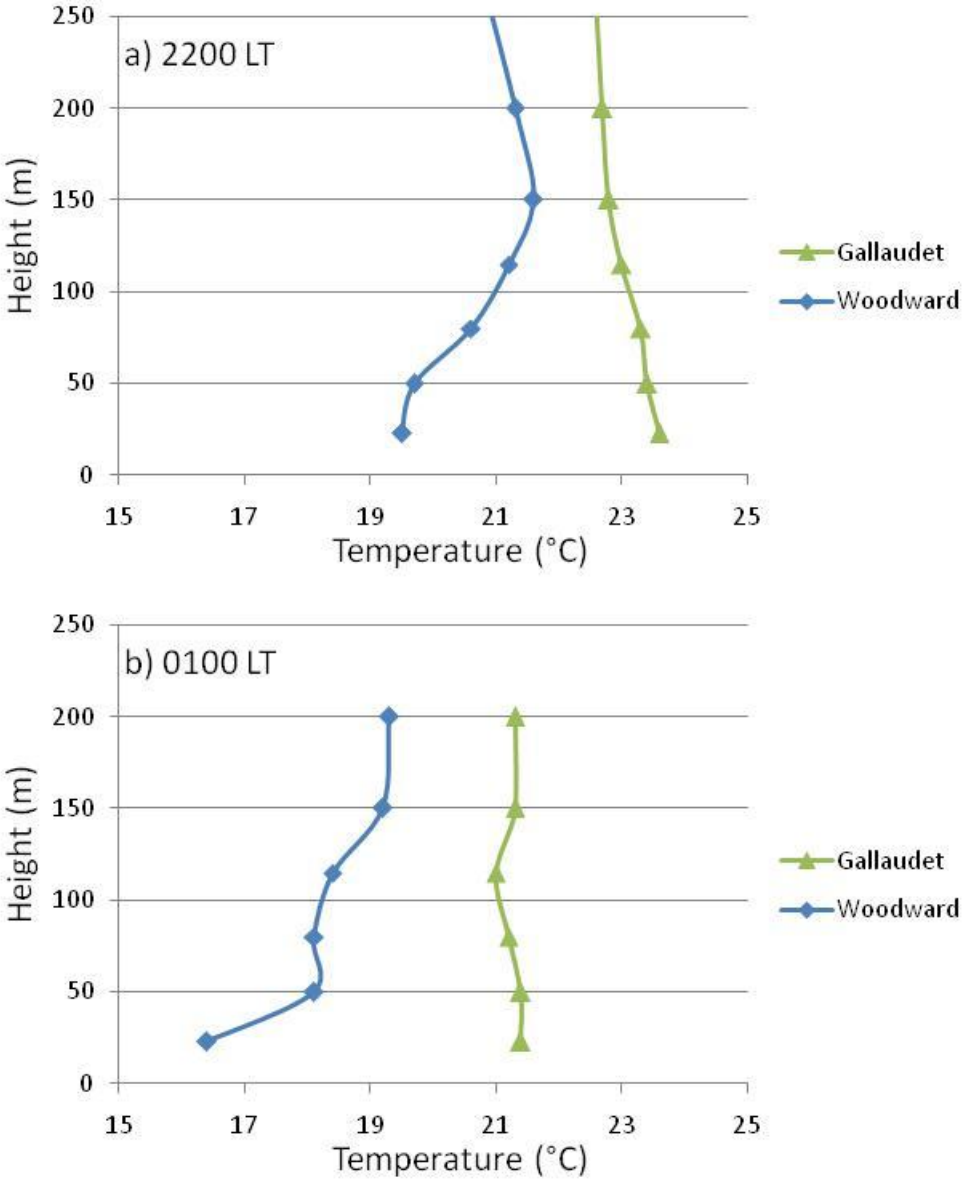

Fig 18: Plot of the observed temperature profiles for each tethersonde site at a) 2200 LT and b) 0100 LT

2) COMPARISON OF NEAR SURFACE OBSERVATIONS WITH MODEL DATA

Figure 19 is a plot of the maximum modeled UHI response (2300 LT), along with the observed data locations indicated. Given expectations from Figs 16-17, the modeled position of the UHI seems reasonable and the time of the maximum was correct, but the

strength is significantly underestimated. The model difference between Reagan and Dulles in the TEB vs. no-TEB simulations maximizes at only 2.3 °C while differences between Gallaudet and Dulles maximizes at 2.6 °C. By the time you reach the beltway, UHI intensity is below 2 °C.

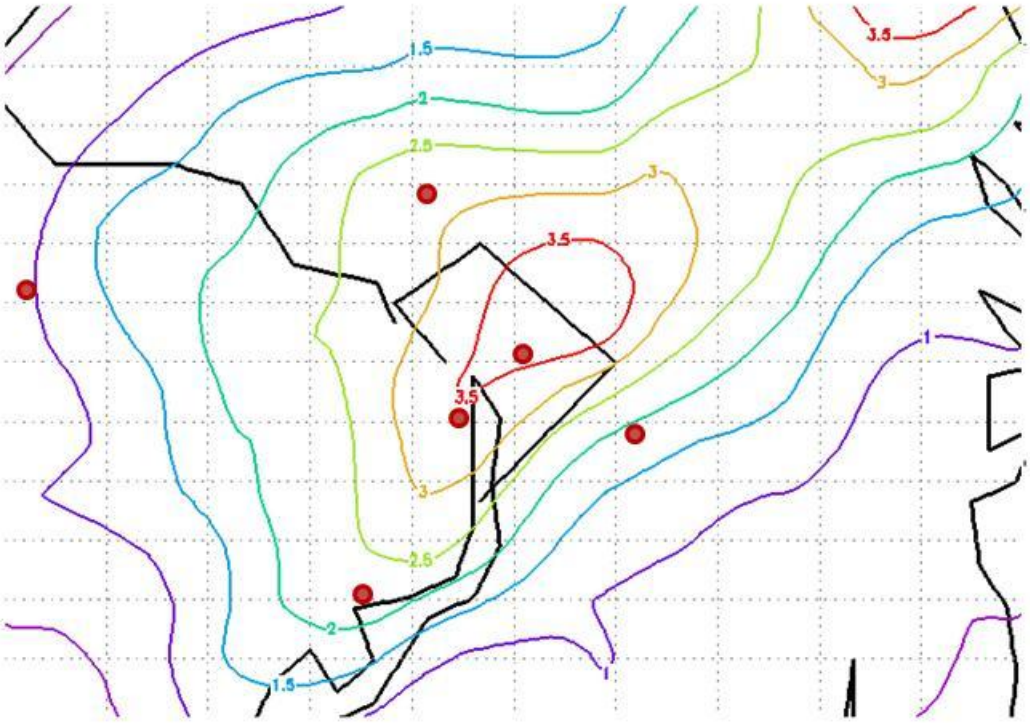

Fig 19: Plot of near surface temperature difference TEB – no-TEB simulation for 2300 LT 26 June with key observation locations indicated.

Figure 20 shows the plot of hourly temperatures observed at Reagan Intl, Dulles, and Andrews AFB with model data from both TEB and non-TEB runs plotted as well. First, starting with Reagan, there is difference between the TEB and no-TEB simulation at night in the city (Reagan), where the TEB run clearly represents the observations better over the time period; however, the startling agreement becomes happenstance when the data from Dulles and Andrews are examined. Looking at these locations it is clear that

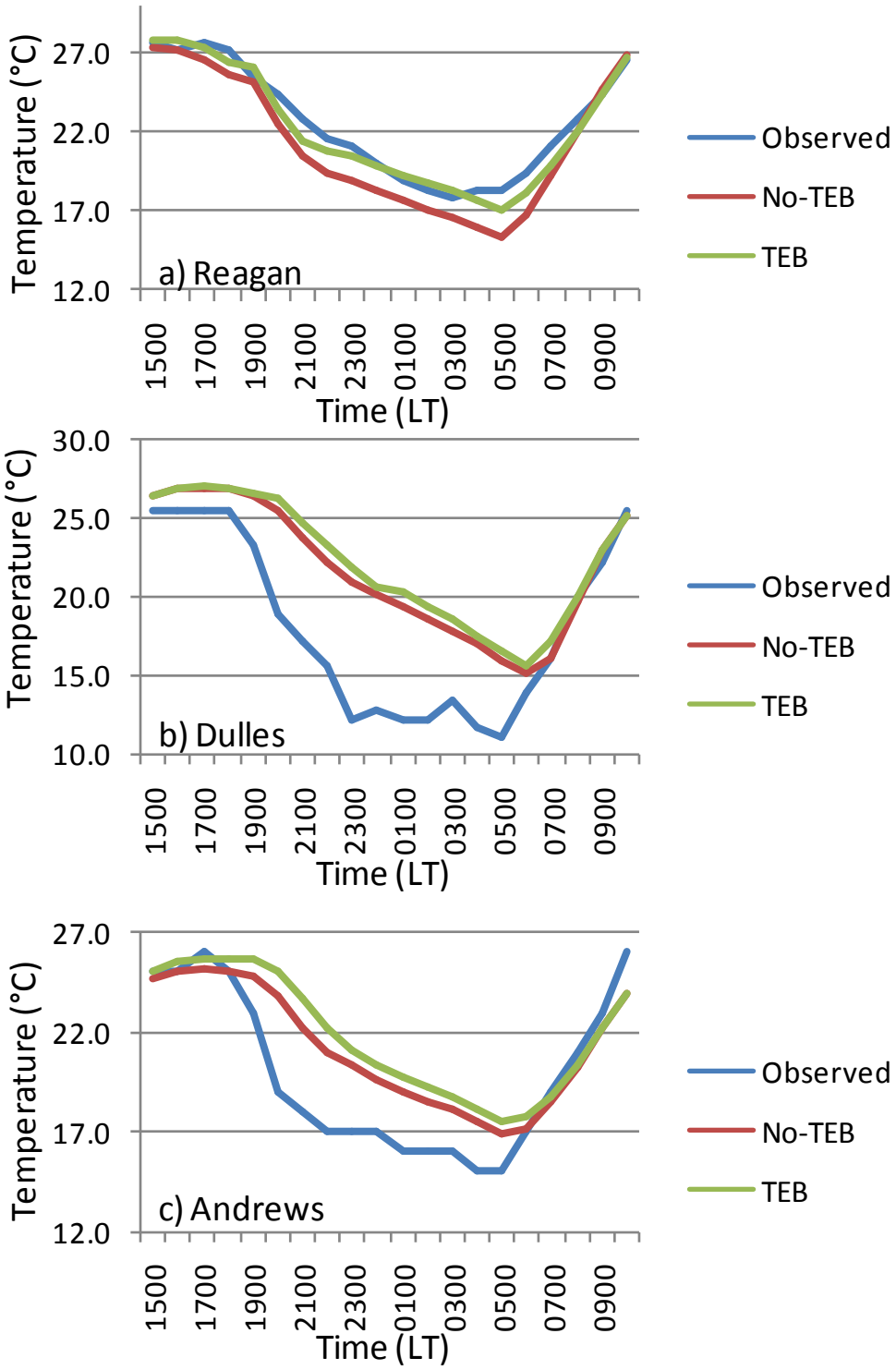

Fig 20: Plots of comparisons of near surface temperatures observed, No-TEB, and TEB for a) Reagan, b)Dulles, and c) Andrews for the night of 26-27 June.

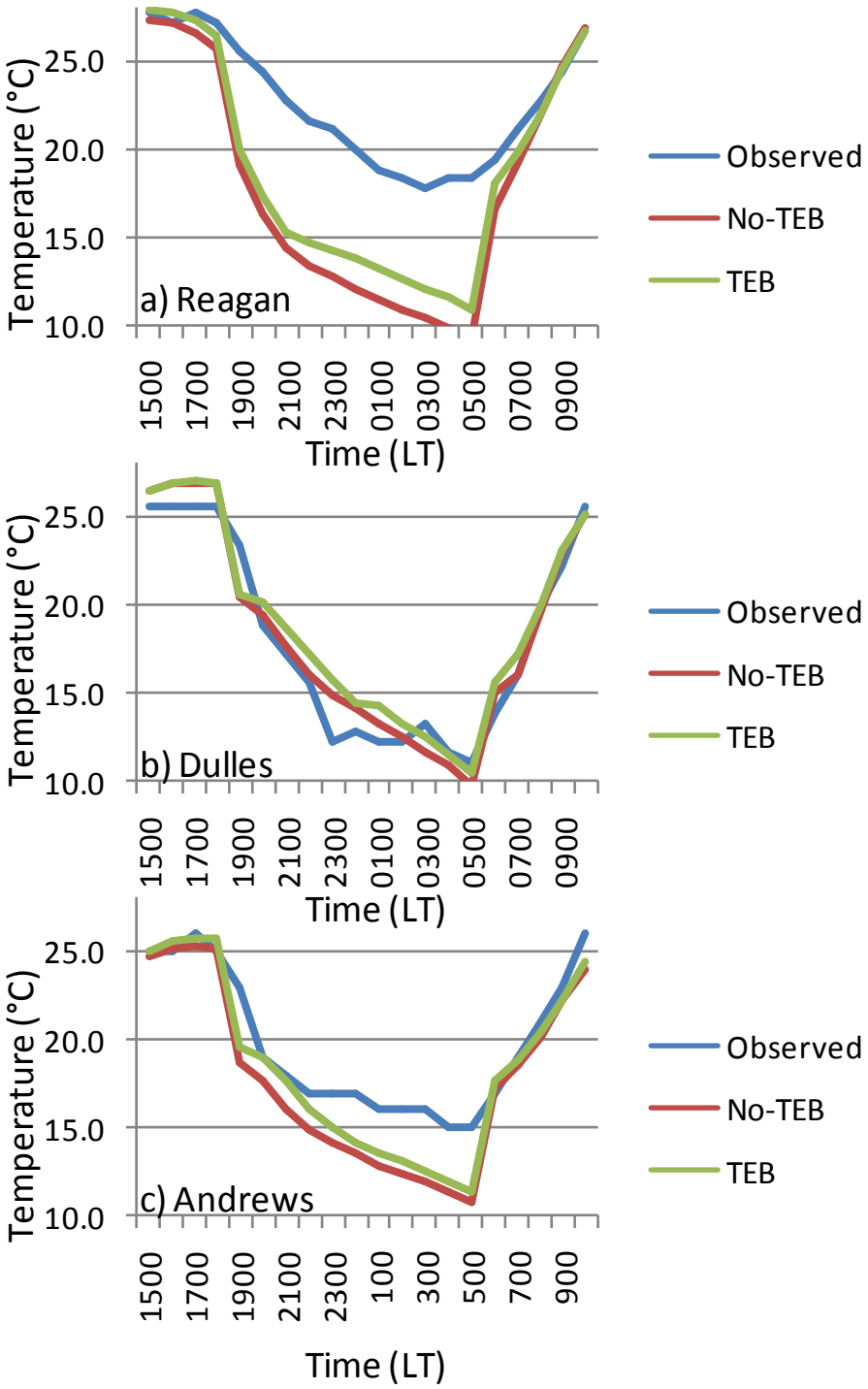

Fig 21: Plots of comparisons of near surface temperatures observed, No-TEB, and TEB for a) Reagan, b)Dulles, and c) Andrews with a Dulles bias correction applied for the night of 26-27 June.

the model has a significant rural nighttime warm bias that has nothing to do with the presence of TEB since it is in both simulations. Figure 21 shows the same plots as figure

20 but with an average bias correction of 6.1 °C applied to the nighttime data (this being the average Dulles bias). This approach is simplistic at best, but it does allow a better examination of the overnight TEB/No-TEB relationship without the excess rural warmth. Removing the bias reduces the agreement at Reagan and accentuates how significantly under forecast the UHI intensity is. However, the TEB simulation does push the temperature nearly 2 °C closer on average to the correct temperature. At Andrews again, in the absence of the bias the TEB simulation would offer a small but positive improvement of the temperature forecast. While the improvement is there, the lack of UHI strength is what stands out in these plots. It is postulated that the lack of UHI strength is a result of the model resolution both horizontal and vertical. For example, TEB was also allowed to run on the 20 km nest and while it did function properly, it produced a UHI response more than 1 °C weaker than the 5 km nest. Ideally, higher resolution runs would be needed to confirm this.

In summary, comparison of the model simulations with observed surface data produced mixed results. On the negative side, the TEB simulation significantly under estimated the strength of the UHI. Additionally, both the TEB and no-TEB simulations had a significant nighttime warm bias. On the positive side, both the shape and timing of the UHI matched well against the observations, and in the absence of the warm bias, the presence of TEB has appeared to improve the overall nighttime surface temperature forecasts at both Reagan and Andrews without degrading the performance at Dulles. Further, as the analysis in Chapter 1 showed, even this UHI was able to generate a UHIC and alter the PBL evolution over the city thus interacting with the mesoscale environment in ways that one would desire.

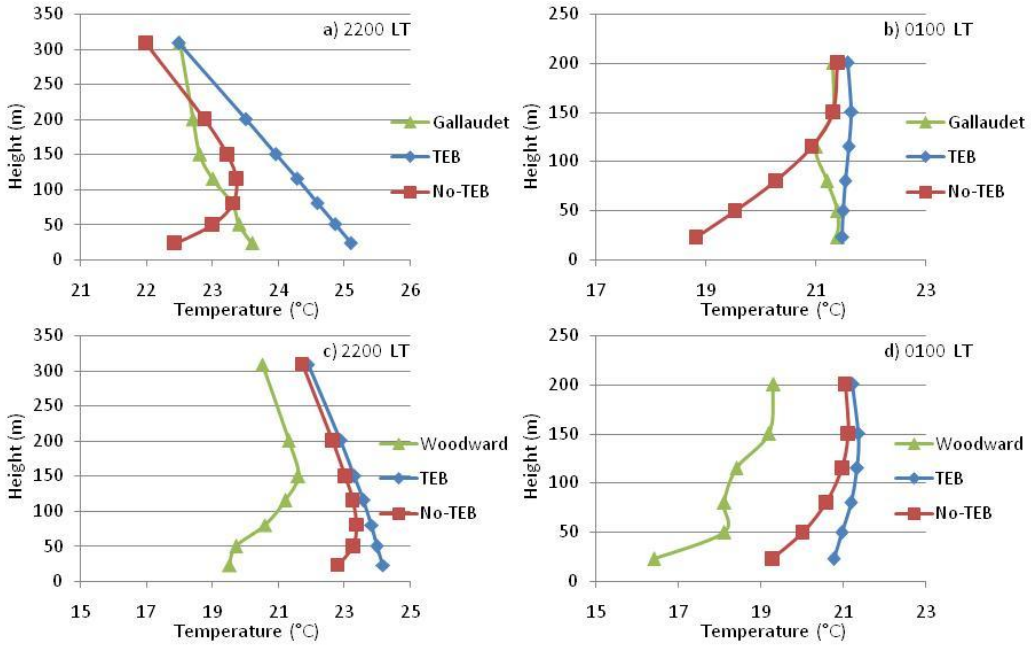

Fig 22: Plots of vertical temperature profiles from observed, No-TEB, and TEB for a) Gallaudet at 2200 LT, b) Gallaudet at 0100 LT c) Woodward at 2200 LT, and d) Woodward at 0100 LT

3) COMPARISONS OF OBSERVATIONS IN THE VERTICAL WITH MODEL DATA

Figure 22 shows the observed, TEB and no-TEB vertical profiles at 2200 and 0100 LT for the Gallaudet and Woodward sites. Starting with Gallaudet, the TEB simulation clearly has a much better vertical profile showing at both 2200 and 0200 LT in line with the observations. On the other hand, the no-TEB simulation produces an inversion in the lowest levels. This difference in ability to simulate the environmental lapse rate is likely very important to many applications that use weather data as input (such as dispersion models). Looking at Woodward, one of the first things we see is again evidence of a warm bias in the model results. Looking beyond that, we can see that in this case the no-TEB model had a more faithful representation of the lower level profile. It is possible that due to 5 km grid cells, the land surface data set over estimated the urban percentage in this segment of the city and thus modeled too much surface flux. One would expect

locations along the gradient between urban and rural to be the most susceptible to issues arising from a lack of fine scale resolution.

4) SUMMARY

During the 26-27 June timeframe under clear skies and building SSW flow, observational evidence suggests that the Washington DC area experienced a strong nighttime UHI reaching a maximum in excess of 10 °C prior to midnight. This UHI provided enough heating support to prevent the core of the city from developing a near surface temperature inversion inside the beltway even well after midnight. In terms of the model simulations, there was a strong nighttime warm bias seen in both TEB and no-TEB simulations which clouded the results a bit. However, overall, in the absence of the bias, the model simulation using the urban parameterization improved the performance of the temperature forecast. The model produced a UHI shape that matched observations well and maximized the intensity at the right time. However, the strength was at best only about 1/3rd of the observed UHI. The TEB simulation did succeed in modeling the correct environmental lapse rate over the heart of the city, but carried this influence too far to the NW. The most likely cause of both the lack of strength of the UHI and the warm lapse rate to the NW is the relatively coarse resolution of the simulation in both the horizontal and vertical. Still, while the overall improvements were at times small, TEB demonstrated that it could add value to the sensible weather forecast in the city. Additionally, the behavior over the core of the city was likely significant enough to be of importance to follow-on applications like air pollution or dispersion modeling efforts.

b.7-8 November, 1984

1) GENERAL OBSERVED CONDITIONS

A large, strong high pressure system built in and dominated the entire eastern seaboard bringing fantastic late fall weather to the entire eastern third of the US. Conditions in the Washington DC area featured scattered to clear skies with highs on both the 7th and 8th in the 10-12 °C range throughout the area. The nighttime temperatures in the area varied significantly from well below freezing in the rural areas to above freezing in the city. Winds during the day on the 7th were brisk NNW to NNE at 5-7 m s^{-1} sustained throughout the area. Overnight, winds in the city stayed at 2.5-5 m s^{-1} while winds in the rural areas near Dulles and Ft. Belvoir eventually went calm or nearly calm.

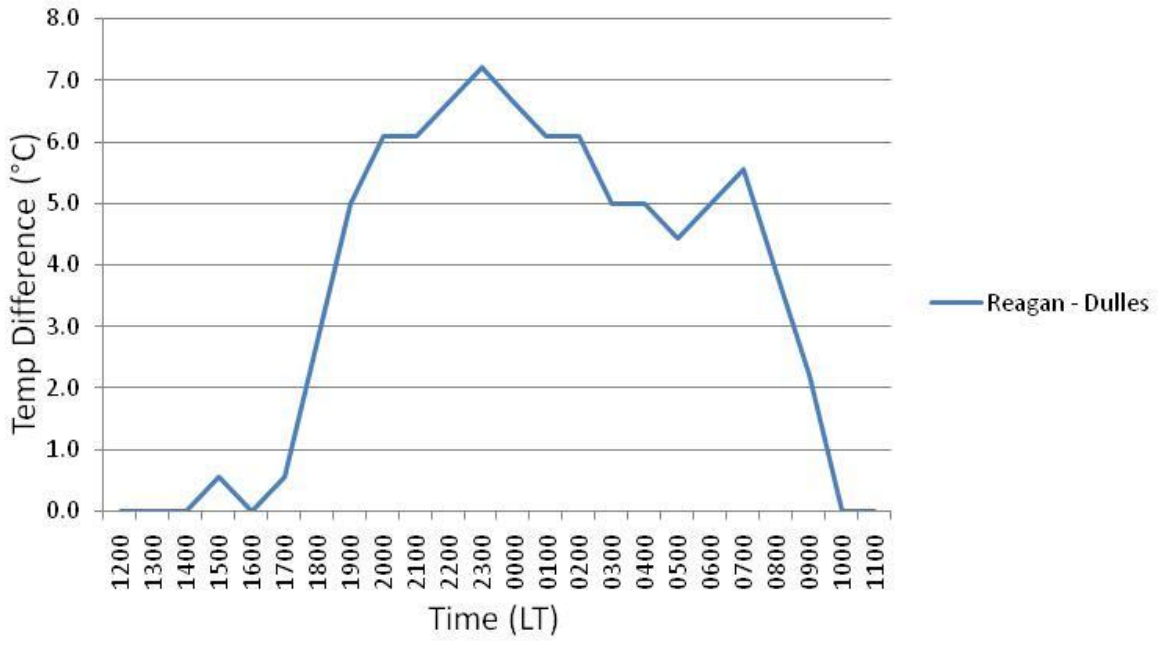

Fig 23: Plot of the temperature difference (in °C) of Reagan – Dulles from 1200 LT 7 November to 1100 LT 8 November 1984.

Figure 23 shows the plot of observed temperature difference between Reagan and Dulles. This time we see no evidence of any daytime heat island but there is another

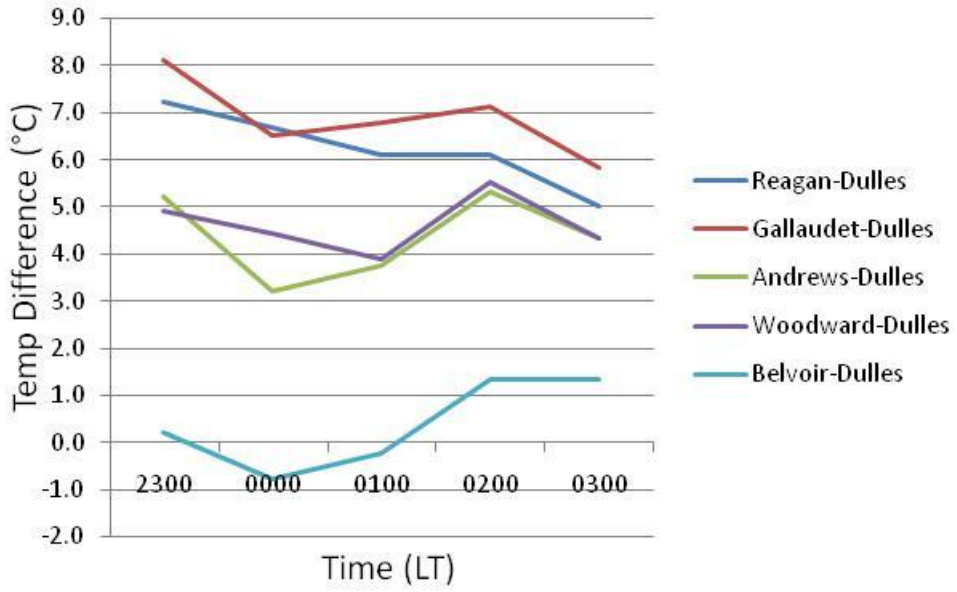

Fig 24: Plot of the temperature difference (in °C) between five sites with Dulles during the night of 7-8 November, 1984

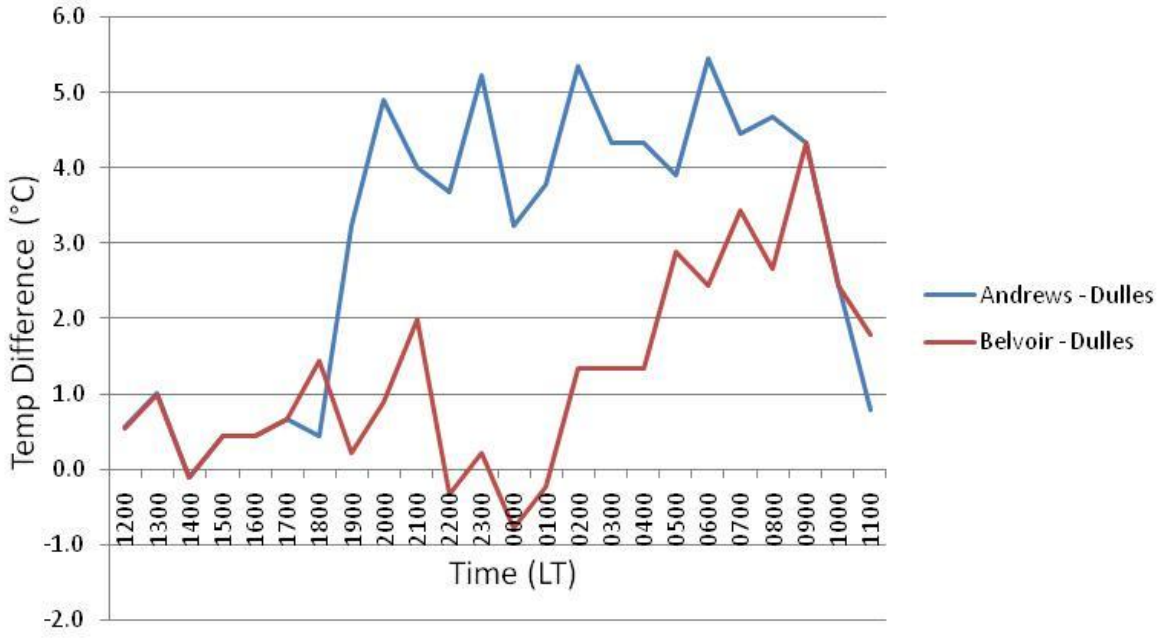

Fig 25: Plot of the temperature difference (in °C) between Andrews with Dulles and Belvoir with Dulles from 1200L 7 November to 1100L 8 November, 1984.

intense nighttime UHI maximizing once again around 2300 LT at > 7 °C. This UHI is slightly less intense than the 26-27 June case. Figure 24 shows the difference plots for the five stations available between 2300-0300 LT. Again the strongest response is in the Gallaudet area. It is also interesting to note that there is again some sense of symmetry in

the evolution of the heat island between the NW and SE portion of the beltway at this time in spite of a totally different wind direction and stronger speed.

Figure 25 shows the difference plot between Belvoir and Andrews with Dulles. Comparing Fig 25 with Fig 23, we see that the Reagan UHI peaks then slowly falls until a brief resurge prior to dawn, the UHI at Andrews remains more or less constant once it peaks, and the UHI at Ft Belvoir is non-existent for most of the night and then suddenly surges. This suggests the possibility that while the UHI was being forced over the center of the city, the effects were being advected east and south during the night by the NW winds.

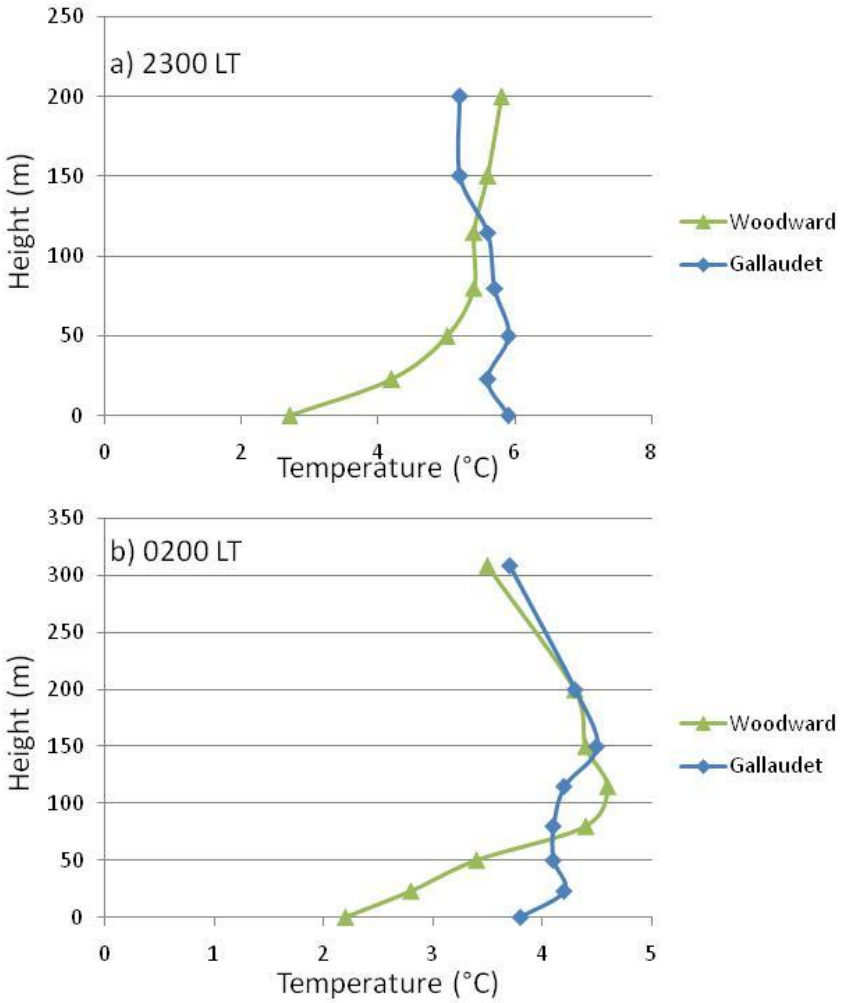

Fig 26: Plot of the observed temperature profiles for each tethersonde site at a) 2300 LT and b) 0200 LT.

Figure 26 shows the observed tethersonde profiles at 2300 and 0300 LT where like the 26-27 June case we see a near neutral profile at Gallaudet with an increasingly stable profile at Woodward.

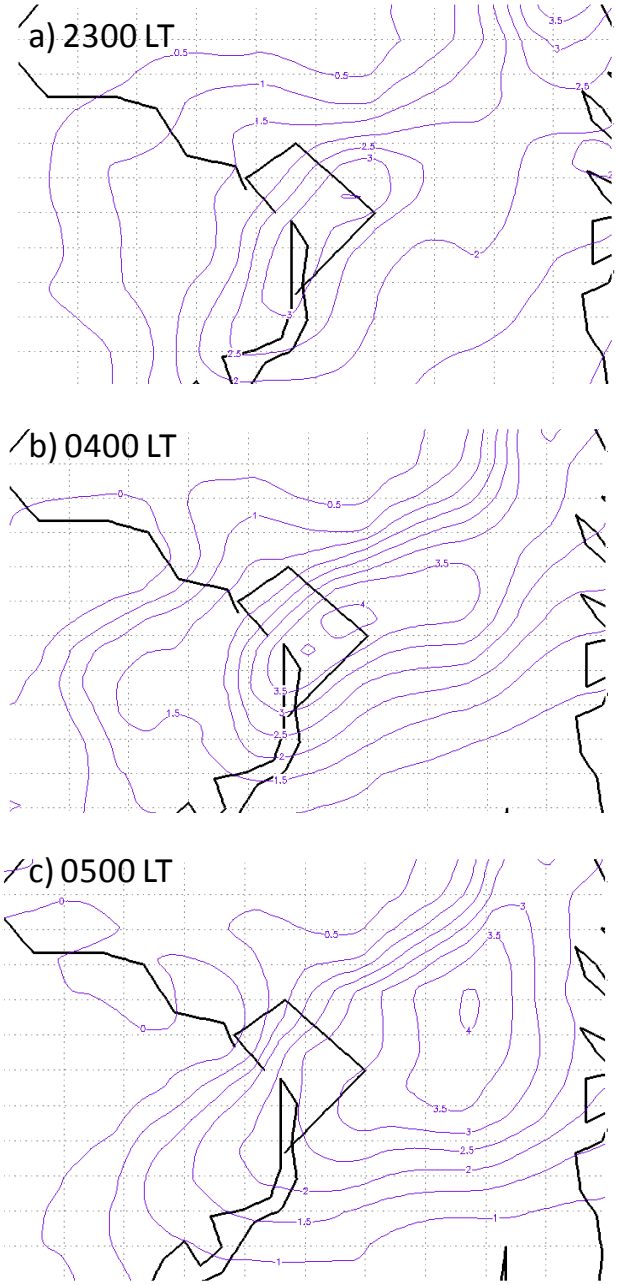

Fig 27: Plot of the TEB minus No-TEB near surface temperatures at a) 2300L, b) 0400L, and c) 0500L

2) COMPARISON OF NEAR SURFACE OBSERVATIONS WITH MODEL DATA

Figure 27 shows the 2300, 0400, and 0500 LT difference between the TEB and no-TEB simulation. In the 2300 LT image we see the strongest part of the UHI dominates the eastern half of the beltway area at >3 °C. This pattern (with some strength variation) is largely maintained up through 0400 LT pictured next. Comparing Woodward surface temperature with Andrews from Fig 24 suggests that the UHI may have been a bit more symmetrical than the model has. Additionally, looking at the UHI pattern to the south of the city suggests the model had a measurable UHI present in the Belvoir area by 2300 LT and decreases the intensity between then and 0400 LT which is not supported by the data (Fig 25). Finally, after 0400 LT, the UHI over the city quickly collapses and the UHI pattern moves away from the city to the ESE moving out over eastern Maryland. Examination of the model flux fields (not shown) revealed that by 0400 LT the positive sensible heat fluxes in the TEB run had dried up, thus the UHI lost its sustainment and the winds then apparently advected the residual pattern off the city. The observed data do not support the early morning collapse of the UHI over the city; however, the model's move to suddenly advect a UHI pattern is intriguing when compared against the sudden appearance of a UHI signature at about this time in the observed data at Ft Belvoir. However, even if the model is hinting at something, it pushed things more eastward than southward, so rather than increasing UHI strength at Belvoir, it eliminates it. In short, as seen with the 26-27 June case, the model fails to capture the peak strength of the central UHI, but once again the model does time the maximum UHI well until about 0400 LT after which the simulation gets quite questionable.

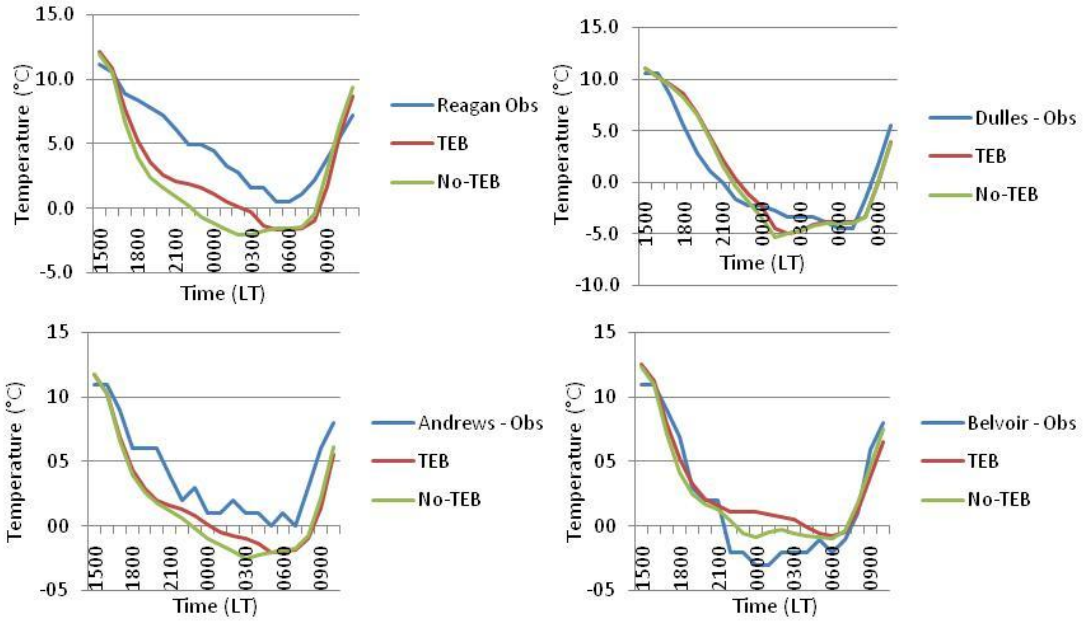

Fig 28: Plot of observed, TEB and No-TEB temperatures at Reagan, Dulles, and Andrews 7-8 Nov 1984.

Figure 28 shows the comparison of hourly temperature at Reagan, Dulles, Andrews, and Belvoir. At Reagan in the heart of the night we see both the TEB and no-TEB run are too cold, but the TEB run is closer to the observations for most of the night until the collapse of the UHI. Also note that the UHI intensity in the TEB simulation is nearly half of the observed, an improvement over 26-27 June. The same basic story exists at Andrews as well. Further, examining Dulles, we do not find the significant bias seen in the simulation of the 26-27 June, so the results prior to 0500 LT are fairly straightforward to interpret. However, at Belvoir we see that the model never catches on to what was happening. In fact the response of the model is the exact opposite of what actually occurs.

In summary, the overall behavior of the near surface temperature is similar to the 26-27 June case where the TEB simulation captured many of the basic features, but under simulated the strength of the UHI. TEB was further able to reduce the error of the temperature forecast prior to 0500 LT. However, in this case, the TEB simulation

seemed to 'run out of gas' in the early morning hours causing a collapse of the UHI over the city, a fact not supported by the surface observations. It is possible that the lower daytime incoming radiation did not allow TEB to store enough energy for nighttime release. Additionally, the model clearly struggled with validation to the south of the city as evidence by the performance at Belvoir.

3) COMPARISONS OF OBSERVATIONS IN THE VERTICAL WITH MODEL DATA

Figure 29 shows the vertical profiles of the TEB, no-TEB, and observation for both tethersonde locations at 2300 LT and 0300 LT. As we saw with the near surface temperatures, both simulations are much too cold but the TEB simulation again reduces the error. In addition the TEB simulation does attempt to produce a better vertical profile but does not have quite the good agreement seen in the 26-27 June case.

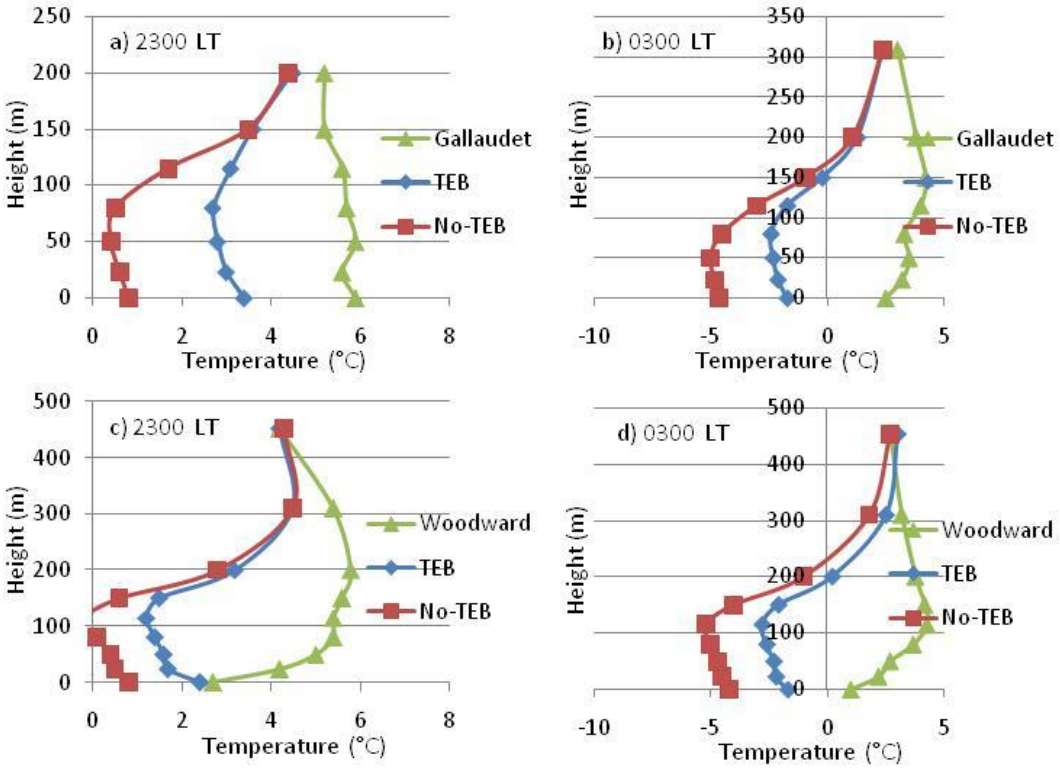

Fig 29: Plots of vertical temperature profiles from observed, TEB, and No-TEB for a) Gallaudet at 2300 LT, b) Gallaudet at 0300 LT c) Woodward at 2300 LT, and d) Woodward at 0300 LT

4) SUMMARY

In this section we examined the UHI behavior of 7-8 November 1984; a day that featured strong high pressure, clear skies and brisk NW winds. From the observations we saw that the city of Washington, DC experienced a weak daytime, strong nighttime UHI signature as seen in the 26-27 June case. However, there was a significant UHI response seen at Belvoir during the early morning hours that was not seen in the 26-27 June case. In terms of the model behavior, up until 0500 LT 8 November, many aspects of the performance were similar to the 26-27 June case in that it modeled the timing and general coverage well, significantly under estimated the strength but did reduce the forecast error significantly, especially inside the Beltway. However, the model really did struggle to reproduce the evolution of the UHI at Belvoir and the model suddenly experienced a collapse of the UHI at about 0500 LT.

c.7-8 January, 1984

1) GENERAL OBSERVED CONDITIONS

This was the one period selected that was not part of an intensive field campaign day, therefore, no tethersonde data are available; however, the period was selected because it offered an interesting synoptic situation featuring variable cloud cover and a significant wind shift without any precipitation in the Washington DC area. This affords the ability to observe the behavior of the parameterization in a more complex synoptic situation.

The 7th and 8th of January featured a longwave trough aloft centered over the eastern third of the US with energy moving through the flow. At the surface on the morning of

the 7th, high pressure was building in behind a retreating low pressure system. Skies were cloudy with mid-level (c. 8000 ft) ceilings. Thanks to the cloud cover, temperatures throughout the metro area were above freezing although the day likely felt brisk with NW winds gusting at times to more than 11 m s^{-1}. As evening approached, winds started to die down and skies cleared. Overnight lows fell into the teens outside the city. Then in the early morning hours, winds suddenly shifted to a southerly direction in what the National Weather Service charts show as a weak frontal passage associated with a quickly approaching Alberta Clipper system and the cloud cover returned with mid level ceilings around 10,000 ft by dawn. There was no snow on the ground in the Washington, DC area or even south of northern Pennsylvania.

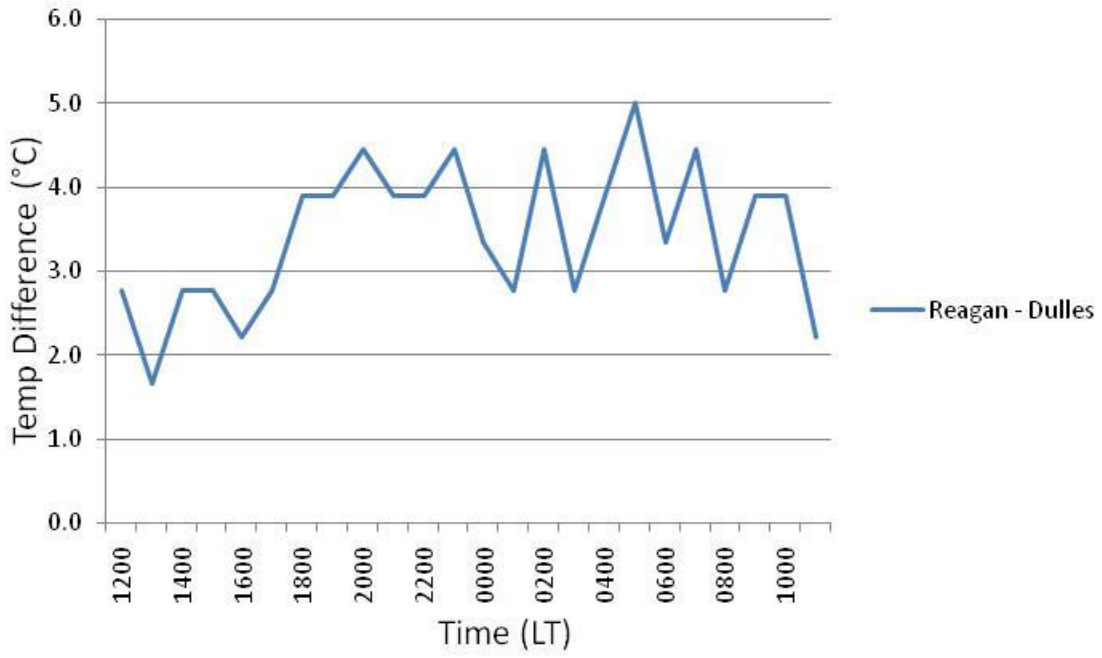

Fig 30: Plot of the temperature difference (in °C) of Reagan – Dulles from 1200 LT 7 January to 1100 LT 8 January 1984.

Figure 30 shows the plot of Reagan – Dulles temperature series. We see a very different plot from the other two periods analyzed previously. Here we see a weak (>2 °C) UHI during the day increase slightly to approximately 4 °C and then vacillate

through the night and next morning between 3-4 °C. This is in stark contrast to the strong nighttime UHI, daytime collapse seen in the previously analyzed periods. Figure 31 shows the differences with Dulles for both Andrews and Belvoir and again we see behavior significantly different than the previous periods. With Andrews we see a very weak afternoon UHI signature followed by a weak to moderate response (2 -3 °C) through the night and into the following morning. This response is qualitatively similar to Reagan, but weaker in magnitude. Belvoir offers something different. Here we see a moderate (c. 3 °C) afternoon UHI response which lingers through the evening hours and then abruptly vanishes shortly after midnight (nearly opposite of the 7-8 November response). The timing of the collapse accompanies the general collapse in moderate NW winds followed by building southerly winds suggesting that the UHI response was an advection of the UHI signature from the urban concentration to the north of Belvoir.

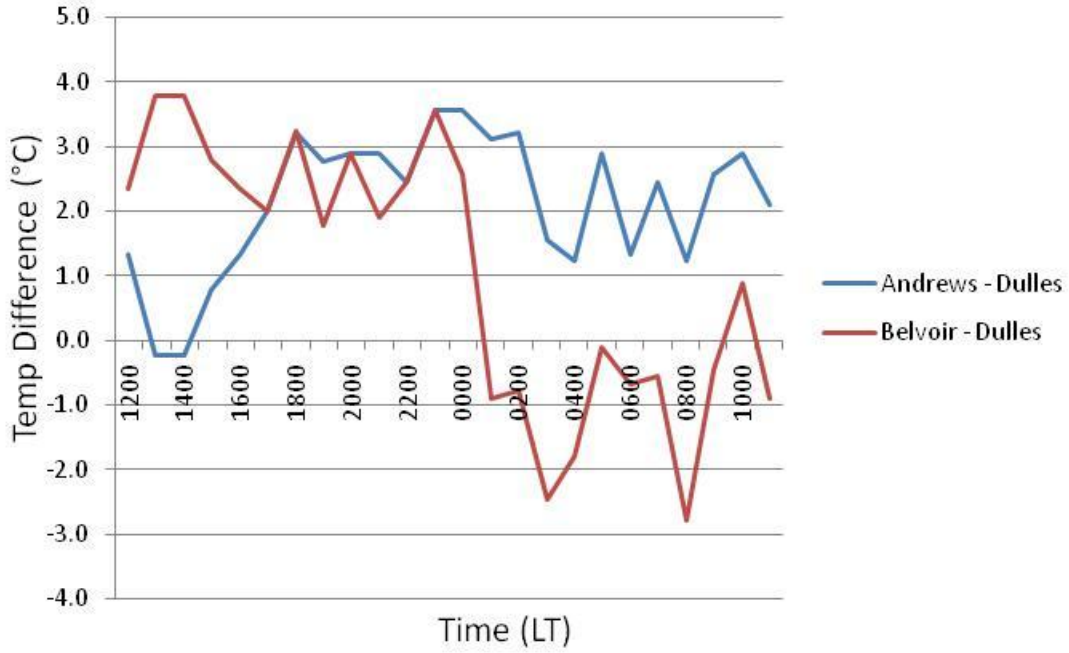

Fig 31: Plot of the temperature difference (in °C) of Andrews – Dulles and Belvoir – Dulles from 1200 LT 7 January to 1100 LT 8 January 1984.

2) COMPARISON OF NEAR SURFACE OBSERVATIONS WITH MODEL DATA

The differences between the TEB and no-TEB runs were examined over the simulation period. TEB only developed a very weak (< .5 °C) UHI during the day. Figure 32a shows a representative image from 1400 LT. The model then begins to develop a more significant UHI (albeit weak) around 1800 LT with a strength of slightly over 1 °C. Figure 32b from 2200 LT shows an image representative of this time period. As we saw in the 26-27 June case, the model intensity is only about 1/3rd of the observed. One somewhat encouraging thing is the shape of the UHI suggests the model carries the warm

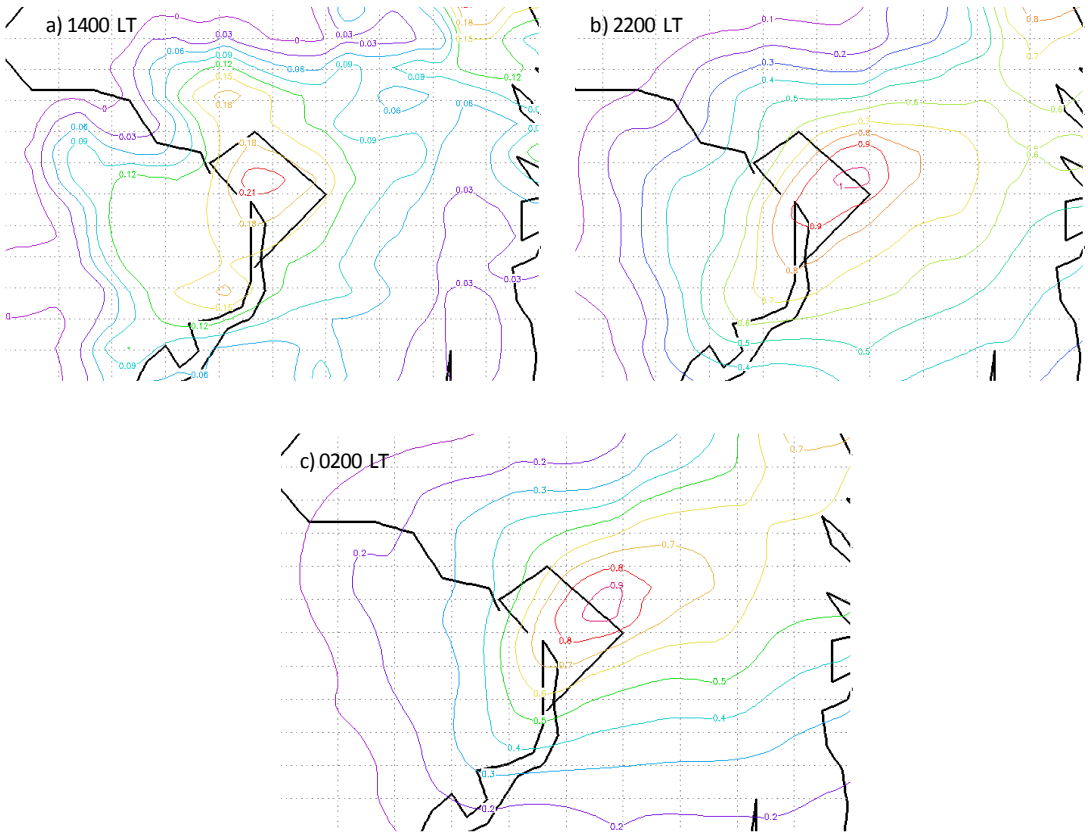

Fig 32: Plot of the temperature difference TEB – No TEB for a) 1400 LT, b) 2200 LT, and c) 0200 LT on 7-8 January, 1984.

well south of the urban area as suggested in the Belvoir observations. The basic intensity stays the same through the night at around 1 °C. As the winds in the model swing to the south after midnight, the model does begin to relax the UHI south of the city decreasing the intensity in the area of Belvoir by about half (Compare figure 32b from 2200 LT with figure 32c from 0200 LT). However, the model does it gradually, not as an abrupt collapse in the UHI as the data suggest. Overall the results are disappointing. The observed daytime UHI is not developed; the nighttime response is again too weak; and the UHI fails to respond in a sudden fashion as the winds switch direction. Still TEB does appear to at least attempt to move things in the correct direction.

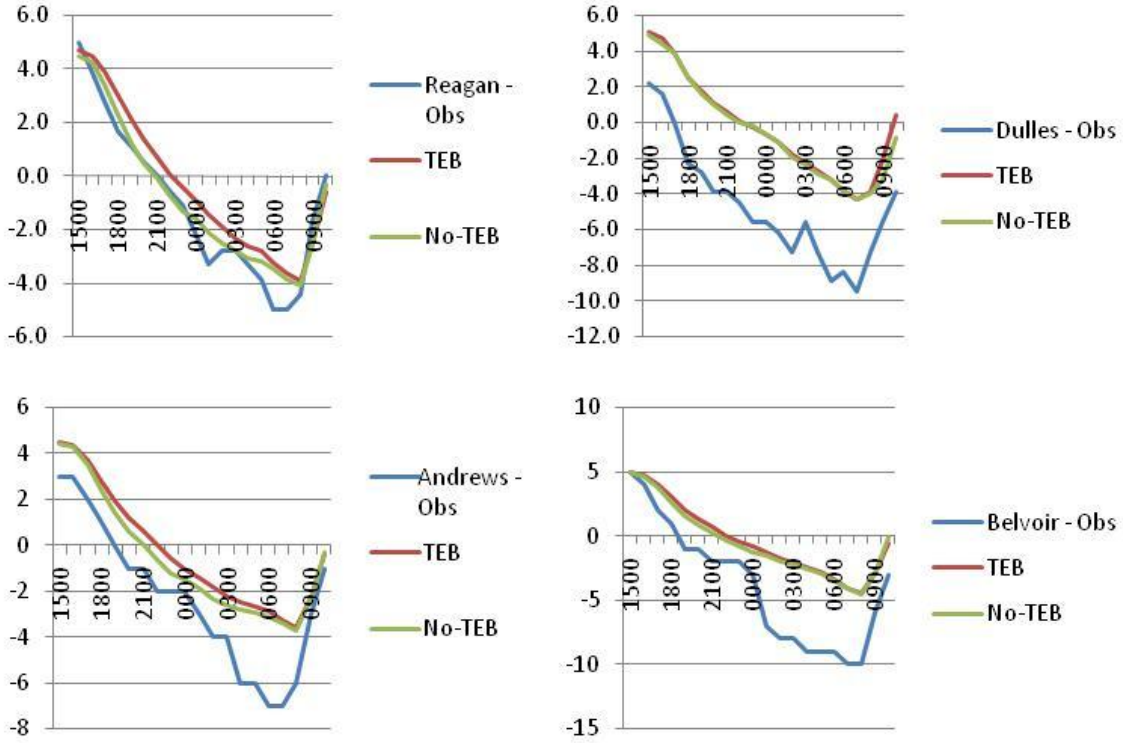

Fig 33: Plot of the temperature series of observed, TEB, and No-TEB values for 4 locations 7-8 June, 1984.

Figure 33 shows the comparisons with the surface plots. First, like 26-27 June, there is a significant rural warm bias. Removing that bias would once again drop temperatures from the models at Reagan, Andrews, and Belvoir well below the observed. The plots

confirm the discussed lack of UHI response from the TEB simulation. The TEB simulation does reduce the bias corrected temperature forecast error, but the improvement is clearly less than in either of the two previous simulations. Also, the TEB simulation does maintain a basically steady nighttime UHI at both Reagan and Andrews. Also it does eventually eliminate the UHI at Belvoir, but the model also eliminates the UHI in the morning at both Reagan and Andrews in disagreement with the observations. It is not entirely obvious why the observed UHI persisted into the morning when in the other days examined it was eliminated at dawn. One possibility could be the fact that mid level clouds built in as the sun was rising. This may have altered the relative heating rates between rural open areas and urban canyon geometry which is typically the reason many locations see a collapse of the UHI in the morning. If this is the reason, then it is all the more interesting since the model simulations did not bring significant cloud cover in on the morning of the 8th and then eliminated the UHI with sunrise. More modeling of UHI behavior with variable cloud cover present should be done to better understand the dynamics of the UHI under this scenario.

3) SUMMARY

The observation data from 7-8th January confirmed that the UHI behavior of the city was significantly different than the other two simulation days with a much less intense UHI that persisted into the day of the 8th. In addition, the UHI at Belvoir, south of the city, quickly eroded once the winds shifted from NW to southerly. The results from the TEB simulation at night were qualitatively similar to the other cases in that TEB generally got the large scale pattern of UHI behavior correct, but significantly under

estimated the intensity. The model failed to carry the UHI into the daytime of the 8th and also gradually faded the UHI out at Belvoir as opposed to modeling a quick collapse. Both simulations also displayed the significant warm bias observed in the 26-27 January case.

5. Conclusions and Recommendations:

This chapter examined the performance of the TEB parameterization against objective data from the Washington DC area for three periods with distinctly different weather in order to evaluate the ability of an urban parameterization to function at the relatively coarse resolution used in operational weather centers. The overall results suggest that the presence of the TEB parameterization did work to reduce the nighttime forecast temperature error in both the horizontal and vertical inside the Beltway of Washington DC. Perhaps most encouragingly, the urban parameterization really improved the model's handling of the near surface environmental lapse rate which would likely have significant impacts in follow-on applications that are sensitive to stability, such as air pollution and dispersion. However, the parameterization consistently under forecasted the intensity of the UHI significantly, likely due to the coarse resolution of the model runs. In addition, TEB struggled with the stability profile at Woodward in the area of transition from significant urbanization and greater rural coverage. This again was likely due to the model's resolution. Finally, the parameterization struggled most in the synoptically complex scenario on 7-8 January, especially when the model failed to sustain the UHI into the 8th, possibly due to the inability of the model to correctly forecast a return of cloud cover on the morning of the 8th. Results from this study are encouraging

enough to recommend a larger effort designed to assess the impact of the parameterization on the root mean square error of forecasted temperature over a longer period (45 days or so) as is done traditionally when assessing changes to operational model configurations. Also, this study highlighted the need for more studies of UHI behavior under a variety of synoptic forcings. Traditionally studies, especially field studies, are generally done in an effort to capture and understand 'golden' days of urban behavior. The documented behavior of Washington, DC on these three days suggests there is a lot to see and learn about UHI behavior in all types of weather situations.

Recommended follow-on efforts would include conducting a higher resolution (1 km horizontal, more vertical levels) simulation of at least one of these days to examine if the lack of UHI strength is a result of coarse resolution. In addition, a more systematic evaluation of TEB should be undertaken to see how the parameterization performs under various levels of synoptic forcing.

APPENDIX A: THE URBAN HEAT ISLAND (UHI) EFFECT AND MOTIVATION FOR CURRENT EFFORT

The purpose of this appendix is to review the basics of the urban energy balance and urban boundary layer theory, provide a description of urban heat island climatology and its interaction with other local flows, discuss the current state of land surface models and the need for urban parameterization, and ultimately, the motivation for the efforts described in this document as a whole.

A.1. UHI Boundary Layer Theory and Climate

A basic review of Planetary Boundary Layer (PBL) theory (e.g. Stull 1988) demonstrates that the structure of the PBL and sensible weather within (temperatures, winds, moisture, and stability) is driven largely by the underlying surface. Different surface types (i.e. water, dirt, evergreen trees, grass or concrete) process the incoming energy differently and thus drive different boundary layer structures producing different sensible weather near the ground. Therefore, it is not surprising that a growing body of literature over the past few decades has demonstrated that urban landscapes have different boundary layer structures than their surrounding landscapes. Because of the noted difference in temperature over the urban area, this effect has commonly become referred to as the Urban Heat Island (UHI). This section will describe urban boundary layer formation from an energy balance perspective, overview basic urban boundary layer

theory, and review observational studies of the UHI in an effort to describe an urban climatology and variation between urban areas.

a. The Urban Energy Balance

Energy balance equations are normally interpreted as if intercepted by a plane surface. However, in an urban area, due to the 3D nature of the urban fabric, it is best to consider the absorbing element as a volume like that depicted in Fig A.1 from Oke (1988) and consider the energy balance at the top of this volume. This volume is referred to as the Urban Canopy Layer (UCL) and contains the buildings, cars, people, vegetation, and water sources such as ponds, rivers, or even a broken water main. All of these elements will influence the energy balance over an urban area, making the urban energy balance an

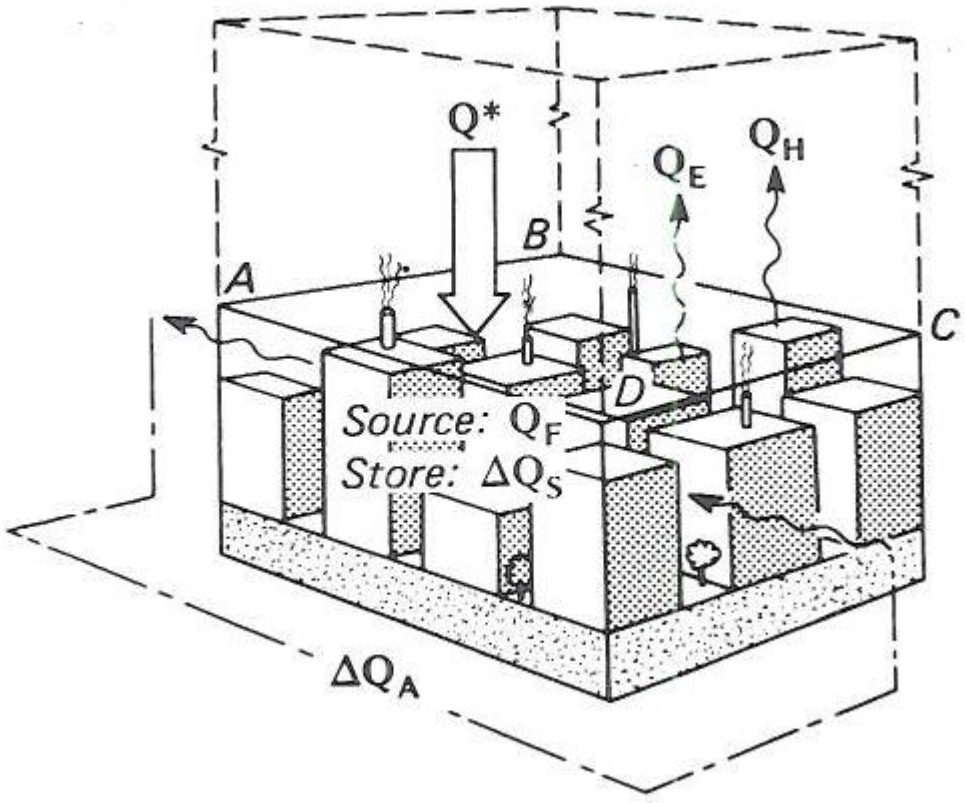

Fig A.1: Surface energy volume (from Oke 1988).

amalgam of a number of different surface types and orientations. This introduces an important caveat to urban energy balance studies; the environment makes traditional energy balance measurements very difficult to obtain. Studies already struggle to properly close the energy balance in well-designed field studies over very homogeneous settings. Cleugh and Oke (1986), Grimmond and Oke (1995), and Grimmond et al. (2004) all note the extreme difficulty with selecting sites for urban measurements and how the vast majority of urban studies done tend to use suburban areas due to their greater homogeneous nature versus urban cores which are often very heterogeneous. Even given these difficulties, much work has been done examining the energy balance of the urban zone.

Equations 1 and 2 represent the energy balance equations for an urban area.

$$Q^* + Q_F = Q_H + Q_E + \Delta Q_S + \Delta Q_A \quad (A.1)$$

$$Q^* = Q(1-\alpha) + LW\Downarrow - LW\Uparrow \quad (A.2)$$

In equation A.1, Q* represents the net radiation absorbed by the volume. Q_F is an additional source term called the anthropogenic heat term, which is not present in the rural energy balance. It represents the input of energy that arises from human generated sources (e.g. industry, cars, or metabolic processes). These two source terms can then be distributed to Q_H, the sensible turbulent heat flux, Q_E, the latent turbulent heat flux, and ΔQ_S, the storage term. The energy budget can also be influenced by horizontal advection from other volumes represented here by the ΔQ_A term. In equation A.2, we see that Q* is made up of the shortwave solar energy Q, reduced by the albedo α, plus a longwave contribution. This longwave contribution consists of $LW\Downarrow$, from the overlying atmosphere, reduced by the loss of longwave energy, $LW\Uparrow$, from the top of the UCL

volume. The following discussion will outline several of the key aspects of the terms in the urban environment.

Q_F is the term unique to the urban area. The anthropogenic heat term recognizes that some energy available to the urban area comes as a by-product of human behavior. Generally, there are three sources: heat exchange from climate controlled buildings, heat from combustion sources (i.e. cars, generators, and industry), and finally, heat from metabolic processes (i.e. human heat waste). The third is often considered much smaller than the other two and is normally disregarded. In his literature review, Arnfield (2003) reports that most estimates of Q_F are less than 50 W/m^2 on a city wide average, making the term generally secondary in importance. However, studies such as Sailor and Fan (2004), Steinecke (1999) and Tomita et al. (2007) found that Q_F can be a dominant term in urban cores during winter. Additionally, Sailor and Lu (2004) looked at Q_F for six US cities and found significant increases in total Q_F output during winter for cities in higher latitudes. They also found vehicles dominated during the summer, with heating waste dominating during the winter in the colder cities. Plus, Ohashi et al., 2007 estimated that air conditioning waste in Tokyo contributed enough heat flux to contribute 1-2 degrees Celsius of heating to the city core in summer. Further, fine scale studies within dense urban cores, with high traffic volume, will likely see Q_F as a significant source term. Another important aspect of this term is its ability to provide a positive heat source at night in the absence of Q*. Q_F is a difficult term to measure directly and is often estimated by scaling up studies of individual generators and cars to citywide values. Further, most researchers that do attempt to consider the term apply a diurnal nature to the term in step with the typical diurnal behavior of a city (e.g. Sailor and Lu 2004;

Grossman-Clarke et al. 2005; Coutts et al. 2007). Ohashi et al. (2007) also found a significant variation of Q_F in the urban core on weekends versus weekdays. All of these studies point to a very dynamic role for Q_F which would have greatest impact as you increase in resolution. Thus, large domain studies can probably represent Q_F impacts with city wide average values, while neighborhood studies will likely want a more dynamic interaction with anthropogenic output.

The advection term, $\Delta Q_{A,}$ attempts to account for horizontal advection effects. In most measurement studies (urban or otherwise) this term is not resolved. Instead, any magnitude it may hold is simply folded into the other terms. Some studies may attempt to account for it by measuring the energy balance over the same portion of a city on days with different wind directions, but this is generally empirical at best. Most observational studies attempt to limit the influence of ΔQ_A by setting up measurements in areas that are spatially homogeneous upwind (e.g. Cleugh and Oke 1986). Both Brandsma et al. (2003) and Haeger-Eugensson and Holmer (1999) found direct evidence of this term in their observational studies, especially near the boundaries of the urban and rural area. This implies that at boundaries between different land uses, ignoring this term may be questionable. However questionable the assumption might be, fact is that the majority of studies will simply acknowledge the potential for error and then go on ignoring it.

The remaining variables are the traditional terms of the energy balance equation: Q*, Q_H, Q_E, and ΔQ_S (alternately labeled Q_G in many rural studies). While traditional, these terms are processed quite differently in urban areas than rural. Figure A.2 presents the measured energy balances from Cleugh and Oke (1986), and will be used as 'typical' to

discuss the remaining terms. The two curves were measured in Vancouver, BC at the same time (one at a suburban location, the other rural), and can be compared directly.

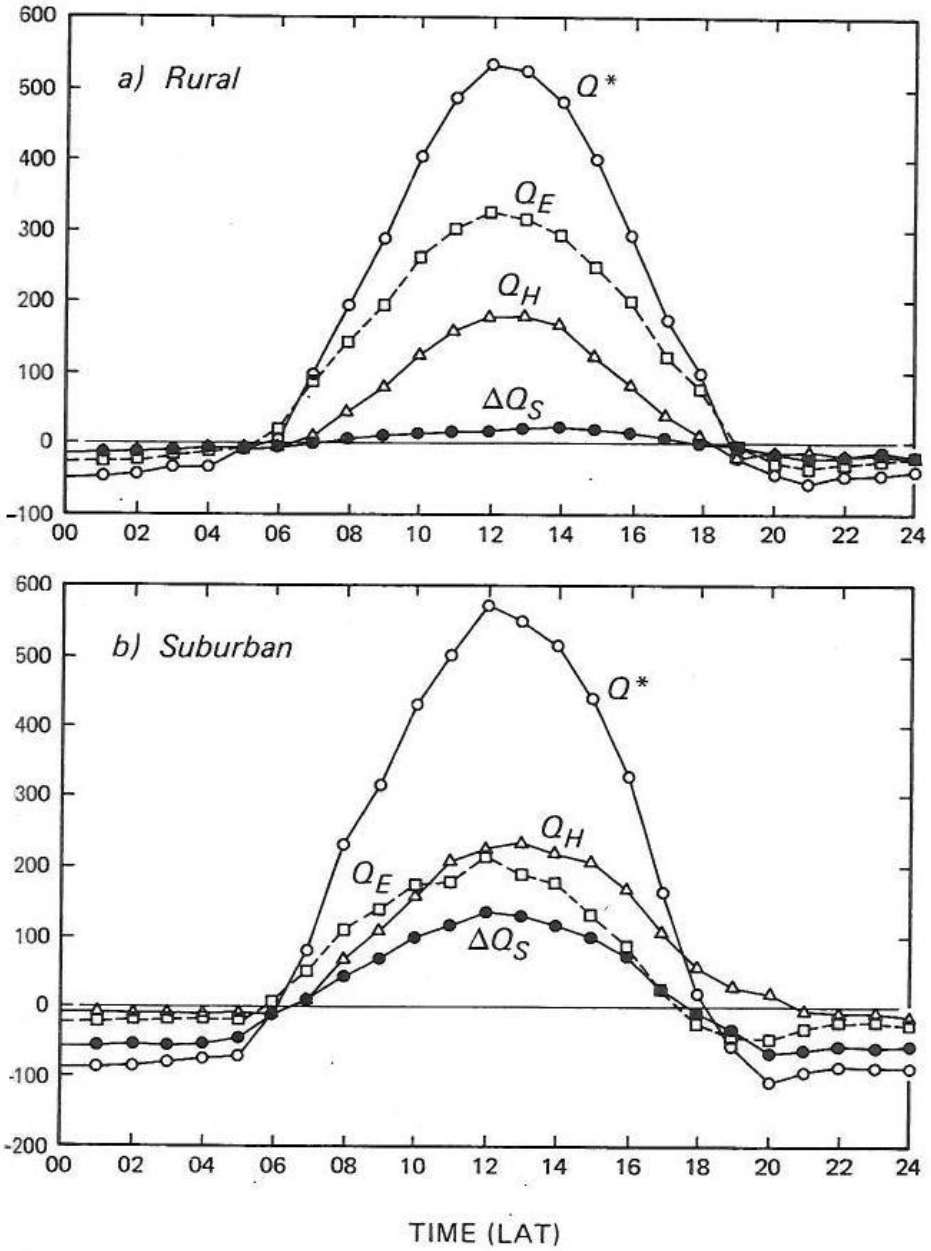

Fig A.2: Energy balance terms in Vancouver from a) rural and b) suburban location. Adapted from Cleugh and Oke (1986).

Note the measurements of Q* from Vancouver in Fig A.2. The curves of Q* are different between rural and suburban settings. In this example we see that the shape of

the suburban curve is sharper and peaks higher than the rural one. These differences can be considered 'typical' and are often attributed to combinations of the following four major effects:

1) SURFACE ALBEDO: In most instances, there is a measurable difference in albedo between the urban and surrounding rural landscape. In general, urban areas tend to have lower albedo and thus, capture a greater percent of incoming solar energy. However, measuring the albedo of an urban area is a complex affair as most urban areas are a large mixture of building colors and roofing materials, plus a mixture of surface concrete and asphalt, making urban albedo strongly heterogeneous.

2) URBAN GEOMETRY: There are two effects here. First, the geometry of the buildings accounts for less Q* in early morning and late afternoon in urban areas due to shading effects. This accounts for the sharper Q* curve seen in Fig A.2. (Rosenzweig, et al. 2009 found evidence of this effect in mid-town Manhattan as well.) Second, the urban geometry is very effective at trapping both incoming shortwave and outgoing longwave radiation, thus increasing Q* in the urban area. This trapping occurs when energy is reflected off several urban surfaces prior to reaching the surface or escaping to the overlying atmosphere. With each reflection, a greater portion of energy is absorbed as compared to a plane surface. As an example, Pearlmutter et al. (2005) found that a two story canyon structure leads to 15-20% higher Q* than a one story canyon. Also, Tomita et al. (2007) found that the sky view factor, a measure of how much of the sky plane is

visible from within an urban canyon, is critical to the observed post sunset delayed cooling, presumably due to trapping of escaping LW.

3) AEROSOLS: Urban areas tend to have greater aerosol loading than the surrounding rural areas. Urban climate studies have long since supposed that this would lead to a decrease in shortwave energy to the ground and a decrease in Q* over an urban area. There has been an increasing number of studies on this effect in the last few years. Xia et al. (2007), Chou et al. (2006), Ganguly et al. (2006a, b, and c), Jin et al. (2005a), Jin et al. (2005b) and Anrfield (2003) all found that the increased aerosol optical thickness decreased the amount of short wave energy reaching the surface by anywhere from 20-60 W m^{-2}. However, all of the same studies found evidence that much of this loss is being directly absorbed by the aerosols within the urban boundary layer leading to an increase in LW$\Downarrow$. The net forcing at the surface is always negative, but the overall magnitude on Q* in the urban UCL volume is harder to comment on. Further, Xia et al. (2007) and Ganguly et al. (2006b) found a large amount of temporal variability in aerosol loading (diurnal and synoptic), and thus in forcing. Studies have also begun to link aerosols with precipitation in urban areas, an impact that will be discussed in a later section.

4) LONGWAVE EFFECTS: The fact that the atmosphere over an urban area is generally warmer than the surrounding rural area may lead to a greater contribution from LW$\Downarrow$, thus increasing Q* over the urban area. However, Arnfield (2003) suggests this term is probably quite small.

These influences are a mixture of both positive and negative influences on Q*. Current thinking is that the overall difference on daily average Q* between urban and surrounding rural areas is probably small. For example, in the Vancouver study cited in Fig A.2, the Q* difference between suburban and rural was on the order of 4%. However, aspects of urban areas like the urban geometry, aerosol loading, and albedo of building materials will vary from urban area to urban area making a broad overarching comment difficult to construct. In addition, while the diurnal average Q* differences may be quite small, the hourly differences in Q* will at times be quite large because of these factors.

From Q*, we will move to ΔQ_S, the storage term. Understanding the effects of storage is vitally important to understanding the urban energy balance. In urban areas, ΔQ_S is far more important than in most rural areas. As seen in Fig A.2, storage represents a sizable percentage in the suburban curve. This increase in storage is a direct result of the properties of urban building materials and the urban geometry. The storage of heat by the urban fabric allows the urban area to release heat at a later time. Tomita et al. (2007), Grimmond and Oke (1999a) and Oke et al. (1991) all conclude that this behavior of ΔQ_S is a critical aspect of the formation of a UHI.

Q_E is probably the most complex energy term in the urban environment. For starters, urban surfaces are generally impervious to water and urban planners go to great lengths to control the presence of surface water (frozen or liquid) in urban areas. When precipitation falls, systems are in place to quickly remove surface water and snow. When conditions are dry, many areas irrigate existing vegetation to keep it healthy. As a result, humans in urban areas heavily modify Q_E. Factors to consider, other than direct human,

include the overall percentage of vegetation and the presence of any natural water sources such as rivers, lakes, and oceans. All of this makes Q_E one of the most variable terms from one urban area to another and even from one part of an urban area to another. Grimmond and Oke (2002) review a number of urban field measurements and conclude that the fraction of vegetated and irrigated surface exerts an important control on Q_E. Arnfield (2003) and Oke (1979) both discuss a feature of irrigation where under the right conditions, Q_E can exceed Q* due to dry air moving over irrigated surfaces. This is part of an effect known as the 'oasis effect' and will be discussed again later. Grimmond and Oke (1995) found evidence of a late afternoon secondary maximum in Q_E which they attribute to late day lawn watering. Grimmond and Oke (1999a) discuss how Q_E is usually minimized in the urban core, yet can remain positive at night, especially in irrigated portions of the city. Avissar (1996) demonstrates that vegetation in urban cores can significantly alter the resulting energy balance and could help reduce the UHI effect. In summary, this term plays a crucial wild card in the resulting nature of a UHI for a particular urban area.

The turbulent sensible heat flux, Q_H, gets whatever remains after ΔQ_S and Q_E are fully accommodated. As seen in Fig A.2, Q_H between the suburban and rural area can compare, even though storage is greater in the suburban area. This can occur because of the reduction in Q_E. Thus, if you have an urban environment with a high Q_E potential, Q_H will suffer, leading to less heat generation and a reduction (or possible elimination) in the UHI effect. Avissar (1996) noted that this type of effect may lead some urban areas to become afternoon 'cool islands'. Also note in Fig A.2 that due to storage release at night, urban areas can exhibit positive Q_H values even after Q* goes to zero. Tomita et

al. (2007) found the greatest difference in cooling rates between urban and non-urban environments in the late afternoon and early evening after sunset. Finally, the presence of significant urban geometry can delay the onset of Q_H relative to rural areas, leading to delayed morning warming of the urban core.

The presence of the urban area significantly alters the processing of arriving energy relative to the surrounding rural areas. As detailed in the following two sections, this will lead to a distinctly different boundary layer over the urban area and greatly altered sensible weather variables.

b. The Structure of the Urban Boundary Layer

The urban geometry, and the materials of the urban elements that have such a large influence on the urban energy balance at the surface, in-turn cause a fundamental difference in the structure of the Urban Boundary Layer (UBL) compared with traditional boundary layer structure. Several papers including Arnfield (2003), Rotach et al. (2001), Roth (2000), Hunter et al. (1990/1991), and Oke (1988), offer comprehensive reviews of the UBL. These reviews all point out that the structure of the UBL is fundamentally different than often considered in standard BL theory, because urban areas are strongly non-homogeneous in the horizontal, thus violating a fundamental assumption made in the development of standard boundary layer parameterizations. Much of the work done in UBL is aimed towards determining to what extent traditional theory can or cannot be applied to the UBL.

One thing that immediately complicates description of the UBL is that no universal terminology has been adapted for describing the layers of the UBL. For this study, I have

adapted Fig A.3 from Oke (1988) to serve as the basis for discussion. The point of departure compared with standard BL is the presence of a 'roughness layer' near the surface where the individual roughness elements strongly influenced the flow (Rotach and others refer to this region as the Roughness Sublayer or RS). The RS is considered to

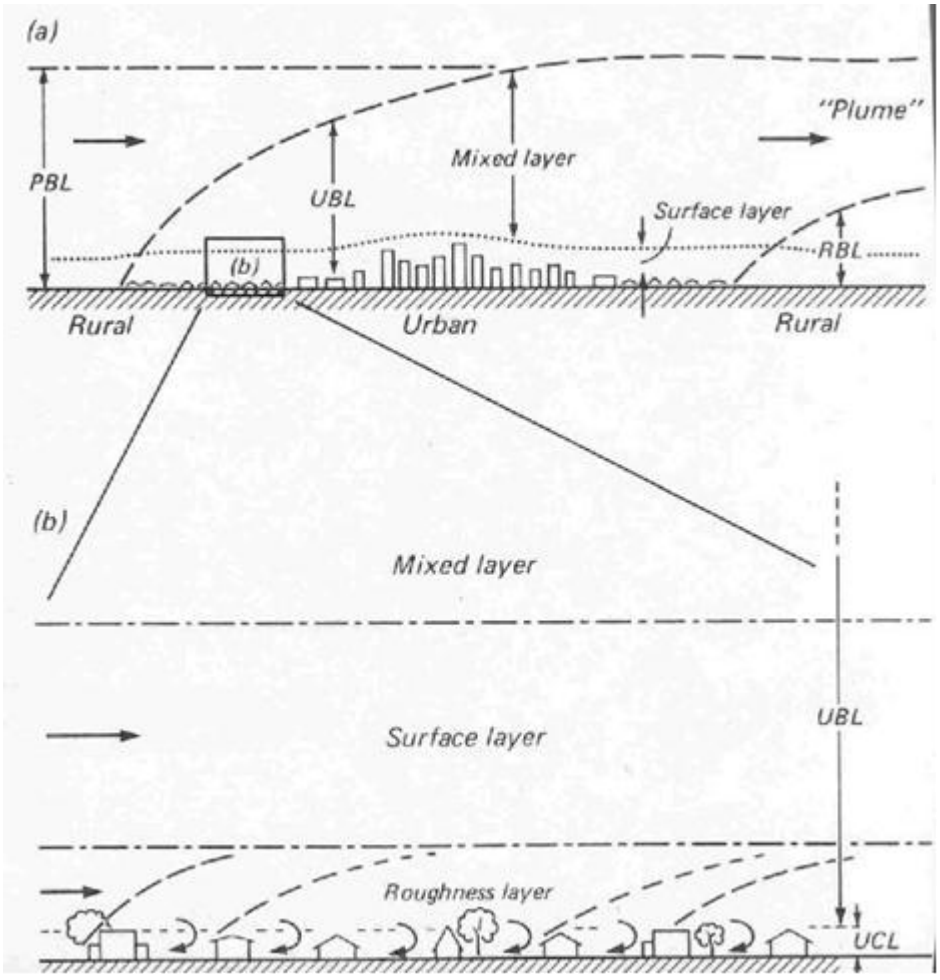

Fig A.3: Schematic of the Urban Boundary Layer. Taken from Oke, 1988

have two layers where the Urban Canopy Layer (UCL) is broken out from the remaining atmosphere above the roofs.

Research in the RS is usually concentrated in two broad areas: 1) studies of the UCL, especially on the exchange of properties (e.g. heat and material) between the UCL and

the remaining RS above the roofs and 2) studies of BL theory in the remaining RS, especially concerning the applicability of Monin-Obukhov Similarity Theory (MOST).

The UCL is the portion of the RS that contains the building elements. Thus, it consists of both buildings and the spaces in between. Generally, the literature refers to this zone as an amalgam of 'urban canyons' where the buildings line either side of a street, forming an artificial canyon like structure. Most of the studies of these urban canyons are interested in studying the behavior of energy transfer within and out of the canyons to the remaining RS above. The studies are a mixture of model, wind tunnel, and field studies. The studies build a case suggesting that interactions with the air above roof level is largely a function of the wind direction relative to the orientation of the canyon, the height-to-width (H/W) ratio of the canyon, and the density of building elements. Vardoulakis et al. (2003) provides a comprehensive review of ventilation related studies in the UCL. Oke (1987) coined three basic flow regimes to describe the interactions when the flow is perpendicular to the canyon (Fig A.4). If the canyons are wide and shallow, and the buildings very isolated (Fig A.4a.), then the flow from roof level tends to regularly flush the air from the canyons and transfer is very vigorous. Many suburban housing neighborhoods likely exist in this type of regime. As elements become more numerous and canyon depth relative to width of the street increases, the air in the canyon becomes increasingly cut off from the overlying flow. At some point the building density becomes so great that the air literally skims over the canyons (Fig A.4c.). In this case, air within the canyon tends to form a vertically rotating vortex allowing some slow interaction with the air overhead.

Many studies have been done to confirm this behavior with models or in wind tunnels, and to try and develop parameterizations of behavior between the canyon and overlying flow. Mills (1993) examined exchanges between UCL and upper RS for a number of

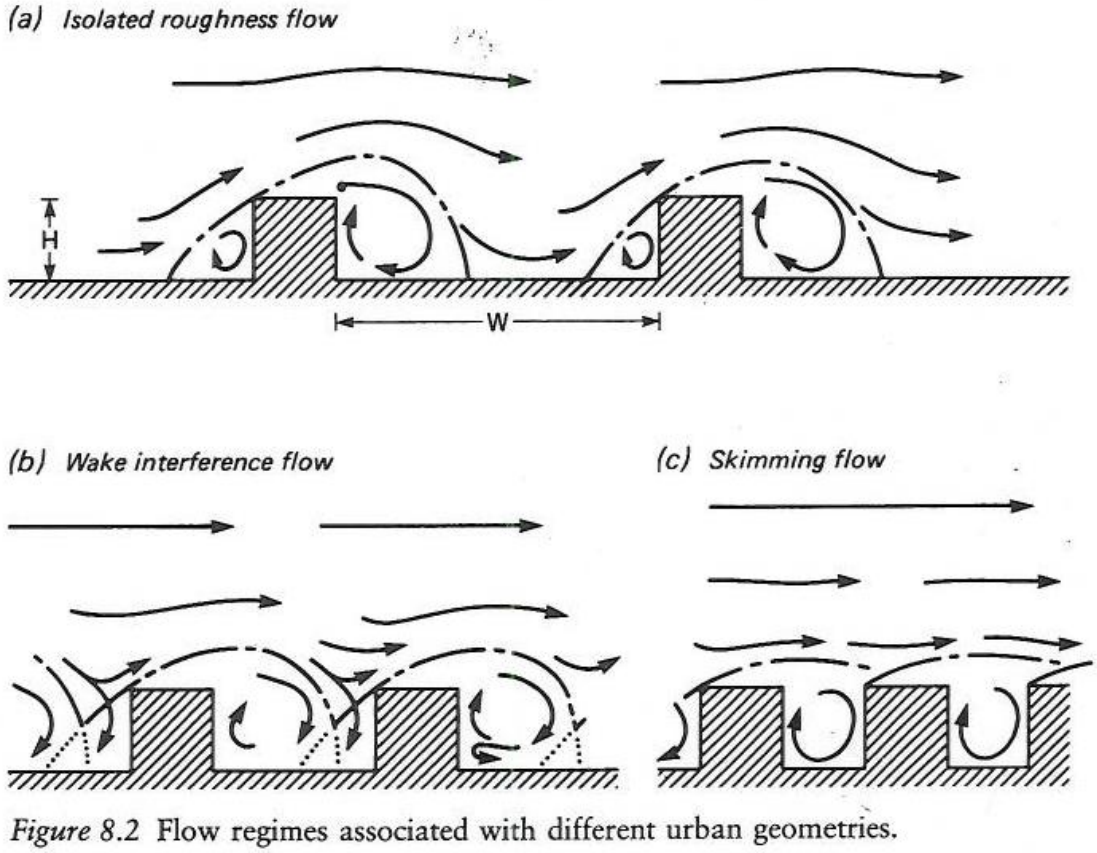

Figure 8.2 Flow regimes associated with different urban geometries.

Fig A.4: UCL flow schemes under perpendicular flow. Taken from Oke (1987)

different configurations. He found sensible heat exchange was most sensitive to wind speed, albedo of the building materials, and H/W ratio with deep central city canyons having the most impeded transfer. Chan et al. (2002) and Barlow and Belcher (2002) also confirmed the importance of H/W to ventilation from the UCL. Meroney et al. (1996) found in wind tunnel studies that isolated canyons were more easily flushed than canyons embedded in an urban setting with other canyons. In fact, they found no

evidence of a re-circulating eddy in the isolated case, but did find one in the heavily urbanized case. Liu and Barth (2002) performed a Large Eddy Simulation study of an urban canyon with perpendicular wind flow. Their model confirmed the general theory by generating an eddy within the canyon once the H/W ratio had grown large enough. Jeong and Andrews (2002) modeled skimming flow under several different H/W in an effort to determine critical values for vortex development. Other modeling work confirming the validity of this basic theory includes Hunter et al. (1990/1991), Lee and Park (1994), and Baik and Kim (1999).

Of course, the real atmosphere is never truly this easily characterized. Street canyons are irregular in shape and building height (especially near city centers) is usually non-uniform, so the flow within the canyons and between the UCL and remaining RS is quite complex. Some modelers have attempted to conduct sensitivity tests using more complex setups. For example, Hoydysh and Dabberdt (1988) studied skimming flow with buildings along the canyon of differing heights, side streets and non-perpendicular wind directions, while Dabberdt and Hoydysh (1991) looked at square block layouts instead of the traditional rectangular street canyons. These more realistic street canyons are generally better ventilated than the traditional designs cited above. All of the above studies only address the mechanical forces of exchange. Kim and Baik (1999) studied the thermal impacts of the canyon circulation. They looked at the impact of irregular heating applied to the upwind wall, downwind wall, and street, and found that this added complexity to the vortex developed.

Logically, several field studies have examined the basic validity of UCL exchange. Vardoulakis et al. (2002) found evidence for vortex formation within street canyons

during a field study in Paris, where isolated hot spots were found during tracer releases. They also found strong dependence of ventilation upon synoptic wind direction. In Mills and Arnfield (1993b), measurements in Columbus, OH generally confirm that the canyon becomes more isolated in terms of heat exchange as H/W increases. DePaul and Sheih (1985) conducted a field study in Chicago and felt that in spite of the complexity, ventilation could be parameterized fairly easily using just wind measurements from roof top. Salmond et al. (2005) looked at nighttime venting of a street canyon in Marseille, France and found evidence of intermittent venting, which they linked to thermally driven releases from sensible heat in the canyon. Klein and Clark (2007) performed field work in Oklahoma City to look at ventilation and concluded that the in-canyon flow is primarily driven by the boundary layer flow above, noting that vortices are seen when flow is perpendicular. However, real flow also contains occasional channeling flows, even under perpendicular flow conditions. Finally, Hanna and Zhou (2009) reported results from the 2005 Midtown Manhattan field experiment and found that the 30 minute average behavior of turbulence structures were surprisingly non-variable. They attributed this to the natural variability of wind direction which was great enough to prevent classic laboratory static flows (e.g. vortices) and presenting a more homogeneous interaction between canyons and overlying air. The conclusion from the field studies is that while the basic construct of the modeled results is verified, the real city structure is far more complicated and the real exchange far more chaotic in nature.

The importance of the UCL to this study is that any attempts to parameterize the behavior of an urban area within a numerical model must somehow account for this

exchange, recognizing that the UCL will interact with the overlying atmosphere not just as a flux source, but also as a source for tracer and mass.

Once you rise above the roofs, the main issue of research centers is how to model this non-homogeneous area of the UBL. Most of the turbulence scaling done in models and parameterizations follows MOST, which is predicated on an assumption of horizontal homogeneous behavior (Stull 1988). However, all researchers agree that the urban landscape creates a lack of flow homogeneity, which likely violates the assumptions in MOST. Roth (2000) presents a comprehensive review of work done on urban boundary layers and concluded that considerable work needs to be done to investigate to what extent similarity theory can be applied to the RS. Perhaps in response, working groups 1 and 2, from a European framework for coordinating national research efforts called COST 715, have set the gold standard in advanced urban boundary layer research. This group held a major workshop 24-25 May 2001, producing several extended abstracts on their efforts. Rotach et al. (2002) provides an overview of the effort, and documentation from this workshop can be obtained at www.iac.ethz.ch/en/research/cost715/cost715_2.html. This effort produced several papers examining the applicability (or lack thereof) of MOST in the RS, and proposes several ideas for how to deal with it. Even the most recent field studies (e.g. Klipp 2007) continue to demonstrate the non-uniform behavior of turbulence above the roof tops.

Of critical importance to gauging the importance of the RS is to determine its vertical extent. Observational studies want to understand what part of the UBL their instruments are sampling and modelers want to understand at what modeling resolutions they need to develop advanced parameterization to deal with the departure from MOST. Roth (2000)

summarizes a number of studies that have attempted to calculate this and concludes the height of the RS extends 2-5 times the height of the roofs. Rotach et al. (2001) suggests that the 5h value may be too high, at least for European cities, and favors a value closer to 2h. Regardless of what height is selected, the more intense the skyline, the deeper the RS impact should be.

From here, the next major effort is to develop an understanding of how turbulence behaves in this region, in an effort to develop schemes aimed at modifying the MOST approach to work in the UBL. As summarized in Rotach et al. (2001), two significant departures from MOST exist in the RS. First, Reynolds stress is not "approximately constant with height". Instead, it increases with height becoming nearly constant, at which point the RS boundary is reached. Second, because of this non-constant behavior, using surface fluxes to derive non-dimensionalized scaling variables cannot be done. The first departure means that a constant value of u* cannot be used in the RS. The effect means that the mean wind is reduced over what MOST would predict. Rotach et al. (2001) recommends using a locally derived value of u*, instead giving rise to a method known as 'local scaling'. Parameterizations using this concept of local scaling are available today and used by some urban parameterizations. For example, Al-Jiboori et al. (2002) and Roulet et al. (2005) describe model development that uses this concept of local similarity theory. Once you have this local u*, the standard non-dimensional scaling can commence.

Even accounting for a more complex Reynolds stress behavior in the RS is itself a simplification of the forces at work. Belcher and Coceal (2001) point out that there is a dispersive stress term at work, representing the transport of momentum by spatial

fluctuations in urban elements. They conclude that for most urban applications it can probably be ignored; however, areas where the buildings have a lot of non-uniform sizes (e.g. central business districts), this may be problematic. Of course, they also point out that observational studies are largely lacking in this environment, so theories on how to account for this term are woefully inadequate. In addition, Rotach et al. (2001) point out that local similarity theory will likely break down near the boundaries between urban and rural areas, and probably significant urban land use boundaries such as central business and suburban, where significant boundary layer blending is occurring. The reality is that most urban parameterizations will be developed over a so called 'urban Kansas' and then applied across the entire domain just as is done today with traditional PBL parameterizations.

The importance of the above sections to this work centers around the need to understand how the urban parameterization used deals with the RS and any potential impacts that may have on the simulations. The Town Energy Balance (TEB) scheme of Masson (2000) [the scheme used in this study] assumes MOST holds within his parameterization. Given the above, that could be concerning. However, since my study is done over Washington, DC where the average building height was determined to be 8m, and my model configuration is set to resemble today's operational configuration (meaning only 1 layer within 2h), the impact of this assumption should be minimized. In short, this modeling configuration lacks the near surface vertical resolution to take advantage of the advanced parameterizations capable of non-MOST treatment of the RS.

In addition to the parameterization of Reynolds stress, another popular parameterized factor in BL theory which is questionable in the UBL, is the roughness length, z_o. As

pointed out by Belcher and Coceal (2001), the roughness length is not a physical length scale; it is derived from the logarithmic wind profile which comes from MOST and likely not valid in the RS. z_o acts to compile the impacts of the rough surface towards the generation and dissipation of turbulence as a result of flow over the surface. Atkinson (2003) demonstrates in UHI sensitivity studies how z_o acts to reduce the intensity of modeled UHI intensity by enhancing the effectiveness of the sensible heat flux and resulting heat loss. Grimmond and Oke (1999b), Roth (2000), Mestayer and Bottema (2001), and Arnfield (2003) all review studies that have attempted to devise ways of calculating z_o over urban areas consistent with RS theory. None of the studies reviewed could make a solid recommendation of how to calculate z_o over an urban area. Several researchers have examined simple and very complex means to determine z_o; however, the issue is really one of observation. Arnfield (2003) stated it best: "Observed values are of insufficient quality to decide truly between competing techniques".

Masson (2000) has adopted the simple approach of setting z_o=10/h, which on the basis of the above studies, seems like reasonable logic. Considering the degree of difficulty present in even measuring z_o, using an overly complex method in this instance would be akin to maintaining several significant digits when accuracy suggests it is unwarranted.

c. UHI Climatology

The first section examined how the 3D urban surface processes the surface energy balance differently than the typical rural area. Section b then explored how the urban landscape would alter the structure of the overlying boundary layer. This section will

now examine the impact both of these have on the so-called sensible weather variables such as temperature, wind, and moisture, attempting to ultimately link the UHI drivers responsible for the sensible weather variable response.

As early as the 1800's, humans have recognized that the climate of urban areas is different from the surrounding rural areas. Both Oke et al. (1991) and Shepherd and Burian (2003) credit Luke Howard with the first documented observation of a temperature difference between an urban area and the surrounding rural area in his 1833 book, Climate of London Deduced from Meteorological Observations. Shepherd and Burian (2003) go on to credit Manley (1958) with first coining the term "urban heat island"; thus forever placing temperature deviation at the heart of urban climate modification. But, studies have clearly shown that urban climate modification extends well beyond just temperature. Oke (1987) offers a comprehensive review of the 'typical' urban climate. Fig A.5 comes from that review and shows the typical temperature behavior across a cross-section of a theoretical urban area on a clear, calm night. It features a temperature maximum located over the urban core with slightly cooler conditions over the sub-urban areas, falling quickly down to a rural background temperature. The UHI intensity is defined as the ΔT in air temperature between the urban and rural area. It is best developed during the evening and generally lessens after midnight. In many cities it is a minimum during the day and may even become negative.

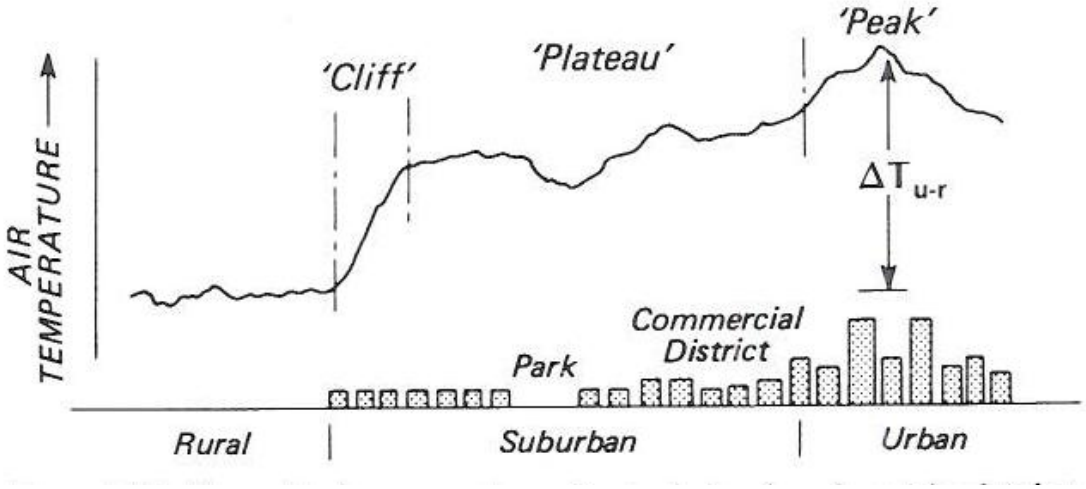

Fig A.5: Cross section of a 'typical' UHI. Taken from Oke (1987).

More subtle than temperature is humidity. Oke (1987) and Robaa (2003) both conclude that, in terms of vapor pressure, the urban area is usually drier by day and slightly more moist at night, but that differences tend to be small and the patterns are very complex.

Wind speeds over the city are generally less compared with rural areas at the same height because of the increased urban roughness. By both day and night, the boundary layer over the urban area is generally deeper and the urban area may suppress stabilization long after sunset. Finally, the precipitation patterns around urban areas tend to show an enhancement in convective precipitation downwind of urban areas with a relative minimum upwind.

While this general climatology of the UHI is a nice aspect to understand, it should not come as a surprise that actual UHIs can and do deviate strongly from this simplistic discussion. For starters, Grimmond and Oke (1995) found strong variability in surface energy balance from one day to the next in their study of four suburban areas. They concluded that a great deal of day to day variation in UHI should be expected. For example, when the urban area is subject to the larger synoptic forcing (e.g. gradient

winds), a UHI may fail to exist at all. DeMarris (1975) examined daily UHI variability for 33 cities using data from 1964 for urban/rural station pairs and found significant daily variability in all of the cities suggesting daily UHI's vary from negative values to highly positive (>10 °F). More recently, Rosenzweig et al. (2009) found such synoptic cycle variation in UHI behavior of New York City as did Basara et al. (2008) in Oklahoma City, OK.

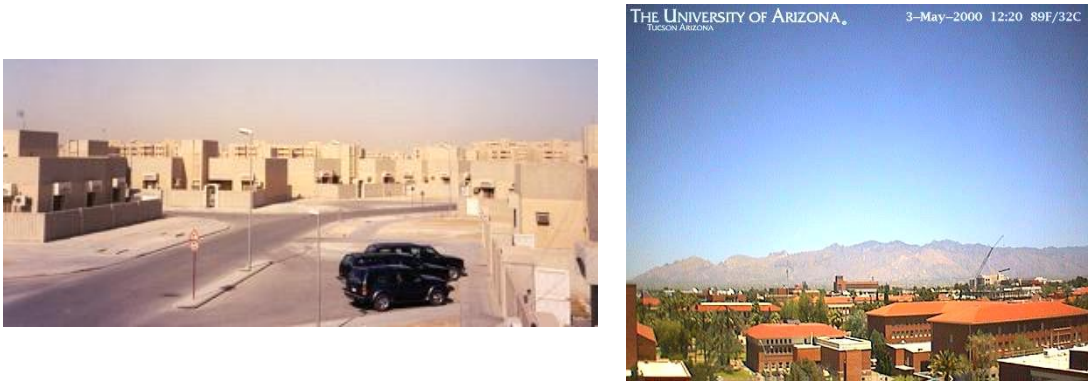

Fig A.6: Photos of two suburban areas in desert areas. A) Image of Eskan Village outside of Riyad Saudi Arabia (photo taken by author) b) Photo of University of Arizona, Tucson (obtained from U. of Arizona website).

At the heart of the UHI is a difference in forcing between the material of the urban fabric and the surrounding rural landscape. Cities are found embedded in every major type of landcover on earth and the differential forcing between a city embedded in a rain forest will be different than one embedded in a desert. Further, cities are not built from standard materials or in a standard layout. Figure A.6 shows two photos of suburban landscapes built in a desert landscape. Clearly these two areas are vastly different and will have very different energy balances relative to their surroundings and thus different UHI forcing. Bounoua et al. (2009) attributed this difference in materials to their finding of no UHI signature in the Mediterranean coastal city of Oran in North Africa. Below are a number of observations about the sensible variables of the UHI obtained from review of various UHI observational studies.

1) TEMPERATURE: One constant factor of UHI existence is the presence of a mean temperature difference between urban and rural regions, especially at night. Based on this, attempts have been made to develop simple bulk parameterizations of UHI intensity. Oke (1987) presented material on efforts to parameterize expected maximum UHI intensity based solely on population, and while he did find a relationship, he found that North American cities had a different curve than European ones due to differences in construction materials, city design, and surrounding landscapes. Torok et al. (2001) looked at population relationships with UHI intensity for Australian cities and found that the more open planning concept of Australian cities led to a less intense UHI than a North American city of similar population. These simple parameterizations may capture the maximum theoretical UHI intensity, but it will fail to capture the fact that the intensity of the UHI will vary spatially within the city, diurnally, synoptically, and seasonally.

Spatially, UHI intensity will change as one moves from section to section within the city. It tends to maximize in the area with the highest building density, especially as measured by H/W ratio. Hawkins et al. (2004) looked at the spatially varying intensity of the UHI around Phoenix, AZ and concluded that varying land cover types in and around the city, plus the changes in building materials/morphology make defining the UHI difficult. Kim and Baik (2005) found strong spatial variations in the UHI of Seoul, South Korea and concluded that it is a response of varying urban land use and diurnal cycle of human activity. Basara et al. (2008) reached similar conclusions concerning Oklahoma City using data from the Joint Urban 2003 Campaign.

Diurnally, it tends to maximize in the early evening; however, here it is worth pointing out an important factor about measuring the UHI. There are two methods used to

measure UHI intensity. One is to measure the air temperature at various points in the city and surrounding rural area. The other is to attempt to measure from satellite. Satellite measurements are actually measuring skin temperature, not air temperature. Satellite studies will generally find maximum UHI intensity in the middle of the day as solar insulation is absorbed by the urban fabric. Jin et al. (2005b) conducted a global analysis of urban areas using satellite data and found measurable UHIs day and night in all seasons. However, air measurements will usually minimize the UHI at midday as much of the absorbed insulation is being stored in the urban fabric. The shedding of the stored heat by the urban fabric at night leads to the maximum observed air temperature difference. Therefore, it is important to recognize how the UHI is being measured. Memon et al. (2009) found such behavior in their study of differences of UHI's measured with satellite vs air temperature. Nichol et al. (2009) did a comparison study of Hong Kong's UHI as it looks to satellite derived vs. traditional in-situ and concluded that the differences are due to fundamental differences in measurement properties. However, Lynn et al. (2009) found that even though the daytime UHI is present as a skin temperature rather than air temperature, that the thermal stress introduced to people walking the streets is still very high. Diurnally, nighttime UHIs as measured by air temperature are nearly exclusively positive while daytime UHIs may be positive or negative. When negative, the UHI is referred to as a 'cool island'. Alonso (2003) found the city of Salamanca, Spain exhibits an average daytime UHI intensity of -0.7 °C. Montavez et al. (2000) found a similar cool island behavior in Granada. Basara et al. (2008) reported daytime UHI cool island for Oklahoma City and were even able to confirm spatial variability of the cool island intensity within the city in much the same

way others have studied in intra-city behavior of heat islands. However, not all cities create cool islands, for example, Kusaka (2002) reports a positive daytime UHI for Tokyo. A result of this diurnal behavior is that many climate trend studies will find strong trends in increasing Tmin of urban areas, with more ambiguous findings for Tmax trends (e.g. Montzvez et al. 2000; Tonkaz and Cetin 2007; Hamdi et al. 2009; Roy and Yuan 2009).

Many studies find significant differences in UHI temperature intensity between seasons. This is generally attributed to seasonal changes in surrounding landscape driving changes in differential forcing (e.g. Offerle et al. 2005; Tonkaz and Cetin 2007; Roth 2007; Wang et al. 2007), or changes in anthropogenic heat output (e.g. Sailor and Fan 2004; Steinecke 1999; and Tomita et al. 2007). Arnfield (2003) concluded that many UHIs maximize during the warm season; however, many studies have found maximum UHI intensities in winter. Wang et al. (2007) in Beijing, Lo et al. (2007) over Hong Kong, and Montavez et al. (2000) in Granada are three examples. Also, Alonso et al. (2003) and Kim and Baik (2005) found maximum nighttime air temperature of UHIs in Salamanca, Spain and Seoul, South Korea respectively during Autumn. Further, locations with two season climates, such as Sub-Saharan Africa, also exhibit strong seasonal variation in UHI with the dry season often having a maximum (Offerle et al. 2005 and Roth 2007).

To summarize, UHI behavior as measured by temperature is highly variable in space and time, fully coupled and responsive to the larger scale environment it is embedded in.

2) HUMIDITY: Again, urban climatology suggests cities are drier by day and more moist by night. However, this is perhaps the most difficult variable to characterize in any uniform way. For one thing, how you choose to measure humidity (absolute or relative) will likely lead to different conclusions. Additionally, while city construction materials are generally non-porous and cities put a lot of effort into efficient water removal mechanisms, cities are often located adjacent to water bodies (rivers, lakes, ocean) or may contain irrigated vegetation zones. Even practices such as cleaning city streets at night can be a factor (Grimmond et al. 2004). Also, since water vapor can be easily advected, interactions of local mesoscale flows (e.g. sea breeze) can greatly complicate things (e.g. Ohashi and Kida 2004). Finally, the surrounding landscape of the city may be heavily modified by irrigated crops (e.g. Tonkaz and Cetin 2007), leading to a very artificial surrounding humidity pattern. Jauregui and Tejeda (1997) found the climatological view of humidity held over Mexico City during the wet season, but that there was little to no difference in humidity behavior between urban and rural areas in the dry season. Holmer and Eliasson (1999) examined four years of vapor pressure differences in Goteborg, Sweden and found the traditional relationship of excess vapor pressure over the city at night and drier conditions during the day exists there. They also examined the feedback this could have on the UHI intensity and concluded that the overall effect was negative. While the impact of the vapor did increase the amount of $LW\Downarrow$ by 12%, this was offset by the LE stimulation of dry air advection from surrounding landscapes. Roth (2007) concludes that wet season air humidity in rural areas was the primary likely reason that wet season UHI intensity decreases as rural areas struggle more to radiate at the higher humidity values.

The dry air advection process mentioned above has been seen in many studies and is termed the 'oasis effect'. The advection of dry air over isolated urban moisture sources (vegetation, anthropogenic moisture waste) leads to greater evaporative potential (increased LE) than landscapes with continuous moisture sources. This is enhanced by the presence of irrigation. Modlers and Olson (2004) found evidence of this effect over Tokyo. Offerele et al. (2006) found the effect in four different cities in Poland. It is worth pointing out that those current land surface models used by mesoscale models will not be able to account for such an effect, and will likely underestimate latent heat fluxes over urban areas.

Unger (1999) examined Szeged, Hungary and found urban vapor excess at all hours. Unger was unable to conclude why this would occur. Studies that look at relative humidity instead of vapor pressure tend to find conditions are drier over the city due to the influence of the excess urban heat on RH calculation (e.g. Robaa 2003).

Overall, the strong variability of observed moisture with its large thermal capacity, make it the wild card in determining inter-urban differences in UHI manifestation.

3) WINDS, STABILITY AND THE UHI CIRCULATION: Winds over urban areas are going to be influenced by two different factors. First, increased roughness associated with the urban morphology will generally lead to slower wind speeds compared with adjacent rural areas measured at the same height. Second, the presence of the UHI (a thermal 'bubble') will tend to produce deeper boundary layers, and the continued SH release in the evening hours will tend to prevent stabilization, allowing winds over the city to remain into the night while the surrounding landscape sees winds approaching

calm. Soriano et al. (2001) found evidence of both in a study of European winds. They found the urban areas as a whole had lighter winds due to roughness; however they observed a positive offset with non-zero winds over the city when rural areas were calm, likely due to stability. Hilderbrand and Ackerman (1984) looked at the stability implications of the UHI and found larger SH over the urban area, driving a deeper convective boundary layer. Basara et al. (2008) confirm the lack of boundary layer stabilization at night in Oklahoma City. Instead the city exhibited a neutral boundary layer throughout the night. Balling and Cerveny, (1987) attribute higher winds of Phoenix, AZ during the early morning hours with decreased nighttime stability over the city as a result of the UHI.

Another aspect of the UHI is the development of a secondary circulation. If the UHI intensity becomes large enough, a thermally forced circulation can develop between the urban and rural area (much like a sea breeze). This secondary circulation is referred to as the UHI Circulation (UHIC) and when superimposed upon the background synoptic flow, it tends to manifest itself as a convergence zone located downwind of the city center. This will be detailed in section A.2.

4) PRECIPITATION AND AEROSOLS: Several studies have confirmed the presence of precipitation anomalies in the vicinity of urban areas (Huff and Changnon 1973; Shepherd and Burian 2003; Mote et al. 2007). Most often studies find enhanced precipitation downwind of urban areas. Next to nighttime temperatures, this may be one of the most consistently observed features of an UHI. Chen et al. (2007) found increases in thunderstorm in and around Taipei as the city has grown. Lo et al. (2007) found

similar results in the Pearl River Delta region of China, which includes Hong Kong. Molders and Olson (2004) found the effect at high latitudes in Fairbanks, AK. Shepherd (2006) found evidence in the desert cities of Phoenix, AZ and Riyadh, Saudi Arabia. Farias et al. (2009) reported enhanced lightning activity over São Paulo in South America. Hand and Shepherd (2009) found statistically significant enhancement of precipitation downwind of Oklahoma City in the absence of strong synoptic forcing. Huff (1986) found a maximum in precipitation over St. Louis and to the NE of the city with a relative minimum to the SW. The prevailing wind during July is from the SW supporting the belief of the convective enhancement downwind. Huff and Changnon (1973) conducted their study at eight different cities in the US and found precipitation enhancement in all. Zhang et al. (2009) also found enhanced precipitation downwind of Beijing, China; however the primary reservoir for the city lies upwind and has seen decreasing precipitation, especially heavy convective type. As we will explore in section A.2, the UHIC and interactions with other mesoscale flows is a leading candidate for cause.

Another aspect of precipitation has to do with city design. The increased precipitation coupled with large areas of non-porous surfaces often exacerbates the potential for flash floods. Bounoua et al. (2009) linked the growing city of Oran in North Africa with the increasing occurrence of devastating flash flood there. Both Huff (1986) over St. Louis and Ntelekos et al. (2007) over Baltimore, MD emphasize the need of city planning to consider this aspect.

There is also some evidence that the presence of the UHI may have impact on frozen precipitation. Changnon (2003) looked at trends in freezing rain and snow events at four

major downtown airport locations (Chicago, New York City, St. Louis, and Washington, D.C.) and found significant reductions in both events at all four locations, but especially at the biggest urban areas, Chicago and New York City.

In addition, increasing evidence is starting to suggest that urban aerosol loading may be affecting precipitation around cities. Huff and Changnon (1973) mention the possibility of a role for aerosols in precipitation modification. Molders and Olson (2004) suggest aerosols are the largest factor for precipitation pattern changes over Fairbanks, AK. Ganguly and Jararaman (2006c) and Ganguly et al. (2006a) show how the aerosol loading changes the surface and near surface heating/cooling rates in Ahmedabad and Delhi, India, which would have an impact on stability and thus precipitation. Rosenfeld et al. (2007) conclude that aerosols from Xi'an, China are changing the dynamics of downwind precipitation over the mountains. They believe the abundance of aerosol is suppressing rainfall by 30-50%. Van Den Heever and Cotton (2007) conducted a series of sensitivity studies with convection initiated downwind of the St. Louis UHI and found that the presence and make-up of the urban aerosols exerted a strong influence on the ultimate development of the convection intensity. Farias et al. (2009) concluded that aerosols are increasing the lifetime of storms over São Paulo but that their influence is secondary when compared to the influence of the UHI. Carrió et al. (2010) demonstrated in their modeling study over Houston that aerosol loading would influence the likelihood of liquid particles reaching supercooled levels which led to both an increase of storm heating and increased electrical activity.

5) PRIMARY DRIVERS OF THE UHI: Urban areas offer many differences from natural landscapes including building materials (includes thermal characteristics such as albedo and capacity), 3D morphology (includes effects on roughness, LW and SW energy trapping), presence of anthropogenic heat sources, alteration of the water budget (non-porous surfaces, irrigation, and the oasis effect), and increased aerosol loading. Many studies have attempted to determine which of the factors play the largest role manifesting a UHI, in order to ensure parameterizations have the necessary elements and also to help urban planners mitigate the effects of the urban landscape.

Oke et al. (1991) is one of the first works to systematically look at the individual factors listed above in a series of modeled sensitivity tests. They found the LW trapping effects of the urban canyons and the thermal properties of the urban fabric that leads to large $\Delta Q_{S,}$ which is then bled off at night, were the two factors that in isolation, could produce a significant UHI. To get large values of ΔQ_S, it was the difference between thermal properties of the dominant urban building materials compared with the rural background thermal characteristics that proved most critical. Anthropogenic heat release could be important, especially at night under cold weather conditions. The UHI was relatively insensitive to albedo/emissivity effects. Cloud cover acted to reduce the intensity of the UHI. Difference between rural and urban moisture levels could be a wild card to UHI intensity.

This result was in agreement with Carlson and Borland (1978) that found the surface thermal inertia critical. They also found that large differences in moisture availability could also be crucial. Offerle et al. (2005) also saw the critical nature of thermal inertia in their study of the city of Ouagadougou in sub-Saharan Africa. In spite of a large

sprawl of urban 'shanty towns', they found a surprising low intensity UHI which they attribute to the lack of building sophistication (dirt alleys, low structures, and natural building materials), versus planned urban development creating less thermal characteristic differences between urban and rural landscape. Tomita et al. (2007) examined the causes behind the reduced cooling rate in the early evening over a medium sized city in Japan. They found a large role for Q_F and the thermal conductivity, with only a small role for trapping effects. Kusaka and Kimura (2004) also concluded the dominant role of storage release and Q_F presence at night as critical for strong UHI formation. Coutts et el. (2007) looked at Melbourne, Australia and found that difference in storage and Q_F were the primary drivers of the UHI there. Atkinson (2003) conducted a similar study to Oke et al. (1991) using a numerical model to examine the sensitivity of the UHI to several forcing variables. He found different forcing was important between day and night. During the day, roughness length and moisture were the most dominant factors of UHI intensity. In this study, the sensitivity of moisture was assessed between a very dry urban core and a moist surrounding, so no oasis effect was considered. Roughness length proved critical for enhancing SH transfer. At night, Q_F played the most critical role. Interestingly, his study showed little influence from thermal inertia effects. Another interesting sensitivity experiment they conducted was to vary the size of the city. They found very little impact on UHI intensity due to the horizontal extent of the city. In Basara et al. (2008) they attribute the Oklahoma City UHI primarily to arise from the LW/SW impacts of the downtown street canyons.

In summary, the factors leading to the formation of the UHI are many and the summation of the studies suggest those factors that dominate are likely somewhat

different from one urban area to another, owing to differences in materials, anthropogenic heat waste, and water availability.

A.2. The UHIC as a forcing mechanism and its interactions with other mesoscale features

a. General

As discussed in A.1.c., the thermal discontinuity between urban and rural areas can give rise to a circulation, the UHIC, in much the same way as the water/land contrast can give rise to the sea breeze. In the absence of any background flow, the resultant induced flow would converge inward to the city center from all directions. Figure A.7 gives an example, taken from Rozoff 2002).

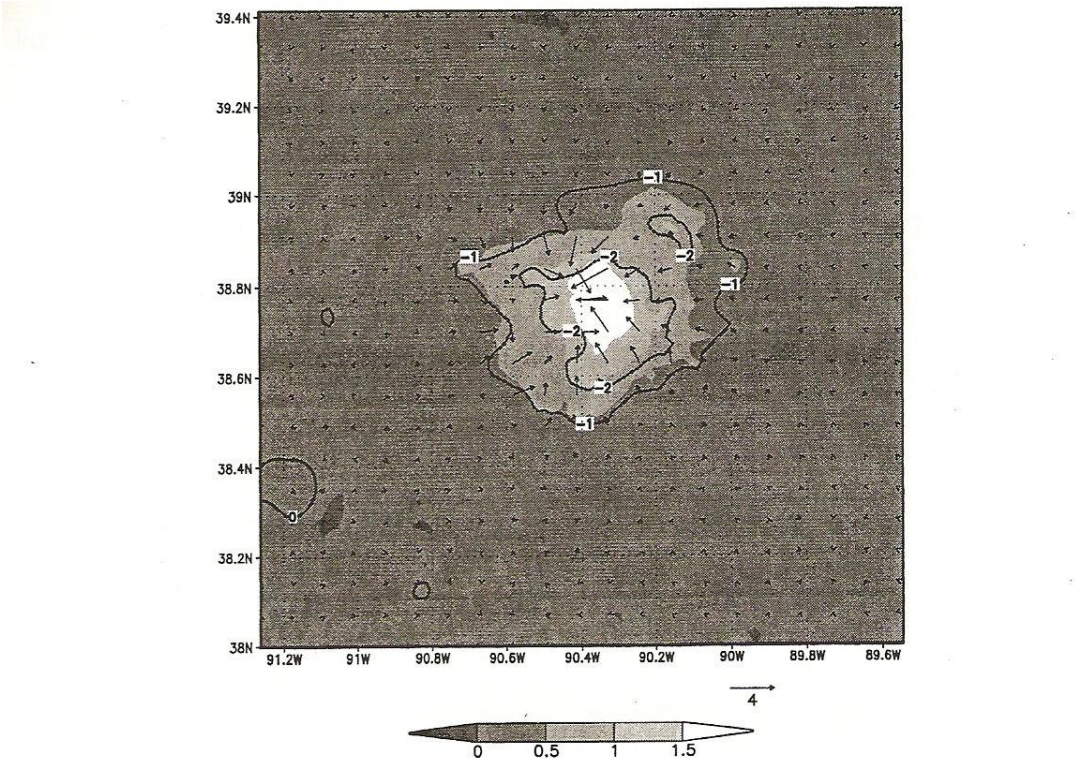

Fig A.7: Convergent flow pattern of a UHIC with no background winds. Adapted from Rozoff (2002).

As one would expect, this convergent flow near the surface would lead to upward vertical motion over the city. Fig A.8.a. is an example of how a flow pattern looks in cross section (taken from Yoshiado 1992). However, there is usually some magnitude of background flow that the UHIC is embedded in. In this case, the thermal forcing is shifted and slightly distorted downwind of the city. The modified forcing is shown in Fig A.8.b (again from Yoshiado 1992).

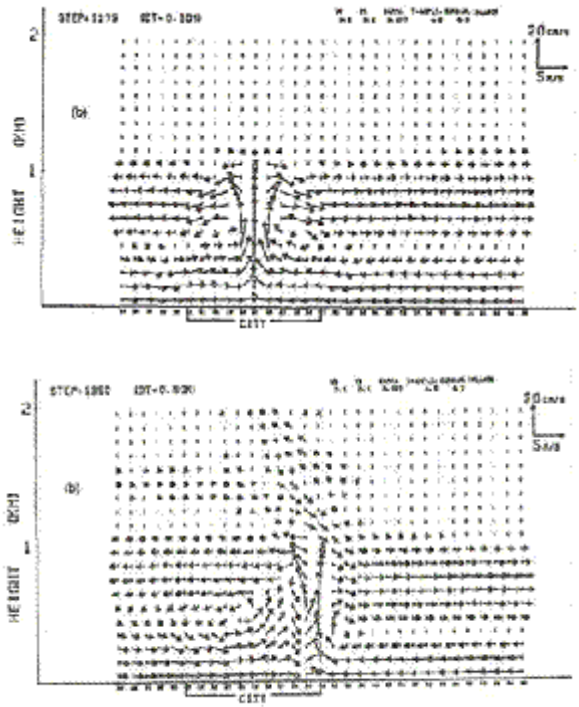

Fig A.8: Cross section of simulated UHIC without (a) and with (b) a background flow. Adapted from Yoshiado (1992)

Baik et al. (2001) examined the impact of the UHIC on vertical motion using a 2D model and found that the UHIC pattern is sufficient enough to exist under a wide range of background synoptic flows and could act as a convective forcing mechanism. Lemonsu and Masson (2002) found evidence of such a flow pattern in their modeling study of Paris, France. Lei et al. (2008) found a similar pattern over Mumbai, India. Bornstein and Lin (2000) found it over Atlanta, GA. Avissar (1996) found that the strength of the

UHIC was very sensitive to the size of the urban area. The UHIC is one of the primary factors believed to stimulate the precipitation maximum observed downwind of many urban areas. Because of this, many studies have looked at the influence of the UHIC on local convection. Details from these studies will follow in the next section.

It should not be surprising, since the UHIC is a response to a thermal imbalance, that the UHIC would act as a thermal regulator on the intensity of the UHI. Haeger-Eugensson and Homer (1999) were able to confirm that effect in the city of Goteborg, Sweden. In addition, one should expect the UHIC to interact with other local mesoscale flow regimes. Brazel et al. (2005) demonstrated that the UHIC influences the evening transition between upslope and downslope flows in the vicinity of Phoenix, AZ. By far, the flow interaction most often studied is interaction of the UHIC with the sea breeze, and results from those studies will follow the convection discussion.

b. Interaction of UHIC with Convection

Observation studies have generally borne out the fact that convective precipitation is enhanced over and downwind of large cities, while it is suppressed upwind. Papers like Pielke (2001) and Pielke et al. (2007) have demonstrated that convective precipitation is sensitive to land use and its alterations. It seems likely that the observed pattern of precipitation around urban areas could be the result of the UHI and the UHIC acting as a forcing mechanism. Huff and Changnon (1973) suspected this was the case, and an increasing number of studies are bearing this out. Craig (2002) confirmed that the UHIC was responsible for a convective event over Atlanta on one day during July, 2000. Dixon and Mote (2003) looked at a longer period in Atlanta and concluded that the UHIC was

probably having the greatest impact on convective precipitation on days when the atmosphere was marginally unstable, where the UHIC can provide that critical lift mechanism needed. Rozoff (2003) used a mesoscale model with an urban parameterization and looked at the impact of the UHIC over St. Louis as a convective initiator and found it was the most important factor for timing and location of convective initiation. Niyogi et al. (2006) conducted a similar experiment with a mesoscale convective system in Oklahoma City and concluded that inclusion of the urban effects improved the model performance, and the key factor to the improvement was the ability to obtain a better representation of the urban-rural heterogeneities. Lei et al. (2008) found that the mesoscale boundary produced by the UHI of Mumbai, India directly contributed to a record breaking heavy rain event there in 2005. Han and Baik (2008) concluded the UHIC could induce upward vertical velocity downwind of a city. Finally, Shepherd et al. (2010) found urban induced circulation features were critical factors leading to increased precipitation in their modeling study over Houston. Further, Gauthier et al. (2010) were able to rule out cell mergers as the primary cause of the local cloud-to-ground lightning maximum over and downwind of Houston leaving UHIC influences as the most probable forcing mechanism.

It is worth noting that the magnitude of effect will be directly related to the intensity of UHI generated by the city of interest. As was pointed out in the last section, the character of the UHI varies from city to city due to that city's particular characteristics. For example, a city that produces an afternoon urban cool island and experiences a convective potential maximum at that time will not likely impact precipitation the same

way (if at all). Therefore, it is essential to understand the character of an urban area prior to assuming its impact on convection.

c. Interaction of the UHIC with a Sea Breeze.

Just as the UHI circulation can act as a focus mechanism for convection, it can also interact with other naturally existing circulation patterns to produce other more complex mesoscale circulations. Given the large number of major urban areas located along the coast, the sea breeze is the mesoscale circulation most considered in urban interaction studies. Figure A.9 is adapted from Yoshikado (1992) and shows the results of a model

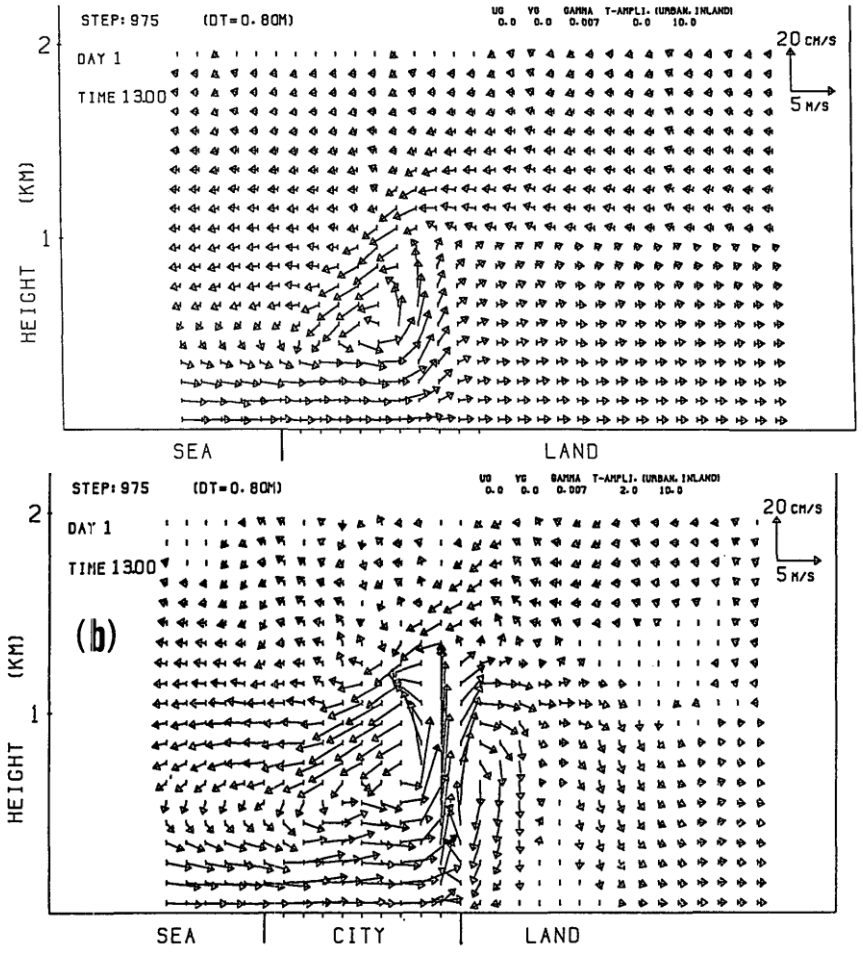

Fig A.9: Simulation of sea breeze without a) and with b) an UHI present. Adapted from Yoshikado (1992).

simulation of a sea breeze: a) without an UHI present and b) with an UHI present. Yoshikado found that this is not simply the addition of the UHI circulation with the sea breeze. Instead, non-linear forces were at work that caused the resultant uplift to be stronger than the sum of the two effects. Areas that derive rainfall triggered by sea breeze interactions should expect impacts if urban areas are present. (Note also that the same caveats given at the end of the last section apply here as well. The nature of the UHI, whether heat or cool island, will ultimately determine the degree of interaction.)

Kusaka (2002) looked at the impact of the growth of Tokyo on the development of the sea breeze using an urban parameterization and found stronger sea breeze system results when urban land class and parameterization are included. In fact, the presence of Tokyo has allowed the sea breeze to routinely penetrate through the entire Kanto Plain, a feature not observed in modeling studies without Tokyo present. Chen et al. (2007) found that precipitation in the Taipei valley has been enhanced by interaction between the UHI and the sea breeze, concluding that the effect has led to a 70% increase in afternoon thunderstorms versus a sea breeze alone. Martilli (2003) conducted a generic 2D modeling study of interaction between an urban area and a sea breeze and found that the sea breeze initiated quicker and grew stronger with an urban area present, but its penetration speed inland was slowed by the urban roughness. Also, the nighttime UHI reduced the intensity of the land breeze. Lo et al. (2007) found an urban parameterization was necessary to generate the observed strength and timing of the sea breeze system over Hong Kong during a modeling study. They found the intense UHI further intensified the land/sea temperature contrast driving a stronger sea breeze, which then drives further

inland. Ohashi and Kida (2002) continued the work of Yoshikado (1992) looking at the interaction of a sea breeze this time with multiple cities, one coastal, one inland. Again they confirmed the enhancement of the sea breeze by the UHI near the coast. This allowed a more powerful interaction with the inland urban area, creating complex flow behavior and significant pollutant transport. Ohashi and Kida (2004) then confirmed the modeled results of their 2002 study using the sea breeze urban behavior of Osaka and Kyoto in Japan. Pullen et al. (2008) showed that heterogeneity had an influence on the interaction of the UHI and sea breeze suggesting the importance of considering the morphology. Finally, Shepherd and Burain (2003) used data from the TRMM satellite to examine convective rainfall behavior around Houston, Texas and concluded that interaction between the UHIC and the sea breeze was the most likely cause of the precipitation anomalies. Shepherd et al. (2010) seemed to collaborate that for Houston when their modeling study showed that interactions between urban and non-urban (e.g. sea breeze) convergence zones contributed to more vigorous and wide spread precipitation then just urban or non-urban zones alone. Carrió et al. (2010) found a similarly strengthened sea-breeze convergence zone (and thus convection) in and around the UHI in their Houston modeling study.

The consensus among the studies reviewed is that the UHIC is a significant enough circulation pattern to interact with (in a non-linear way) other significant mesoscale circulation systems like the sea breeze, creating new and more complex flow patterns and forcings.

A.3. Current handling of Urban land surface in mesoscale models

a. General

Mesoscale models are routinely used to simulate boundary layer properties such as temperature, moisture, and wind at ever increasing resolution. Even the models used to make operational weather forecasts for civilian and military customers routinely use grid dimensions of 4-12 km, permitting them to simulate not just the synoptic scale effects on boundary layer properties, but the mesoscale effects as well (for example the impacts of a sea breeze, valley breeze, or a squall line). Many of these mesoscale flow systems are driven or influenced by features of the land surface. Avissar and Pielke (1989) demonstrated the value and necessity of coupling mesoscale models to a land surface model (LSM) capable of handling many different types of land surface characteristics in order to simulate these flow systems well. Since then, many different land surface models have been created to provide surface fluxes to parent mesoscale models. Henderson-Sellers et al. (1993, 1995) give a basic overview of several different types of land surface models available. More currently, Ek et al. (2003) provides details on the NOAH land surface model, which is the one coupled to operational mesoscale models used by both the Air Force and National Centers for Environmental Prediction (NCEP).

Regardless of the LSM, all are designed to process the surface energy balance for a number of different land surface types, including soil, vegetation (usually several types), water, and urban areas. Their output are surface fluxes (SH, LH, and momentum), used to drive the boundary layers of the parent mesoscale models. These models have tended

to concentrate on the processing of energy by vegetative, water, and soil surfaces, as these land class types represent the vast majority of land cover (more than 98% of the land cover in the US). Urban land class tends to be treated as a modified vegetation type given a higher roughness and different thermal properties that are a mix of concrete and vegetation. However, as demonstrated in earlier sections, the critical factors driving the processing of the urban energy balance includes the three dimensional urban geometry and anthropogenic sources. Without these features, it should come as no surprise if the current LSMs struggle to re-create a typical UHI and any subsequent UHIC. For example, Zehnder (2002) noted MM5 struggled to create a UHI over Phoenix, AZ. Georgescu et al. (2008) noted their lack of LSM urban representation hindered their ability to account for some of the UHI characteristics over Phoenix, AZ in their modeling study. In this study, the Regional Atmospheric Modeling System (RAMS) model will be used to simulate the mesoscale atmosphere. RAMS utilizes the Land Ecosystem-Atmosphere Feedback-2 (LEAF-2) model as its land surface model and is described in detail in the following section.

b. LEAF-2

The LEAF model is a vegetation parameterization model developed for use in the RAMS model. It was designed to calculate the exchange of momentum, energy, and water at the surface. The detailed description of the initial development of LEAF can be found in Lee (1992) and Lee et al. (1995).

Walko et al. (2000) describe the upgraded LEAF-2 model which added several new features to the original, including subgrid patch representation of land surface type, the

ability to handle snow and freezing/thawing soil, plus a better treatment of runoff. This is the version of LEAF used in this study. Soil and snowcover are divided into multiple vertical levels while vegetation is represented by a single level with an additional zone identified as 'canopy air'. LEAF-2 has the ability to offer multiple land surface patches. A given grid cell can have multiple sub-patches each with its own vegetation, soil and snowcover. The total flux for the grid cell is an area weighted average from the multiple patches. This allows effective utilization of land surface data at a higher resolution than what is being modeled in the parent mesoscale model. In vegetated areas, LEAF-2 models turbulent exchanges between the vegetation and the canopy air. Formation of dew or frost on the vegetation and ability to model vegetation intercepted precipitation are also features of LEAF-2. The model assumes that multiple longwave reflections do not occur.

LEAF-2 uses the Biosphere-Atmosphere Transfer Scheme (BATS) vegetation classes to define many of its land surface type parameters. BATS was originally developed for the NCAR community climate model and is described in Dickinson et al. (1986). Specifically the model uses leaf area index, fractional coverage, displacement height, roughness height, albedo, and emissivity for 18 specific classes of vegetation. In addition, another 12 classes were defined from the NASA/NOAA Land Data Assimilation System (LDAS) bring the total number of classes available in RAMS to 30. Table A.1 provides the details for each land class type. Leaf area index and fractional coverage have a simple seasonal dependence and thus vary from season to season. The table represents the highest or summer value.

TABLE A.1: Land Surface Properties used by LEAF-2. 0-17 based on BATS, 18-30 on LDAS

LEAF-2 Code	Type	Albedo	Emiss	LAI	dLAI	veg frac	d veg frac	z_o	zdisp	root depth
0	Ocean	0.14	0.99	0	0	0	0	0	0.1	0
1	Rivers, Streams (inland water)	0.14	0.99	0	0	0	0	0	0.1	0
2	Ice cap/glacier	0.4	0.82	0	0	0	0	0.01	0.1	0
3	Evergreen needleleaf tree	0.1	0.97	6	1	0.8	0.1	1	15	1.5
4	Deciduous needleleaf tree	0.1	0.95	6	5	0.8	0.3	1	20	1.5
5	Deciduous broadleaf tree	0.2	0.95	6	5	0.8	0.3	0.8	15	2
6	Evergreen broadleaf tree	0.15	0.95	6	1	0.9	0.5	2	20	1.5
7	Short grass	0.26	0.96	2	1.5	0.8	0.1	0.02	0.2	1
8	Tall grass	0.16	0.96	6	5.5	0.8	0.3	0.1	1	1
9	Desert	0.3	0.86	0	0	0	0	0.05	0.1	1
10	Semi-desert	0.25	0.96	6	5.5	0.1	0.1	0.1	0.5	1
11	Tundra	0.2	0.95	6	5.5	0.6	0.2	0.04	0.1	1
12	Evergreen Shrub	0.1	0.97	6	1	0.8	0.2	0.1	1	1
13	Deciduous shrub	0.2	0.97	6	5	0.8	0.3	0.1	1	1
14	Mixed woodland	0.15	0.96	6	3	0.8	0.2	0.8	20	2
15	Crop/mixed farming	0.2	0.95	6	5.5	0.85	0.6	0.06	0.7	1
16	Irrigated crop	0.18	0.95	6	5.5	0.8	0.6	0.06	0.7	1
17	Bog or marsh	0.12	0.98	6	5.5	0.8	0.4	0.03	1	1
18	Evergreen needleleaf forest	0.06	0.97	6	1	0.8	0.1	0.98	10.2	1
19	Evergreen broadleaf forest	0.08	0.95	6	1	0.9	0.5	2.21	20.7	1.2
20	Deciduous needleleaf forest	0.06	0.95	6	5	0.8	0.3	0.92	9.2	1
21	Deciduous broadleaf forest	0.09	0.95	6	5	0.8	0.3	0.91	7.2	1.2
22	Mixed cover	0.07	0.96	6	3.1	0.8	0.21	0.87	6.5	1.1
23	Woodland	0.08	0.96	5.7	2.3	0.8	0.17	0.83	7.4	1
24	Wooded grassland	0.18	0.96	5	4	0.8	0.2	0.51	3.6	1
25	Closed shrubland	0.1	0.97	5.1	3.7	0.63	0.19	0.14	1.4	0.7
26	Open shrubland	0.12	0.97	6	5.4	0.22	0.12	0.08	0.2	0.6
27	Grassland	0.11	0.96	2.6	2	0.73	0.11	0.04	0.2	0.7
28	Cropland	0.1	0.95	6	5.2	0.84	0.55	0.11	0.2	0.7
29	Bare ground	0.16	0.86	0.7	0.6	0.07	0.03	0.05	0.2	0.5
30	Urban and built up	0.15	0.9	4.8	3.6	0.74	0.31	0.8	1.1	0.8

In order for LEAF-2 to function it must have a land surface database in order to assign land class to the various patches. In this study, two different land surface data sets were used in order to assess the sensitivity of the system to land surface resolution. The first is the standard data set supplied with the RAMS model. It is derived from the 1-km Global

Ecosystem data set archived at the EROS Data Center. This data was collected in the 1992-1993 timeframe using the AVHRR instrument on NOAA polar orbiting satellites. This data set actually has a total of 94 land surface classes which have been cross referenced to the 30 types available in RAMS and then written to a latitude-longitude grid at 30-arc-second spacing. It will be referred to as the 30-sec land class data set (30 s). The second data set is a Land Use/Land Cover (LULC) 30 m high resolution land class data set. It was collected by the LANDSAT TM instrument in 1992-1993. It also was based on the 94 land classes and was re-binned into the 30 types available within RAMS. It will be referred to as the 30-meter land class data set (30 m). When doing a modeling study over an urban area it is important to note when the land class data set was collected as urban areas change significantly on decadal or even annual basis. This was a factor for this study and details on how this was dealt with are contained in the main chapters.

Both generations of LEAF have been featured in several validation efforts demonstrating the model's ability to couple with a mesoscale model to create realistic PBL structure and to drive important mesoscale features. Studies include Lee (1992), Lee et al. (1995), Vidale et al. (1997), Taylor et al. (1998), Pielke et al. (1999), Mihailovic et al. (2000), and Walko et al. (2000). However, these studies were all concerned with vegetative landscapes or interactions between vegetation and water or snowcover. As mentioned previously, the urban land class (#30) is really treated as another type of vegetation. This study hypothesizes that LEAF-2 will struggle to develop an UHI. By using LAI, LEAF-2 will process incoming energy and transpire as vegetation and not as artificial, non-porous surface. The roughness length is 0.8 which is exceeded by most large tree categories. The displacement height is likewise significantly

lower than most urban areas would see. Also, there is no ability to alter either the roughness length or displacement height from city to city although the morphology changes greatly between them. In addition, the roughness length has been shown to factor into convective initiation in cities (e.g. Rozoff 2003) and larger values should be assigned when warranted. In fact, there is evidence (Gaffen and Bornstein 1988; Loose and Bornstein 1977) that the extreme roughness of New York City can influence the passage of synoptic cold fronts. There is no accounting here for the difference in thermal capacity of the urban material, no capability to allow for LW or SW energy trapping within the urban canopy, and no capacity for including output from anthropogenic sources. In short, this LSM is not designed to develop an UHI, any UHIC that the UHI would drive, and thus any non-linear interaction with other mesoscale flow systems the model may actually be capable of developing. This shortfall is one of the primary factors motivating this study.

A.4. Motivation for improving mesoscale model handling of the urban PBL

From the above sections several conclusions may be drawn that begin to construct a case to motivate this research:

- The altered landscape of the urban area will process the surface energy balance differently then the surrounding landscape.
- This altered energy balance will drive the formation of an altered boundary layer over the urban area leading to altered sensible weather variables compared to the surrounding rural landscape.
- If the differences are great enough it will force a mesoscale flow system in an effort to restore balance, and this flow system will react with other natural mesoscale flow systems in the area, which will ultimately drive further alteration of the sensible weather in the vicinity of the urban area.
- Mesoscale models routinely used to create operational weather forecasts are modeling in the 4-12 km range and are coupled to LSMs in order to account for differing mesoscale PBL forcing and their impacts to near-surface sensible weather.

- Today's LSMs are not well designed to simulate the forcing introduced by the urban area, lacking most of the correct parameters important to urban PBL forcing.
- Therefore, today's operational weather forecasts in urban areas will not capture the mesoscale impacts of the urban area on the sensible weather, without altering current LSM to better account for the urban forcing.
- This urban effect is forced by a number of competing effects and interacts in a non-linear fashion with the surroundings, making a simple bulk approach inappropriate for mesoscale modeling needs.

The next task is to examine why it should be important for operational weather forecasts to incorporate the impact of urban areas into their forecasts of near-surface sensible weather variables.

While the urban land surface does not make up much of the land surface, it does hold an increasing percentage of population. Cohen (2003) states that in 2000 nearly 50% of the human population lived in urban areas, and of the 2.2 billion people expected to be added to the global population over the next 30 years, 2.1 billion of them will likely reside in urban areas. So while the urban area is small, the environment in and around it is experienced by a majority of the earth's population. Dabberdt et al. (2000) emphasized the need to improve mesoscale model performance in and around urban areas, especially in light of the relative percentage of population impacted by their effects. Sensible weather, from heat to precipitation, can have negative impacts on human populations and if the urban area is altering the likelihood of given weather events, then forecast models should be able to anticipate it. For example, Rosenzweig et al. (2009) found synoptic variation of UHI signature with UHI intensity greater during heat waves, further exacerbating the negative impacts of the heat!

Further, there are a number of civilian and military concerns that are impacted by near-surface sensible weather variables. There is an increasing interest in the day-to-day

impacts of air pollution and dispersion of hazardous materials (whether accidentally or purposely released). Military personnel need to predict the performance of precision weapons, night vision goggles, and even acoustical propagation. These agencies have created applications aimed at helping them forecast the impact of the above concerns from air quality to acoustical propagation. In the military, the term 'decision aid' has been applied to such applications. To avoid potential confusion in this study, the term 'model' will apply to the atmospheric mesoscale model and the term 'decision aid' will apply to these follow-on applications that use data from the weather model.

The decision aids used by civilian and military personnel require sensible weather input and most can accept data from gridded mesoscale model output. NCEP uses gridded output from its mesoscale model to drive their operational air quality and dispersion (HYSPLIT) decision aids. Military users routinely drive their military oriented decision aids with gridded mesoscale model output. Otte et al. (2005) describe a version of National Air Quality Forecasting System which consists of a chemistry decision aid driven by gridded output from an atmospheric mesoscale model and emphasizes the importance of performance over urban areas. Angevine and Mitchell (2001) and Banta et al. (2005) discuss the importance of the quality of mesoscale model output to the quality of results from an Air Quality decision aid. In particular, they emphasize the importance of the model's capability to simulate the PBL under clear skies, light winds, conditions most conducive to an UHI. Dr. Barron stated in his testimony before Congress (Barron 2003) that our mesoscale models are "not well designed for [the] urban environment." In addition, a 2003 National Academies study (Serafin 2003) on tracking and predicting atmospheric dispersion concluded a need for

improving the capability of meteorological models to account for urban surfaces. Masson (2006) calls for more studies to examine the impacts of urban parameterizations developed boundary layers vs. non-urban parameterization efforts. Baik et al. (2009) noted that dispersion models normally don't do that well when initialized by just routine urban observations because they are not temporally or spatially fine enough. Studies like Pullen et al. (2008), Chan and Leach (2007), Martilli (2007) and Collier et al. (2005) suggest that dispersion decision aids could benefit from more accurate gridded model input. Lemonsu et al. (2009) describes an effort to include urban effects in the Canadian GEM model in an effort to create better grids for decision aids to use as initialization.

Best (2006) recognizes that little work has been done to integrate urban parameterizations into wx forecast models and challenges the forecast community to demonstrate the importance of urban impacts to weather forecasts. To date, neither the National Centers for Environmental Prediction (NCEP) or the military weather centers utilize an urban parameterization in their operational models.

Summarizing, civilian and military personnel routinely rely on gridded atmospheric model data fields to drive decision aids that are sensitive to the quality of the atmospheric data provided. Based on today's LSM, it is suspected that mesoscale flow interactions and sensible weather are not being handled particularly well around urban areas. Thus, the primary motivation for this study is to evaluate the usefulness of an urban parameterization to supplement the LSM in an atmospheric model typical of that used by operational centers to improve atmospheric representation in and around urban areas.

A.5. Urban Parameterization Development Efforts

a. General

This is not the first study to recognize the need for a specific urban parameterization. Several urban parameterizations of varying sophistication have been developed for use in numerical weather models. Martilli (2007), Masson (2006), Best (2006), and Craig and Bornstein (2001) provides a general overview of techniques available. Efforts can generally be grouped into three classes of increasing sophistication.

The first are methods that use bulk parameterizations. Here, aspects of urban modification not included in common land surface schemes are provided and modeled in a simple bulk format. For example, a study may add a sky view factor and an anthropogenic flux directly to the land surface flux calculation, or they may provide many different types of urban land classes and alter the specific albedo, emissivity, etc in an effort to generate differences. Seaman et al. (1989) describes changes made to MM5 to account for St. Louis. These alterations did not explicitly consider the city as a 3D volume; instead each type of urban cover was given unique values of albedo, emissivity, thermal inertia, moisture and roughness. Run at 2.5 km on the inner nest, the model nudged things in the right direction, but it was underestimating the UHI intensity. In Taha (1999), instead of calculating the fluxes for various surfaces their integrated effect is accounted for instead. He found they could produce an UHI over Atlanta, GA with a 2 km inner nest, though the intensity was underestimated. Fan and Sailor (2005) injected just an anthropogenic term into the flux equations using MM5 and successfully generated

a UHI. Grossman-Clarke et al. (2005) used the bulk approach by injecting a skyview factor and anthropogenic term and by sub-dividing the urban land surface into three different types. They verified their model in a 2 km inner nest study over Phoenix, AZ. They returned to this study in Grossman-Clarke et al. (2008) and ran their model for a longer period of time than their original 3-day study (a total of 53 days) and found consistently improved 2 m temperatures and 10 m winds versus having no urban representation. Dandou et al. (2005) performed a bulk modification to MM5 to study the UHI over Athens in Greece. Biak et al. (2009) did a similar approach for urban study over Seoul, South Korea to provide initial fields to a dispersion model using MM5 with an inner nest of 1 km. Shem and Shepherd (2009) describe a bulk approach study using WRF over Atlanta, GA to study the impact of urban land cover on thunderstorms there. While their model did produce a UHI, they acknowledged the bulk approach as a limitation of their study. Both Silva et al. (2009) (over Phoenix, AZ) and Lynn et al. (2009) (over New York City) argued these bulk approaches as a cost effective tool to help public decision makers develop UHI mitigation strategies. Rozenzweig et al. (2009) used MM5 with a 1.3 km inner nest to study UHI mitigation strategies for New York City and was able to capture first order UHI effects with a simple bulk scheme. Shepherd et al. (2010) used a bulk approach in MM5 with an inner nest of 1.5 km to study the sensitivity of precipitation to changes in land surface in and around Houston expected over the next 25 years and found it produced the expected sensitivity. These are the simplest schemes and offer the advantage of not needing specific morphology information to operate and generally require less modification of the parent model.

Next up in terms of sophistication are the slab, pseudo slab, or single layer schemes. These schemes replace the land surface model for urban land class areas with a thermal model capable of modeling the effects of canyon geometry and thermal conductivity. They also account for anthropogenic fluxes by direct insertion or simple modeling. They are referred to as pseudo slabs or single layer schemes because the calculations treat the urban area as a volume for the purpose of flux calculation, but all of those fluxes are coupled to the surface only even if the morphology of the city extends up into the lower levels of the numerical model. These schemes also tend to assume MOST holds over an urban area, so no local scaling is done. These schemes need a description of the urban morphology to work. The Town Energy Balance (Masson 2000) model is an example of such a scheme and is the one selected for this work. Details on this particular model will be provided in the next section. Dupont and Mestayer (2006) describe the Soil Model for Sub-Mesoscale, Urbanized version (SM2-U), a parameterization meant for sub-1km simulations and verified it in a 1km single grid cell study. Jin et al. (2007) developed a slab scheme for application in large scale climate models and applied it to the CAM2/CLM2 model. Lo et al. (2007) used MM5 and a slab urban model parameterization to study sea breeze, UHI and pollution interaction over Hong Kong and found the urban area was necessary to describe the resultant winds and temperature patterns. Holt and Pullen (2007) used COAMPS over NYC to study the relative performance of two different types of urban parameterizations at very fine resolutions (.44 km inner nest) and generally found the slab model approach did as good or even better than more sophisticated multi-level model. Zhang et al. (2008) coupled the urban canopy model of Kusaka and Kimura (2004) to RAMS demonstrating its necessity in

modeling the presence of a UHI over a Chinese city. This same model was also coupled to WRF 2.2 and used to study the UHI of Beijing, China (Miao et al. 2009) at very high resolution (inner nest of 0.5 km) and found it reproduced most of the UHI characteristics observed on a day in Aug 2005. However, they did comment that at these high resolutions you are limited by the lack of vertical layer integration.

Finally, the most sophisticated schemes add local u* scaling to the thermal pseudo slab. In this case, the model is fully 3-D and interacts with the first several layers of the model to allow u* to vary by height. This also allows the model to provide the urban fluxes to the layer where the flux is released. These models require an urban morphology to perform the calculations and the resolution of the model must be fine enough to allow several vertical layers in the urban canopy in order for the scheme to work well. The multilayer Brown and Williams (1998) model seems to be one of the first developed. Otte et al. (2004) adapted this model for use in the MM5 urban canopy model. They found it did much better at reproducing the observations in urban areas. Martilli et al. (2002) described a multi layer urban parameterization for use in mesoscale models. It combines both a parameterized drag approach for momentum and TKE with the thermal effects on the surface energy balance. They demonstrated an ability to better reproduce the shape of vertical profiles of the turbulent momentum fluxes over urban areas than approaches that didn't use the parameterization. Their multi-layer approach permits momentum dissipation at levels other than the surface. They also are able to handle the alteration to the surface heat budget. They did not allow for direct input of anthropogenic (though it does allow heat escape from buildings). In Martilli (2003) the model was applied to the study of sea breeze interactions with an urban area at 1 km horizontal grid spacing. He

did tests with and without a 10 km wide city and found significant impact to the intensity and timing of the resultant sea breeze which had large impact on a hypothetical dispersion simulation. In Martilli et al. (2003) the model was applied to Athens at 2 km horizontal grid spacing and no variable morphology. They demonstrated the importance of including urban effects in pollution modeling. Roulet et al. (2005) used Martelli approach with a 1D column model approach and finds that inclusion of an urban parameterization improves the vertical profiles of fluxes against a tower in and above a street canyon.

The vast majority of studies with these urban parameterizations have been in UHI cause/effect or case studies of specific mesoscale flow interactions. In addition, nearly all of the studies sited in this review conducted their simulations at horizontal grid spacing of 2km or less. In contrast, very little attention has been paid to the readiness of these parameterizations for operational applications and the value they may bring to daily meteorological forecasts. These models are run every day in all types of meteorological regimes and are generally run at grid increments of 4 km or greater.

This study will explore the application of an urban parameterization to a model set to match a typical operational setting. The TEB model was selected in part because work has already been done to couple the model to RAMS (Rozoff 2002). But it was also selected because the high complexity urban parameterizations require greater low level vertical resolution than available in today's operational models and because Masson claims the parameterization is usable with horizontal grid increments up to 'several kilometers'. The following section will describe the parameterization in detail.

b. The Town Energy Balance (TEB) Model

Masson (2000) provides the foundation description of the model. The model is designed to replace the traditional land surface scheme approach and instead treat the urban area as a 3D volume with each grid cell containing a local street canyon system of roofs, walls, and roads. This allows the 3D geometry of the canyon to be simulated and its dynamic/thermodynamic impacts on the fluxes to be accounted for. The scheme tracks separate evolutions for roofs, walls, and roads which it aggregates to calculate the final fluxes. However, as mentioned above, all of the fluxes calculated in this 3D volume are provided as surface inputs to the parent model, even if the actual morphology of the urban area extends into the lower layers of the model. In order to function, the scheme requires a description of local urban morphology. The details of what is required will be discussed in Appendix B. The advantage of using morphological input is that it allows the model to develop a unique urban impact for each modeled city. In addition, there is no need to develop multiple urban land class use categories; the morphological data set describes the land use for the given cell and allows an infinite number of nuances in land use as are found in actual urban areas. The scheme also permits the addition of anthropogenic fluxes, though it does not model with them; instead it treats them as additions to the calculated natural fluxes. Finally the scheme has an internal building temperature model that permits climate controlled internal temperatures to interact with the natural climate outdoors. Masson et al. (2002) describes minor modifications to the original model and it is this version of the model used for this work.

As incorporated here, the model replaces the land surface scheme (LEAF-2) whenever the land surface patch is identified as 'urban'. Specifically, TEB is used to calculate surface sensible heat, latent heat, and turbulent fluxes over urban patches of grid cells. This original coupling of TEB to LEAF-2 was accomplished by Rozoff (2002). In addition to incorporating the newer 2002 version for this effort, the TEB scheme was also incorporated into the calculation of surface albedo and upward longwave radiation from the surface as calculated in the surface radiation scheme of the RAMS model. Another addition to Rozoff (2002) made here is the ability to vary the urban morphology by grid cell.

The TEB scheme has been validated in the literature and found capable of simulating the UHI effect. Lemonsu and Masson (2002) used TEB to successfully simulate the UHI of Paris, France demonstrating the impact of the urban area upon the local circulation pattern. Rozoff et al. (2003) used TEB to study convection initiation around St. Louis and found the urban parameterization improved the simulation by initiating convection along the urban heat island convergence zone down wind of the city as observed. Lemonsu et al. (2004) used TEB over Marseille, France and found its simulations compared well to measured sensible heat fluxes and urban fabric storage. Offerle et al. (2005) used TEB to study a major city in sub-Saharan Africa and found the parameterization did a reasonable job reproducing the urban cycle concluding that TEB was fit for use in mesoscale models. Roberts et al. (2006) uses TEB, again over Marseille, France, and found that it did a remarkable job simulating the urban heat storage. Van Den Heever and Cotton (2007) also used TEB to study influence of urban aerosols and concluded that TEB faithfully simulated the UHI. Hamdi et al. (2009) used

TEB to study the UHI signature as it related to the climate stability of Brussels and found that UHI signatures were likely contributing to climate change measurements. Trusilova et al. (2009) coupled TEB to MM5 in order to study potential effects of urban expansion in Europe. They found TEB able to simulate urban effects with their relatively coarse grid increment of only 10km. Lemonsu et al. (2009) describes an effort to integrate TEB into the Canadian GEM model in order to create a Canadian Numerical Urban Modeling System. For this effort, TEB was used whenever the model grid was 2.5km or finer. Finally, Carrió et al. (2010) coupled TEB to RAMS for their cloud resolving modeling study over Houston and found the system developed the expected UHI response.

A.6. Scope of this Effort

This effort will assess the impact of an urban parameterization (TEB) in a mesoscale model (RAMS). Unlike most previous studies of urban parameterizations that ran with very fine inner nests (<2 km), this effort will run in a configuration closely matching current operational configurations in the civilian and military forecast centers (>4 km). Thus, a primary question to be addressed is the ability of the urban parameterization to function at relatively 'coarse' resolution. In addition, this work will build upon Rozoff (2002) efforts to couple TEB to RAMS by adding the ability to vary the morphology by grid cell.

Simulations were run for 26-27 Jun 1984 over Washington DC, a night when an UHI was expected to form. Primary interest is to assess the impact of TEB by validating against near-surface sensible weather obtained from the METREX campaign conducted in Washington, DC that year. Sensitivity tests will also be performed to assess how

aspects of today's operational model configuration will affect implementation of an urban parameterization like TEB and to determine how detailed morphology information needs to be at today's modeling resolution. Simulations were also conducted under two different synoptic conditions (building fall high pressure on 7-8 Nov 84, and a variably cloudy air mass exchange day on 7-8 Jan 84) to assess the impact of TEB when stronger synoptic forcing was present.

It is hypothesized that inclusion of the urban parameterization will improve the performance of the sensible weather prediction over the urban area as measured during METREX. The sensitivity tests will also provide data to consider when deciding how to implement an urban parameterization into an operational model.

APPENDIX B: CREATION OF A MORPHOLOGY AND LAND SURFACE DATASET FOR WASHINGTON, DC

B.1. Creation of an Urban Morphology for Washington, DC

TEB requires morphology information in order perform its calculations. Table B1 describes the elements TEB expects. In the original coupling of RAMS/TEB (Rozoff, 2002) morphology information was not allowed to vary by gridpoint, so a city wide average was used at each point instead. However, Pullen et al. (2008) suggests that morphology heterogeneity plays a role in UHI development, thus for this study, the RAMS/TEB interface was altered to allow the morphology variables to vary by grid point, thus allowing a more complete treatment of a city's morphology. To take advantage of this, a morphology database of Washington DC was needed.

In the aftermath of September 11, 2001, a vigorous program to create city morphologies emerged. Most are taking advantage of Geographic Information Systems (GIS) technology (e.g. Burian et al. 2005). Such a database could have been available for use in this study. However there are a couple of problems with this for the purpose of the study. First, this approach only estimates 4 of the 16 variables listed in Table B1, which limits the amount of grid cell variation that can be assessed. Further, any database made today will depict Washington DC as it is in the 21st century, while the time period of interest is the mid 1980's. Census data shows that the Washington DC area population grew by nearly 30% from 1990 and 2000. Further, a study by Johnston and Watters

(1996) used Landsat imagery to demonstrate that the amount of urban fabric increased 7% between 1982 and 1993, growth they referred to as 'explosive'. Hamdi et al. (2009) found decadal changes to Brussels morphology landscape has led to measureable changes in the city's UHI signature. Therefore a database created using data from 2000 could be suspect for use in the mid 1980's.

Table B1: Elements TEB requires from the morphology file with a description.

Morphology Element	Description
Building Height (h)	Average building height within a grid cell in Meters. Information varies by grid cell.
Fractional area of buildings (bld)	Identifies the fraction of urban fabric occupied by roof area. The remaining fraction is classified as road. Information varies by grid cell.
Building Aspect Ratio (h/l)	Identifies the shape of the urban canyons and is the ratio of the height of the building to the distance between buildings. This is critical to determine dynamic flow category and to determine the sky view for radiation calculations. Information varies by grid cell.
Dynamic Roughness (Zo)	Used to determine the amount of dynamic drag induced by the urban fabric. For this study, Zo=h/10. Information varies by grid cell.
Albedo / emissivity Roads (aroad, eroad)	Albedo and Emissivity values for roads. Area of concrete vs. asphalt was estimated. Resultant value is an area weighted average of characteristics from concrete and asphalt. Information varies by grid cell.
Albedo / emissivity Roofs (aroof, eroof)	Albedo and Emissivity values for roofs. All roofs categorized as housing, non-housing light, or non-housing dark. Resultant value is an area weighted average of the categories. Information varies by grid cell.
Albedo / emissivity Walls (awall, ewall)	Albedo and Emissivity values for walls. Value drawn from Rozoff (2002). Information fixed for all grid cells.
Building material characteristics	Includes number and thickness of road, roof, and wall layers with thermal conductivity and heat capacity of each layer. All values were drawn from Rozoff (2002) and information remained fixed for all grid cells.
Internal Building Temperature (tbld)	Set at 293.16K. Used along with building material characteristics to calculate the temperature wave. Fixed for all grid cells.
Sensible and Latent heat from traffic (sh_traffic, le_traffic)	Values of sensible and latent heat generated from traffic. Three categories of traffic use identified: housing, downtown, and interstate and given different values. Grid cell total is an area weighted average and therefore varies.
Sensible and Latent heat from industry (sh_industry, le_industry)	Values of sensible and latent heat generated from industry. Value set to 10 and 5 W/M^2 respectively for any grid cell identified with industry present, zero otherwise. Value varies by grid cell as a binary value.

Given these shortcomings, an effort was undertaken to construct a unique morphology database for Washington, DC more representative of a time closer to the mid -1980's. Figure B1 is a plot of the 30-second (approx 1 km) land surface data set provided with RAMS. Yellow represents urban cells, green is vegetation, and blue is water. Using this plot, a rectangular area (red outline 36 X 32 km on the figure) was identified within which the morphology would be created. Three sources were used to construct the

database. The USGS 1:24,000 map series for the counties surrounding Washington DC provided details on land use, and a readymade 1 km grid layout. A series of high altitude photographs (also at 1:24,000) obtained from USGS provided specific details on the urban fabric, and the book "Above Washington DC" (Camaron 2000) provided detailed photography of various neighborhoods to provide additional morphology details.

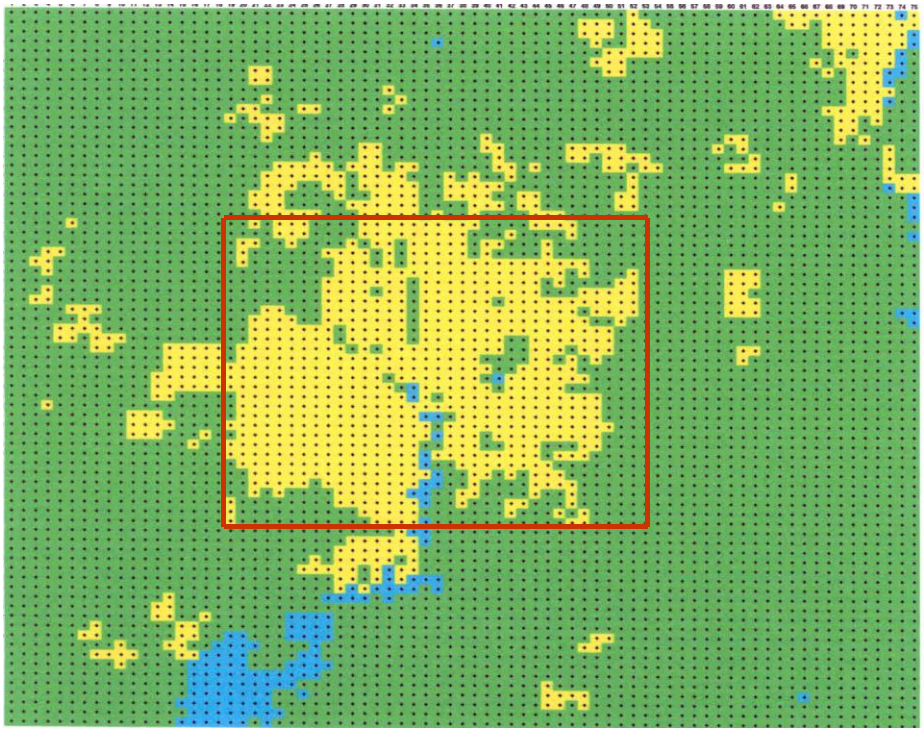

Fig B1: 1km land surface data plot around Washington DC. Yellow is urban, green vegetation, and blue is water. Red rectangle indicates boundaries of the created morphology.

The dates on the USGS maps ranged from 1979-1984 and the photographs used were taken in Apr 1981 and Mar 1983, thus the resulting morphology is estimated to be a good representation of the Washington DC area for the early 1980's. Using these sources, the values for 11 of the 16 elements were estimated and thus would be able to vary by grid cell. The remaining variables were assigned a default value from the literature and remained fixed for all grid cells.

Each of the USGS maps contains a 1 km grid that became the grid layout for the morphology. There are a total of 1152 grid cells in the 36 X 32 km area. For each grid cell the USGS maps and corresponding area on the photographs were used to determine the morphology characteristics. Carmaron's book was used to provide specific information on the nature of various neighborhoods and specific landmarks around the city. To aid in the process, a scaled 1 km grid square was traced onto a sheet of transparency. Stenciled within this larger grid were 16 equally sized, smaller grids. This transparency was then placed over both the USGS cell and the corresponding area on the photograph, allowing the area of various land types to be estimated in 16ths. Figure B2 shows an example of the procedure for a grid cell on the Washington West USGS map. Here $2/16^{th}$ of the area was identified as vegetation due to the presence of Washington Circle while the remainder of the area was classified as downtown structures averaging 7 stories in height.

Data for each grid cell were entered onto a standard form shown in Figure B3. Each grid cell on the map was given a name indicating which USGS chart it appeared on and where the grid cell was located on the chart (e.g. 'Washington West row 3/ column 7'), plus the central latitude/longitude was documented. The total 16ths of water and vegetation was estimated. For the vegetation, the area was then further broken down by type.

When it came to the urban portion of a cell, it became apparent that the majority of the urban fabric was made up of housing. Further, these housing areas could be largely grouped into four classes or types, each of which was given a default set of characteristics. The total 16ths for each housing type was estimated and entered into the

a) b)

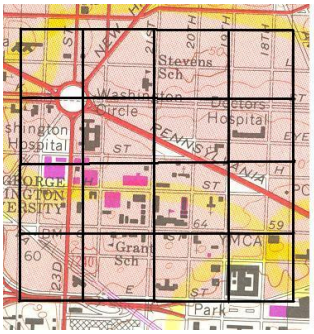

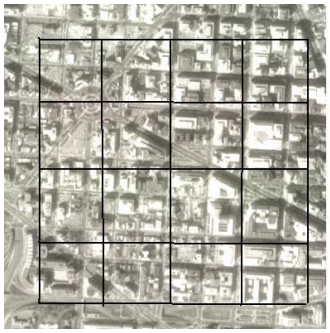

c)

Fig B2: Examples of a) USGS map, b) High Altitude Photo, and c) Photo from "Above Washington" (note rotated orientation) for one 1km grid cell. In this example, 14/16ths were identified as 'downtown' with avg height of 21m (7-stories), 70% roofs/30% roads, aspect ratio of 1, and roughness of 2.1m (h/10). The remaining 2/16ths were categorized as vegetation, 70% grass, 30 % trees.

MAP:_____ LAT:_____ LONG:_____

_____ 16th Water

_____ 16th Veg ____Trees ____Grass ____ Mixed _____Crops ____ Bare

_____ Sub-Urban
h=7m, h/l=.3, bld=.4, gray roofs, veg 40%, 15% trees, 85% grass

_____ Sub-Urban M
h=7m, h/l=.3, bld=.4, gray roofs, veg 40%, 50% trees, 50% grass

_____ Gridded "7"
h=7m, h/l=.5, bld= 5, gray roofs, veg 30%, 50% trees, 50% grass

_____ Gridded "10"
h=10m, h/l=.75, bld=.6, gray roofs, veg 20%,60% trees, 40% grass

_____ Other: ____ h, _____ h/l, _____ bld, _____ d/l roofs, _____ veg

_____ Other: ____ h, _____ h/l, _____ bld, _____ d/l roofs, _____ veg

_____ Other: ____ h, _____ h/l, _____ bld, _____ d/l roofs, _____ veg

_____ Other: ____ h, _____ h/l, _____ bld, _____ d/l roofs, _____ veg

_____ Other: ____ h, _____ h/l, _____ bld, _____ d/l roofs, _____ veg

_____ Ratio Asphalt / Concrete Roods.

Remarks:

Fig B3: Sample sheet used to document morphology elements for each 1km grid cell.

sheet just below the vegetation. Fig B4 shows an example of each of the four sub-classes as seen in the high altitude photographs and from Camaron's book (where available), and Table B2 discusses the characteristics of each type. In general, the four types of housing areas form growth rings around the city. The oldest (nearest to the city core) neighborhoods are the 'gridded-10', with the 'gridded-7' and two sub-urban types further from the core respectively. For simplicity all housing roofs were assigned the characteristics of an Aspen Grey asphalt shingle (albedo .18, emissivity .91 from Parker et al. 2000) which was in the middle of characteristics presented for various types of asphalt shingles.

Urban areas that could not be classified as a type of housing were dealt with independently and classified as 'Other' on the sheet in Figure B3. Using the available sources, an attempt was made to determine the specific nature of the features (e.g. shopping center, rail yard, interstate, commercial district, hotel) and then the characteristics of that type were estimated and entered separately in the form. Albedo and emissivity for the roofs in these areas were dealt with by examining their appearance in the high altitude photographs. The percentage of 'dark' roofs (d roofs) were estimated and used to calculate a weighted average of albedo between .05 (very dark) and .25 (very light) and a weighted average of emissivity between .91 and .88. Note also that all urban areas were given some vegetation percentage to account for landscaping around the buildings and parking lots. Finally at the bottom of the sheet in Fig B3, the characteristics of the roads in this grid cell were estimated by providing the ratio of dark asphalt vs. lighter concrete. Several studies, including Pomerantz et al. (1998) showed that while fresh asphalt may have an albedo a low as .04, they quickly weathered to an

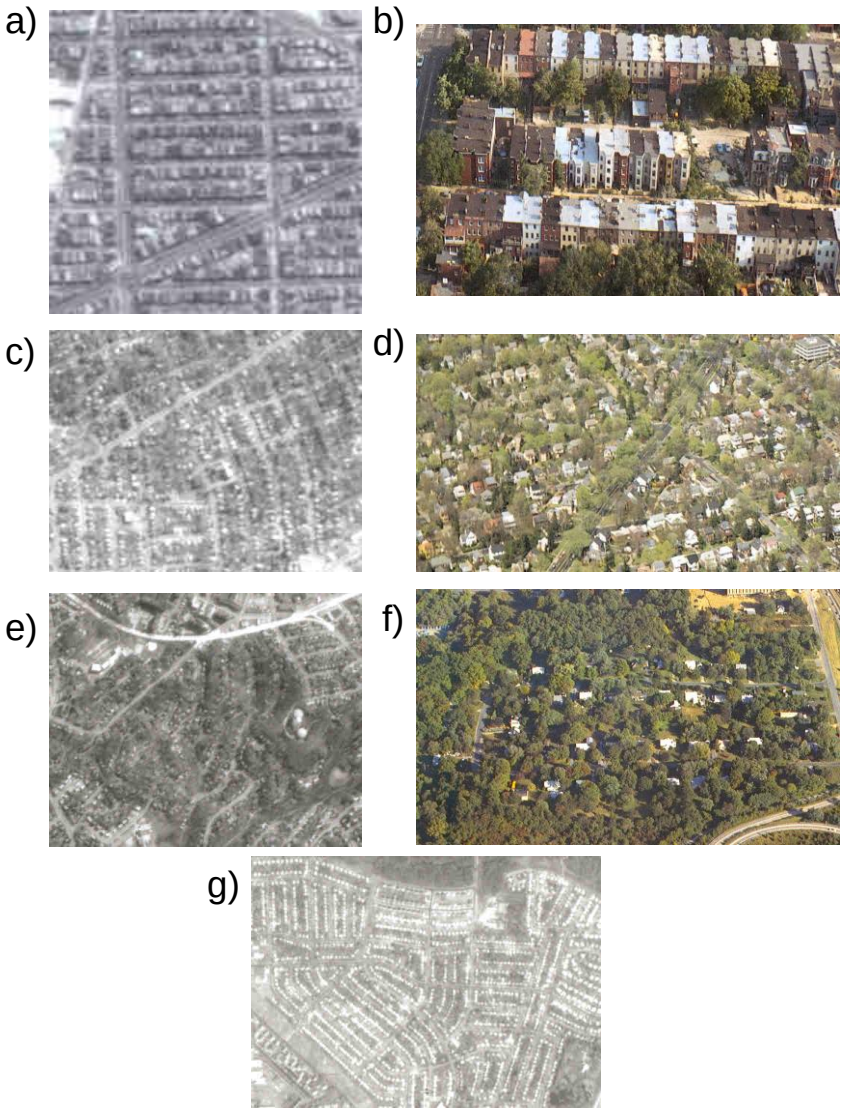

Fig B4: Photos of the four different residential neighborhoods: a) & b) 'Gridded-10', c) & d) 'Gridded-7', e) & f) 'Sub-Urban Mature' and g) 'Sub-Urban' (no color picture).

albedo of .12. Likewise, fresh concrete could have an albedo above .5, but they quickly darkened due to road grime to values around .25. Thus the final road albedo was weighted against the ratio of asphalt to concrete using an asphalt albedo of .12 and a concrete albedo of .25. Emissivity values were weighed between .95 and .90 based on similar data.

Table B2: Description of details for the four residential categories.

Name	Description	Bld Height (m)	aspect ratio	Fractional area of roofs vs. roads	% Veg	% Trees	% Grass
Gridded-10	Oldest residential areas. Row houses generally 3 or 4 stories with flat roofs, Houses are densely packed with little vegetation and narrow streets	10	0.75	0.6	20%	60%	40%
Gridded-7	First sub-urban areas. Mature neighborhoods with lots of trees. Houses are generally 1-2 stories with pitched roofs. Steets are generally gridded, houses have small yards.	7	0.5	0.5	30%	50%	50%
Sub-Urban Mature	Next major wave of sub-urban building. 1-2 stories situated on larger lots with winding and wider streets. Area is old enough to have mature tree growth	7	0.3	0.4	40%	50%	50%
Sub-Urban	Newest neighborhoods, similar in structure to 'Sub-Urban Mature', but without the mature tree growth.	7	0.3	0.4	40%	15%	85%

TEB also uses anthropogenic information on traffic and industry. Grid cell variations of these were allowed by using some simple calculations. First, the contribution of industry was calculated by determining if there was any commercial or industrial percentage in the cell. If there was, then default values of $10W/m^2$ and $5W/m^2$ were assigned to sensible and latent heating respectively. For traffic a bit more involved procedure was used. Traffic volume maps were examined and it became apparent that traffic volume was highest along the interstates and downtown areas with significantly

lower values in the sub-urban areas. To account for this spatially varying traffic volume a weighted average system was devised based on the number of 16^{th} of sub-urban vs. downtown infrastructure identified with a plus-up added for those grid cells that contained an interstate segment. The final formula created potential values that varied from zero to a theoretical maximum of 25 W m^{-2} for sensible heat. Latent heat for traffic was assumed to be zero. Also, no effort was made to introduce a diurnal variation, though efforts along this line may make a worthy follow-on effort.

All of this information for each of the 1152 grid cells was entered into a spreadsheet. The end result was a morphology database that contained not only the urban fabric estimations, but also an estimated vegetation characterization as well. Tables B3 and B4 (at the end of this appendix) presents the database for all 1152 grid cells. Table B3 shows the raw data collected into the sheets where table B4 shows the resulting TEB values. The total domain averages for the TEB values were also calculated (last set of values in table B4) and was used to conduct a sensitivity test using just one average value for all grid cells. This 1 km database was then aggregated up to 5 and 20 km to allow it to be used in the current study.

B.2. Creation of the Land Surface Dataset

One of the primary advantages to using variable morphology is that there is no need for many different types of urban land class categories such as ‘industrial’, ‘residential’, or ‘commercial’ in order to model the land surface variations within the city. Instead, one ‘urban’ land class can be used and the TEB model will model different urban areas based on the provided morphology.

Even with this relative simplicity, there is still the matter of what source to use for land surface information. There are a number of land surface data sources available varying both in method of obtaining and also in resolution. The RAMS model comes with a standard 30 s (approximately 1 km) land class data set derived from Advanced Very High Resolution Radiometer (AVHRR) data in 1992-1993 and made available from the United States Geological Survey (USGS) Earth Resources Observation System (EROS). In addition, for this study, a land use/land class (LULC) data set collected at a resolution of 30 m was obtained for a 75 X 75 km area around Washington, DC. This data was collected by a joint effort of the USGS and the U.S. Environmental Protection Agency. A number of sources were used, including the Landsat Thermatic Mapper, high resolution terrain databases, Bureau of Census; USGS land use and land cover, plus the National Wetlands Inventory. The end result is collectively known as the National Land Cover Data (NLCD).

One of the fallouts of the morphology data base creation is an independent urban, water, vegetation estimation for the 36 X 32 km area over Washington, DC. Because of the sources, this estimate should be more representative of the early 1980's. However, it also attempted to account for the fact that even the most urban areas (shopping malls, business districts etc) are not pure artificial surface, but contain at least some vegetation, a practice not used with the other two sources. Thus this urban estimate is likely more an estimate of the percentage of impervious surface and should be much lower. It is worth noting that this is the type of information TEB expects as it deals only with impervious surface leaving all vegetation to the parent land surface model.

In the end, for the area immediately around Washington DC, three land surface data sets were created; the RAMS and LULC raw data sets formed the first two. For the third, the morphology derived urban and vegetation numbers were used to overwrite the LULC data over the Washington, DC area creating a LULC-Modified data set. These three sets were used to test the sensitivity of the modeled UHI to total urban land cover.

RAMS also offers the capability to model multiple land surface patches for each grid cell. Information from the land surface data sets were aggregated up to the resolution of each nested grid and percentages of land class types were calculated based on the number of patches modeled for each grid cell. For this study, the land surface model was run with four patches for each grid cell; once for any water percentage, and then three more times for the leading three land surface types present. Total grid cell fluxes are then simply a weighted average of the contribution from each of the four patches.

Once these three sets were aggregated to 5 km for use on the inner model nest, there was little visual difference between the RAMS and LULC database in terms of the dominant land class of the first patch. However, when the actual percentage of urban land class is calculated for each in the 1152 square kilometer area centered on the city (this is the area within the 5 km inner nest that contains the variable morphology area), the differences can be seen. The AVHRR is 72% urban, the LULC is 60% and the LULC-Mod is 37%.

Table B.3: Raw morphology/land surface data for each 1152 1 km grid cells

USGS Map Information			Grid Center		16th's		Housing Areas - Total 16th's				Other Urban						
map	row	col	lat	long	Veg	Water	Sub-U	Sub-U-M	Gridded "7"	Gridded "10"	16th's	height	bld	d roofs	h/l	veg	asphalt
ROCKVILLE	4	2	39.0319	-77.2359	16												
ROCKVILLE	4	3	39.0321	-77.2243	15			1									1
ROCKVILLE	4	4	39.0323	-77.2127	14			2									1
ROCKVILLE	4	5	39.0325	-77.2011	14.5	0.5					1	10	1	0	0	1	1
ROCKVILLE	4	6	39.0327	-77.1895	14		2										1
ROCKVILLE	4	7	39.0329	-77.1779	7		9										1
ROCKVILLE	4	8	39.0331	-77.1664	7		5				4	10	1	0	0	0	1
ROCKVILLE	4	9	39.0333	-77.1548	14		1				1	10	1	0	0	0	1
ROCKVILLE	4	10	39.0335	-77.1432	13						3	10	0	0.3	0	0	1
ROCK/KENS	B4		39.0338	-77.1316	8		7				1	7	0	0.47	0	0	1

KENSINGTON	4	1	39.0340	-77.1200	14		1				1	10	1	0	0	1	1
KENSINGTON	4	2	39.0342	-77.1084	10.5		1.5	3			1	10	1	0	0	1	1
KENSINGTON	4	3	39.0344	-77.0968	2			9.5			4.5	10	1	0.17	0	0	1
KENSINGTON	4	4	39.0346	-77.0853	6			10									1
KENSINGTON	4	5	39.0348	-77.0737	2			14									1
KENSINGTON	4	6	39.0350	-77.0621	3.5			10.5			2	8.5	0	0.25	0	0	1
KENSINGTON	4	7	39.0352	-77.0505	1		3.5	6			5.5	8.1	1	0.32	0	0	1
KENSINGTON	4	8	39.0355	-77.0389	7			8			1	7	1	0.5	0	0	1
KENSINGTON	4	9	39.0357	-77.0273	7			6			3	10	1	0.25	0	0	1
KENSINGTON	4	10	39.0359	-77.0157	6.5			9.5									1
KENS/BELT	B4		39.0361	-77.0042	8	0.5		7.5									1
BELTSVILLE	4	1	39.0363	-76.9926	6		6				4	20	0	0.5	0	0	0.66
BELTSVILLE	4	2	39.0365	-76.9810	12						4	10	0	0	1	0	1
BELTSVILLE	4	3	39.0367	-76.9694	14.7	0.3					1	7	0	0.3	0	1	1
BELTSVILLE	4	4	39.0369	-76.9578	16												
BELTSVILLE	4	5	39.0371	-76.9462	9			5.5			1.5	10	0	1	1	0	0.83
BELTSVILLE	4	6	39.0374	-76.9346	11.7	0.3	1				3	10	0	0.5	1	0	0.2
BELTSVILLE	4	7	39.0376	-76.9231	7		9										1
BELTSVILLE	4	8	39.0378	-76.9115	2		14										1
BELTSVILLE	4	9	39.0380	-76.8999	8.5		1				6.5	7	1	0.4	1	0	1
BELTSVILLE	4	10	39.0382	-76.8883	16												
BELT/LAUREL	B4		39.0384	-76.8767	16												
LAUREL	4	1	39.0386	-76.8651	16												
LAUREL	4	2	39.0388	-76.8535	13.5						2.5	8	0	0.5	0	0	1
LAUREL	4	3	39.0391	-76.8420	16												
LAUREL	4	4	39.0393	-76.8304	16												
ROCKVILLE	3	2	39.0229	-77.2356	14	2											
ROCKVILLE	3	3	39.0231	-77.2240	14			2									1
ROCKVILLE	3	4	39.0233	-77.2124	13			2			1	10	1	0	0	1	1
ROCKVILLE	3	5	39.0235	-77.2008	14		1	1									1
ROCKVILLE	3	6	39.0237	-77.1892	15						1	10	1	0	0	0	1
ROCKVILLE	3	7	39.0239	-77.1777	11		4	1									1
ROCKVILLE	3	8	39.0241	-77.1661	8		5				3	10	0	0	0	0	1
ROCKVILLE	3	9	39.0243	-77.1545	8	1		1			6	36	0	0.4	1	0	1
ROCKVILLE	3	10	39.0245	-77.1429	6						10	9	0	0.2	0	0	1
ROCK/KENS	B3		39.0248	-77.1313	6		2	1			7	24	0	0.4	0	0	1
KENSINGTON	3	1	39.0250	-77.1197	4.5			9			2.5	8.5	0	0.2	0	0	1
KENSINGTON	3	2	39.0252	-77.1081	9	0.5		1.5			5	50	0	0.1	0	1	1
KENSINGTON	3	3	39.0254	-77.0966	10			3			3	10	1	0.37	0	0	1
KENSINGTON	3	4	39.0256	-77.0850	2		3.5	9			1.5	7	1	0.5	0	0	1
KENSINGTON	3	5	39.0258	-77.0734	2		2	6			6	8	1	0.5	0	0	0.8
KENSINGTON	3	6	39.0260	-77.0618	2.5		5	8.5									1
KENSINGTON	3	7	39.0262	-77.0502			10	4.5			1.5	9	0	0.5	0	0	0.8
KENSINGTON	3	8	39.0265	-77.0386			10	2.5			3.5	10	1	0	0	1	1
KENSINGTON	3	9	39.0267	-77.0271	4		8	4									1
KENSINGTON	3	10	39.0269	-77.0155	3		7	5			1	7	0	0.47	0	0	0.7
KENS/BELT	B3		39.0271	-77.0039	9			7									0.9
BELTSVILLE	3	1	39.0273	-76.9923	8		8										1
BELTSVILLE	3	2	39.0275	-76.9807	4			11.5			0.5	7	0	0.47	0	0	0.7
BELTSVILLE	3	3	39.0277	-76.9691	1.5			12			2.5	12	0	0	1	0	1
BELTSVILLE	3	4	39.0279	-76.9576	9.5	0.5	6										1
BELTSVILLE	3	5	39.0282	-76.9460	14.5						1.5	0.1	0	0	0	0	0
BELTSVILLE	3	6	39.0284	-76.9344	15	1											
BELTSVILLE	3	7	39.0286	-76.9228	5.5		5				5.5	7.81	1	0.6	1	0	1
BELTSVILLE	3	8	39.0288	-76.9112	1			1			14	10	1	0.3	1	0	1
BELTSVILLE	3	9	39.0290	-76.8996	16												
BELTSVILLE	3	10	39.0292	-76.8881	15						1	10	0	0	1	0	1
BELT/LAUREL	B3		39.0294	-76.8765	16												
LAUREL	3	1	39.0296	-76.8649	16												
LAUREL	3	2	39.0298	-76.8533	14.5						1.5	0.1	0	0	0	0	1
LAUREL	3	3	39.0301	-76.8417	16												
LAUREL	3	4	39.0303	-76.8301	16												
ROCKVILLE	2	2	39.0139	-77.2353	14	1	1										1
ROCKVILLE	2	3	39.0141	-77.2237	14		2										1
ROCKVILLE	2	4	39.0143	-77.2121	9.5		2	3			1.5	7	1	0.5	0	0	1
ROCKVILLE	2	5	39.0145	-77.2005	12		2	2									1
ROCKVILLE	2	6	39.0147	-77.1890	16												
ROCKVILLE	2	7	39.0149	-77.1774	13		3										1
ROCKVILLE	2	8	39.0151	-77.1658	12	0.5		3			0.5	10	1	0.1	0	0	1
ROCKVILLE	2	9	39.0153	-77.1542	11.5	0.5		3			1	7	0	0.47	0	0	1
ROCKVILLE	2	10	39.0155	-77.1426	9		2.5	2			2.5	7	0	0.47	0	0	1
ROCK/KENS	B2		39.0158	-77.1310	1		2	12			1	7	0	0.47	0	0	1
KENSINGTON	2	1	39.0160	-77.1195	1.5			12.5			2	7	0	0.47	0	0	1
KENSINGTON	2	2	39.0162	-77.1079	8.5			2.5			5	45	0	0.2	0	0	0.9

KENSINGTON	2	3	39.0164	-77.0963	7			7.5			1.5	7	0	0.47	0	0	0.8
KENSINGTON	2	4	39.0166	-77.0847				15			1	10	1	0	0	0	0.8
KENSINGTON	2	5	39.0168	-77.0731				14.5			1.5	10	1	0.8	0	1	0.8
KENSINGTON	2	6	39.0170	-77.0615	12			3			1	7	0	0.47	0	0	1
KENSINGTON	2	7	39.0172	-77.0500	6		5	2			3	10	0	0.2	0	0	1
KENSINGTON	2	8	39.0175	-77.0384	3		7	2			4	12.5	0	0.2	0	0	0.5
KENSINGTON	2	9	39.0177	-77.0268	4		8	3			1	7	0	0.47	0	0	0.5
KENSINGTON	2	10	39.0179	-77.0152	2.5		8	2.5			3	7	0	0.47	0	0	0.3
KENS/BELT	B2		39.0181	-77.0036	2		3	7.5			3.5	10	0	0	0	0	0.4
BELTSVILLE	2	1	39.0183	-76.9921	9		6				1	7	0	0.47	0	0	0.5
BELTSVILLE	2	2	39.0185	-76.9805	0.75		9.75				5.5	12.3	0	1	0	0	0.3
BELTSVILLE	2	3	39.0187	-76.9689			13				3	20	0	0.1	1	0	0.5
BELTSVILLE	2	4	39.0189	-76.9573	8		4				4	7	0	0.47	0	0	0.3
BELTSVILLE	2	5	39.0191	-76.9457	13	0.5					2.5	0.1	0	0	0	0	0
BELTSVILLE	2	6	39.0194	-76.9341	10		1				5	21	0	0.2	1	0	0.4
BELTSVILLE	2	7	39.0196	-76.9226	5		1		3		7	7.75	0	0.13	1	0	0.5
BELTSVILLE	2	8	39.0198	-76.9110	11		3				2	10	0	0.3	1	0	0.5
BELTSVILLE	2	9	39.0200	-76.8994	16												
BELTSVILLE	2	10	39.0202	-76.8878	15	1											
BELT/LAUREL	B2		39.0204	-76.8762	16												
LAUREL	2	1	39.0206	-76.8647	16												
LAUREL	2	2	39.0209	-76.8531	15.5						0.5	0.1	0	0	0	0	1
LAUREL	2	3	39.0211	-76.8415	16												
LAUREL	2	4	39.0213	-76.8299	16												
ROCKVILLE	1	2	39.0049	-77.2348	15		1										1
ROCKVILLE	1	3	39.0051	-77.2233	15		1										1
ROCKVILLE	1	4	39.0053	-77.2117	11		5										1
ROCKVILLE	1	5	39.0055	-77.2001	14			2									1
ROCKVILLE	1	6	39.0057	-77.1885	15			1									1
ROCKVILLE	1	7	39.0059	-77.1769	12		1	3									1
ROCKVILLE	1	8	39.0061	-77.1654	8.5	0.5		7									1
ROCKVILLE	1	9	39.0063	-77.1538	6.5			8.5			1	7	0	0.47	0	0	1
ROCKVILLE	1	10	39.0065	-77.1422	10			6									1
ROCK/KENS	B1		39.0068	-77.1306	5.5		3	5.5			2	10	1	0	0	1	1
KENSINGTON	1	1	39.0070	-77.1190	1.5			14.5									1
KENSINGTON	1	2	39.0072	-77.1075	8		2	6									1
KENSINGTON	1	3	39.0074	-77.0959	7.5		4	4			0.5	7	0	0.47	0	0	0.8
KENSINGTON	1	4	39.0076	-77.0843	7.5		0.5	5			3	12	0	0	0	0	0.8
KENSINGTON	1	5	39.0078	-77.0727	6			8			2	7	0	0.47	0	0	1
KENSINGTON	1	6	39.0080	-77.0611	10			5			1	7	0	0.47	0	0	1
KENSINGTON	1	7	39.0082	-77.0496	3.5		3	3.5			6	7	1	0.3	0	0	1
KENSINGTON	1	8	39.0085	-77.0380	2		3	9			2	12	0	0.1	0	0	0.7
KENSINGTON	1	9	39.0087	-77.0264	6		2	8									1
KENSINGTON	1	10	39.0089	-77.0148	1.5			14.5									0.8
KENS/BELT	B1		39.0091	-77.0032	2		2	10			2	12	0	0	0	0	0.8
BELTSVILLE	1	1	39.0093	-76.9917	8.2	0.3	7.5										
BELTSVILLE	1	2	39.0095	-76.9801	2.5		4				9.5	10	0	0.75	1	1	0.6
BELTSVILLE	1	3	39.0097	-76.9685	10		4.5				1.5	10	0	0.8	1	1	1
BELTSVILLE	1	4	39.0099	-76.9569	11.7		3.5				0.8	10	1	0	1	0	1
BELTSVILLE	1	5	39.0101	-76.9453	12.7	0.3	3										1
BELTSVILLE	1	6	39.0104	-76.9338	13.5	0.5					2	7	0	0.5	1	0	1
BELTSVILLE	1	7	39.0106	-76.9222					14		2	7	0	0.5	1	0	1
BELTSVILLE	1	8	39.0108	-76.9106	12				3.5		0.5	7	0	0.47	1	0	0.66
BELTSVILLE	1	9	39.0110	-76.8990	13.5						2.5	12	0	0	1	0	0.2
BELTSVILLE	1	10	39.0112	-76.8874	10		5				1	10	1	1	1	0	1
BELT/LAUREL	B1		39.0114	-76.8759	7.5		3				5.5	10	0	0	1	1	1
LAUREL	1	1	39.0116	-76.8643	15						1	0.1	0	0	0	0	1
LAUREL	1	2	39.0119	-76.8527	16												
LAUREL	1	3	39.0121	-76.8411	16												
LAUREL	1	4	39.0123	-76.8295	16												
ROCK/FALLS		B2	38.9959	-77.2347	14		2										1
ROCK/FALLS		B3	38.9961	-77.2231	12		4										1
ROCK/FALLS		B4	38.9963	-77.2115	12	0.5	3.5										1
ROCK/FALLS		B5	38.9965	-77.1999	15		1										1
ROCK/FALLS		B6	38.9967	-77.1884	13		3										1
ROCK/FALLS		B7	38.9969	-77.1768	14.5	0.5	1										1
ROCK/FALLS		B8	38.9971	-77.1652	9.5	0.5		6									1
ROCK/FALLS		B9	38.9973	-77.1536	11			4			1	7	0	0.47	0	0	1
ROCK/FALLS		B10	38.9975	-77.1421	11			5									1
RO/FA/KEN/WW	B1		38.9978	-77.1305	10.5			5.5									1
KENN/WASHW		B1	38.9980	-77.1189			5	10			1	10	1	0.3	0	1	1
KENN/WASHW		B2	38.9982	-77.1073	3.5			5.5			7	21	1	0.4	0	0	1
KENN/WASHW		B3	38.9984	-77.0957	6.5			1.5			8	16.5	1	0.3	0	0	1
KENN/WASHW		B4	38.9986	-77.0842	10.5			2.5			3	15	1	0.2	0	0	1

KENN/WASHW		B5	38.9988	-77.0726	4			8			4	10.7	0	0.47	0	0	0.8
KENN/WASHW		B6	38.9990	-77.0610	10.5			3			2.5	7	1	0.4	0	0	1
KENN/WASHW		B7	38.9992	-77.0494	5.5		4	2.5			4	7	1	0.1	0	0	1
KENN/WASHW		B8	38.9995	-77.0378	5.5		1	5			4.5	13	1	0.3	0	0	0.8
KENN/WASHW		B9	38.9997	-77.0263				9			7	24	1	0.3	1	0	0.9
KENN/WASHW		B10	38.9999	-77.0147	5		2	6.5			2.5	11.2	1	0.48	0	0	1
KEN/BE/WE/WW	B1		39.0001	-77.0031	1.5			11.5			3	7	0	0.2	0	0	1
BELT/WASHE		B1	39.0003	-76.9915	2.5	0.5		8.5			4.5	8.5	0	0.3	0	0	1
BELT/WASHE		B2	39.0005	-76.9799	9.5	0.5		4			2	10	0	1	1	0	1
BELT/WASHE		B3	39.0007	-76.9684	6			8			2	7	0	0.4	0	0	1
BELT/WASHE		B4	39.0009	-76.9568	13.5	0.5	2										1
BELT/WASHE		B5	39.0012	-76.9452	12		3.5				0.5	7	0	0.47	0	0	1
BELT/WASHE		B6	39.0014	-76.9336	10			3			3	7	0	0.4	0	0	1
BELT/WASHE		B7	39.0016	-76.9221	8			7			1	7	0	0.47	0	0	1
BELT/WASHE		B8	39.0018	-76.9105	8.5						7.5	8	0	0.27	0	0	1
BELT/WASHE		B9	39.0020	-76.8989	4.5						12	9.5	0	0	0	0	0.4
BELT/WASHE		B10	39.0022	-76.8873	7.5	2	1.5	1			4	7	0	0.4	1	0	0.7
BE/LAUR/WE/LANH	B1		39.0024	-76.8757	2			9			5	8.8	0	0.12	1	0	1
LAUREL/LANHAM		B1	39.0026	-76.8642	11						5	10	0	1	1	0	1
LAUREL/LANHAM		B2	39.0029	-76.8526	13.5						2.5	12	0	0.1	0	0	1
LAUREL/LANHAM		B3	39.0031	-76.8410	15						1	10	1	0	0	1	1
LAUREL/LANHAM		B4	39.0033	-76.8294	16												
FALLS CHURCH	13	2	38.9869	-77.2344	15	1											
FALLS CHURCH	13	3	38.9871	-77.2228	11			5									1
FALLS CHURCH	13	4	38.9873	-77.2112	11			5									1
FALLS CHURCH	13	5	38.9875	-77.1997	12.5	0.5		3									1
FALLS CHURCH	13	6	38.9877	-77.1881	12.5	0.5		2			1	10	1	0	0	0	1
FALLS CHURCH	13	7	38.9879	-77.1765	13.5			2.5									1
FALLS CHURCH	13	8	38.9881	-77.1649	13			3									
FALLS CHURCH	13	9	38.9883	-77.1534	9.5			3.5			3	7	0	0.47	0	0	0.8
FALLS CHURCH	13	10	38.9886	-77.1418	9.5		3	3			0.5	7	0	0.47	0	0	0.8
FALLS/WAW	B13		38.9888	-77.1302	5.5		3	6.5			1	10	1	0.2	0	0	1
WASH WEST	13	1	38.9890	-77.1186	6		2	8									1
WASH WEST	13	2	38.9892	-77.1071			1	14			1	30	0	0	0	0	1
WASH WEST	13	3	38.9894	-77.0955	1			6.5			8.5	21	1	0.3	1	0	0.7
WASH WEST	13	4	38.9896	-77.0839	6			9			1	18	1	0.4	0	0	1
WASH WEST	13	5	38.9898	-77.0723	5		2	8			1	10	1	0	0	0	1
WASH WEST	13	6	38.9900	-77.0607	8.5	0.5	4	3									1
WASH WEST	13	7	38.9902	-77.0492	9.5		2.5	2			2	10	1	0.3	0	0	1
WASH WEST	13	8	38.9905	-77.0376	6		4.5	3			2.5	27	0	0.2	0	0	0.9
WASH WEST	13	9	38.9907	-77.0260				6			10	14.7	1	0.27	1	0	0.9
WASH WEST	13	10	38.9909	-77.0144	3		2	9			2	7	1	0.1	0	0	1
WAW/WAE	B13		38.9911	-77.0029	2	0.5	2.5	11									1
WASH EAST	13	1	38.9913	-76.9913			5	6			5	7	0	0.73	0	0	1
WASH EAST	13	2	38.9915	-76.9797	1.5	0.5	8				6	10	1	0.6	1	0	1
WASH EAST	13	3	38.9917	-76.9681	10.5	0.5	5										1
WASH EAST	13	4	38.9919	-76.9565	11	1	3				1	7	0	0.47	0	0	1
WASH EAST	13	5	38.9922	-76.9450	3.5						13	15	0	0.8	0	0	1
WASH EAST	13	6	38.9924	-76.9334	4.5	0.5		4			7	10.6	0	0.36	0	0	1
WASH EAST	13	7	38.9926	-76.9218	6.5	0.5	2	7									1
WASH EAST	13	8	38.9928	-76.9102			2	13.5			0.5	7	0	0.47	0	0	1
WASH EAST	13	9	38.9930	-76.8987	11			1			4	12	0	0.3	1	0	1
WASH EAST	13	10	38.9932	-76.8871	8						8	7	0	0.1	0	0	0.2
WE/LANHAM	B13		38.9934	-76.8755	9.5			1			5.5	7	0	0	0	0	1
LANHAM	13	1	38.9936	-76.8639	11						5	7.9	0	0.49	0	0	1
LANHAM	13	2	38.9939	-76.8523	3.5						13	17.1	0	0.08	0	0	1
LANHAM	13	3	38.9941	-76.8408	13.5						2.5	18	0	0	0	0	1
LANHAM	13	4	38.9943	-76.8292	11						5	12	0	0.4	0	0	1
FALLS CHURCH	12	2	38.9779	-77.2341	13	3											
FALLS CHURCH	12	3	38.9781	-77.2225	10.5	3.5	2										1
FALLS CHURCH	12	4	38.9783	-77.2110	11.5	2.5	2										1
FALLS CHURCH	12	5	38.9785	-77.1994	11		2				3	7	1	0	0	0	1
FALLS CHURCH	12	6	38.9787	-77.1878	12.5		2				1.5	7	1	0	0	0	1
FALLS CHURCH	12	7	38.9789	-77.1762	12		2				2	7	0	0.47	0	0	1
FALLS CHURCH	12	8	38.9791	-77.1647	12			3			1	7	0	0.47	0	0	1
FALLS CHURCH	12	9	38.9793	-77.1531	12.5	0.5		3									1
FALLS CHURCH	12	10	38.9796	-77.1415	11.5			4.5									0.9
FALLS/WW	B12		38.9798	-77.1299	7.5			7			1.5	7	1	0	0	0	0.7
WASH WEST	12	1	38.9800	-77.1183	3		3	10									1
WASH WEST	12	2	38.9802	-77.1068	3		2	11									0.9
WASH WEST	12	3	38.9804	-77.0952	1			4.5			11	18.9	1	0.3	1	0	0.7
WASH WEST	12	4	38.9806	-77.0836	3		1	11			1	27	1	0.2	1	0	1
WASH WEST	12	5	38.9808	-77.0721	1			15									1
WASH WEST	12	6	38.9810	-77.0605	6		3	7									1

WASH WEST	12	7	38.9812	-77.0489	14	0.5		1.5									1
WASH WEST	12	8	38.9815	-77.0373	4.5			3	7.5		1	12	1	0.4	0	0	1
WASH WEST	12	9	38.9817	-77.0257	3			4.5	5.5		3	15	0	0.4	1	0	0.9
WASH WEST	12	10	38.9819	-77.0142	2.5		3	9.5			1	12	1	0.1	0	0	1
WW/WE	B12		38.9821	-77.0026	2.7	0.3		7			6	10	1	0.2	1	0	1
WASH EAST	12	1	38.9823	-76.9910	2.5		1.5	10			2	10	0	0.8	0	0	1
WASH EAST	12	2	38.9825	-76.9794	1		6				9	10	0	0	1	0	1
WASH EAST	12	3	38.9827	-76.9679	5.5	0.5	9.5				0.5	10	1	0	1	0	1
WASH EAST	12	4	38.9829	-76.9563	6	0.5	3.5	1			5	10	0	0.3	0	0	0.7
WASH EAST	12	5	38.9832	-76.9447	2			2.5			12	15	0	0.8	0	1	0.7
WASH EAST	12	6	38.9834	-76.9331	2.5	0.5			6		7	15	0	0.8	0	1	0.8
WASH EAST	12	7	38.9836	-76.9216	8.5	1.5					6	7.5	0	0.58	0	1	1
WASH EAST	12	8	38.9838	-76.9100	6		8.5				1.5	7	0	0.47	0	0	1
WASH EAST	12	9	38.9840	-76.8984	16												
WASH EAST	12	10	38.9842	-76.8868	13.5		1				1.5	7	0	0.47	0	0	1
WE/LANHAM	B12		38.9844	-76.8753	9		3.5				3.5	10	0	0.2	0	0	0.4
LANHAM	12	1	38.9846	-76.8637	7.5		5.5				3	8	1	0.47	1	0	1
LANHAM	12	2	38.9849	-76.8521	8		8										1
LANHAM	12	3	38.9851	-76.8405	7			4			5	7	0	0.44	0	0	1
LANHAM	12	4	38.9853	-76.8289	14						2	7	1	0.8	0	0	1
FALLS CHURCH	11	2	38.9689	-77.2338	16												
FALLS CHURCH	11	3	38.9691	-77.2222	13.5	2.5											
FALLS CHURCH	11	4	38.9693	-77.2107	10.5	4.5	1										1
FALLS CHURCH	11	5	38.9695	-77.1991	11	5											
FALLS CHURCH	11	6	38.9697	-77.1875	8.5	3	1				3.5	7	1	0	0	0	1
FALLS CHURCH	11	7	38.9699	-77.1759	10	3					3	0.1	0	0	0	0	1
FALLS CHURCH	11	8	38.9701	-77.1644	9.5	5		1.5									1
FALLS CHURCH	11	9	38.9703	-77.1528	7.5	6	1	1.5									1
FALLS CHURCH	11	10	38.9706	-77.1412	11	0.5	1.5	3									1
FALLS/WW	B11		38.9708	-77.1297	8.5		2	5.5									1
WASH WEST	11	1	38.9710	-77.1181	5		3	6.5			1.5	10	0	0	0	0	0.8
WASH WEST	11	2	38.9712	-77.1065	7			9									1
WASH WEST	11	3	38.9714	-77.0949	4		2	10									1
WASH WEST	11	4	38.9716	-77.0833	11.5			4.5									1
WASH WEST	11	5	38.9718	-77.0718	1			15									1
WASH WEST	11	6	38.9720	-77.0602	0.5			13.5			2	10	1	0.8	1	0	1
WASH WEST	11	7	38.9722	-77.0486	16												
WASH WEST	11	8	38.9725	-77.0370	9.5	0.5			3		3	12	1	0.5	0	0	1
WASH WEST	11	9	38.9727	-77.0255	2				11		3	15	1	0.4	0	0	1
WASH WEST	11	10	38.9729	-77.0139	4			7	2		3	7	0	0.2	0	0	1
WW/WE	B11		38.9731	-77.0023	1			15									1
WASH EAST	11	1	38.9733	-76.9907	5			9			2	7	1	0.7	1	0	0.8
WASH EAST	11	2	38.9735	-76.9792	5		7	3			1	7	0	0.47	0	0	0.7
WASH EAST	11	3	38.9737	-76.9676	5.5	0.5	10										1
WASH EAST	11	4	38.9739	-76.9560	7		2	1			6	10	0	0.23	0	0	1
WASH EAST	11	5	38.9742	-76.9444			3	13									1
WASH EAST	11	6	38.9744	-76.9329	6			7			3	7	0	0.6	0	0	1
WASH EAST	11	7	38.9746	-76.9213	11.5	0.5					4	7	1	0.5	1	0	1
WASH EAST	11	8	38.9748	-76.9097	14		1				1	7	0	0.47	0	0	1
WASH EAST	11	9	38.9750	-76.8981	13		2				1	7	0	0.47	0	0	1
WASH EAST	11	10	38.9752	-76.8866	6		10										1
WAE/LANHAM	B11		38.9754	-76.8750	3		4	8			1	7	0	0.47	0	0	0.7
LANHAM	11	1	38.9756	-76.8634	8		2	2			4	7	0	0	0	1	1
LANHAM	11	2	38.9759	-76.8518	2		7	7									1
LANHAM	11	3	38.9761	-76.8403	7		4	4			1	7	0	0.47	0	0	1
LANHAM	11	4	38.9763	-76.8287	16												
FALLS CHURCH	10	2	38.9599	-77.2335	10		6										1
FALLS CHURCH	10	3	38.9601	-77.2220	14		2										1
FALLS CHURCH	10	4	38.9603	-77.2104	14		2										1
FALLS CHURCH	10	5	38.9605	-77.1988	14		2										1
FALLS CHURCH	10	6	38.9607	-77.1872	9		4				3	7	0	0.47	0	0	1
FALLS CHURCH	10	7	38.9609	-77.1757	13		2				1	7	0	0.47	0	0	1
FALLS CHURCH	10	8	38.9611	-77.1641	15			1									1
FALLS CHURCH	10	9	38.9613	-77.1525	15	1											
FALLS CHURCH	10	10	38.9616	-77.1409	9	7											
FALLS/WAW	B10		38.9618	-77.1294	4	1		11									1
WASH WEST	10	1	38.9620	-77.1178				15.5			0.5	10	1	1	0	0	1
WASH WEST	10	2	38.9622	-77.1062	2	0.5		4			9.5	10.5	1	0.31	0	0	0.8
WASH WEST	10	3	38.9624	-77.0947	2		2	8			4	27.5	1	0.55	1	0	0.9
WASH WEST	10	4	38.9626	-77.0831	1.5			8.5		1.5	4.5	30	1	0.4	1	0	1
WASH WEST	10	5	38.9628	-77.0715				7	7		2	10	1	0.5	1	0	1
WASH WEST	10	6	38.9630	-77.0599	3			11			2	12	1	0.6	0	0	1
WASH WEST	10	7	38.9633	-77.0484	16												
WASH WEST	10	8	38.9635	-77.0368	8				5	3							1

WASH WEST	10	9	38.9637	-77.0252					9	2	5	13.2	1	0.46	0	0	1
WASH WEST	10	10	38.9639	-77.0136	2.5				7	1.5	5	12	1	0.34	1	0	1
WAW/WAE	B10		38.9641	-77.0021	2			9			5	7	1	0.5	1	0	0.9
WASH EAST	10	1	38.9643	-76.9905	5		3	6			2	7	0	0.3	1	0	0.8
WASH EAST	10	2	38.9645	-76.9789	4.5	0.5	5	5			1	7	0	1	0	0	1
WASH EAST	10	3	38.9647	-76.9673	11		1	3			1	7	0	0.47	0	0	0.75
WASH EAST	10	4	38.9649	-76.9558	4			6			6	9	0	0.8	0	0	0.8
WASH EAST	10	5	38.9652	-76.9442				14			2	7	0	0.4	1	0	1
WASH EAST	10	6	38.9654	-76.9326	2			9			5	8.5	0	0.3	0	0	1
WASH EAST	10	7	38.9656	-76.9210	7.5	0.5		6.5			1.5	7	0	0.2	0	0	0.6
WASH EAST	10	8	38.9658	-76.9095	4			9			3	10	0	0	1	0	1
WASH EAST	10	9	38.9660	-76.8979	7		5				4	10	0	0	1	0	1
WASH EAST	10	10	38.9662	-76.8863	2		11				3	10	1	0	1	1	1
WAE/LANHAM	B10		38.9664	-76.8748			11	5									1
LANHAM	10	1	38.9666	-76.8632	3			12			1	7	0	0.47	0	0	0.7
LANHAM	10	2	38.9669	-76.8516			2	13			1	7	0	0.47	0	0	1
LANHAM	10	3	38.9671	-76.8400	5		2	7.5			1.5	7	0	0	0	0	1
LANHAM	10	4	38.9673	-76.8285	14		2										1
FALLS CHURCH	9	2	38.9509	-77.2332	12			4									1
FALLS CHURCH	9	3	38.9511	-77.2217	13.5	0.5		2									1
FALLS CHURCH	9	4	38.9513	-77.2101	11			5									1
FALLS CHURCH	9	5	38.9515	-77.1985	9			5			2	7	0	0.47	0	0	1
FALLS CHURCH	9	6	38.9517	-77.1870	9			6			1	10	1	0	0	0	1
FALLS CHURCH	9	7	38.9519	-77.1754	10			6									1
FALLS CHURCH	9	8	38.9521	-77.1638	12.5			2.5			1	10	1	0.2	0	0	1
FALLS CHURCH	9	9	38.9523	-77.1522	13						3	12	0	0	0	0	1
FALLS CHURCH	9	10	38.9526	-77.1407	12	2					2	30	0	0	1	0	1
FALLS/WAW	B9		38.9528	-77.1291	6.5	6		3			0.5	7	0	0.47	0	0	1
WASH WEST	9	1	38.9530	-77.1175	1.5			10.5			4	17.3	0	0.6	0	0	1
WASH WEST	9	2	38.9532	-77.1059	3.5	0.5		12									1
WASH WEST	9	3	38.9534	-77.0944	1			8.5	6.5								1
WASH WEST	9	4	38.9536	-77.0828	2				9.5		4.5	11.1	1	0.36	1	0	1
WASH WEST	9	5	38.9538	-77.0712	4				8		4	15	1	0.7	1	0	1
WASH WEST	9	6	38.9540	-77.0597	7.5	0.5		7	1								1
WASH WEST	9	7	38.9543	-77.0481	14.5	0.5		1									1
WASH WEST	9	8	38.9545	-77.0365	6.5					8.5	1	4	0	0.5	0	0	1
WASH WEST	9	9	38.9547	-77.0249					3	11	2	12	1	0.5	1	0	1
WASH WEST	9	10	38.9549	-77.0134	2					14							1
WAW/WAE	B9		38.9551	-77.0018	3.5			6.5		1	5	7	0	0.4	0	0	1
WASH EAST	9	1	38.9553	-76.9902	6.5			9.5									1
WASH EAST	9	2	38.9555	-76.9787	6.7	0.3		3			6	10.7	1	0.7	1	0	1
WASH EAST	9	3	38.9557	-76.9671	2	1		2.5			11	6.1	0	0.31	0	0	0.8
WASH EAST	9	4	38.9559	-76.9555	2			14									1
WASH EAST	9	5	38.9562	-76.9439				10			6	8.5	0	0.6	1	0	1
WASH EAST	9	6	38.9564	-76.9324	4	0.5		8			3.5	7	1	0.3	1	0	1
WASH EAST	9	7	38.9566	-76.9208	3.5	0.25	3	2.25			7	8	0	0.6	0	0	0.75
WASH EAST	9	8	38.9568	-76.9092	5.5		6.5	2.5			1.5	7	0	0.47	0	0	1
WASH EAST	9	9	38.9570	-76.8977	7.5		8.5										1
WASH EAST	9	10	38.9572	-76.8861	10		6										1
WAE/LANHAM	B9		38.9574	-76.8745	1		3	2			10	7.9	0	0.17	0	0	1
LANHAM	9	1	38.9576	-76.8629				6			10	10	0	0	1	0	0.7
LANHAM	9	2	38.9579	-76.8514	6.5		6.5	3									1
LANHAM	9	3	38.9581	-76.8398	7		4				5	7	1	0	0	0	1
LANHAM	9	4	38.9583	-76.8282	12			4									1
FALLS CHURCH	8	2	38.9419	-77.2329	14			2									1
FALLS CHURCH	8	3	38.9421	-77.2214	5			11									1
FALLS CHURCH	8	4	38.9423	-77.2098	7.5			7.5			1	7	0	0.47	0	0	1
FALLS CHURCH	8	5	38.9425	-77.1982	9			6.5			0.5	7	0	0.47	0	0	1
FALLS CHURCH	8	6	38.9427	-77.1867	9.5			6.5									1
FALLS CHURCH	8	7	38.9429	-77.1751	10			6									1
FALLS CHURCH	8	8	38.9431	-77.1635	11			5									1
FALLS CHURCH	8	9	38.9433	-77.1519	8			6			2	10	0	0	0	0	0.7
FALLS CHURCH	8	10	38.9436	-77.1404	13			3									0.9
FALLS/WAW	B8		38.9438	-77.1288	11	5											
WASH WEST	8	1	38.9440	-77.1172	8	2	1	3			2	24	0	0.3	0	0	1
WASH WEST	8	2	38.9442	-77.1057	8.5	2	1.5	4									1
WASH WEST	8	3	38.9444	-77.0941	2.5			4.5	7.5		1.5	15	1	0.2	0	0	1
WASH WEST	8	4	38.9446	-77.0825	1	0.5	1		6		7.5	12	1	0.42	1	0	1
WASH WEST	8	5	38.9448	-77.0710	1				10		5	15.6	1	0.42	1	0	1
WASH WEST	8	6	38.9450	-77.0594	9			2	1		4	24	1	0.2	1	0	1
WASH WEST	8	7	38.9453	-77.0478	13				3								1
WASH WEST	8	8	38.9455	-77.0362	0.5				8.5	4	3	12	1	0.6	0	0	1
WASH WEST	8	9	38.9457	-77.0247					3	10	3	15	1	0.4	0	0	1
WASH WEST	8	10	38.9459	-77.0131	8					7	1	12	0	0.8	0	0	1

WAW/WAE	B8		38.9461	-77.0015	6				1	2.5	6.5	7	0	0.5	1	0	1
WASH EAST	8	1	38.9463	-76.9900	4				10.5		1.5	12	0	0.3	1	0	1
WASH EAST	8	2	38.9465	-76.9784	3.5			4.5	8								0.9
WASH EAST	8	3	38.9467	-76.9668	1			7			8	9.6	1	0.68	0	0	0.8
WASH EAST	8	4	38.9469	-76.9553	4	0.5		11.5									1
WASH EAST	8	5	38.9472	-76.9437	5.5	1		5			4.5	7	1	0.5	1	0	1
WASH EAST	8	6	38.9474	-76.9321	1.5	0.5		7.5			6.5	7	0	0.25	0	0	0.8
WASH EAST	8	7	38.9476	-76.9205	1.5			13			1.5	10	1	0	1	0	0.9
WASH EAST	8	8	38.9478	-76.9090	7		5				4	10	0	0	1	0	1
WASH EAST	8	9	38.9480	-76.8974	1		15										1
WASH EAST	8	10	38.9482	-76.8858	4		5.5	0.5			6	7	0	0.1	0	0	1
WAE/LANHAM	B8		38.9484	-76.8743	6.5			4			5.5	7	0	0.47	0	0	1
LANHAM	8	1	38.9486	-76.8627	6.5						9.5	7	0	0.1	0	0	0.7
LANHAM	8	2	38.9489	-76.8511	6.5		7				2.5	7	0	0.47	0	1	0.9
LANHAM	8	3	38.9491	-76.8396	12						4	7	0	0.5	0	0	0.8
LANHAM	8	4	38.9493	-76.8280	15						1	0.1	0	0	0	0	0
FALLS CHURCH	7	2	38.9329	-77.2326	13						3	45	0	0	1	0	1
FALLS CHURCH	7	3	38.9331	-77.2211	10.5			2.5			3	12	0	0.5	0	0	1
FALLS CHURCH	7	4	38.9333	-77.2095	4			2			10	10	0	0	0	1	1
FALLS CHURCH	7	5	38.9335	-77.1979	11			5									1
FALLS CHURCH	7	6	38.9337	-77.1864	7			9									1
FALLS CHURCH	7	7	38.9339	-77.1748	9			7									1
FALLS CHURCH	7	8	38.9341	-77.1632	12.5	0.5		3									1
FALLS CHURCH	7	9	38.9343	-77.1517	10	0.5	5				0.5	30	1	0	0	0	1
FALLS CHURCH	7	10	38.9346	-77.1401	13.5	0.5		2									1
FALLS/WAW	B7		38.9348	-77.1285	11.5	0.5		3			1	7	0	0.47	0	0	1
WASH WEST	7	1	38.9350	-77.1170	8	3		3			2	4	1	0.1	0	0	1
WASH WEST	7	2	38.9352	-77.1054	4			11			1	18	0	0.8	0	0	0.9
WASH WEST	7	3	38.9354	-77.0938	2			10			4	15	1	0.5	1	0	1
WASH WEST	7	4	38.9356	-77.0823	6			1	1		8	18.8	1	0.5	1	0	1
WASH WEST	7	5	38.9358	-77.0707					10.5		5.5	15	0	0.7	1	0	1
WASH WEST	7	6	38.9360	-77.0591	8				4		4	10	1	0.5	0	0	1
WASH WEST	7	7	38.9363	-77.0476	12				2	2							1
WASH WEST	7	8	38.9365	-77.0360	4.5				2.5	9							1
WASH WEST	7	9	38.9367	-77.0244						13	3	12	1	0.6	1	0	1
WASH WEST	7	10	38.9369	-77.0128	11					3	2	12	1	0.7	0	0	1
WAW/WAE	B7		38.9371	-77.0013							16	12	1	0.7	0	1	1
WASH EAST	7	1	38.9373	-76.9897	2				10		4	8.1	0	0.88	0	0	1
WASH EAST	7	2	38.9375	-76.9781	5				11								1
WASH EAST	7	3	38.9377	-76.9666	3.5				12.5								1
WASH EAST	7	4	38.9379	-76.9550					12		4	7	1	0.8	1	0	1
WASH EAST	7	5	38.9382	-76.9434	6	2			5		3	7	1	0.6	1	0	0.7
WASH EAST	7	6	38.9384	-76.9319	3			4			9	8	1	0.6	1	0	1
WASH EAST	7	7	38.9386	-76.9203				8			8	12	0	0.42	0	0	0.6
WASH EAST	7	8	38.9388	-76.9087	5.5		0.5	1.5			8.5	8.3	0	0.33	0	0	1
WASH EAST	7	9	38.9390	-76.8972	3		10				3	9	0	0.33	0	0	1
WASH EAST	7	10	38.9392	-76.8856	2		7.5				6.5	7	0	0.2	0	0	1
WAE/LANHAM	B7		38.9394	-76.8740	7		1.5				7.5	7	1	0.3	0	0	1
LANHAM	7	1	38.9396	-76.8624	2		4				10	7	0	0.3	1	0	1
LANHAM	7	2	38.9399	-76.8509	7		7.5				1.5	7	0	0.47	0	0	0.5
LANHAM	7	3	38.9401	-76.8393	15		1										1
LANHAM	7	4	38.9403	-76.8277	13		3										1
FALLS CHURCH	6	2	38.9239	-77.2324	4						12	45	0	0.3	0	0	1
FALLS CHURCH	6	3	38.9241	-77.2208	9						7	30	0	0.3	0	0	1
FALLS CHURCH	6	4	38.9243	-77.2092	7						9	21.4	0	0.34	0	0	1
FALLS CHURCH	6	5	38.9245	-77.1977	7		4	3			2	7	0	0.47	0	0	1
FALLS CHURCH	6	6	38.9247	-77.1861	8		4	4									1
FALLS CHURCH	6	7	38.9249	-77.1745	9			7									1
FALLS CHURCH	6	8	38.9251	-77.1629	7			8			1	10	0	0.1	0	0	1
FALLS CHURCH	6	9	38.9254	-77.1514	9.5		4	2.5									1
FALLS CHURCH	6	10	38.9256	-77.1398	10.2	0.3		5.5									1
FALLS/WAW	B6		38.9258	-77.1283	8			8									1
WASH WEST	6	1	38.9260	-77.1167	10.5	2.5		3									1
WASH WEST	6	2	38.9262	-77.1051	6	1		9									1
WASH WEST	6	3	38.9264	-77.0936	11			5									1
WASH WEST	6	4	38.9266	-77.0820	7			3		1	5	27	1	0.4	1	0	1
WASH WEST	6	5	38.9268	-77.0704	3				6	3	4	20.3	1	0.7	1	0	1
WASH WEST	6	6	38.9270	-77.0589	4				7	2	3	15	1	0.8	1	0	1
WASH WEST	6	7	38.9273	-77.0473	10.5	0.5				5							1
WASH WEST	6	8	38.9275	-77.0357						7	9	15	1	0.5	1	0	1
WASH WEST	6	9	38.9277	-77.0242		1				11	4	12	1	0.4	1	0	1
WASH WEST	6	10	38.9279	-77.0126	9.5	1.5					5	21	1	0.3	0	0	1
WAW/WAE	B6		38.9281	-77.0010	5					4	7	15	1	0.7	0	1	0.9
WASH EAST	6	1	38.9283	-76.9894					15		1	7	0	0.47	1	0	1

WASH EAST	6	2	38.9285	-76.9779					16									1
WASH EAST	6	3	38.9287	-76.9663					13.5		2.5	7	1	1	1	0	1
WASH EAST	6	4	38.9289	-76.9547	9				1		6	10	1	0.6	1	0	1
WASH EAST	6	5	38.9292	-76.9432	12.5	2.5			1								1
WASH EAST	6	6	38.9294	-76.9316	2						14	7	0	0.3	0	0	0.8
WASH EAST	6	7	38.9296	-76.9200	4.5			4.5			7	12	0	0	0	1	1
WASH EAST	6	8	38.9298	-76.9085	3			13									1
WASH EAST	6	9	38.9300	-76.8969	3		4				9	7	0	0.8	1	0	0.7
WASH EAST	6	10	38.9302	-76.8853	2			1.5			13	7	1	0.2	1	0	1
WAE/LANHAM	B6		38.9304	-76.8738	10		2				4	8	0	0.7	1	0	1
LANHAM	6	1	38.9306	-76.8622	4		4	6.5			1.5	10	0	0	1	0	1
LANHAM	6	2	38.9309	-76.8506	5.5		4	5.5			1	7	0	0.47	0	0	0.7
LANHAM	6	3	38.9311	-76.8391	15		1										1
LANHAM	6	4	38.9313	-76.8275	14		2										1
FALLS CHURCH	5	2	38.9149	-77.2322	2			4.5			9.5	24	0	0.3	0	0	1
FALLS CHURCH	5	3	38.9151	-77.2206	5						11	9.1	0	0.4	0	0	1
FALLS CHURCH	5	4	38.9153	-77.2091	2		3	6			5	16	1	0.35	0	0	1
FALLS CHURCH	5	5	38.9155	-77.1975	6		5	5									1
FALLS CHURCH	5	6	38.9157	-77.1860	6.5		3	6			0.5	7	0	0.47	0	0	1
FALLS CHURCH	5	7	38.9159	-77.1744	6		3	7									1
FALLS CHURCH	5	8	38.9161	-77.1628	8			8									1
FALLS CHURCH	5	9	38.9164	-77.1513	11.5			2			2.5	7	1	0.2	0	0	1
FALLS CHURCH	5	10	38.9166	-77.1397	7.5			7.5			1	10	1	0	0	0	1
FALLS/WAW	B5		38.9168	-77.1281	4			12									1
WASH WEST	5	1	38.9170	-77.1165	8			8									1
WASH WEST	5	2	38.9172	-77.1050	11.5	3.5		1									1
WASH WEST	5	3	38.9174	-77.0934	8.5	1.5		6									1
WASH WEST	5	4	38.9176	-77.0818	13					3							1
WASH WEST	5	5	38.9178	-77.0703	8					5	3	15	1	0.3	1	0	1
WASH WEST	5	6	38.9180	-77.0587	11.5	0.5			3		1	10	1	0.6	1	0	1
WASH WEST	5	7	38.9183	-77.0471	3					5	8	15	1	0.7	1	0	1
WASH WEST	5	8	38.9185	-77.0356	1					7	8	15	1	0.7	1	0	1
WASH WEST	5	9	38.9187	-77.0240						4.5	12	13.6	1	0.51	1	0	1
WASH WEST	5	10	38.9189	-77.0125	2	1				11.5	1.5	12	1	0.4	0	0	1
WAW/WAE	B5		38.9191	-77.0009	3.5					4.5	8	12	0	0.6	1	0	1
WASH EAST	5	1	38.9193	-76.9893						2	14	7.6	0	0.76	0	0	1
WASH EAST	5	2	38.9195	-76.9778	1.5				4		11	7	0	0.75	1	0	1
WASH EAST	5	3	38.9197	-76.9662	4				3		9	7	1	0.6	1	0	1
WASH EAST	5	4	38.9199	-76.9546	14						2	7	1	0.6	1	0	1
WASH EAST	5	5	38.9202	-76.9431	13	2					1	0.1	0	0	0	0	1
WASH EAST	5	6	38.9204	-76.9315	8						8	7	0	0.5	1	0	0.8
WASH EAST	5	7	38.9206	-76.9199	2			7.5			6.5	7	0	0.5	1	0	1
WASH EAST	5	8	38.9208	-76.9084	1.5			4			11	7	0	0.3	0	0	1
WASH EAST	5	9	38.9210	-76.8968	9		3				4	10	1	0	0	1	1
WASH EAST	5	10	38.9212	-76.8852	1		15										1
WAE/LANHAM	B5		38.9214	-76.8737	2.5		9.5				4	9.4	0	0	1	0	1
LANHAM	5	1	38.9216	-76.8621	7.5		1				7.5	10	0	0.23	1	0	1
LANHAM	5	2	38.9219	-76.8505	8.5		1				6.5	10	0	0	0	0	0.1
LANHAM	5	3	38.9221	-76.8390	16												
LANHAM	5	4	38.9223	-76.8274	16												
FALLS CHURCH	4	2	38.9059	-77.2319	11			5									1
FALLS CHURCH	4	3	38.9061	-77.2203	12			1			3	21	0	0.2	0	0	1
FALLS CHURCH	4	4	38.9063	-77.2088	5			8			3	20	1	0.1	1	0	1
FALLS CHURCH	4	5	38.9065	-77.1972	8.5			7.5									1
FALLS CHURCH	4	6	38.9067	-77.1857	10			5			1	7	0	0.47	0	0	1
FALLS CHURCH	4	7	38.9069	-77.1741	10			4			2	10	1	0	0	0	1
FALLS CHURCH	4	8	38.9071	-77.1625	11			5									1
FALLS CHURCH	4	9	38.9074	-77.1510	8			7			1	10	1	0	0	0	1
FALLS CHURCH	4	10	38.9076	-77.1394	7			9									1
FALLS/WAW	B4		38.9078	-77.1278	7			7			2	7	0	0.1	0	0	1
WASH WEST	4	1	38.9080	-77.1163	9.5			6.5									1
WASH WEST	4	2	38.9082	-77.1047	8	1	4	3									1
WASH WEST	4	3	38.9084	-77.0931	8.5	5.5		2									1
WASH WEST	4	4	38.9086	-77.0816	6	2		5			3	18	1	0.7	1	0	0.7
WASH WEST	4	5	38.9088	-77.0700	3	0.5				8.5	4	18	1	0.7	1	0	1
WASH WEST	4	6	38.9091	-77.0584	3.5	0.5				11	1	21	1	0.2	1	0	1
WASH WEST	4	7	38.9093	-77.0469	2.5					5	8.5	17.3	1	0.28	1	0	1
WASH WEST	4	8	38.9095	-77.0353						7	9	17.7	1	0.41	1	0	1
WASH WEST	4	9	38.9097	-77.0238						10	6	19	1	0.23	1	0	1
WASH WEST	4	10	38.9099	-77.0122						8.5	7.5	11.2	1	0.64	1	0	1
WAW/WAE	B4		38.9101	-77.0006						3	13	10.9	0	0.28	0	0	1
WASH EAST	4	1	38.9103	-76.9891						7.5	8.5	12	0	0.7	0	1	1
WASH EAST	4	2	38.9105	-76.9775	12				2	2							1
WASH EAST	4	3	38.9107	-76.9659	14	1			1								1

WASH EAST	4	4	38.9109	-76.9544	11.5	4					0.5	10	1	0.2	1	0	1
WASH EAST	4	5	38.9112	-76.9428	8.5	3			3.5		1	10	1	0	1	0	1
WASH EAST	4	6	38.9114	-76.9312	2				8.5		5.5	7.9	1	0.14	1	0	0.9
WASH EAST	4	7	38.9116	-76.9197	5			6			5	10	1	0.8	1	0	1
WASH EAST	4	8	38.9118	-76.9081	11			3			2	7	1	0.4	0	0	1
WASH EAST	4	9	38.9120	-76.8966	3			3			10	7	1	0.4	0	0	1
WASH EAST	4	10	38.9122	-76.8850	11			2.5			2.5	12	0	0	1	0	1
WAE/LANHAM	B4		38.9124	-76.8734	7		7				2	7	0	0	0	0	1
LANHAM	4	1	38.9126	-76.8619	13.5		1.5				1	7	0	0	0	0	1
LANHAM	4	2	38.9129	-76.8503	11.5						4.5	7	0	0.8	1	0	0.4
LANHAM	4	3	38.9131	-76.8387	15						1	0.1	0	0	0	0	1
LANHAM	4	4	38.9133	-76.8272	16												
FALLS CHURCH	3	2	38.8969	-77.2316	6		1	8			1	7	1	0	0	0	1
FALLS CHURCH	3	3	38.8971	-77.2201	12			3			1	7	0	0.47	0	0	1
FALLS CHURCH	3	4	38.8973	-77.2085	6.5			9			0.5	7	0	0.47	0	0	0.8
FALLS CHURCH	3	5	38.8975	-77.1969	8			4.5			3.5	7	0	0.47	0	0	1
FALLS CHURCH	3	6	38.8977	-77.1854	9			4.5			2.5	7	0	0.47	0	0	1
FALLS CHURCH	3	7	38.8979	-77.1738	3			12			1	7	0	0.47	0	0	1
FALLS CHURCH	3	8	38.8981	-77.1622	1.5	0.5		13			1	10	1	0.2	0	0	1
FALLS CHURCH	3	9	38.8984	-77.1507				15			1	7	1	0.3	0	0	1
FALLS CHURCH	3	10	38.8986	-77.1391	1			12			3	8.5	0	0.55	0	0	1
FALLS/WAW	B3		38.8988	-77.1276				14			2	7	1	0.8	0	0	0.9
WASH WEST	3	1	38.8990	-77.1160	4			8.5			3.5	12	1	0.8	1	0	0.8
WASH WEST	3	2	38.8992	-77.1044	3			10			3	10	0	0.7	0	0	0.9
WASH WEST	3	3	38.8994	-77.0929	6			6			4	22	0	0.65	0	0	0.8
WASH WEST	3	4	38.8996	-77.0813	6	3					7	10	0	0.8	0	0	0.9
WASH WEST	3	5	38.8998	-77.0697	4.5	6.5			1		4	30	0	0.5	1	0	0.5
WASH WEST	3	6	38.9000	-77.0582	3	3.5					9.5	17.4	0	0.53	1	0	1
WASH WEST	3	7	38.9003	-77.0466						2	14	21	1	0.2	1	0	1
WASH WEST	3	8	38.9005	-77.0351							16	22.3	1	0.39	1	0	1
WASH WEST	3	9	38.9007	-77.0235						3	13	18.2	1	0.51	1	0	1
WASH WEST	3	10	38.9009	-77.0119						8	8	21	1	0.2	1	0	1
WAW/WAE	B3		38.9011	-77.0004						12	4	18	0	0	0	0	1
WASH EAST	3	1	38.9013	-76.9888						15	1	12	0	0	0	1	1
WASH EAST	3	2	38.9015	-76.9772						11	5	8.8	1	0.3	0	0	0.9
WASH EAST	3	3	38.9017	-76.9657	8	5					3	12	0	0.8	1	0	1
WASH EAST	3	4	38.9020	-76.9541	9	1					6	11.3	1	0.4	0	1	1
WASH EAST	3	5	38.9022	-76.9425	1.5				12		2.5	10	0	0.75	0	0	1
WASH EAST	3	6	38.9024	-76.9310					15		1	7	1	1	1	0	1
WASH EAST	3	7	38.9026	-76.9194	2		4	9			1	10	1	0	0	0	1
WASH EAST	3	8	38.9028	-76.9079	3			12			1	10	1	0	0	0	1
WASH EAST	3	9	38.9030	-76.8963	5		6	3			2	9	0	0.3	0	0	1
WASH EAST	3	10	38.9032	-76.8847	15						1	12	1	0.2	0	0	1
WAE/LANHAM	B3		38.9034	-76.8732	11.5		2				2.5	10	0	0	0	0	1
LANHAM	3	1	38.9036	-76.8616	16												
LANHAM	3	2	38.9039	-76.8500	8.5						7.5	16.7	0	0.07	0	0	0.7
LANHAM	3	3	38.9041	-76.8385	16												
LANHAM	3	4	38.9043	-76.8269	16												
FALLS CHURCH	2	2	38.8879	-77.2313	4.5		9	1			1.5	10	0	0.2	0	0	0.8
FALLS CHURCH	2	3	38.8881	-77.2198	5.5			5			5.5	7	0	0.47	0	0	0.3
FALLS CHURCH	2	4	38.8883	-77.2082	9			6			1	7	0	0.47	0	0	0.7
FALLS CHURCH	2	5	38.8885	-77.1966	3			13									1
FALLS CHURCH	2	6	38.8887	-77.1851	7			9									1
FALLS CHURCH	2	7	38.8889	-77.1735	8			8									1
FALLS CHURCH	2	8	38.8891	-77.1620	1.5			10			4.5	7	0	0.7	0	0	1
FALLS CHURCH	2	9	38.8894	-77.1504				15.5			0.5	7	0	0.47	0	0	1
FALLS CHURCH	2	10	38.8896	-77.1388	1			14			1	7	0	0.7	0	0	1
FALLS/WAW	B2		38.8898	-77.1273	1		1	12.5			1.5	15	1	0.8	1	0	1
WASH WEST	2	1	38.8900	-77.1157	0.5			14.5			1	7	0	0.47	0	0	0.8
WASH WEST	2	2	38.8902	-77.1041	1			12			3	12	0	0.1	0	0	0.8
WASH WEST	2	3	38.8904	-77.0926				12			4	7	0	0.8	0	0	1
WASH WEST	2	4	38.8906	-77.0810	4				6		6	18	0	0.3	0	0	1
WASH WEST	2	5	38.8908	-77.0695	7.5	1					7.5	20.2	0	0.45	1	0	0.7
WASH WEST	2	6	38.8910	-77.0579	5.5	8					2.5	12	0	0.4	0	0	1
WASH WEST	2	7	38.8913	-77.0463	9.5	1					5.5	24	1	0.3	1	0	1
WASH WEST	2	8	38.8915	-77.0348	11.5						4.5	24	1	0.3	1	0	0.7
WASH WEST	2	9	38.8917	-77.0232	4						12	21.8	1	0.28	1	0	0.7
WASH WEST	2	10	38.8919	-77.0117	8	0.5					7.5	18	1	0.23	1	0	0.7
WAW/WAE	B2		38.8921	-77.0001	1.5					11.5	3	20	1	0	1	0	1
WASH EAST	2	1	38.8923	-76.9885	1					15							1
WASH EAST	2	2	38.8925	-76.9770	1					10	5	25	0	0	0	0	1
WASH EAST	2	3	38.8927	-76.9654	5	6			1		4	25	0	0	0	0	0.8
WASH EAST	2	4	38.8930	-76.9538	2					6	8	10	0	0.8	1	0	1
WASH EAST	2	5	38.8932	-76.9423	4				6		6	8	1	0.5	1	0	1

WASH EAST	2	6	38.8934	-76.9307	1				11		4	10	1	0	1	1	0.9
WASH EAST	2	7	38.8936	-76.9192					9		7	10.6	1	0.36	1	0	0.8
WASH EAST	2	8	38.8938	-76.9076					14		2	10	0	0	0	0	1
WASH EAST	2	9	38.8940	-76.8960	5		11										1
WASH EAST	2	10	38.8942	-76.8845	5		11										1
WAE/LANHAM	B2		38.8944	-76.8729	12.5		3.5										1
LANHAM	2	1	38.8946	-76.8614	14		2										1
LANHAM	2	2	38.8949	-76.8498	9		1				6	7	0	0.3	0	0	0.2
LANHAM	2	3	38.8951	-76.8382	15						1	0.1	0	0	0	0	1
LANHAM	2	4	38.8953	-76.8267	11						5	10	0	0.6	1	0	1
FALLS CHURCH	1	2	38.8789	-77.2310	4.5		1.5	1			9	7	1	0.6	1	0	0.4
FALLS CHURCH	1	3	38.8791	-77.2195	6	0.5		3.5			6	7	0	0.7	1	0	1
FALLS CHURCH	1	4	38.8793	-77.2079	11		5										1
FALLS CHURCH	1	5	38.8795	-77.1964	10.5			5.5									1
FALLS CHURCH	1	6	38.8797	-77.1848	6			10									1
FALLS CHURCH	1	7	38.8799	-77.1732	9			7									1
FALLS CHURCH	1	8	38.8801	-77.1617	2			14									1
FALLS CHURCH	1	9	38.8804	-77.1501	2			12			2	27	0	0.8	1	0	1
FALLS CHURCH	1	10	38.8806	-77.1386	2			8.5			5.5	11.3	0	0.6	0	0	0.9
FALLS/WAW	B1		38.8808	-77.1270	2			12			2	7	0	0.47	0	0	0.9
WASH WEST	1	1	38.8810	-77.1154	2			7			7	12	0	0.5	0	0	1
WASH WEST	1	2	38.8812	-77.1039				7			9	15	0	0.6	0	0	1
WASH WEST	1	3	38.8814	-77.0923				14			2	10	0	0.6	0	0	0.8
WASH WEST	1	4	38.8816	-77.0808	8						8	10	1	0.8	1	0	1
WASH WEST	1	5	38.8818	-77.0692	15						1	0.1	0	0	0	0	1
WASH WEST	1	6	38.8821	-77.0576	10.5	4.5					1	0.1	0	0	0	0	1
WASH WEST	1	7	38.8823	-77.0461	4.5	11.5											
WASH WEST	1	8	38.8825	-77.0345	5.5	6.5					4	24	0	0.4	1	0	0.8
WASH WEST	1	9	38.8827	-77.0230	2	1					13	19.3	1	0.27	1	0	1
WASH WEST	1	10	38.8829	-77.0114						4	12	18.5	1	0.3	1	0	1
WAW/WAE	B1		38.8831	-76.9998						15	1	20	1	0	1	0	1
WASH EAST	1	1	38.8833	-76.9883						16							1
WASH EAST	1	2	38.8835	-76.9767	4	1				5	6	18	0	0.2	1	0	1
WASH EAST	1	3	38.8837	-76.9652	10	3				2	1	10	0	0.47	1	0	1
WASH EAST	1	4	38.8840	-76.9536	6					5	5	10	1	0.6	0	0	1
WASH EAST	1	5	38.8842	-76.9420	6		6				4	10	1	0.5	1	0	1
WASH EAST	1	6	38.8844	-76.9305	2				1.5	12.5							1
WASH EAST	1	7	38.8846	-76.9189					13		3	18.3	1	0	1	0	0.9
WASH EAST	1	8	38.8848	-76.9073	5		3		8								0.6
WASH EAST	1	9	38.8850	-76.8958	9		6				1	10	1	0	1	0	0.5
WASH EAST	1	10	38.8852	-76.8842	12		4										0.3
WAE/LANHAM	B1		38.8854	-76.8727	10.5		3.5				2	7	0	1	0	0	0.4
LANHAM	1	1	38.8857	-76.8611	8						8	7	1	0.3	1	0	0.8
LANHAM	1	2	38.8859	-76.8496	8.5						7.5	10	0	0.3	0	0	0.8
LANHAM	1	3	38.8861	-76.8380	12		1				3	10	0	0.7	1	0	0.7
LANHAM	1	4	38.8863	-76.8264	12.5						3.5	10.6	1	0.5	1	0	1
FALLS/ANNAN		B2	38.8699	-77.2309	3.5						13	8.6	1	0.43	0	0	1
FALLS/ANNAN		B3	38.8701	-77.2193	3.5	1.5		1.5			9.5	24	0	0.3	0	0	0.4
FALLS/ANNAN		B4	38.8703	-77.2078	6			8			2	10	1	0	0	0	0.8
FALLS/ANNAN		B5	38.8705	-77.1962	4		6	5			1	7	0	0.47	0	0	0.7
FALLS/ANNAN		B6	38.8707	-77.1847	4		5	6			1	7	0	0.47	0	0	0.7
FALLS/ANNAN		B7	38.8709	-77.1731	8		1	6			1	7	0	0.47	0	0	0.7
FALLS/ANNAN		B8	38.8711	-77.1615	4		6	5			1	7	0	0.47	0	0	0.7
FALLS/ANNAN		B9	38.8714	-77.1500	3.5			1			12	9.3	0	0.7	0	0	0.8
FALLS/ANNAN		B10	38.8716	-77.1384	6.5		4	2			3.5	7	0	0.8	0	0	0.8
FA/AN/WW/ALEX	B1		38.8718	-77.1269	7.5			8.5									1
WAW/ALEX		B1	38.8720	-77.1153	4.5			6			5.5	10.9	1	0.71	0	0	1
WAW/ALEX		B2	38.8722	-77.1037	3			7			6	10	0	0.72	0	0	0.8
WAW/ALEX		B3	38.8724	-77.0922	1			12			3	12	0	0.1	0	0	1
WAW/ALEX		B4	38.8726	-77.0806	6			5			5	10	0	0.5	0	0	1
WAW/ALEX		B5	38.8728	-77.0691	13						3	15	1	0.4	1	0	1
WAW/ALEX		B6	38.8731	-77.0575	6						10	15	0	0.7	2	0	1
WAW/ALEX		B7	38.8733	-77.0460	3.5	8					4.5	0.1	0	0	0	0	0.9
WAW/ALEX		B8	38.8735	-77.0344	6	8.5					1.5	4	0	0	0	0	1
WAW/ALEX		B9	38.8737	-77.0228	4.5	5.5					6	24	1	0.5	1	0	1
WAW/ALEX		B10	38.8739	-77.0113		0.5					16	13.2	1	0.5	0	0	1
WW/WE/ALEX/AN	B1		38.8741	-76.9997		5				4	7	20	1	0.5	1	0	1
WAE/ANACOSTIA		B1	38.8743	-76.9882	2.5	5				3	5.5	22.5	1	0.6	1	0	1
WAE/ANACOSTIA		B2	38.8745	-76.9766	6	3.5			4.5		2	7	0	0.47	0	0	0.8
WAE/ANACOSTIA		B3	38.8747	-76.9650	4		3	3.5	5		0.5	7	0	0.47	0	0	1
WAE/ANACOSTIA		B4	38.8750	-76.9535	10.5			5.5									1
WAE/ANACOSTIA		B5	38.8752	-76.9419	10		3	3									1
WAE/ANACOSTIA		B6	38.8754	-76.9304	1.5			13.5			1	7	0	0.9	0	0	1
WAE/ANACOSTIA		B7	38.8756	-76.9188	4.5			11.5									1

WAE/ANACOSTIA		B8	38.8758	-76.9072	14.5			1.5									1
WAE/ANACOSTIA		B9	38.8760	-76.8957	13		1				2	10	1	0.7	0	0	1
WAE/ANACOSTIA		B10	38.8762	-76.8841	9.5		4.5				2	10	1	0.6	0	0	1
WE/LANH/AN+A1144/UM	B1		38.8764	-76.8726	12.5		3.5										1
LANHAM/UMARL		B1	38.8766	-76.8610	13		1				2	7	0	0.6	0	0	1
LANHAM/UMARL		B2	38.8769	-76.8495	12						4	7	0	0.2	0	0	1
LANHAM/UMARL		B3	38.8771	-76.8379	9			6			1	7	0	0.47	0	0	0.5
LANHAM/UMARL		B4	38.8773	-76.8263	11		5										1
ANNANDLE, VA	13	2	38.8609	-77.2305	9						7	15.7	0	0.5	0	0	1
ANNANDLE, VA	13	3	38.8611	-77.2189	11.5		2				2.5	45	0	0	0	0	0.6
ANNANDLE, VA	13	4	38.8613	-77.2073	5.5	0.5	3	4			3	24	1	0	0	0	1
ANNANDLE, VA	13	5	38.8615	-77.1958	3.5		6	6.5									1
ANNANDLE, VA	13	6	38.8617	-77.1842	3		6	7									1
ANNANDLE, VA	13	7	38.8619	-77.1727	8.5		3.5	4									1
ANNANDLE, VA	13	8	38.8621	-77.1611	9		4	3									1
ANNANDLE, VA	13	9	38.8624	-77.1496	7		6	3									1
ANNANDLE, VA	13	10	38.8626	-77.1380	7.5	0.5	4	3.5			0.5	7	0	0.47	0	0	0.8
ANNAN/ALEX	B13		38.8628	-77.1264	7			7			2	10	0	0	0	0	0.8
ALEXANDRIA, VA	13	1	38.8630	-77.1149	6.5	0.5		9									1
ALEXANDRIA, VA	13	2	38.8632	-77.1033	11			5									1
ALEXANDRIA, VA	13	3	38.8634	-77.0918	3			13									1
ALEXANDRIA, VA	13	4	38.8636	-77.0802	6			10									1
ALEXANDRIA, VA	13	5	38.8638	-77.0687	7			3			6	7	0	0	1	0	1
ALEXANDRIA, VA	13	6	38.8641	-77.0571	9.5			2			4.5	7	0	0.47	0	0	1
ALEXANDRIA, VA	13	7	38.8643	-77.0455	8	3					5	27	0	0.2	1	0	1
ALEXANDRIA, VA	13	8	38.8645	-77.0340	2	14											
ALEXANDRIA, VA	13	9	38.8647	-77.0224	6	8					2	8	1	0.5	1	1	1
ALEXANDRIA, VA	13	10	38.8649	-77.0109	2	7.5					6.5	9	1	0.5	0	0	1
ALEX/ANAC	B13		38.8651	-76.9993	7	1.5				1.5	6	8	0	0.3	0	0	0.9
ANACOSTIA, MD	13	1	38.8653	-76.9878	2	0.5				11	2.5	10	0	0.1	0	0	1
ANACOSTIA, MD	13	2	38.8655	-76.9762	6.5				4.5	4	1	10	1	0.4	1	0	1
ANACOSTIA, MD	13	3	38.8658	-76.9646	6			5.5		3	1.5	10	1	0.1	0	0	1
ANACOSTIA, MD	13	4	38.8660	-76.9531	4.5			9			2.5	9.4	1	0.56	1	0	1
ANACOSTIA, MD	13	5	38.8662	-76.9415	3			11			2	10	0	0.6	0	0	0.7
ANACOSTIA, MD	13	6	38.8664	-76.9300	6		2	6			2	12	0	0.3	1	0	1
ANACOSTIA, MD	13	7	38.8666	-76.9184	8			3			5	10.3	0	0.28	0	0	0.6
ANACOSTIA, MD	13	8	38.8668	-76.9069	13.5		1	1			0.5	10	1	0.1	0	0	1
ANACOSTIA, MD	13	9	38.8670	-76.8953	12	1.5					2.5	10	1	0.2	0	0	1
ANACOSTIA, MD	13	10	38.8672	-76.8837	12		2				2	10	1	0.4	0	0	1
ANAC/UMARL	B13		38.8674	-76.8722	13		3										1
UPPER MARLBORO	13	1	38.8677	-76.8606	12		3				1	7	1	0.7	0	1	1
UPPER MARLBORO	13	2	38.8679	-76.8491	15.5						0.5	0.1	0	0	0	0	0
UPPER MARLBORO	13	3	38.8681	-76.8375	14.5						1.5	4	0	0	1	0	0.3
UPPER MARLBORO	13	4	38.8683	-76.8260	16												
ANNANDLE, VA	12	2	38.8519	-77.2303	7			7			2	10	1	1	0	0	1
ANNANDLE, VA	12	3	38.8521	-77.2187	7		3	5			1	7	0	0.47	0	0	0.9
ANNANDLE, VA	12	4	38.8523	-77.2072	10.5		2	3.5									1
ANNANDLE, VA	12	5	38.8525	-77.1956	11.5	0.5	2	2									1
ANNANDLE, VA	12	6	38.8527	-77.1841	8		5	3									1
ANNANDLE, VA	12	7	38.8529	-77.1725	10		4	2									1
ANNANDLE, VA	12	8	38.8532	-77.1610	6.5	0.5	2	7									1
ANNANDLE, VA	12	9	38.8534	-77.1494	9.5	1.5		5									1
ANNANDLE, VA	12	10	38.8536	-77.1379	8		1	7									1
ANNAN/ALEX	B12		38.8538	-77.1263	9			6			1	7	0	0.47	0	0	1
ALEXANDRIA, VA	12	1	38.8540	-77.1147	7			9									1
ALEXANDRIA, VA	12	2	38.8542	-77.1032	7.5	0.5		8									1
ALEXANDRIA, VA	12	3	38.8544	-77.0916	2			14									1
ALEXANDRIA, VA	12	4	38.8546	-77.0801	12			4									1
ALEXANDRIA, VA	12	5	38.8548	-77.0685	6			9			1	7	0	0.47	0	0	1
ALEXANDRIA, VA	12	6	38.8551	-77.0570	6				9		1	7	0	0.47	1	0	1
ALEXANDRIA, VA	12	7	38.8553	-77.0454	2						14	17	0	0.33	0	0	0.8
ALEXANDRIA, VA	12	8	38.8555	-77.0339	6	6.5					3.5	0.1	0	0	0	0	0.9
ALEXANDRIA, VA	12	9	38.8557	-77.0223	1.5	14.5											
ALEXANDRIA, VA	12	10	38.8559	-77.0107	6.5	1					8.5	8	0	0.2	0	0	1
ALEX/ANAC	B12		38.8561	-76.9992	9					4	3	7	0	0.5	0	0	1
ANACOSTIA, MD	12	1	38.8563	-76.9876	5					4	7	9.5	1	0.35	0	0	1
ANACOSTIA, MD	12	2	38.8565	-76.9761	7.5	0.5			4.5		3.5	7	1	0.4	1	0	1
ANACOSTIA, MD	12	3	38.8568	-76.9645	5				5	4	2	8.5	0	0.65	0	0	1
ANACOSTIA, MD	12	4	38.8570	-76.9530	10			5			1	10	1	0.3	1	0	1
ANACOSTIA, MD	12	5	38.8572	-76.9414	15						1	10	1	0.9	0	0	1
ANACOSTIA, MD	12	6	38.8574	-76.9299	5			9			2	10	1	0.2	1	0	1
ANACOSTIA, MD	12	7	38.8576	-76.9183	6		3				7	10	0	0.28	0	0	0.6
ANACOSTIA, MD	12	8	38.8578	-76.9067	6			5			5	7.6	0	0.2	0	0	0.8
ANACOSTIA, MD	12	9	38.8580	-76.8952	3		1.5	9			2.5	10	0	0.6	0	0	1

ANACOSTIA, MD	12	10	38.8582	-76.8836			16										1
ANAC/UMARL	B12		38.8584	-76.8721	4		9	3									1
UPPER MARLBORO	12	1	38.8587	-76.8605	12		3				1	5	0	0.2	0	0	0.9
UPPER MARLBORO	12	2	38.8589	-76.8490	13			1			2	4	0	0	1	0	0.2
UPPER MARLBORO	12	3	38.8591	-76.8374	15						1	4	1	0	1	0	1
UPPER MARLBORO	12	4	38.8593	-76.8259	16												
ANNANDLE, VA	11	2	38.8429	-77.2299	7			9									1
ANNANDLE, VA	11	3	38.8431	-77.2183	10		2	4									1
ANNANDLE, VA	11	4	38.8433	-77.2068	10		1	5									1
ANNANDLE, VA	11	5	38.8435	-77.1952	5		2	9									1
ANNANDLE, VA	11	6	38.8437	-77.1836	4		4	8									1
ANNANDLE, VA	11	7	38.8439	-77.1721	10.5	0.5		5									1
ANNANDLE, VA	11	8	38.8441	-77.1605	8	2	2	4									1
ANNANDLE, VA	11	9	38.8444	-77.1490	8	5	1	2									1
ANNANDLE, VA	11	10	38.8446	-77.1374	8			8									1
ANNAN/ALEX	B11		38.8448	-77.1259	11			5									1
ALEXANDRIA, VA	11	1	38.8450	-77.1143	10			6									1
ALEXANDRIA, VA	11	2	38.8452	-77.1028	9			7									1
ALEXANDRIA, VA	11	3	38.8454	-77.0912	5			7			4	7	1	0	1	0	1
ALEXANDRIA, VA	11	4	38.8456	-77.0797	6			4			6	24	0	0.2	0	0	1
ALEXANDRIA, VA	11	5	38.8458	-77.0681	9.5	0.5		6									1
ALEXANDRIA, VA	11	6	38.8461	-77.0566	9	1		4			2	7	0	0	0	0	1
ALEXANDRIA, VA	11	7	38.8463	-77.0450	4.5						12	9.1	0	0.13	0	0	0.7
ALEXANDRIA, VA	11	8	38.8465	-77.0334	6	6.5					3.5	0.1	0	0	0	0	1
ALEXANDRIA, VA	11	9	38.8467	-77.0219	3	10.5					2.5	7	1	0.4	0	0	1
ALEXANDRIA, VA	11	10	38.8469	-77.0103	12						4	7	0	0.3	0	0	1
ALEX/ANAC	B11		38.8471	-76.9988	6				6		4	10	1	0.6	0	0	1
ANACOSTIA, MD	11	1	38.8473	-76.9872	9.5	0.5					6	8.25	1	0.6	0	0	1
ANACOSTIA, MD	11	2	38.8475	-76.9757	3						13	7	1	0.6	1	0	1
ANACOSTIA, MD	11	3	38.8478	-76.9641	8		3.5		3.5		1	10	1	0.3	0	0	1
ANACOSTIA, MD	11	4	38.8480	-76.9526	8		4				4	7	1	0.4	0	0	1
ANACOSTIA, MD	11	5	38.8482	-76.9410	13.5						2.5	9.2	1	0.14	0	0	1
ANACOSTIA, MD	11	6	38.8484	-76.9295	6			2.5			7.5	10.7	0	0.55	1	0	0.9
ANACOSTIA, MD	11	7	38.8486	-76.9179	7		3				6	7	1	0.4	1	0	1
ANACOSTIA, MD	11	8	38.8488	-76.9063	8.5			5.5			2	10	0	0.9	1	0	0.6
ANACOSTIA, MD	11	9	38.8490	-76.8948	5		6				5	8.5	0	0.55	0	0	1
ANACOSTIA, MD	11	10	38.8492	-76.8832	4.5		4.5				7	7.9	0	0.23	0	0	1
ANAC/UMARL	B11		38.8494	-76.8717	4		4.5	4			3.5	7	0	0.4	0	0	1
UPPER MARLBORO	11	1	38.8497	-76.8601	12.5		1	1			1.5	7	0	0.47	0	0	0.3
UPPER MARLBORO	11	2	38.8499	-76.8486	13		1	2									1
UPPER MARLBORO	11	3	38.8501	-76.8370	16												
UPPER MARLBORO	11	4	38.8503	-76.8255	16												
ANNANDLE, VA	10	2	38.8339	-77.2560	10			6									1
ANNANDLE, VA	10	3	38.8341	-77.2445	8			2			6	10	0	0	0	0	1
ANNANDLE, VA	10	4	38.8343	-77.2329	8		5	2			1	7	0	0.47	0	0	1
ANNANDLE, VA	10	5	38.8345	-77.2214	6		4	6									1
ANNANDLE, VA	10	6	38.8347	-77.2098	6		4	6									1
ANNANDLE, VA	10	7	38.8349	-77.1983	12	0.5	1.5	2									1
ANNANDLE, VA	10	8	38.8352	-77.1867	7		3	6									1
ANNANDLE, VA	10	9	38.8354	-77.1752	1			15									1
ANNANDLE, VA	10	10	38.8356	-77.1636	7			8			1	10	1	0.1	0	0	1
ANNAN/ALEX	B10		38.8358	-77.1521	3			10			3	10	1	0.3	0	0	1
ALEXANDRIA, VA	10	1	38.8360	-77.1405	3			5.5			7.5	18	1	0.59	0	0	1
ALEXANDRIA, VA	10	2	38.8362	-77.1290	5			3			8	12.8	0	0.72	0	0	0.8
ALEXANDRIA, VA	10	3	38.8364	-77.1174				4			12	10	0	0.8	0	0	0.9
ALEXANDRIA, VA	10	4	38.8366	-77.1059				16									1
ALEXANDRIA, VA	10	5	38.8368	-77.0943	1.5		3.5	11									1
ALEXANDRIA, VA	10	6	38.8371	-77.0828	6	0.5			4		5.5	11.2	1	0.75	1	0	1
ALEXANDRIA, VA	10	7	38.8373	-77.0712	3.5	6.5					6	0.1	0	0	0	0	1
ALEXANDRIA, VA	10	8	38.8375	-77.0597	1.5	14.5											
ALEXANDRIA, VA	10	9	38.8377	-77.0481		6					10	7.5	0	0.53	0	0	1
ALEXANDRIA, VA	10	10	38.8379	-77.0365	4.5			2	3		6.5	8	0	0.4	0	0	1
ALEX/ANAC	B10		38.8381	-77.0250	5.5	0.5			5		5	10	1	0.47	0	0	1
ANACOSTIA, MD	10	1	38.8383	-77.0134	8				4		4	9.3	0	0.7	0	0	1
ANACOSTIA, MD	10	2	38.8385	-77.0019	16												
ANACOSTIA, MD	10	3	38.8388	-76.9903	4.5		7.5				4	10	1	0.7	1	0	1
ANACOSTIA, MD	10	4	38.8390	-76.9788	1		9	2			4	7.8	1	0.3	0	0	1
ANACOSTIA, MD	10	5	38.8392	-76.9672	9			1			6	7.5	0	0.14	0	0	1
ANACOSTIA, MD	10	6	38.8394	-76.9557	9			1.5			5.5	10	0	0.8	0	0	0.8
ANACOSTIA, MD	10	7	38.8396	-76.9441	10		2	2			2	8	1	0.7	0	0	1
ANACOSTIA, MD	10	8	38.8398	-76.9326	13.5			0.5			2	10	1	0.6	0	0	1
ANACOSTIA, MD	10	9	38.8400	-76.9210	10						6	10	1	0.5	0	0	1
ANACOSTIA, MD	10	10	38.8402	-76.9095	7		4.5				4.5	10	0	0.29	0	0	1
ANAC/UMARL	B10		38.8404	-76.8979	5.5		3				7.5	7	0	0.2	0	0	0.7

UPPER MARLBORO	10	1	38.8407	-76.8864	9			2.5			4.5	7	0	0	1	0	0.6
UPPER MARLBORO	10	2	38.8409	-76.8748	16												
UPPER MARLBORO	10	3	38.8411	-76.8633	14		2										1
UPPER MARLBORO	10	4	38.8413	-76.8517	16												
ANNANDLE, VA	9	2	38.8249	-77.2293	10			6									1
ANNANDLE, VA	9	3	38.8251	-77.2177	7						9	9.6	1	0.62	0	0	1
ANNANDLE, VA	9	4	38.8253	-77.2062	9		2	5									1
ANNANDLE, VA	9	5	38.8255	-77.1946	8		2	6									1
ANNANDLE, VA	9	6	38.8257	-77.1831	11		2	3									1
ANNANDLE, VA	9	7	38.8259	-77.1715	10			6									1
ANNANDLE, VA	9	8	38.8262	-77.1600	6			6			4	10	0	0.7	0	0	0.8
ANNANDLE, VA	9	9	38.8264	-77.1484	5.5			9			1.5	10	1	0.6	1	0	1
ANNANDLE, VA	9	10	38.8266	-77.1369	3		4	8			1	10	1	0.3	0	0	1
ANNAN/ALEX	B9		38.8268	-77.1253	7.5	0.5					8	10	1	0.2	0	0	1
ALEXANDRIA, VA	9	1	38.8270	-77.1138	6		1	1			8	11.3	0	0.37	0	0	1
ALEXANDRIA, VA	9	2	38.8272	-77.1022	12		2	1			1	10	0	0.5	0	0	1
ALEXANDRIA, VA	9	3	38.8274	-77.0907	6.5		0.5				9	8	1	0.7	0	0	1
ALEXANDRIA, VA	9	4	38.8276	-77.0791	2			11			3	7	0	0.6	0	0	1
ALEXANDRIA, VA	9	5	38.8278	-77.0676	6.5		2	5	2.5								1
ALEXANDRIA, VA	9	6	38.8281	-77.0560					13.5		2.5	8.2	1	0.56	0	0	1
ALEXANDRIA, VA	9	7	38.8283	-77.0445	10	1					5	0.1	0	0	0	0	1
ALEXANDRIA, VA	9	8	38.8285	-77.0329		16											
ALEXANDRIA, VA	9	9	38.8287	-77.0214	2.5	1	2.5				10	11.3	0	0.41	0	0	1
ALEXANDRIA, VA	9	10	38.8289	-77.0098	5			2.5		8	0.5	9.29	0	0.47	1	0	1
ALEX/ANAC	B9		38.8291	-76.9983	3.5				3		9.5	10.2	1	0.69	0	0	1
ANACOSTIA, MD	9	1	38.8293	-76.9867	8						8	10	0	0.67	0	0	1
ANACOSTIA, MD	9	2	38.8295	-76.9752	12		4										1
ANACOSTIA, MD	9	3	38.8298	-76.9636	5.5		7.5				3	12	0	0.5	0	0	1
ANACOSTIA, MD	9	4	38.8300	-76.9521	2.5		11				2.5	10	1	0.1	0	0	1
ANACOSTIA, MD	9	5	38.8302	-76.9405	5.5		3				7.5	7	0	0.51	0	0	1
ANACOSTIA, MD	9	6	38.8304	-76.9290	11		1.5				3.5	7	0	0	0	0	1
ANACOSTIA, MD	9	7	38.8306	-76.9174	14.5			0.5			1	7	0	0.2	0	0	1
ANACOSTIA, MD	9	8	38.8308	-76.9059	12	1	3										1
ANACOSTIA, MD	9	9	38.8310	-76.8943	4.5		1.5	10									1
ANACOSTIA, MD	9	10	38.8312	-76.8827	12.5						3.5	8	1	0.2	0	0	0.7
ANAC/UMARL	B9		38.8314	-76.8712	10.5			1			4.5	7	0	0.7	0	0	0.7
UPPER MARLBORO	9	1	38.8317	-76.8596	12.5						3.5	7	0	0.1	0	0	0.7
UPPER MARLBORO	9	2	38.8319	-76.8481	16												
UPPER MARLBORO	9	3	38.8321	-76.8365	16												
UPPER MARLBORO	9	4	38.8323	-76.8250	16												
ANNANDLE, VA	8	2	38.8159	-77.2290	12.8	0.75		2			0.5	10	0	0	0	0	1
ANNANDLE, VA	8	3	38.8161	-77.2174	4.5		6.5				5	10	0	0.4	0	0	0.7
ANNANDLE, VA	8	4	38.8163	-77.2059	8.5	0.5	2	5									1
ANNANDLE, VA	8	5	38.8165	-77.1943	11		2	3									1
ANNANDLE, VA	8	6	38.8167	-77.1828	11		2	3									1
ANNANDLE, VA	8	7	38.8169	-77.1712	8		7				1	10	1	0	1	0	1
ANNANDLE, VA	8	8	38.8172	-77.1597	4.5			10			1.5	9	1	0.27	0	0	1
ANNANDLE, VA	8	9	38.8174	-77.1482	6			2.5			7.5	9.1	0	0.67	0	0	1
ANNANDLE, VA	8	10	38.8176	-77.1366	1.5			0.5			14	20.4	0	0.45	0	0	1
ANNAN/ALEX	B8		38.8178	-77.1250	2.5	0.5	3.5				9.5	27.1	0	0.43	0	0	1
ALEXANDRIA, VA	8	1	38.8180	-77.1135	7		5.5				3.5	10	1	0.5	0	0	1
ALEXANDRIA, VA	8	2	38.8182	-77.1019	6.5		4.5	2.5			2.5	7.6	1	0.3	0	0	1
ALEXANDRIA, VA	8	3	38.8184	-77.0904	10		4	2									1
ALEXANDRIA, VA	8	4	38.8186	-77.0789	7.5	0.5	2	6									1
ALEXANDRIA, VA	8	5	38.8188	-77.0673	4			5	7								1
ALEXANDRIA, VA	8	6	38.8191	-77.0558					11		5	15	0	0.2	1	0	1
ALEXANDRIA, VA	8	7	38.8193	-77.0442	1	1.5					14	11.2	1	0.6	1	0	1
ALEXANDRIA, VA	8	8	38.8195	-77.0326	0.5	15.5											
ALEXANDRIA, VA	8	9	38.8197	-77.0211	2.5	3.5					10	8	1	0.2	1	0	1
ALEXANDRIA, VA	8	10	38.8199	-77.0095	11					4	1	7	0	0.3	0	0	1
ALEX/ANAC	B8		38.8201	-76.9980	2.5			5			8.5	8.9	0	0.66	0	0	0.9
ANACOSTIA, MD	8	1	38.8203	-76.9865	8		1	1.5			5.5	10	1	0.3	0	0	1
ANACOSTIA, MD	8	2	38.8205	-76.9749	9.5			5.5			1	10	1	0	1	0	1
ANACOSTIA, MD	8	3	38.8208	-76.9634	13			3									1
ANACOSTIA, MD	8	4	38.8210	-76.9518	7		1	5			3	8	0	0.17	0	0	1
ANACOSTIA, MD	8	5	38.8212	-76.9402	9	1					6	7.3	0	0.43	0	0	0.6
ANACOSTIA, MD	8	6	38.8214	-76.9287	12.5			2			1.5	7	0	0.47	0	0	0.2
ANACOSTIA, MD	8	7	38.8216	-76.9171	5.5			2			8.5	10	0	0.5	0	0	0.4
ANACOSTIA, MD	8	8	38.8218	-76.9056	6.5			7.5			2	10	0	0	0	0	0.6
ANACOSTIA, MD	8	9	38.8220	-76.8941	9	0.5		3			3.5	7	0	0.5	0	0	0.7
ANACOSTIA, MD	8	10	38.8222	-76.8825	11	0.5	1				3.5	8	0	0.4	0	0	0.2
ANAC/UMARL	B8		38.8224	-76.8710	14						2	0.1	0	0	0	0	0.9
UPPER MARLBORO	8	1	38.8227	-76.8594	8.5		0.5				7	10.8	0	0.44	0	0	0.5
UPPER MARLBORO	8	2	38.8229	-76.8478	13.5						2.5	4	0	0	1	0	1

UPPER MARLBORO	8	3	38.8231	-76.8363	16												
UPPER MARLBORO	8	4	38.8233	-76.8247	16												
ANNANDLE, VA	7	2	38.8069	-77.2288	10		6										1
ANNANDLE, VA	7	3	38.8071	-77.2173	3		3.5				9.5	18	0	0.4	1	0	0.7
ANNANDLE, VA	7	4	38.8073	-77.2058	2		7	7									1
ANNANDLE, VA	7	5	38.8075	-77.1942	10		2	4									1
ANNANDLE, VA	7	6	38.8077	-77.1826	11		2	3									1
ANNANDLE, VA	7	7	38.8079	-77.1711	7.5		4	3			1.5	7	0	0.4	0	0	1
ANNANDLE, VA	7	8	38.8082	-77.1596	7.5		0.5	5			3	8	0	0.2	0	0	1
ANNANDLE, VA	7	9	38.8084	-77.1480	11.5		0.5	0.5			3.5	60	0	0.4	1	0	1
ANNANDLE, VA	7	10	38.8086	-77.1365	2						14	21.3	0	0.33	1	0	1
ANNAN/ALEX	B7		38.8088	-77.1249	4						12	8.3	1	0.48	1	0	1
ALEXANDRIA, VA	7	1	38.8090	-77.1134	6	1	2				7	7	0	0.63	1	0	1
ALEXANDRIA, VA	7	2	38.8092	-77.1018	5		4	2			5	7	0	0.6	1	0	1
ALEXANDRIA, VA	7	3	38.8094	-77.0903	4		2.5	4			5.5	8	0	0.3	0	0	1
ALEXANDRIA, VA	7	4	38.8096	-77.0787	3		2	4	2		5	8	0	0	0	0	1
ALEXANDRIA, VA	7	5	38.8099	-77.0672	6	0.5			8.5		1	7	0	0.47	1	0	1
ALEXANDRIA, VA	7	6	38.8101	-77.0556					4		12	12	1	0.5	1	0	1
ALEXANDRIA, VA	7	7	38.8103	-77.0441		0.5					16	14	1	0.5	1	0	1
ALEXANDRIA, VA	7	8	38.8105	-77.0325	1	15											
ALEXANDRIA, VA	7	9	38.8107	-77.0210	3	8					5	7	0	0.58	0	0	1
ALEXANDRIA, VA	7	10	38.8109	-77.0094	10	1.5		2.5			2	7	0	0.8	0	0	1
ALEX/ANAC	B7		38.8111	-76.9979	3.5			11			1.5	10	0	0.1	1	0	0.7
ANACOSTIA, MD	7	1	38.8113	-76.9863	8		8										1
ANACOSTIA, MD	7	2	38.8115	-76.9748	6.5		5				4.5	7	0	0.6	0	0	0.5
ANACOSTIA, MD	7	3	38.8118	-76.9632	8			2			6	12	0	0.1	0	0	0.4
ANACOSTIA, MD	7	4	38.8120	-76.9517	9.5			5			1.5	10	0	0	0	0	0.6
ANACOSTIA, MD	7	5	38.8122	-76.9401	7.5			8.5									1
ANACOSTIA, MD	7	6	38.8124	-76.9286	4.5		3	8.5									1
ANACOSTIA, MD	7	7	38.8126	-76.9170	7.5		2	6			0.5	7	0	0.47	0	0	0.7
ANACOSTIA, MD	7	8	38.8128	-76.9055	13.5			2			0.5	7	0	0.47	0	0	0.4
ANACOSTIA, MD	7	9	38.8130	-76.8939	4.5			2.5			9	8.2	0	0.29	0	0	1
ANACOSTIA, MD	7	10	38.8132	-76.8824							16	11.4	0	0.28	0	0	0.6
ANAC/UMARL	B7		38.8134	-76.8709	11						5	0.1	0	0	0	0	0
UPPER MARLBORO	7	1	38.8137	-76.8593	5						11	7	0	0	0	0	0.3
UPPER MARLBORO	7	2	38.8139	-76.8477	12						4	6.3	1	0.13	0	0	0.8
UPPER MARLBORO	7	3	38.8141	-76.8362	15						1	0.1	0	0	0	0	1
UPPER MARLBORO	7	4	38.8143	-76.8247	14						2	0.1	0	0	0	0	1
ANNANDLE, VA	6	2	38.7979	-77.2286	11.5	1	3.5										1
ANNANDLE, VA	6	3	38.7981	-77.2170	9	3	4										1
ANNANDLE, VA	6	4	38.7983	-77.2055	9		1	5			1	7	0	0.47	0	0	0.8
ANNANDLE, VA	6	5	38.7985	-77.1939	6.5		2	6			1.5	7	0	0.47	0	0	0.8
ANNANDLE, VA	6	6	38.7987	-77.1824	8			2			6	7	1	0	0	0	0.9
ANNANDLE, VA	6	7	38.7989	-77.1708	3	2					11	7	1	0.8	1	0	1
ANNANDLE, VA	6	8	38.7992	-77.1593	6.5		4				5.5	7.8	0	0.64	0	0	1
ANNANDLE, VA	6	9	38.7994	-77.1477	9			4			3	8.5	0	0.6	0	0	1
ANNANDLE, VA	6	10	38.7996	-77.1362	7						9	7	0	0.3	1	0	1
ANNAN/ALEX	B6		38.7998	-77.1246	6.5			2			7.5	12.7	0	0.48	1	0	1
ALEXANDRIA, VA	6	1	38.8000	-77.1131	7.5			5			3.5	7	0	0.6	1	0	1
ALEXANDRIA, VA	6	2	38.8002	-77.1015	12	1	2				1	7	0	0.47	0	0	1
ALEXANDRIA, VA	6	3	38.8004	-77.0900	8.5		5.5				2	7	0	0.47	0	0	1
ALEXANDRIA, VA	6	4	38.8006	-77.0784	8	1	2				5	10	0	0.3	0	0	1
ALEXANDRIA, VA	6	5	38.8008	-77.0669	8	1		2			5	18.5	0	0.5	0	0	1
ALEXANDRIA, VA	6	6	38.8011	-77.0554	4	0.5					12	9.9	0	0.37	1	0	1
ALEXANDRIA, VA	6	7	38.8013	-77.0438	1.5	1					14	11.6	1	0.47	1	0	1
ALEXANDRIA, VA	6	8	38.8015	-77.0323		16											
ALEXANDRIA, VA	6	9	38.8017	-77.0207	8	6.5					1.5	0.1	0	0	0	0	0
ALEXANDRIA, VA	6	10	38.8019	-77.0092	15.5						0.5	0.1	0	0	0	0	0
ALEX/ANAC	B6		38.8021	-76.9976	9.5		1.5				5	7	0	0.8	0	0	0.2
ANACOSTIA, MD	6	1	38.8023	-76.9861	6			2			8	9	0	0.4	0	0	0.7
ANACOSTIA, MD	6	2	38.8025	-76.9745	8.5			2.5			5	9.4	0	0.16	0	0	1
ANACOSTIA, MD	6	3	38.8028	-76.9630	16												
ANACOSTIA, MD	6	4	38.8030	-76.9514	9.5			0.5			6	8	0	0.47	0	0	1
ANACOSTIA, MD	6	5	38.8032	-76.9399	10		3	3									1
ANACOSTIA, MD	6	6	38.8034	-76.9283	5		9	2									1
ANACOSTIA, MD	6	7	38.8036	-76.9168	2.5		10.5	2			1	10	1	0	1	1	1
ANACOSTIA, MD	6	8	38.8038	-76.9052	6		2				8	8	0	0.2	1	0	0.7
ANACOSTIA, MD	6	9	38.8040	-76.8937	2						14	7	1	0.34	1	0	1
ANACOSTIA, MD	6	10	38.8042	-76.8821	10						6	7.5	0	0.4	0	0	0.3
ANAC/UMARL	B6		38.8045	-76.8706	13						3	0.1	0	0	0	0	0
UPPER MARLBORO	6	1	38.8047	-76.8591	11						5	7	0	0.1	0	0	0.2
UPPER MARLBORO	6	2	38.8049	-76.8475	10		1				5	4.3	1	0	0	0	0.7
UPPER MARLBORO	6	3	38.8051	-76.8360	14		2										1
UPPER MARLBORO	6	4	38.8053	-76.8244	16												

ANNANDLE, VA	5	2	38.7889	-77.2283	9		2	5									1
ANNANDLE, VA	5	3	38.7891	-77.2167	11	0.5	1.5	3									1
ANNANDLE, VA	5	4	38.7893	-77.2052	8	0.5	2	4			1.5	7	1	0	1	0	1
ANNANDLE, VA	5	5	38.7895	-77.1936	2		2	12									1
ANNANDLE, VA	5	6	38.7897	-77.1821	4		1	7			4	7	0	0.47	0	0	0.5
ANNANDLE, VA	5	7	38.7899	-77.1705	7.5		5.5				3	7	0	0.47	0	0	0.9
ANNANDLE, VA	5	8	38.7902	-77.1590	13.5		1				1.5	7	0	0.47	0	0	1
ANNANDLE, VA	5	9	38.7904	-77.1474	13.5		1	1			0.5	7	0	0.47	0	0	1
ANNANDLE, VA	5	10	38.7906	-77.1359	9.5			6.5									1
ANNAN/ALEX	B5		38.7908	-77.1243	8			8									1
ALEXANDRIA, VA	5	1	38.7910	-77.1128	6		7	3									1
ALEXANDRIA, VA	5	2	38.7912	-77.1013	8		6	2									1
ALEXANDRIA, VA	5	3	38.7914	-77.0897	11.5		2.5	2									1
ALEXANDRIA, VA	5	4	38.7916	-77.0782	7.5		6	1			1.5	9	1	0.47	0	0	0.9
ALEXANDRIA, VA	5	5	38.7918	-77.0666	6.5	1	4	0.5			4	45	0	0.3	0	0	1
ALEXANDRIA, VA	5	6	38.7921	-77.0551	7.5	3					5.5	10.7	0	0.5	1	0	0.8
ALEXANDRIA, VA	5	7	38.7923	-77.0435	3	9.5					3.5	15.4	1	0.37	1	0	1
ALEXANDRIA, VA	5	8	38.7925	-77.0320		15					1	0.1	0	0	0	0	0
ALEXANDRIA, VA	5	9	38.7927	-77.0204	3	9.5					3.5	0.1	0	0	0	1	0
ALEXANDRIA, VA	5	10	38.7929	-77.0089	12.5			2.5			1	7	0	0.47	0	1	0.5
ALEX/ANAC	B5		38.7931	-76.9973	6.5		7				2.5	9	0	0.27	0	0	1
ANACOSTIA, MD	5	1	38.7933	-76.9858	10		6										1
ANACOSTIA, MD	5	2	38.7935	-76.9743	9.5		6.5										1
ANACOSTIA, MD	5	3	38.7938	-76.9627	10		2				4	8	0	0.1	0	1	1
ANACOSTIA, MD	5	4	38.7940	-76.9512	13.5						2.5	7	1	0.5	0	0	1
ANACOSTIA, MD	5	5	38.7942	-76.9396	15		1										1
ANACOSTIA, MD	5	6	38.7944	-76.9281	7.5		4.5				4	7	0	0.1	0	0	1
ANACOSTIA, MD	5	7	38.7946	-76.9165	2		14										
ANACOSTIA, MD	5	8	38.7948	-76.9050	7.5		8				0.5	7	0	0.47	0	0	0.8
ANACOSTIA, MD	5	9	38.7950	-76.8934	9						7	7	0	0.5	1	0	0.7
ANACOSTIA, MD	5	10	38.7952	-76.8819	14						2	4	1	0.4	0	1	1
ANAC/UMARL	B5		38.7955	-76.8704	15						1	0.1	0	0	0	0	0
UPPER MARLBORO	5	1	38.7957	-76.8588	15.5						0.5	0.1	0	0	0	0	0
UPPER MARLBORO	5	2	38.7959	-76.8473	14		2										1
UPPER MARLBORO	5	3	38.7961	-76.8357	13		3										
UPPER MARLBORO	5	4	38.7963	-76.8242	16												
ANNANDLE, VA	4	2	38.7799	-77.2280	14		2										1
ANNANDLE, VA	4	3	38.7801	-77.2164	7		3	6									1
ANNANDLE, VA	4	4	38.7803	-77.2049	11.5	1		3.5									1
ANNANDLE, VA	4	5	38.7805	-77.1933	6		6	4									1
ANNANDLE, VA	4	6	38.7807	-77.1818	7.5			3.5			5	7	0	0	0	0	0.8
ANNANDLE, VA	4	7	38.7809	-77.1702	7		6				3	8	0	0.7	0	0	0.5
ANNANDLE, VA	4	8	38.7812	-77.1587	10		3	1			2	7	0	0	0	0	0.8
ANNANDLE, VA	4	9	38.7814	-77.1472	7.5		4	3.5			1	7	0	0.3	0	0	1
ANNANDLE, VA	4	10	38.7816	-77.1356	9.5		3	2			1.5	10	1	1	0	0	1
ANNAN/ALEX	B4		38.7818	-77.1241	8		2.5	2.5			3	8.5	0	0.2	0	0	1
ALEXANDRIA, VA	4	1	38.7820	-77.1125	4		12										1
ALEXANDRIA, VA	4	2	38.7822	-77.1010	5		7	4									1
ALEXANDRIA, VA	4	3	38.7824	-77.0894	11		5										1
ALEXANDRIA, VA	4	4	38.7826	-77.0779	5		4	1			6	7	0	0.7	0	0	1
ALEXANDRIA, VA	4	5	38.7829	-77.0663	6.5			8.5			1	30	0	0.7	0	0	1
ALEXANDRIA, VA	4	6	38.7831	-77.0548	6.5	7.5		2									1
ALEXANDRIA, VA	4	7	38.7833	-77.0433		16											
ALEXANDRIA, VA	4	8	38.7835	-77.0317		16											
ALEXANDRIA, VA	4	9	38.7837	-77.0202	5	11											
ALEXANDRIA, VA	4	10	38.7839	-77.0086	11		3	2									1
ALEX/ANAC	B4		38.7841	-76.9971	6		5	2			3	8.5	0	0.3	0	0	1
ANACOSTIA, MD	4	1	38.7843	-76.9855	12		3				1	7	0	0.6	0	0	1
ANACOSTIA, MD	4	2	38.7845	-76.9740	15			1									1
ANACOSTIA, MD	4	3	38.7848	-76.9624	6		10										1
ANACOSTIA, MD	4	4	38.7850	-76.9509	8		8										1
ANACOSTIA, MD	4	5	38.7852	-76.9394	8		8										1
ANACOSTIA, MD	4	6	38.7854	-76.9278	12.5		3.5										1
ANACOSTIA, MD	4	7	38.7856	-76.9163	11.5		4.5										1
ANACOSTIA, MD	4	8	38.7858	-76.9047	7.5		4.5	2			2	7	1	0.3	0	0	1
ANACOSTIA, MD	4	9	38.7860	-76.8932	7.5			1			7.5	8.2	0	0.08	0	0	0.8
ANACOSTIA, MD	4	10	38.7862	-76.8816	15			1									1
ANAC/UMARL	B4		38.7865	-76.8701	14.5	1.5											
UPPER MARLBORO	4	1	38.7867	-76.8586	15.5		0.5										1
UPPER MARLBORO	4	2	38.7869	-76.8470	13.5		2.5										1
UPPER MARLBORO	4	3	38.7871	-76.8355	10		4				2	7	1	0	1	0	1
UPPER MARLBORO	4	4	38.7873	-76.8239	16												
ANNANDLE, VA	3	2	38.7709	-77.2277	7.5	0.5	4	4									1
ANNANDLE, VA	3	3	38.7711	-77.2161	10.5	0.5	4	1									1

ANNANDLE, VA	3	4	38.7713	-77.2046	14.5	0.5	1										1
ANNANDLE, VA	3	5	38.7715	-77.1931	10		2	4									1
ANNANDLE, VA	3	6	38.7717	-77.1815	4.5		2.5				9	7	0	0.8	0	0	1
ANNANDLE, VA	3	7	38.7719	-77.1700	9			5			2	7	0	0.2	0	0	0.2
ANNANDLE, VA	3	8	38.7722	-77.1584	10						6	8.5	1	0.8	1	0	1
ANNANDLE, VA	3	9	38.7724	-77.1469	13		3										1
ANNANDLE, VA	3	10	38.7726	-77.1353	16												
ANNAN/ALEX	B3		38.7728	-77.1238	15.5	0.5											
ALEXANDRIA, VA	3	1	38.7730	-77.1123	11		5										1
ALEXANDRIA, VA	3	2	38.7732	-77.1007	8.5		5.5	2									1
ALEXANDRIA, VA	3	3	38.7734	-77.0892	4.5		1	7.5			3	10	1	0.1	0	0	1
ALEXANDRIA, VA	3	4	38.7736	-77.0776	3		2	6.5			4.5	7	0	0.4	0	0	1
ALEXANDRIA, VA	3	5	38.7739	-77.0661	7.5		4	2			2.5	7.6	0	0.1	0	0	1
ALEXANDRIA, VA	3	6	38.7741	-77.0545	6.5			3			6.5	13.1	0	0.25	0	0	1
ALEXANDRIA, VA	3	7	38.7743	-77.0430	2	14											
ALEXANDRIA, VA	3	8	38.7745	-77.0314	3.5	12.5											
ALEXANDRIA, VA	3	9	38.7747	-77.0199	12.5			3.5									1
ALEXANDRIA, VA	3	10	38.7749	-77.0084	12.5		1.5	1.5			0.5	12	1	0	0	0	1
ALEX/ANAC	B3		38.7751	-76.9968	9		4.5				2.5	6	0	0.12	0	0	0.8
ANACOSTIA, MD	3	1	38.7753	-76.9853	15		1										1
ANACOSTIA, MD	3	2	38.7756	-76.9737	16												
ANACOSTIA, MD	3	3	38.7758	-76.9622	14		2										1
ANACOSTIA, MD	3	4	38.7760	-76.9506	9			7									1
ANACOSTIA, MD	3	5	38.7762	-76.9391	12.5			3.5									1
ANACOSTIA, MD	3	6	38.7764	-76.9276	16												
ANACOSTIA, MD	3	7	38.7766	-76.9160	14	1	1										1
ANACOSTIA, MD	3	8	38.7768	-76.9045	10		5				1	4	0	0	0	0	0.7
ANACOSTIA, MD	3	9	38.7770	-76.8929	11		3				2	7	0	0.3	1	0	0.7
ANACOSTIA, MD	3	10	38.7772	-76.8814	13			1			2	7	0	0	0	0	0.8
ANAC/UMARL	B3		38.7775	-76.8698	8.5		4.5				3	7	1	0.1	1	0	1
UPPER MARLBORO	3	1	38.7777	-76.8583	13.5		2.5										1
UPPER MARLBORO	3	2	38.7779	-76.8468	16												
UPPER MARLBORO	3	3	38.7781	-76.8352	13		3										1
UPPER MARLBORO	3	4	38.7783	-76.8237	16												
ANNANDLE, VA	2	2	38.7619	-77.2274	9		4	3									1
ANNANDLE, VA	2	3	38.7621	-77.2158	7.5		6	1			1.5	7	0	0.47	0	0	1
ANNANDLE, VA	2	4	38.7623	-77.2043	14.5	0.5	1										1
ANNANDLE, VA	2	5	38.7625	-77.1928	13		3										1
ANNANDLE, VA	2	6	38.7627	-77.1812	6.5	0.5	4				5	7	0	0.8	0	0	0.8
ANNANDLE, VA	2	7	38.7629	-77.1697	10			3			3	10	0	0.87	0	0	0.4
ANNANDLE, VA	2	8	38.7632	-77.1581	12.5			3.5									1
ANNANDLE, VA	2	9	38.7634	-77.1466	15		1										1
ANNANDLE, VA	2	10	38.7636	-77.1351	14		2										1
ANNAN/ALEX	B2		38.7638	-77.1235	13	0.5	1.5				1	10	1	0.9	0	0	1
ALEXANDRIA, VA	2	1	38.7640	-77.1120	10		6										1
ALEXANDRIA, VA	2	2	38.7642	-77.1004	12.5		3.5										1
ALEXANDRIA, VA	2	3	38.7644	-77.0889	5.5			5.5			5	7	1	0.6	1	0	1
ALEXANDRIA, VA	2	4	38.7646	-77.0774	3		2	8			3	10	1	0.9	0	1	1
ALEXANDRIA, VA	2	5	38.7648	-77.0658	7		7	2									1
ALEXANDRIA, VA	2	6	38.7651	-77.0543	10			6									1
ALEXANDRIA, VA	2	7	38.7653	-77.0427	2	14											
ALEXANDRIA, VA	2	8	38.7655	-77.0312	4	12											
ALEXANDRIA, VA	2	9	38.7657	-77.0197	2.5			13.5									1
ALEXANDRIA, VA	2	10	38.7659	-77.0081	13.5		2				0.5	12	1	0	0	0	1
ALEX/ANAC	B2		38.7661	-76.9966	12		2				2	10	0	0	1	0	1
ANACOSTIA, MD	2	1	38.7663	-76.9850	10		3				3	10	1	0	1	0	1
ANACOSTIA, MD	2	2	38.7666	-76.9735	16												
ANACOSTIA, MD	2	3	38.7668	-76.9619	12		4										1
ANACOSTIA, MD	2	4	38.7670	-76.9504	11.5		4				0.5	10	1	0	0	0	1
ANACOSTIA, MD	2	5	38.7672	-76.9389	12		4										1
ANACOSTIA, MD	2	6	38.7674	-76.9273	13		1.5				1.5	4	1	0	1	0	1
ANACOSTIA, MD	2	7	38.7676	-76.9158	7.5		8.5										1
ANACOSTIA, MD	2	8	38.7678	-76.9042	12			3			1	20	0	0.3	0	0	1
ANACOSTIA, MD	2	9	38.7680	-76.8927	8			4			4	10	1	0.2	1	0	1
ANACOSTIA, MD	2	10	38.7682	-76.8812	9			3.5			3.5	7	0	0	0	0	0.7
ANAC/UMARL	B2		38.7685	-76.8696	9.5		6.5										1
UPPER MARLBORO	2	1	38.7687	-76.8581	13		3										1
UPPER MARLBORO	2	2	38.7689	-76.8465	15.5	0.5											
UPPER MARLBORO	2	3	38.7691	-76.8350	13.5		2.5										1
UPPER MARLBORO	2	4	38.7693	-76.8234	14.5	0.5	1										1
ANNANDLE, VA	1	2	38.7529	-77.2271	9.5	0.5	6										1
ANNANDLE, VA	1	3	38.7531	-77.2156	13		3										1
ANNANDLE, VA	1	4	38.7533	-77.2040	15.5	0.5											
ANNANDLE, VA	1	5	38.7535	-77.1925	12.5						3.5	7	0	0.5	0	0	1

ANNANDLE, VA	1	6	38.7537	-77.1809	12	0.5	1				2.5	7	0	0.47	0	0	1
ANNANDLE, VA	1	7	38.7539	-77.1694	13		2				1	10	1	0.4	1	0	1
ANNANDLE, VA	1	8	38.7542	-77.1579	12.5	0.5	3										1
ANNANDLE, VA	1	9	38.7544	-77.1463	13	1					2	10	1	0.5	1	0	1
ANNANDLE, VA	1	10	38.7546	-77.1348	8		8										1
ANNAN/ALEX	B1		38.7548	-77.1232	16												
ALEXANDRIA, VA	1	1	38.7550	-77.1117	16												
ALEXANDRIA, VA	1	2	38.7552	-77.1002	16												
ALEXANDRIA, VA	1	3	38.7554	-77.0886	9.5		3				3.5	7	0	0.6	0	0	1
ALEXANDRIA, VA	1	4	38.7556	-77.0771	5.5			5.5			5	10	0	0.7	0	0	1
ALEXANDRIA, VA	1	5	38.7559	-77.0655	4			12									1
ALEXANDRIA, VA	1	6	38.7561	-77.0540	8.5			7.5									1
ALEXANDRIA, VA	1	7	38.7563	-77.0425	3	13											
ALEXANDRIA, VA	1	8	38.7565	-77.0309	1	14		1									1
ALEXANDRIA, VA	1	9	38.7567	-77.0194	6	0.5	4	5			0.5	10	1	0	0	0	1
ALEXANDRIA, VA	1	10	38.7569	-77.0078	15			1									1
ALEX/ANAC	B1		38.7571	-76.9963	13						3	8	0	0.2	0	0	1
ANACOSTIA, MD	1	1	38.7573	-76.9848	14.5		1.5										1
ANACOSTIA, MD	1	2	38.7576	-76.9732	12.5		3.5										1
ANACOSTIA, MD	1	3	38.7578	-76.9617	11		5										1
ANACOSTIA, MD	1	4	38.7580	-76.9501	15.5		0.5										1
ANACOSTIA, MD	1	5	38.7582	-76.9386	16												
ANACOSTIA, MD	1	6	38.7584	-76.9271	15.5		0.5										1
ANACOSTIA, MD	1	7	38.7586	-76.9155	11.5		4				0.5	10	0	0	0	1	1
ANACOSTIA, MD	1	8	38.7588	-76.9040	10.5		5				0.5	10	1	0.8	1	0	1
ANACOSTIA, MD	1	9	38.7590	-76.8924	9.5		5	0.5			1	10	1	0	1	0	1
ANACOSTIA, MD	1	10	38.7592	-76.8809	13		1	1			1	7	0	0.47	0	0	1
ANAC/UMARL	B1		38.7595	-76.8694	12		4										1
UPPER MARLBORO	1	1	38.7597	-76.8578	14		2										1
UPPER MARLBORO	1	2	38.7599	-76.8463	16												
UPPER MARLBORO	1	3	38.7601	-76.8347	14		2										1
UPPER MARLBORO	1	4	38.7603	-76.8232	9		7										1

Table B.4: TEB values derived from the raw morphology data for each 1152 1 km grid cells

USGS Map Information			**Grid Center**		**TEB Parameters**												
map	row	col	lat	long	bld	h	h/l	zo	aroof	aroad	awall	eroof	eroad	ewall	Traffic SH	Industry SH	Industry LE
ROCKVILLE	4	2	39.0319	-77.2359	0.00	0.0	0.00	0.0	0.00	0.00	0.00	0.00	0.00	0.00	0.00	0.00	0.00
ROCKVILLE	4	3	39.0321	-77.2243	0.40	7.0	0.30	0.7	0.18	0.12	0.25	0.91	0.95	0.90	0.31	0.00	0.00
ROCKVILLE	4	4	39.0323	-77.2127	0.40	7.0	0.30	0.7	0.18	0.12	0.25	0.91	0.95	0.90	0.63	0.00	0.00
ROCKVILLE	4	5	39.0325	-77.2011	0.60	10.0	0.20	1.0	0.25	0.12	0.25	0.88	0.95	0.90	0.63	10.00	5.00
ROCKVILLE	4	6	39.0327	-77.1895	0.40	7.0	0.30	0.7	0.18	0.12	0.25	0.91	0.95	0.90	0.63	0.00	0.00
ROCKVILLE	4	7	39.0329	-77.1779	0.40	7.0	0.30	0.7	0.18	0.12	0.25	0.91	0.95	0.90	2.81	0.00	0.00
ROCKVILLE	4	8	39.0331	-77.1664	0.49	8.3	0.34	0.8	0.21	0.12	0.25	0.90	0.95	0.90	4.06	10.00	5.00
ROCKVILLE	4	9	39.0333	-77.1548	0.50	8.5	0.35	0.9	0.22	0.12	0.25	0.90	0.95	0.90	0.94	10.00	5.00
ROCKVILLE	4	10	39.0335	-77.1432	0.23	10.0	0.20	1.0	0.19	0.12	0.25	0.88	0.95	0.90	11.88	10.00	5.00
ROCK/KENS	B4		39.0338	-77.1316	0.35	7.0	0.30	0.7	0.18	0.12	0.25	0.91	0.95	0.90	12.81	10.00	5.00
KENSINGTON	4	1	39.0340	-77.1200	0.45	8.5	0.35	0.9	0.22	0.12	0.25	0.90	0.95	0.90	0.94	10.00	5.00
KENSINGTON	4	2	39.0342	-77.1084	0.42	7.5	0.32	0.8	0.19	0.12	0.25	0.90	0.95	0.90	2.03	10.00	5.00
KENSINGTON	4	3	39.0344	-77.0968	0.44	8.0	0.31	0.8	0.19	0.12	0.25	0.90	0.95	0.90	5.78	10.00	5.00
KENSINGTON	4	4	39.0346	-77.0853	0.40	7.0	0.30	0.7	0.18	0.12	0.25	0.91	0.95	0.90	3.13	0.00	0.00
KENSINGTON	4	5	39.0348	-77.0737	0.40	7.0	0.30	0.7	0.18	0.12	0.25	0.91	0.95	0.90	4.38	0.00	0.00
KENSINGTON	4	6	39.0350	-77.0621	0.41	7.2	0.29	0.7	0.18	0.12	0.25	0.91	0.95	0.90	4.53	10.00	5.00
KENSINGTON	4	7	39.0352	-77.0505	0.45	7.4	0.30	0.7	0.18	0.12	0.25	0.90	0.95	0.90	6.41	10.00	5.00
KENSINGTON	4	8	39.0355	-77.0389	0.41	7.0	0.29	0.7	0.18	0.12	0.25	0.91	0.95	0.90	3.13	10.00	5.00
KENSINGTON	4	9	39.0357	-77.0273	0.45	8.0	0.33	0.8	0.19	0.12	0.25	0.90	0.95	0.90	3.75	10.00	5.00
KENSINGTON	4	10	39.0359	-77.0157	0.40	7.0	0.30	0.7	0.18	0.12	0.25	0.91	0.95	0.90	2.97	0.00	0.00
KENS/BELT	B4		39.0361	-77.0042	0.40	7.0	0.30	0.7	0.18	0.12	0.25	0.91	0.95	0.90	2.34	0.00	0.00
BELTSVILLE	4	1	39.0363	-76.9926	0.33	12.2	0.36	1.2	0.17	0.16	0.25	0.90	0.93	0.90	14.38	10.00	5.00
BELTSVILLE	4	2	39.0365	-76.9810	0.40	10.0	0.50	1.0	0.25	0.12	0.25	0.88	0.95	0.90	2.50	10.00	5.00
BELTSVILLE	4	3	39.0367	-76.9694	0.30	7.0	0.25	0.7	0.19	0.12	0.25	0.88	0.95	0.90	0.63	10.00	5.00
BELTSVILLE	4	4	39.0369	-76.9578	0.00	0.0	0.00	0.0	0.00	0.00	0.00	0.00	0.00	0.00	0.00	0.00	0.00
BELTSVILLE	4	5	39.0371	-76.9462	0.39	7.6	0.34	0.8	0.15	0.14	0.25	0.90	0.94	0.90	7.66	10.00	5.00
BELTSVILLE	4	6	39.0374	-76.9346	0.23	9.3	0.45	0.9	0.16	0.22	0.25	0.89	0.91	0.90	7.19	10.00	5.00
BELTSVILLE	4	7	39.0376	-76.9231	0.40	7.0	0.30	0.7	0.18	0.12	0.25	0.91	0.95	0.90	2.81	0.00	0.00
BELTSVILLE	4	8	39.0378	-76.9115	0.40	7.0	0.30	0.7	0.18	0.12	0.25	0.91	0.95	0.90	4.38	0.00	0.00
BELTSVILLE	4	9	39.0380	-76.8999	0.49	7.0	0.91	0.7	0.17	0.12	0.25	0.88	0.95	0.90	4.38	10.00	5.00
BELTSVILLE	4	10	39.0382	-76.8883	0.00	0.0	0.00	0.0	0.00	0.00	0.00	0.00	0.00	0.00	0.00	0.00	0.00
BELT/LAUREL	B4		39.0384	-76.8767	0.00	0.0	0.00	0.0	0.00	0.00	0.00	0.00	0.00	0.00	0.00	0.00	0.00
LAUREL	4	1	39.0386	-76.8651	0.00	0.0	0.00	0.0	0.00	0.00	0.00	0.00	0.00	0.00	0.00	0.00	0.00
LAUREL	4	2	39.0388	-76.8535	0.24	8.0	0.30	0.8	0.15	0.12	0.25	0.88	0.95	0.90	6.56	10.00	5.00
LAUREL	4	3	39.0391	-76.8420	0.00	0.0	0.00	0.0	0.00	0.00	0.00	0.00	0.00	0.00	0.00	0.00	0.00

LAUREL	4	4	39.0393	-76.8304	0.00	0.0	0.00	0.0	0.00	0.00	0.00	0.00	0.00	0.00	0.00	0.00	0.00
ROCKVILLE	3	2	39.0229	-77.2356	0.00	0.0	0.00	0.0	0.00	0.00	0.00	0.00	0.00	0.00	0.00	0.00	0.00
ROCKVILLE	3	3	39.0231	-77.2240	0.40	7.0	0.30	0.7	0.18	0.12	0.25	0.91	0.95	0.90	0.63	0.00	0.00
ROCKVILLE	3	4	39.0233	-77.2124	0.47	8.0	0.27	0.8	0.20	0.12	0.25	0.90	0.95	0.90	1.25	10.00	5.00
ROCKVILLE	3	5	39.0235	-77.2008	0.40	7.0	0.30	0.7	0.18	0.12	0.25	0.91	0.95	0.90	0.63	0.00	0.00
ROCKVILLE	3	6	39.0237	-77.1892	0.70	10.0	0.20	1.0	0.25	0.12	0.25	0.88	0.95	0.90	0.63	10.00	5.00
ROCKVILLE	3	7	39.0239	-77.1777	0.40	7.0	0.30	0.7	0.18	0.12	0.25	0.91	0.95	0.90	1.56	0.00	0.00
ROCKVILLE	3	8	39.0241	-77.1661	0.40	8.1	0.30	0.8	0.21	0.12	0.25	0.90	0.95	0.90	8.44	10.00	5.00
ROCKVILLE	3	9	39.0243	-77.1545	0.34	31.9	0.56	3.2	0.17	0.12	0.25	0.88	0.95	0.90	9.06	10.00	5.00
ROCKVILLE	3	10	39.0245	-77.1429	0.22	9.0	0.29	0.9	0.21	0.12	0.25	0.88	0.95	0.90	21.25	10.00	5.00
ROCK/KENS	B3		39.0248	-77.1313	0.40	18.9	0.30	1.9	0.17	0.12	0.25	0.89	0.95	0.90	10.31	10.00	5.00
KENSINGTON	3	1	39.0250	-77.1197	0.39	7.3	0.28	0.7	0.19	0.12	0.25	0.90	0.95	0.90	9.38	10.00	5.00
KENSINGTON	3	2	39.0252	-77.1081	0.28	40.1	0.30	4.0	0.22	0.12	0.25	0.89	0.95	0.90	13.59	10.00	5.00
KENSINGTON	3	3	39.0254	-77.0966	0.45	8.5	0.35	0.9	0.18	0.12	0.25	0.90	0.95	0.90	2.81	10.00	5.00
KENSINGTON	3	4	39.0256	-77.0850	0.41	7.0	0.31	0.7	0.18	0.12	0.25	0.91	0.95	0.90	4.84	10.00	5.00
KENSINGTON	3	5	39.0258	-77.0734	0.44	7.4	0.34	0.7	0.17	0.15	0.25	0.90	0.94	0.90	6.25	10.00	5.00
KENSINGTON	3	6	39.0260	-77.0618	0.40	7.0	0.30	0.7	0.18	0.12	0.25	0.91	0.95	0.90	4.22	0.00	0.00
KENSINGTON	3	7	39.0262	-77.0502	0.40	7.2	0.30	0.7	0.18	0.15	0.25	0.91	0.94	0.90	5.47	10.00	5.00
KENSINGTON	3	8	39.0265	-77.0386	0.42	7.7	0.32	0.8	0.20	0.12	0.25	0.90	0.95	0.90	6.09	10.00	5.00
KENSINGTON	3	9	39.0267	-77.0271	0.40	7.0	0.30	0.7	0.18	0.12	0.25	0.91	0.95	0.90	3.75	0.00	0.00
KENSINGTON	3	10	39.0269	-77.0155	0.37	7.0	0.30	0.7	0.18	0.16	0.25	0.91	0.94	0.90	4.38	10.00	5.00
KENS/BELT	B3		39.0271	-77.0039	0.40	7.0	0.30	0.7	0.18	0.13	0.25	0.91	0.95	0.90	2.19	0.00	0.00
BELTSVILLE	3	1	39.0273	-76.9923	0.40	7.0	0.30	0.7	0.18	0.12	0.25	0.91	0.95	0.90	2.50	0.00	0.00
BELTSVILLE	3	2	39.0275	-76.9807	0.38	7.0	0.30	0.7	0.18	0.16	0.25	0.91	0.94	0.90	3.91	10.00	5.00
BELTSVILLE	3	3	39.0277	-76.9691	0.38	7.9	0.38	0.8	0.19	0.12	0.25	0.90	0.95	0.90	5.31	10.00	5.00
BELTSVILLE	3	4	39.0279	-76.9576	0.40	7.0	0.30	0.7	0.18	0.12	0.25	0.91	0.95	0.90	1.88	0.00	0.00
BELTSVILLE	3	5	39.0282	-76.9460	0.01	0.1	0.01	0.0	0.25	0.25	0.25	0.88	0.90	0.90	10.94	10.00	5.00
BELTSVILLE	3	6	39.0284	-76.9344	0.00	0.0	0.00	0.0	0.00	0.00	0.00	0.00	0.00	0.00	0.00	0.00	0.00
BELTSVILLE	3	7	39.0286	-76.9228	0.50	7.4	0.58	0.7	0.15	0.12	0.25	0.89	0.95	0.90	5.00	10.00	5.00
BELTSVILLE	3	8	39.0288	-76.9112	0.59	9.8	0.72	1.0	0.19	0.12	0.25	0.88	0.95	0.90	9.06	10.00	5.00
BELTSVILLE	3	9	39.0290	-76.8996	0.00	0.0	0.00	0.0	0.00	0.00	0.00	0.00	0.00	0.00	0.00	0.00	0.00
BELTSVILLE	3	10	39.0292	-76.8881	0.40	10.0	0.50	1.0	0.25	0.12	0.25	0.88	0.95	0.90	0.63	10.00	5.00
BELT/LAUREL	B3		39.0294	-76.8765	0.00	0.0	0.00	0.0	0.00	0.00	0.00	0.00	0.00	0.00	0.00	0.00	0.00
LAUREL	3	1	39.0296	-76.8649	0.00	0.0	0.00	0.0	0.00	0.00	0.00	0.00	0.00	0.00	0.00	0.00	0.00
LAUREL	3	2	39.0298	-76.8533	0.01	0.1	0.01	0.0	0.25	0.12	0.25	0.88	0.95	0.90	10.94	10.00	5.00
LAUREL	3	3	39.0301	-76.8417	0.00	0.0	0.00	0.0	0.00	0.00	0.00	0.00	0.00	0.00	0.00	0.00	0.00
LAUREL	3	4	39.0303	-76.8301	0.00	0.0	0.00	0.0	0.00	0.00	0.00	0.00	0.00	0.00	0.00	0.00	0.00
ROCKVILLE	2	2	39.0139	-77.2353	0.40	7.0	0.30	0.7	0.18	0.12	0.25	0.91	0.95	0.90	0.31	0.00	0.00
ROCKVILLE	2	3	39.0141	-77.2237	0.40	7.0	0.30	0.7	0.18	0.12	0.25	0.91	0.95	0.90	0.63	0.00	0.00
ROCKVILLE	2	4	39.0143	-77.2121	0.42	7.0	0.32	0.7	0.17	0.12	0.25	0.90	0.95	0.90	2.50	10.00	5.00
ROCKVILLE	2	5	39.0145	-77.2005	0.40	7.0	0.30	0.7	0.18	0.12	0.25	0.91	0.95	0.90	1.25	0.00	0.00
ROCKVILLE	2	6	39.0147	-77.1890	0.00	0.0	0.00	0.0	0.00	0.00	0.00	0.00	0.00	0.00	0.00	0.00	0.00
ROCKVILLE	2	7	39.0149	-77.1774	0.40	7.0	0.30	0.7	0.18	0.12	0.25	0.91	0.95	0.90	0.94	0.00	0.00
ROCKVILLE	2	8	39.0151	-77.1658	0.43	7.4	0.30	0.7	0.19	0.12	0.25	0.91	0.95	0.90	1.25	10.00	5.00
ROCKVILLE	2	9	39.0153	-77.1542	0.30	7.0	0.30	0.7	0.17	0.12	0.25	0.90	0.95	0.90	6.56	10.00	5.00
ROCKVILLE	2	10	39.0155	-77.1426	0.26	7.0	0.30	0.7	0.17	0.12	0.25	0.90	0.95	0.90	17.97	10.00	5.00
ROCK/KENS	B2		39.0158	-77.1310	0.37	7.0	0.30	0.7	0.18	0.12	0.25	0.91	0.95	0.90	15.00	10.00	5.00
KENSINGTON	2	1	39.0160	-77.1195	0.34	7.0	0.30	0.7	0.18	0.12	0.25	0.91	0.95	0.90	15.16	10.00	5.00
KENSINGTON	2	2	39.0162	-77.1079	0.29	32.3	0.37	3.2	0.20	0.13	0.25	0.89	0.95	0.90	13.91	10.00	5.00
KENSINGTON	2	3	39.0164	-77.0963	0.33	7.0	0.30	0.7	0.18	0.15	0.25	0.91	0.94	0.90	13.28	10.00	5.00
KENSINGTON	2	4	39.0166	-77.0847	0.41	7.2	0.30	0.7	0.18	0.15	0.25	0.91	0.94	0.90	5.31	10.00	5.00
KENSINGTON	2	5	39.0168	-77.0731	0.41	7.3	0.29	0.7	0.17	0.15	0.25	0.91	0.94	0.90	5.47	10.00	5.00
KENSINGTON	2	6	39.0170	-77.0615	0.30	7.0	0.30	0.7	0.17	0.12	0.25	0.90	0.95	0.90	11.56	10.00	5.00
KENSINGTON	2	7	39.0172	-77.0500	0.38	7.9	0.33	0.8	0.19	0.12	0.25	0.90	0.95	0.90	14.06	10.00	5.00
KENSINGTON	2	8	39.0175	-77.0384	0.34	8.7	0.30	0.9	0.19	0.19	0.25	0.90	0.93	0.90	15.31	10.00	5.00
KENSINGTON	2	9	39.0177	-77.0268	0.37	7.0	0.30	0.7	0.18	0.19	0.25	0.91	0.93	0.90	14.06	10.00	5.00
KENSINGTON	2	10	39.0179	-77.0152	0.31	7.0	0.30	0.7	0.17	0.21	0.25	0.90	0.92	0.90	15.16	10.00	5.00
KENS/BELT	B2		39.0181	-77.0036	0.34	7.8	0.30	0.8	0.20	0.20	0.25	0.90	0.92	0.90	15.47	10.00	5.00
BELTSVILLE	2	1	39.0183	-76.9921	0.34	7.0	0.30	0.7	0.18	0.19	0.25	0.91	0.93	0.90	12.50	10.00	5.00
BELTSVILLE	2	2	39.0185	-76.9805	0.32	8.9	0.27	0.9	0.13	0.21	0.25	0.90	0.92	0.90	16.48	10.00	5.00
BELTSVILLE	2	3	39.0187	-76.9689	0.38	9.4	0.49	0.9	0.19	0.19	0.25	0.90	0.93	0.90	15.94	10.00	5.00
BELTSVILLE	2	4	39.0189	-76.9573	0.20	7.0	0.30	0.7	0.17	0.21	0.25	0.90	0.92	0.90	13.75	10.00	5.00
BELTSVILLE	2	5	39.0191	-76.9457	0.01	0.1	0.01	0.0	0.25	0.25	0.25	0.88	0.90	0.90	11.56	10.00	5.00
BELTSVILLE	2	6	39.0194	-76.9341	0.17	18.7	0.88	1.9	0.21	0.20	0.25	0.89	0.92	0.90	13.44	10.00	5.00
BELTSVILLE	2	7	39.0196	-76.9226	0.33	7.5	0.48	0.7	0.21	0.19	0.25	0.89	0.93	0.90	15.63	10.00	5.00
BELTSVILLE	2	8	39.0198	-76.9110	0.34	8.2	0.48	0.8	0.18	0.19	0.25	0.90	0.93	0.90	12.19	10.00	5.00
BELTSVILLE	2	9	39.0200	-76.8994	0.00	0.0	0.00	0.0	0.00	0.00	0.00	0.00	0.00	0.00	0.00	0.00	0.00
BELTSVILLE	2	10	39.0202	-76.8878	0.00	0.0	0.00	0.0	0.00	0.00	0.00	0.00	0.00	0.00	0.00	0.00	0.00
BELT/LAUREL	B2		39.0204	-76.8762	0.00	0.0	0.00	0.0	0.00	0.00	0.00	0.00	0.00	0.00	0.00	0.00	0.00
LAUREL	2	1	39.0206	-76.8647	0.00	0.0	0.00	0.0	0.00	0.00	0.00	0.00	0.00	0.00	0.00	0.00	0.00
LAUREL	2	2	39.0209	-76.8531	0.01	0.1	0.01	0.0	0.25	0.12	0.25	0.88	0.95	0.90	10.31	10.00	5.00
LAUREL	2	3	39.0211	-76.8415	0.00	0.0	0.00	0.0	0.00	0.00	0.00	0.00	0.00	0.00	0.00	0.00	0.00
LAUREL	2	4	39.0213	-76.8299	0.00	0.0	0.00	0.0	0.00	0.00	0.00	0.00	0.00	0.00	0.00	0.00	0.00
ROCKVILLE	1	2	39.0049	-77.2348	0.40	7.0	0.30	0.7	0.18	0.12	0.25	0.91	0.95	0.90	0.31	0.00	0.00

ROCKVILLE	1	3	39.0051	-77.2233	0.40	7.0	0.30	0.7	0.18	0.12	0.25	0.91	0.95	0.90	0.31	0.00	0.00
ROCKVILLE	1	4	39.0053	-77.2117	0.40	7.0	0.30	0.7	0.18	0.12	0.25	0.91	0.95	0.90	1.56	0.00	0.00
ROCKVILLE	1	5	39.0055	-77.2001	0.40	7.0	0.30	0.7	0.18	0.12	0.25	0.91	0.95	0.90	0.63	0.00	0.00
ROCKVILLE	1	6	39.0057	-77.1885	0.40	7.0	0.30	0.7	0.18	0.12	0.25	0.91	0.95	0.90	0.31	0.00	0.00
ROCKVILLE	1	7	39.0059	-77.1769	0.40	7.0	0.30	0.7	0.18	0.12	0.25	0.91	0.95	0.90	1.25	0.00	0.00
ROCKVILLE	1	8	39.0061	-77.1654	0.40	7.0	0.30	0.7	0.18	0.12	0.25	0.91	0.95	0.90	2.19	0.00	0.00
ROCKVILLE	1	9	39.0063	-77.1538	0.36	7.0	0.30	0.7	0.18	0.12	0.25	0.91	0.95	0.90	13.28	10.00	5.00
ROCKVILLE	1	10	39.0065	-77.1422	0.40	7.0	0.30	0.7	0.18	0.12	0.25	0.91	0.95	0.90	1.88	0.00	0.00
ROCK/KENS	B1		39.0068	-77.1306	0.44	7.6	0.30	0.8	0.19	0.12	0.25	0.90	0.95	0.90	3.91	10.00	5.00
KENSINGTON	1	1	39.0070	-77.1190	0.40	7.0	0.30	0.7	0.18	0.12	0.25	0.91	0.95	0.90	4.53	0.00	0.00
KENSINGTON	1	2	39.0072	-77.1075	0.40	7.0	0.30	0.7	0.18	0.12	0.25	0.91	0.95	0.90	2.50	0.00	0.00
KENSINGTON	1	3	39.0074	-77.0959	0.38	7.0	0.30	0.7	0.18	0.15	0.25	0.91	0.94	0.90	7.81	10.00	5.00
KENSINGTON	1	4	39.0076	-77.0843	0.32	8.8	0.30	0.9	0.20	0.15	0.25	0.90	0.94	0.90	13.59	10.00	5.00
KENSINGTON	1	5	39.0078	-77.0727	0.32	7.0	0.30	0.7	0.18	0.12	0.25	0.90	0.95	0.90	13.75	10.00	5.00
KENSINGTON	1	6	39.0080	-77.0611	0.33	7.0	0.30	0.7	0.18	0.12	0.25	0.91	0.95	0.90	12.19	10.00	5.00
KENSINGTON	1	7	39.0082	-77.0496	0.45	7.0	0.35	0.7	0.18	0.12	0.25	0.90	0.95	0.90	5.78	10.00	5.00
KENSINGTON	1	8	39.0085	-77.0380	0.38	7.7	0.30	0.8	0.19	0.16	0.25	0.91	0.94	0.90	10.00	10.00	5.00
KENSINGTON	1	9	39.0087	-77.0264	0.40	7.0	0.30	0.7	0.18	0.12	0.25	0.91	0.95	0.90	3.13	0.00	0.00
KENSINGTON	1	10	39.0089	-77.0148	0.40	7.0	0.30	0.7	0.18	0.15	0.25	0.91	0.94	0.90	4.53	0.00	0.00
KENS/BELT	B1		39.0091	-77.0032	0.39	7.7	0.30	0.8	0.19	0.15	0.25	0.91	0.94	0.90	10.00	10.00	5.00
BELTSVILLE	1	1	39.0093	-76.9917	0.40	7.0	0.30	0.7	0.18	0.25	0.25	0.91	0.90	0.90	2.34	0.00	0.00
BELTSVILLE	1	2	39.0095	-76.9801	0.35	9.1	0.53	0.9	0.12	0.17	0.25	0.89	0.93	0.90	12.19	10.00	5.00
BELTSVILLE	1	3	39.0097	-76.9685	0.40	7.8	0.41	0.8	0.16	0.12	0.25	0.90	0.95	0.90	2.34	10.00	5.00
BELTSVILLE	1	4	39.0099	-76.9569	0.42	7.6	0.34	0.8	0.19	0.12	0.25	0.90	0.95	0.90	1.59	10.00	5.00
BELTSVILLE	1	5	39.0101	-76.9453	0.40	7.0	0.30	0.7	0.18	0.12	0.25	0.91	0.95	0.90	0.94	0.00	0.00
BELTSVILLE	1	6	39.0104	-76.9338	0.40	7.0	0.50	0.7	0.15	0.12	0.25	0.88	0.95	0.90	1.25	10.00	5.00
BELTSVILLE	1	7	39.0106	-76.9222	0.49	7.0	0.50	0.7	0.18	0.12	0.25	0.91	0.95	0.90	5.63	10.00	5.00
BELTSVILLE	1	8	39.0108	-76.9106	0.44	7.0	0.50	0.7	0.18	0.16	0.25	0.91	0.93	0.90	6.41	10.00	5.00
BELTSVILLE	1	9	39.0110	-76.8990	0.24	12.0	0.80	1.2	0.25	0.22	0.25	0.88	0.91	0.90	11.56	10.00	5.00
BELTSVILLE	1	10	39.0112	-76.8874	0.43	7.5	0.42	0.8	0.16	0.12	0.25	0.91	0.95	0.90	2.19	10.00	5.00
BELT/LAUREL	B1		39.0114	-76.8759	0.40	8.9	0.49	0.9	0.23	0.12	0.25	0.89	0.95	0.90	4.38	10.00	5.00
LAUREL	1	1	39.0116	-76.8643	0.01	0.1	0.01	0.0	0.25	0.12	0.25	0.88	0.95	0.90	10.63	10.00	5.00
LAUREL	1	2	39.0119	-76.8527	0.00	0.0	0.00	0.0	0.00	0.00	0.00	0.00	0.00	0.00	0.00	0.00	0.00
LAUREL	1	3	39.0121	-76.8411	0.00	0.0	0.00	0.0	0.00	0.00	0.00	0.00	0.00	0.00	0.00	0.00	0.00
LAUREL	1	4	39.0123	-76.8295	0.00	0.0	0.00	0.0	0.00	0.00	0.00	0.00	0.00	0.00	0.00	0.00	0.00
ROCK/FALLS		B2	38.9959	-77.2347	0.40	7.0	0.30	0.7	0.18	0.12	0.25	0.91	0.95	0.90	0.63	0.00	0.00
ROCK/FALLS		B3	38.9961	-77.2231	0.40	7.0	0.30	0.7	0.18	0.12	0.25	0.91	0.95	0.90	1.25	0.00	0.00
ROCK/FALLS		B4	38.9963	-77.2115	0.40	7.0	0.30	0.7	0.18	0.12	0.25	0.91	0.95	0.90	1.09	0.00	0.00
ROCK/FALLS		B5	38.9965	-77.1999	0.40	7.0	0.30	0.7	0.18	0.12	0.25	0.91	0.95	0.90	0.31	0.00	0.00
ROCK/FALLS		B6	38.9967	-77.1884	0.40	7.0	0.30	0.7	0.18	0.12	0.25	0.91	0.95	0.90	0.94	0.00	0.00
ROCK/FALLS		B7	38.9969	-77.1768	0.40	7.0	0.30	0.7	0.18	0.12	0.25	0.91	0.95	0.90	0.31	0.00	0.00
ROCK/FALLS		B8	38.9971	-77.1652	0.40	7.0	0.30	0.7	0.18	0.12	0.25	0.91	0.95	0.90	1.88	0.00	0.00
ROCK/FALLS		B9	38.9973	-77.1536	0.32	7.0	0.30	0.7	0.18	0.12	0.25	0.90	0.95	0.90	11.88	10.00	5.00
ROCK/FALLS		B10	38.9975	-77.1421	0.40	7.0	0.30	0.7	0.18	0.12	0.25	0.91	0.95	0.90	1.56	0.00	0.00
RO/FA/KEN/WW	B1		38.9978	-77.1305	0.40	7.0	0.30	0.7	0.18	0.12	0.25	0.91	0.95	0.90	1.72	0.00	0.00
KENN/WASHW		B1	38.9980	-77.1189	0.41	7.2	0.29	0.7	0.18	0.12	0.25	0.91	0.95	0.90	5.31	10.00	5.00
KENN/WASHW		B2	38.9982	-77.1073	0.51	14.8	0.30	1.5	0.17	0.12	0.25	0.89	0.95	0.90	6.09	10.00	5.00
KENN/WASHW		B3	38.9984	-77.0957	0.48	15.0	0.43	1.5	0.19	0.12	0.25	0.88	0.95	0.90	5.47	10.00	5.00
KENN/WASHW		B4	38.9986	-77.0842	0.51	11.4	0.30	1.1	0.20	0.12	0.25	0.89	0.95	0.90	2.66	10.00	5.00
KENN/WASHW		B5	38.9988	-77.0726	0.40	8.2	0.31	0.8	0.17	0.15	0.25	0.90	0.94	0.90	10.00	10.00	5.00
KENN/WASHW		B6	38.9990	-77.0610	0.45	7.0	0.35	0.7	0.18	0.12	0.25	0.90	0.95	0.90	2.50	10.00	5.00
KENN/WASHW		B7	38.9992	-77.0494	0.44	7.0	0.34	0.7	0.20	0.12	0.25	0.90	0.95	0.90	4.53	10.00	5.00
KENN/WASHW		B8	38.9995	-77.0378	0.47	9.6	0.37	1.0	0.18	0.15	0.25	0.90	0.94	0.90	4.69	10.00	5.00
KENN/WASHW		B9	38.9997	-77.0263	0.49	14.4	0.43	1.4	0.18	0.13	0.25	0.90	0.95	0.90	7.19	10.00	5.00
KENN/WASHW		B10	38.9999	-77.0147	0.44	8.0	0.32	0.8	0.17	0.12	0.25	0.90	0.95	0.90	4.22	10.00	5.00
KEN/BE/WE/WW	B1		39.0001	-77.0031	0.38	7.0	0.30	0.7	0.19	0.12	0.25	0.90	0.95	0.90	5.47	10.00	5.00
BELT/WASHE		B1	39.0003	-76.9915	0.40	7.5	0.32	0.8	0.18	0.12	0.25	0.90	0.95	0.90	10.47	10.00	5.00
BELT/WASHE		B2	39.0005	-76.9799	0.39	8.0	0.37	0.8	0.14	0.12	0.25	0.90	0.95	0.90	7.50	10.00	5.00
BELT/WASHE		B3	39.0007	-76.9684	0.38	7.0	0.30	0.7	0.18	0.12	0.25	0.90	0.95	0.90	3.75	10.00	5.00
BELT/WASHE		B4	39.0009	-76.9568	0.40	7.0	0.30	0.7	0.18	0.12	0.25	0.91	0.95	0.90	0.63	0.00	0.00
BELT/WASHE		B5	39.0012	-76.9452	0.35	7.0	0.30	0.7	0.18	0.12	0.25	0.91	0.95	0.90	6.41	10.00	5.00
BELT/WASHE		B6	39.0014	-76.9336	0.34	7.0	0.35	0.7	0.18	0.12	0.25	0.90	0.95	0.90	7.81	10.00	5.00
BELT/WASHE		B7	39.0016	-76.9221	0.35	7.0	0.30	0.7	0.18	0.12	0.25	0.91	0.95	0.90	7.81	10.00	5.00
BELT/WASHE		B8	39.0018	-76.9105	0.43	8.0	0.37	0.8	0.20	0.12	0.25	0.88	0.95	0.90	4.69	10.00	5.00
BELT/WASHE		B9	39.0020	-76.8989	0.26	9.5	0.45	1.0	0.25	0.20	0.25	0.88	0.92	0.90	17.19	10.00	5.00
BELT/WASHE		B10	39.0022	-76.8873	0.34	7.0	0.42	0.7	0.17	0.16	0.25	0.89	0.94	0.90	13.28	10.00	5.00
BE/LAUR/WE/LANH	B1		39.0024	-76.8757	0.40	7.6	0.46	0.8	0.20	0.12	0.25	0.90	0.95	0.90	5.94	10.00	5.00
LAUREL/LANHAM		B1	39.0026	-76.8642	0.30	10.0	0.75	1.0	0.05	0.12	0.25	0.88	0.95	0.90	13.13	10.00	5.00
LAUREL/LANHAM		B2	39.0029	-76.8526	0.30	12.0	0.30	1.2	0.23	0.12	0.25	0.88	0.95	0.90	1.56	10.00	5.00
LAUREL/LANHAM		B3	39.0031	-76.8410	0.60	10.0	0.20	1.0	0.25	0.12	0.25	0.88	0.95	0.90	0.63	10.00	5.00
LAUREL/LANHAM		B4	39.0033	-76.8294	0.00	0.0	0.00	0.0	0.00	0.00	0.00	0.00	0.00	0.00	0.00	0.00	0.00
FALLS CHURCH	13	2	38.9869	-77.2344	0.00	0.0	0.00	0.0	0.00	0.00	0.00	0.00	0.00	0.00	0.00	0.00	0.00
FALLS CHURCH	13	3	38.9871	-77.2228	0.40	7.0	0.30	0.7	0.18	0.12	0.25	0.91	0.95	0.90	1.56	0.00	0.00
FALLS CHURCH	13	4	38.9873	-77.2112	0.40	7.0	0.30	0.7	0.18	0.12	0.25	0.91	0.95	0.90	1.56	0.00	0.00

FALLS CHURCH	13	5	38.9875	-77.1997	0.40	7.0	0.30	0.7	0.18	0.12	0.25	0.91	0.95	0.90	0.94	0.00	0.00
FALLS CHURCH	13	6	38.9877	-77.1881	0.47	8.0	0.33	0.8	0.20	0.12	0.25	0.90	0.95	0.90	1.25	10.00	5.00
FALLS CHURCH	13	7	38.9879	-77.1765	0.40	7.0	0.30	0.7	0.18	0.12	0.25	0.91	0.95	0.90	0.78	0.00	0.00
FALLS CHURCH	13	8	38.9881	-77.1649	0.40	7.0	0.30	0.7	0.18	0.25	0.25	0.91	0.90	0.90	0.94	0.00	0.00
FALLS CHURCH	13	9	38.9883	-77.1534	0.22	7.0	0.30	0.7	0.17	0.15	0.25	0.90	0.94	0.90	12.97	10.00	5.00
FALLS CHURCH	13	10	38.9886	-77.1418	0.37	7.0	0.30	0.7	0.18	0.15	0.25	0.91	0.94	0.90	7.19	10.00	5.00
FALLS/WAW	B13		38.9888	-77.1302	0.42	7.3	0.31	0.7	0.18	0.12	0.25	0.91	0.95	0.90	3.59	10.00	5.00
WASH WEST	13	1	38.9890	-77.1186	0.40	7.0	0.30	0.7	0.18	0.12	0.25	0.91	0.95	0.90	3.13	0.00	0.00
WASH WEST	13	2	38.9892	-77.1071	0.40	8.4	0.30	0.8	0.18	0.12	0.25	0.91	0.95	0.90	5.31	10.00	5.00
WASH WEST	13	3	38.9894	-77.0955	0.46	14.9	0.53	1.5	0.19	0.16	0.25	0.89	0.94	0.90	7.34	10.00	5.00
WASH WEST	13	4	38.9896	-77.0839	0.43	8.1	0.31	0.8	0.18	0.12	0.25	0.91	0.95	0.90	3.44	10.00	5.00
WASH WEST	13	5	38.9898	-77.0723	0.42	7.3	0.31	0.7	0.19	0.12	0.25	0.91	0.95	0.90	3.75	10.00	5.00
WASH WEST	13	6	38.9900	-77.0607	0.40	7.0	0.30	0.7	0.18	0.12	0.25	0.91	0.95	0.90	2.19	0.00	0.00
WASH WEST	13	7	38.9902	-77.0492	0.43	7.9	0.33	0.8	0.18	0.12	0.25	0.90	0.95	0.90	2.66	10.00	5.00
WASH WEST	13	8	38.9905	-77.0376	0.38	12.0	0.33	1.2	0.19	0.13	0.25	0.90	0.95	0.90	3.91	10.00	5.00
WASH WEST	13	9	38.9907	-77.0260	0.50	11.8	0.45	1.2	0.19	0.13	0.25	0.89	0.95	0.90	8.13	10.00	5.00
WASH WEST	13	10	38.9909	-77.0144	0.43	7.0	0.32	0.7	0.19	0.12	0.25	0.91	0.95	0.90	4.69	10.00	5.00
WAW/WAE	B13		38.9911	-77.0029	0.40	7.0	0.30	0.7	0.18	0.12	0.25	0.91	0.95	0.90	4.22	0.00	0.00
WASH EAST	13	1	38.9913	-76.9913	0.36	7.0	0.28	0.7	0.16	0.12	0.25	0.90	0.95	0.90	11.56	10.00	5.00
WASH EAST	13	2	38.9915	-76.9797	0.44	8.3	0.43	0.8	0.16	0.12	0.25	0.90	0.95	0.90	6.25	10.00	5.00
WASH EAST	13	3	38.9917	-76.9681	0.40	7.0	0.30	0.7	0.18	0.12	0.25	0.91	0.95	0.90	1.56	0.00	0.00
WASH EAST	13	4	38.9919	-76.9565	0.30	7.0	0.30	0.7	0.17	0.12	0.25	0.90	0.95	0.90	1.56	10.00	5.00
WASH EAST	13	5	38.9922	-76.9450	0.38	15.0	0.40	1.5	0.09	0.12	0.25	0.88	0.95	0.90	12.81	10.00	5.00
WASH EAST	13	6	38.9924	-76.9334	0.36	9.3	0.36	0.9	0.18	0.12	0.25	0.89	0.95	0.90	5.63	10.00	5.00
WASH EAST	13	7	38.9926	-76.9218	0.40	7.0	0.30	0.7	0.18	0.12	0.25	0.91	0.95	0.90	2.81	0.00	0.00
WASH EAST	13	8	38.9928	-76.9102	0.39	7.0	0.30	0.7	0.18	0.12	0.25	0.91	0.95	0.90	10.16	10.00	5.00
WASH EAST	13	9	38.9930	-76.8987	0.38	11.0	0.46	1.1	0.19	0.12	0.25	0.89	0.95	0.90	12.81	10.00	5.00
WASH EAST	13	10	38.9932	-76.8871	0.11	7.0	0.30	0.7	0.23	0.22	0.25	0.88	0.91	0.90	20.00	10.00	5.00
WE/LANHAM	B13		38.9934	-76.8755	0.20	7.0	0.30	0.7	0.24	0.12	0.25	0.88	0.95	0.90	13.75	10.00	5.00
LANHAM	13	1	38.9936	-76.8639	0.44	7.9	0.34	0.8	0.15	0.12	0.25	0.88	0.95	0.90	3.13	10.00	5.00
LANHAM	13	2	38.9939	-76.8523	0.22	17.1	0.27	1.7	0.23	0.12	0.25	0.88	0.95	0.90	7.81	10.00	5.00
LANHAM	13	3	38.9941	-76.8408	0.16	18.0	0.20	1.8	0.25	0.12	0.25	0.88	0.95	0.90	1.56	10.00	5.00
LANHAM	13	4	38.9943	-76.8292	0.35	12.0	0.35	1.2	0.17	0.12	0.25	0.88	0.95	0.90	3.13	10.00	5.00
FALLS CHURCH	12	2	38.9779	-77.2341	0.00	0.0	0.00	0.0	0.00	0.00	0.00	0.00	0.00	0.00	0.00	0.00	0.00
FALLS CHURCH	12	3	38.9781	-77.2225	0.40	7.0	0.30	0.7	0.18	0.12	0.25	0.91	0.95	0.90	0.63	0.00	0.00
FALLS CHURCH	12	4	38.9783	-77.2110	0.40	7.0	0.30	0.7	0.18	0.12	0.25	0.91	0.95	0.90	0.63	0.00	0.00
FALLS CHURCH	12	5	38.9785	-77.1994	0.52	7.0	0.24	0.7	0.22	0.12	0.25	0.89	0.95	0.90	2.50	10.00	5.00
FALLS CHURCH	12	6	38.9787	-77.1878	0.57	7.0	0.34	0.7	0.21	0.12	0.25	0.90	0.95	0.90	1.56	10.00	5.00
FALLS CHURCH	12	7	38.9789	-77.1762	0.20	7.0	0.30	0.7	0.17	0.12	0.25	0.90	0.95	0.90	11.88	10.00	5.00
FALLS CHURCH	12	8	38.9791	-77.1647	0.30	7.0	0.30	0.7	0.17	0.12	0.25	0.90	0.95	0.90	11.56	10.00	5.00
FALLS CHURCH	12	9	38.9793	-77.1531	0.40	7.0	0.30	0.7	0.18	0.12	0.25	0.91	0.95	0.90	0.94	0.00	0.00
FALLS CHURCH	12	10	38.9796	-77.1415	0.40	7.0	0.30	0.7	0.18	0.13	0.25	0.91	0.95	0.90	1.41	0.00	0.00
FALLS/WW	B12		38.9798	-77.1299	0.44	7.0	0.32	0.7	0.19	0.16	0.25	0.90	0.94	0.90	3.13	10.00	5.00
WASH WEST	12	1	38.9800	-77.1183	0.40	7.0	0.30	0.7	0.18	0.12	0.25	0.91	0.95	0.90	4.06	0.00	0.00
WASH WEST	12	2	38.9802	-77.1068	0.40	7.0	0.30	0.7	0.18	0.13	0.25	0.91	0.95	0.90	4.06	0.00	0.00
WASH WEST	12	3	38.9804	-77.0952	0.48	15.3	0.50	1.5	0.19	0.16	0.25	0.89	0.94	0.90	7.97	10.00	5.00
WASH WEST	12	4	38.9806	-77.0836	0.42	8.5	0.35	0.9	0.18	0.12	0.25	0.91	0.95	0.90	4.38	10.00	5.00
WASH WEST	12	5	38.9808	-77.0721	0.40	7.0	0.30	0.7	0.18	0.12	0.25	0.91	0.95	0.90	4.69	0.00	0.00
WASH WEST	12	6	38.9810	-77.0605	0.40	7.0	0.30	0.7	0.18	0.12	0.25	0.91	0.95	0.90	3.13	0.00	0.00
WASH WEST	12	7	38.9812	-77.0489	0.40	7.0	0.30	0.7	0.18	0.12	0.25	0.91	0.95	0.90	0.47	0.00	0.00
WASH WEST	12	8	38.9815	-77.0373	0.48	7.4	0.42	0.7	0.18	0.12	0.25	0.91	0.95	0.90	3.91	10.00	5.00
WASH WEST	12	9	38.9817	-77.0257	0.45	8.8	0.45	0.9	0.18	0.13	0.25	0.90	0.95	0.90	5.00	10.00	5.00
WASH WEST	12	10	38.9819	-77.0142	0.42	7.4	0.29	0.7	0.18	0.12	0.25	0.91	0.95	0.90	4.53	10.00	5.00
WW/WE	B12		38.9821	-77.0026	0.45	8.4	0.39	0.8	0.19	0.12	0.25	0.90	0.95	0.90	5.94	10.00	5.00
WASH EAST	12	1	38.9823	-76.9910	0.39	7.4	0.30	0.7	0.17	0.12	0.25	0.91	0.95	0.90	4.84	10.00	5.00
WASH EAST	12	2	38.9825	-76.9794	0.41	8.8	0.57	0.9	0.22	0.12	0.25	0.89	0.95	0.90	12.50	10.00	5.00
WASH EAST	12	3	38.9827	-76.9679	0.41	7.2	0.32	0.7	0.18	0.12	0.25	0.91	0.95	0.90	3.28	10.00	5.00
WASH EAST	12	4	38.9829	-76.9563	0.29	8.6	0.30	0.9	0.19	0.16	0.25	0.89	0.94	0.90	9.53	10.00	5.00
WASH EAST	12	5	38.9832	-76.9447	0.40	13.6	0.38	1.4	0.11	0.16	0.25	0.89	0.94	0.90	7.97	10.00	5.00
WASH EAST	12	6	38.9834	-76.9331	0.39	11.3	0.45	1.1	0.13	0.15	0.25	0.89	0.94	0.90	6.25	10.00	5.00
WASH EAST	12	7	38.9836	-76.9216	0.35	7.5	0.48	0.8	0.13	0.12	0.25	0.88	0.95	0.90	3.75	10.00	5.00
WASH EAST	12	8	38.9838	-76.9100	0.34	7.0	0.30	0.7	0.18	0.12	0.25	0.91	0.95	0.90	8.59	10.00	5.00
WASH EAST	12	9	38.9840	-76.8984	0.00	0.0	0.00	0.0	0.00	0.00	0.00	0.00	0.00	0.00	0.00	0.00	0.00
WASH EAST	12	10	38.9842	-76.8868	0.16	7.0	0.30	0.7	0.17	0.12	0.25	0.89	0.95	0.90	11.25	10.00	5.00
WE/LANHAM	B12		38.9844	-76.8753	0.42	8.5	0.35	0.9	0.20	0.20	0.25	0.90	0.92	0.90	13.28	10.00	5.00
LANHAM	12	1	38.9846	-76.8637	0.48	7.4	0.45	0.7	0.17	0.12	0.25	0.90	0.95	0.90	3.59	10.00	5.00
LANHAM	12	2	38.9849	-76.8521	0.40	7.0	0.30	0.7	0.18	0.12	0.25	0.91	0.95	0.90	2.50	0.00	0.00
LANHAM	12	3	38.9851	-76.8405	0.42	7.0	0.38	0.7	0.17	0.12	0.25	0.89	0.95	0.90	4.38	10.00	5.00
LANHAM	12	4	38.9853	-76.8289	0.50	7.0	0.30	0.7	0.09	0.12	0.25	0.88	0.95	0.90	1.25	10.00	5.00
FALLS CHURCH	11	2	38.9689	-77.2338	0.00	0.0	0.00	0.0	0.00	0.00	0.00	0.00	0.00	0.00	0.00	0.00	0.00
FALLS CHURCH	11	3	38.9691	-77.2222	0.00	0.0	0.00	0.0	0.00	0.00	0.00	0.00	0.00	0.00	0.00	0.00	0.00
FALLS CHURCH	11	4	38.9693	-77.2107	0.40	7.0	0.30	0.7	0.18	0.12	0.25	0.91	0.95	0.90	0.31	0.00	0.00
FALLS CHURCH	11	5	38.9695	-77.1991	0.00	0.0	0.00	0.0	0.00	0.00	0.00	0.00	0.00	0.00	0.00	0.00	0.00
FALLS CHURCH	11	6	38.9697	-77.1875	0.48	7.0	0.38	0.7	0.23	0.12	0.25	0.89	0.95	0.90	2.50	10.00	5.00

FALLS CHURCH	11	7	38.9699	-77.1759	0.01	0.1	0.01	0.0	0.25	0.12	0.25	0.88	0.95	0.90	11.88	10.00	5.00
FALLS CHURCH	11	8	38.9701	-77.1644	0.40	7.0	0.30	0.7	0.18	0.12	0.25	0.91	0.95	0.90	0.47	0.00	0.00
FALLS CHURCH	11	9	38.9703	-77.1528	0.40	7.0	0.30	0.7	0.18	0.12	0.25	0.91	0.95	0.90	0.78	0.00	0.00
FALLS CHURCH	11	10	38.9706	-77.1412	0.40	7.0	0.30	0.7	0.18	0.12	0.25	0.91	0.95	0.90	1.41	0.00	0.00
FALLS/WW	B11		38.9708	-77.1297	0.40	7.0	0.30	0.7	0.18	0.12	0.25	0.91	0.95	0.90	2.34	0.00	0.00
WASH WEST	11	1	38.9710	-77.1181	0.40	7.4	0.31	0.7	0.19	0.15	0.25	0.91	0.94	0.90	8.91	10.00	5.00
WASH WEST	11	2	38.9712	-77.1065	0.40	7.0	0.30	0.7	0.18	0.12	0.25	0.91	0.95	0.90	2.81	0.00	0.00
WASH WEST	11	3	38.9714	-77.0949	0.40	7.0	0.30	0.7	0.18	0.12	0.25	0.91	0.95	0.90	3.75	0.00	0.00
WASH WEST	11	4	38.9716	-77.0833	0.40	7.0	0.30	0.7	0.18	0.12	0.25	0.91	0.95	0.90	1.41	0.00	0.00
WASH WEST	11	5	38.9718	-77.0718	0.40	7.0	0.30	0.7	0.18	0.12	0.25	0.91	0.95	0.90	4.69	0.00	0.00
WASH WEST	11	6	38.9720	-77.0602	0.43	7.4	0.34	0.7	0.17	0.12	0.25	0.91	0.95	0.90	5.47	10.00	5.00
WASH WEST	11	7	38.9722	-77.0486	0.00	0.0	0.00	0.0	0.00	0.00	0.00	0.00	0.00	0.00	0.00	0.00	0.00
WASH WEST	11	8	38.9725	-77.0370	0.55	9.5	0.40	1.0	0.17	0.12	0.25	0.90	0.95	0.90	2.81	10.00	5.00
WASH WEST	11	9	38.9727	-77.0255	0.54	8.7	0.48	0.9	0.18	0.12	0.25	0.90	0.95	0.90	5.31	10.00	5.00
WASH WEST	11	10	38.9729	-77.0139	0.38	7.0	0.31	0.7	0.19	0.12	0.25	0.90	0.95	0.90	4.69	10.00	5.00
WW/WE	B11		38.9731	-77.0023	0.40	7.0	0.30	0.7	0.18	0.12	0.25	0.91	0.95	0.90	4.69	0.00	0.00
WASH EAST	11	1	38.9733	-76.9907	0.42	7.0	0.35	0.7	0.17	0.15	0.25	0.90	0.94	0.90	4.06	10.00	5.00
WASH EAST	11	2	38.9735	-76.9792	0.36	7.0	0.30	0.7	0.18	0.16	0.25	0.91	0.94	0.90	8.75	10.00	5.00
WASH EAST	11	3	38.9737	-76.9676	0.40	7.0	0.30	0.7	0.18	0.12	0.25	0.91	0.95	0.90	3.13	0.00	0.00
WASH EAST	11	4	38.9739	-76.9560	0.29	9.0	0.33	0.9	0.20	0.12	0.25	0.89	0.95	0.90	4.69	10.00	5.00
WASH EAST	11	5	38.9742	-76.9444	0.40	7.0	0.30	0.7	0.18	0.12	0.25	0.91	0.95	0.90	5.00	0.00	0.00
WASH EAST	11	6	38.9744	-76.9329	0.40	7.0	0.33	0.7	0.17	0.12	0.25	0.90	0.95	0.90	4.06	10.00	5.00
WASH EAST	11	7	38.9746	-76.9213	0.50	7.0	0.50	0.7	0.15	0.12	0.25	0.88	0.95	0.90	2.50	10.00	5.00
WASH EAST	11	8	38.9748	-76.9097	0.20	7.0	0.30	0.7	0.17	0.12	0.25	0.90	0.95	0.90	5.94	10.00	5.00
WASH EAST	11	9	38.9750	-76.8981	0.27	7.0	0.30	0.7	0.17	0.12	0.25	0.90	0.95	0.90	11.25	10.00	5.00
WASH EAST	11	10	38.9752	-76.8866	0.40	7.0	0.30	0.7	0.18	0.12	0.25	0.91	0.95	0.90	3.13	0.00	0.00
WAE/LANHAM	B11		38.9754	-76.8750	0.37	7.0	0.30	0.7	0.18	0.16	0.25	0.91	0.94	0.90	14.38	10.00	5.00
LANHAM	11	1	38.9756	-76.8634	0.35	7.0	0.20	0.7	0.22	0.12	0.25	0.90	0.95	0.90	3.75	10.00	5.00
LANHAM	11	2	38.9759	-76.8518	0.40	7.0	0.30	0.7	0.18	0.12	0.25	0.91	0.95	0.90	4.38	0.00	0.00
LANHAM	11	3	38.9761	-76.8403	0.36	7.0	0.30	0.7	0.18	0.12	0.25	0.91	0.95	0.90	3.13	10.00	5.00
LANHAM	11	4	38.9763	-76.8287	0.00	0.0	0.00	0.0	0.00	0.00	0.00	0.00	0.00	0.00	0.00	0.00	0.00
FALLS CHURCH	10	2	38.9599	-77.2335	0.40	7.0	0.30	0.7	0.18	0.12	0.25	0.91	0.95	0.90	1.88	0.00	0.00
FALLS CHURCH	10	3	38.9601	-77.2220	0.40	7.0	0.30	0.7	0.18	0.12	0.25	0.91	0.95	0.90	0.63	0.00	0.00
FALLS CHURCH	10	4	38.9603	-77.2104	0.40	7.0	0.30	0.7	0.18	0.12	0.25	0.91	0.95	0.90	0.63	0.00	0.00
FALLS CHURCH	10	5	38.9605	-77.1988	0.40	7.0	0.30	0.7	0.18	0.12	0.25	0.91	0.95	0.90	0.63	0.00	0.00
FALLS CHURCH	10	6	38.9607	-77.1872	0.23	7.0	0.30	0.7	0.17	0.12	0.25	0.90	0.95	0.90	18.13	10.00	5.00
FALLS CHURCH	10	7	38.9609	-77.1757	0.27	7.0	0.30	0.7	0.17	0.12	0.25	0.90	0.95	0.90	6.25	10.00	5.00
FALLS CHURCH	10	8	38.9611	-77.1641	0.40	7.0	0.30	0.7	0.18	0.12	0.25	0.91	0.95	0.90	0.31	0.00	0.00
FALLS CHURCH	10	9	38.9613	-77.1525	0.00	0.0	0.00	0.0	0.00	0.00	0.00	0.00	0.00	0.00	0.00	0.00	0.00
FALLS CHURCH	10	10	38.9616	-77.1409	0.00	0.0	0.00	0.0	0.00	0.00	0.00	0.00	0.00	0.00	0.00	0.00	0.00
FALLS/WAW	B10		38.9618	-77.1294	0.40	7.0	0.30	0.7	0.18	0.12	0.25	0.91	0.95	0.90	3.44	0.00	0.00
WASH WEST	10	1	38.9620	-77.1178	0.41	7.1	0.30	0.7	0.18	0.12	0.25	0.91	0.95	0.90	5.16	10.00	5.00
WASH WEST	10	2	38.9622	-77.1062	0.47	9.5	0.42	0.9	0.19	0.15	0.25	0.89	0.94	0.90	7.19	10.00	5.00
WASH WEST	10	3	38.9624	-77.0947	0.43	12.9	0.39	1.3	0.17	0.13	0.25	0.90	0.95	0.90	5.63	10.00	5.00
WASH WEST	10	4	38.9626	-77.0831	0.47	14.4	0.44	1.4	0.18	0.12	0.25	0.90	0.95	0.90	6.41	10.00	5.00
WASH WEST	10	5	38.9628	-77.0715	0.46	7.4	0.43	0.7	0.18	0.12	0.25	0.91	0.95	0.90	5.63	10.00	5.00
WASH WEST	10	6	38.9630	-77.0599	0.42	7.8	0.32	0.8	0.17	0.12	0.25	0.91	0.95	0.90	4.69	10.00	5.00
WASH WEST	10	7	38.9633	-77.0484	0.00	0.0	0.00	0.0	0.00	0.00	0.00	0.00	0.00	0.00	0.00	0.00	0.00
WASH WEST	10	8	38.9635	-77.0368	0.59	8.1	0.59	0.8	0.18	0.12	0.25	0.91	0.95	0.90	3.44	10.00	5.00
WASH WEST	10	9	38.9637	-77.0252	0.54	9.3	0.53	0.9	0.17	0.12	0.25	0.90	0.95	0.90	7.19	10.00	5.00
WASH WEST	10	10	38.9639	-77.0136	0.58	9.2	0.59	0.9	0.18	0.12	0.25	0.90	0.95	0.90	6.25	10.00	5.00
WAW/WAE	B10		38.9641	-77.0021	0.47	7.0	0.37	0.7	0.17	0.13	0.25	0.90	0.95	0.90	5.94	10.00	5.00
WASH EAST	10	1	38.9643	-76.9905	0.40	7.0	0.37	0.7	0.18	0.15	0.25	0.90	0.94	0.90	4.06	10.00	5.00
WASH EAST	10	2	38.9645	-76.9789	0.38	7.0	0.29	0.7	0.17	0.12	0.25	0.91	0.95	0.90	3.75	10.00	5.00
WASH EAST	10	3	38.9647	-76.9673	0.32	7.0	0.30	0.7	0.18	0.15	0.25	0.90	0.94	0.90	6.88	10.00	5.00
WASH EAST	10	4	38.9649	-76.9558	0.32	8.0	0.35	0.8	0.14	0.15	0.25	0.90	0.94	0.90	10.63	10.00	5.00
WASH EAST	10	5	38.9652	-76.9442	0.40	7.0	0.33	0.7	0.18	0.12	0.25	0.91	0.95	0.90	5.63	10.00	5.00
WASH EAST	10	6	38.9654	-76.9326	0.40	7.5	0.34	0.8	0.18	0.12	0.25	0.90	0.95	0.90	10.94	10.00	5.00
WASH EAST	10	7	38.9656	-76.9210	0.38	7.0	0.32	0.7	0.19	0.17	0.25	0.90	0.93	0.90	7.97	10.00	5.00
WASH EAST	10	8	38.9658	-76.9095	0.38	7.8	0.41	0.8	0.20	0.12	0.25	0.90	0.95	0.90	14.69	10.00	5.00
WASH EAST	10	9	38.9660	-76.8979	0.42	8.3	0.50	0.8	0.21	0.12	0.25	0.90	0.95	0.90	14.06	10.00	5.00
WASH EAST	10	10	38.9662	-76.8863	0.44	7.6	0.34	0.8	0.20	0.12	0.25	0.90	0.95	0.90	5.31	10.00	5.00
WAE/LANHAM	B10		38.9664	-76.8748	0.40	7.0	0.30	0.7	0.18	0.12	0.25	0.91	0.95	0.90	5.00	0.00	0.00
LANHAM	10	1	38.9666	-76.8632	0.37	7.0	0.30	0.7	0.18	0.16	0.25	0.91	0.94	0.90	14.38	10.00	5.00
LANHAM	10	2	38.9669	-76.8516	0.38	7.0	0.30	0.7	0.18	0.12	0.25	0.91	0.95	0.90	5.31	10.00	5.00
LANHAM	10	3	38.9671	-76.8400	0.40	7.0	0.29	0.7	0.19	0.12	0.25	0.91	0.95	0.90	3.91	10.00	5.00
LANHAM	10	4	38.9673	-76.8285	0.40	7.0	0.30	0.7	0.18	0.12	0.25	0.91	0.95	0.90	0.63	0.00	0.00
FALLS CHURCH	9	2	38.9509	-77.2332	0.40	7.0	0.30	0.7	0.18	0.12	0.25	0.91	0.95	0.90	1.25	0.00	0.00
FALLS CHURCH	9	3	38.9511	-77.2217	0.40	7.0	0.30	0.7	0.18	0.12	0.25	0.91	0.95	0.90	0.63	0.00	0.00
FALLS CHURCH	9	4	38.9513	-77.2101	0.40	7.0	0.30	0.7	0.18	0.12	0.25	0.91	0.95	0.90	1.56	0.00	0.00
FALLS CHURCH	9	5	38.9515	-77.1985	0.29	7.0	0.30	0.7	0.17	0.12	0.25	0.90	0.95	0.90	12.81	10.00	5.00
FALLS CHURCH	9	6	38.9517	-77.1870	0.43	7.4	0.29	0.7	0.19	0.12	0.25	0.91	0.95	0.90	2.50	10.00	5.00
FALLS CHURCH	9	7	38.9519	-77.1754	0.40	7.0	0.30	0.7	0.18	0.12	0.25	0.91	0.95	0.90	1.88	0.00	0.00
FALLS CHURCH	9	8	38.9521	-77.1638	0.43	7.9	0.33	0.8	0.19	0.12	0.25	0.90	0.95	0.90	1.41	10.00	5.00

FALLS CHURCH	9	9	38.9523	-77.1522	0.20	12.0	0.20	1.2	0.25	0.12	0.25	0.88	0.95	0.90	1.88	10.00	5.00
FALLS CHURCH	9	10	38.9526	-77.1407	0.35	30.0	0.70	3.0	0.25	0.12	0.25	0.88	0.95	0.90	1.25	10.00	5.00
FALLS/WAW	B9		38.9528	-77.1291	0.34	7.0	0.30	0.7	0.18	0.12	0.25	0.91	0.95	0.90	1.25	10.00	5.00
WASH WEST	9	1	38.9530	-77.1175	0.37	9.8	0.28	1.0	0.17	0.12	0.25	0.90	0.95	0.90	5.78	10.00	5.00
WASH WEST	9	2	38.9532	-77.1059	0.40	7.0	0.30	0.7	0.18	0.12	0.25	0.91	0.95	0.90	3.75	0.00	0.00
WASH WEST	9	3	38.9534	-77.0944	0.44	7.0	0.39	0.7	0.18	0.12	0.25	0.91	0.95	0.90	4.69	0.00	0.00
WASH WEST	9	4	38.9536	-77.0828	0.53	8.3	0.52	0.8	0.18	0.12	0.25	0.90	0.95	0.90	5.78	10.00	5.00
WASH WEST	9	5	38.9538	-77.0712	0.53	9.7	0.60	1.0	0.16	0.12	0.25	0.90	0.95	0.90	5.00	10.00	5.00
WASH WEST	9	6	38.9540	-77.0597	0.41	7.0	0.33	0.7	0.18	0.12	0.25	0.91	0.95	0.90	2.50	0.00	0.00
WASH WEST	9	7	38.9543	-77.0481	0.40	7.0	0.30	0.7	0.18	0.12	0.25	0.91	0.95	0.90	0.31	0.00	0.00
WASH WEST	9	8	38.9545	-77.0365	0.68	9.4	0.68	0.9	0.18	0.12	0.25	0.91	0.95	0.90	5.94	10.00	5.00
WASH WEST	9	9	38.9547	-77.0249	0.68	9.7	0.68	1.0	0.18	0.12	0.25	0.91	0.95	0.90	9.06	10.00	5.00
WASH WEST	9	10	38.9549	-77.0134	0.75	10.0	0.75	1.0	0.18	0.12	0.25	0.91	0.95	0.90	8.75	10.00	5.00
WAW/WAE	B9		38.9551	-77.0018	0.39	7.2	0.38	0.7	0.18	0.12	0.25	0.90	0.95	0.90	5.78	10.00	5.00
WASH EAST	9	1	38.9553	-76.9902	0.40	7.0	0.30	0.7	0.18	0.12	0.25	0.91	0.95	0.90	2.97	0.00	0.00
WASH EAST	9	2	38.9555	-76.9787	0.49	9.5	0.55	0.9	0.13	0.12	0.25	0.89	0.95	0.90	4.69	10.00	5.00
WASH EAST	9	3	38.9557	-76.9671	0.38	6.3	0.34	0.6	0.19	0.15	0.25	0.89	0.94	0.90	7.34	10.00	5.00
WASH EAST	9	4	38.9559	-76.9555	0.40	7.0	0.30	0.7	0.18	0.12	0.25	0.91	0.95	0.90	4.38	0.00	0.00
WASH EAST	9	5	38.9562	-76.9439	0.40	7.6	0.41	0.8	0.16	0.12	0.25	0.90	0.95	0.90	6.88	10.00	5.00
WASH EAST	9	6	38.9564	-76.9324	0.43	7.0	0.44	0.7	0.18	0.12	0.25	0.90	0.95	0.90	4.69	10.00	5.00
WASH EAST	9	7	38.9566	-76.9208	0.40	7.6	0.36	0.8	0.15	0.15	0.25	0.89	0.94	0.90	6.02	10.00	5.00
WASH EAST	9	8	38.9568	-76.9092	0.34	7.0	0.30	0.7	0.18	0.12	0.25	0.91	0.95	0.90	13.75	10.00	5.00
WASH EAST	9	9	38.9570	-76.8977	0.40	7.0	0.30	0.7	0.18	0.12	0.25	0.91	0.95	0.90	2.66	0.00	0.00
WASH EAST	9	10	38.9572	-76.8861	0.40	7.0	0.30	0.7	0.18	0.12	0.25	0.91	0.95	0.90	1.88	0.00	0.00
WAE/LANHAM	B9		38.9574	-76.8745	0.33	7.6	0.36	0.8	0.20	0.12	0.25	0.89	0.95	0.90	7.81	10.00	5.00
LANHAM	9	1	38.9576	-76.8629	0.29	8.9	0.43	0.9	0.22	0.16	0.25	0.89	0.94	0.90	18.13	10.00	5.00
LANHAM	9	2	38.9579	-76.8514	0.40	7.0	0.30	0.7	0.18	0.12	0.25	0.91	0.95	0.90	2.97	0.00	0.00
LANHAM	9	3	38.9581	-76.8398	0.46	7.0	0.30	0.7	0.22	0.12	0.25	0.89	0.95	0.90	4.38	10.00	5.00
LANHAM	9	4	38.9583	-76.8282	0.40	7.0	0.30	0.7	0.18	0.12	0.25	0.91	0.95	0.90	1.25	0.00	0.00
FALLS CHURCH	8	2	38.9419	-77.2329	0.40	7.0	0.30	0.7	0.18	0.12	0.25	0.91	0.95	0.90	0.63	0.00	0.00
FALLS CHURCH	8	3	38.9421	-77.2214	0.40	7.0	0.30	0.7	0.18	0.12	0.25	0.91	0.95	0.90	3.44	0.00	0.00
FALLS CHURCH	8	4	38.9423	-77.2098	0.35	7.0	0.30	0.7	0.18	0.12	0.25	0.91	0.95	0.90	12.97	10.00	5.00
FALLS CHURCH	8	5	38.9425	-77.1982	0.37	7.0	0.30	0.7	0.18	0.12	0.25	0.91	0.95	0.90	7.34	10.00	5.00
FALLS CHURCH	8	6	38.9427	-77.1867	0.40	7.0	0.30	0.7	0.18	0.12	0.25	0.91	0.95	0.90	2.03	0.00	0.00
FALLS CHURCH	8	7	38.9429	-77.1751	0.40	7.0	0.30	0.7	0.18	0.12	0.25	0.91	0.95	0.90	1.88	0.00	0.00
FALLS CHURCH	8	8	38.9431	-77.1635	0.40	7.0	0.30	0.7	0.18	0.12	0.25	0.91	0.95	0.90	1.56	0.00	0.00
FALLS CHURCH	8	9	38.9433	-77.1519	0.34	7.8	0.30	0.8	0.20	0.16	0.25	0.90	0.94	0.90	8.13	10.00	5.00
FALLS CHURCH	8	10	38.9436	-77.1404	0.40	7.0	0.30	0.7	0.18	0.13	0.25	0.91	0.95	0.90	0.94	0.00	0.00
FALLS/WAW	B8		38.9438	-77.1288	0.00	0.0	0.00	0.0	0.00	0.00	0.00	0.00	0.00	0.00	0.00	0.00	0.00
WASH WEST	8	1	38.9440	-77.1172	0.37	12.7	0.27	1.3	0.18	0.12	0.25	0.90	0.95	0.90	2.50	10.00	5.00
WASH WEST	8	2	38.9442	-77.1057	0.40	7.0	0.30	0.7	0.18	0.12	0.25	0.91	0.95	0.90	1.72	0.00	0.00
WASH WEST	8	3	38.9444	-77.0941	0.47	7.9	0.42	0.8	0.18	0.12	0.25	0.91	0.95	0.90	4.69	10.00	5.00
WASH WEST	8	4	38.9446	-77.0825	0.51	9.6	0.53	1.0	0.17	0.12	0.25	0.89	0.95	0.90	6.88	10.00	5.00
WASH WEST	8	5	38.9448	-77.0710	0.53	9.9	0.63	1.0	0.18	0.12	0.25	0.90	0.95	0.90	6.25	10.00	5.00
WASH WEST	8	6	38.9450	-77.0594	0.59	16.7	0.73	1.7	0.20	0.12	0.25	0.89	0.95	0.90	3.44	10.00	5.00
WASH WEST	8	7	38.9453	-77.0478	0.50	7.0	0.50	0.7	0.18	0.12	0.25	0.91	0.95	0.90	0.94	0.00	0.00
WASH WEST	8	8	38.9455	-77.0362	0.56	8.7	0.53	0.9	0.17	0.12	0.25	0.90	0.95	0.90	7.03	10.00	5.00
WASH WEST	8	9	38.9457	-77.0247	0.68	10.4	0.62	1.0	0.18	0.12	0.25	0.90	0.95	0.90	9.06	10.00	5.00
WASH WEST	8	10	38.9459	-77.0131	0.71	10.3	0.69	1.0	0.17	0.12	0.25	0.91	0.95	0.90	5.00	10.00	5.00
WAW/WAE	B8		38.9461	-77.0015	0.51	7.8	0.56	0.8	0.16	0.12	0.25	0.89	0.95	0.90	5.94	10.00	5.00
WASH EAST	8	1	38.9463	-76.9900	0.49	7.6	0.53	0.8	0.18	0.12	0.25	0.91	0.95	0.90	4.22	10.00	5.00
WASH EAST	8	2	38.9465	-76.9784	0.46	7.0	0.43	0.7	0.18	0.13	0.25	0.91	0.95	0.90	3.91	0.00	0.00
WASH EAST	8	3	38.9467	-76.9668	0.50	8.4	0.39	0.8	0.14	0.15	0.25	0.89	0.94	0.90	7.19	10.00	5.00
WASH EAST	8	4	38.9469	-76.9553	0.40	7.0	0.30	0.7	0.18	0.12	0.25	0.91	0.95	0.90	3.59	0.00	0.00
WASH EAST	8	5	38.9472	-76.9437	0.45	7.0	0.39	0.7	0.17	0.12	0.25	0.90	0.95	0.90	4.38	10.00	5.00
WASH EAST	8	6	38.9474	-76.9321	0.40	7.0	0.30	0.7	0.19	0.15	0.25	0.90	0.94	0.90	6.41	10.00	5.00
WASH EAST	8	7	38.9476	-76.9205	0.41	7.3	0.32	0.7	0.19	0.13	0.25	0.91	0.95	0.90	5.00	10.00	5.00
WASH EAST	8	8	38.9478	-76.9090	0.39	8.3	0.39	0.8	0.21	0.12	0.25	0.90	0.95	0.90	14.06	10.00	5.00
WASH EAST	8	9	38.9480	-76.8974	0.40	7.0	0.30	0.7	0.18	0.12	0.25	0.91	0.95	0.90	4.69	0.00	0.00
WASH EAST	8	10	38.9482	-76.8858	0.38	7.0	0.35	0.7	0.21	0.12	0.25	0.90	0.95	0.90	5.63	10.00	5.00
WAE/LANHAM	B8		38.9484	-76.8743	0.17	7.0	0.30	0.7	0.17	0.12	0.25	0.89	0.95	0.90	14.69	10.00	5.00
LANHAM	8	1	38.9486	-76.8627	0.09	7.0	0.30	0.7	0.23	0.16	0.25	0.88	0.94	0.90	20.94	10.00	5.00
LANHAM	8	2	38.9489	-76.8511	0.29	7.0	0.30	0.7	0.17	0.13	0.25	0.90	0.95	0.90	13.75	10.00	5.00
LANHAM	8	3	38.9491	-76.8396	0.38	7.0	0.30	0.7	0.15	0.15	0.25	0.88	0.94	0.90	12.50	10.00	5.00
LANHAM	8	4	38.9493	-76.8280	0.01	0.1	0.01	0.0	0.25	0.25	0.25	0.88	0.90	0.90	10.63	10.00	5.00
FALLS CHURCH	7	2	38.9329	-77.2326	0.20	45.0	0.50	4.5	0.25	0.12	0.25	0.88	0.95	0.90	11.88	10.00	5.00
FALLS CHURCH	7	3	38.9331	-77.2211	0.25	9.7	0.25	1.0	0.16	0.12	0.25	0.89	0.95	0.90	12.66	10.00	5.00
FALLS CHURCH	7	4	38.9333	-77.2095	0.15	9.5	0.22	1.0	0.24	0.12	0.25	0.89	0.95	0.90	21.88	10.00	5.00
FALLS CHURCH	7	5	38.9335	-77.1979	0.40	7.0	0.30	0.7	0.18	0.12	0.25	0.91	0.95	0.90	1.56	0.00	0.00
FALLS CHURCH	7	6	38.9337	-77.1864	0.40	7.0	0.30	0.7	0.18	0.12	0.25	0.91	0.95	0.90	2.81	0.00	0.00
FALLS CHURCH	7	7	38.9339	-77.1748	0.40	7.0	0.30	0.7	0.18	0.12	0.25	0.91	0.95	0.90	2.19	0.00	0.00
FALLS CHURCH	7	8	38.9341	-77.1632	0.40	7.0	0.30	0.7	0.18	0.12	0.25	0.91	0.95	0.90	0.94	0.00	0.00
FALLS CHURCH	7	9	38.9343	-77.1517	0.41	9.1	0.29	0.9	0.19	0.12	0.25	0.91	0.95	0.90	1.88	10.00	5.00
FALLS CHURCH	7	10	38.9346	-77.1401	0.40	7.0	0.30	0.7	0.18	0.12	0.25	0.91	0.95	0.90	0.63	0.00	0.00

FALLS/WAW	B7		38.9348	-77.1285	0.30	7.0	0.30	0.7	0.17	0.12	0.25	0.90	0.95	0.90	6.56	10.00	5.00
WASH WEST	7	1	38.9350	-77.1170	0.56	5.8	0.26	0.6	0.20	0.12	0.25	0.90	0.95	0.90	2.19	10.00	5.00
WASH WEST	7	2	38.9352	-77.1054	0.39	7.9	0.29	0.8	0.17	0.13	0.25	0.91	0.95	0.90	4.06	10.00	5.00
WASH WEST	7	3	38.9354	-77.0938	0.43	9.3	0.36	0.9	0.17	0.12	0.25	0.90	0.95	0.90	5.63	10.00	5.00
WASH WEST	7	4	38.9356	-77.0823	0.55	16.4	0.48	1.6	0.16	0.12	0.25	0.89	0.95	0.90	5.63	10.00	5.00
WASH WEST	7	5	38.9358	-77.0707	0.43	9.8	0.50	1.0	0.16	0.12	0.25	0.90	0.95	0.90	6.72	10.00	5.00
WASH WEST	7	6	38.9360	-77.0591	0.50	8.5	0.45	0.9	0.17	0.12	0.25	0.90	0.95	0.90	3.75	10.00	5.00
WASH WEST	7	7	38.9363	-77.0476	0.63	8.5	0.63	0.9	0.18	0.12	0.25	0.91	0.95	0.90	1.88	10.00	5.00
WASH WEST	7	8	38.9365	-77.0360	0.70	9.3	0.70	0.9	0.18	0.12	0.25	0.91	0.95	0.90	6.41	10.00	5.00
WASH WEST	7	9	38.9367	-77.0244	0.72	10.4	0.76	1.0	0.17	0.12	0.25	0.90	0.95	0.90	10.00	10.00	5.00
WASH WEST	7	10	38.9369	-77.0128	0.73	10.8	0.61	1.1	0.15	0.12	0.25	0.90	0.95	0.90	3.13	10.00	5.00
WAW/WAE	B7		38.9371	-77.0013	0.50	12.0	0.20	1.2	0.11	0.12	0.25	0.88	0.95	0.90	10.00	10.00	5.00
WASH EAST	7	1	38.9373	-76.9897	0.46	7.3	0.46	0.7	0.15	0.12	0.25	0.90	0.95	0.90	5.63	10.00	5.00
WASH EAST	7	2	38.9375	-76.9781	0.50	7.0	0.50	0.7	0.18	0.12	0.25	0.91	0.95	0.90	3.44	0.00	0.00
WASH EAST	7	3	38.9377	-76.9666	0.50	7.0	0.50	0.7	0.18	0.12	0.25	0.91	0.95	0.90	3.91	0.00	0.00
WASH EAST	7	4	38.9379	-76.9550	0.53	7.0	0.53	0.7	0.16	0.12	0.25	0.90	0.95	0.90	6.25	10.00	5.00
WASH EAST	7	5	38.9382	-76.9434	0.54	7.0	0.50	0.7	0.16	0.16	0.25	0.90	0.94	0.90	3.44	10.00	5.00
WASH EAST	7	6	38.9384	-76.9319	0.47	7.7	0.44	0.8	0.15	0.12	0.25	0.89	0.95	0.90	6.88	10.00	5.00
WASH EAST	7	7	38.9386	-76.9203	0.42	9.5	0.40	1.0	0.17	0.17	0.25	0.90	0.93	0.90	12.50	10.00	5.00
WASH EAST	7	8	38.9388	-76.9087	0.27	8.1	0.28	0.8	0.18	0.12	0.25	0.89	0.95	0.90	15.94	10.00	5.00
WASH EAST	7	9	38.9390	-76.8972	0.42	7.5	0.32	0.7	0.18	0.12	0.25	0.90	0.95	0.90	5.00	10.00	5.00
WASH EAST	7	10	38.9392	-76.8856	0.36	7.0	0.30	0.7	0.19	0.12	0.25	0.90	0.95	0.90	16.41	10.00	5.00
WAE/LANHAM	B7		38.9394	-76.8740	0.48	7.0	0.30	0.7	0.19	0.12	0.25	0.89	0.95	0.90	5.16	10.00	5.00
LANHAM	7	1	38.9396	-76.8624	0.45	7.0	0.44	0.7	0.19	0.12	0.25	0.89	0.95	0.90	7.50	10.00	5.00
LANHAM	7	2	38.9399	-76.8509	0.33	7.0	0.30	0.7	0.18	0.19	0.25	0.91	0.93	0.90	13.28	10.00	5.00
LANHAM	7	3	38.9401	-76.8393	0.40	7.0	0.30	0.7	0.18	0.12	0.25	0.91	0.95	0.90	0.31	0.00	0.00
LANHAM	7	4	38.9403	-76.8277	0.40	7.0	0.30	0.7	0.18	0.12	0.25	0.91	0.95	0.90	0.94	0.00	0.00
FALLS CHURCH	6	2	38.9239	-77.2324	0.20	45.0	0.20	4.5	0.19	0.12	0.25	0.88	0.95	0.90	7.50	10.00	5.00
FALLS CHURCH	6	3	38.9241	-77.2208	0.13	30.0	0.20	3.0	0.19	0.12	0.25	0.88	0.95	0.90	14.38	10.00	5.00
FALLS CHURCH	6	4	38.9243	-77.2092	0.24	21.4	0.28	2.1	0.18	0.12	0.25	0.88	0.95	0.90	15.63	10.00	5.00
FALLS CHURCH	6	5	38.9245	-77.1977	0.31	7.0	0.30	0.7	0.17	0.12	0.25	0.90	0.95	0.90	13.44	10.00	5.00
FALLS CHURCH	6	6	38.9247	-77.1861	0.40	7.0	0.30	0.7	0.18	0.12	0.25	0.91	0.95	0.90	2.50	0.00	0.00
FALLS CHURCH	6	7	38.9249	-77.1745	0.40	7.0	0.30	0.7	0.18	0.12	0.25	0.91	0.95	0.90	2.19	0.00	0.00
FALLS CHURCH	6	8	38.9251	-77.1629	0.40	7.3	0.30	0.7	0.19	0.12	0.25	0.91	0.95	0.90	3.13	10.00	5.00
FALLS CHURCH	6	9	38.9254	-77.1514	0.40	7.0	0.30	0.7	0.18	0.12	0.25	0.91	0.95	0.90	2.03	0.00	0.00
FALLS CHURCH	6	10	38.9256	-77.1398	0.40	7.0	0.30	0.7	0.18	0.12	0.25	0.91	0.95	0.90	1.72	0.00	0.00
FALLS/WAW	B6		38.9258	-77.1283	0.40	7.0	0.30	0.7	0.18	0.12	0.25	0.91	0.95	0.90	2.50	0.00	0.00
WASH WEST	6	1	38.9260	-77.1167	0.40	7.0	0.30	0.7	0.18	0.12	0.25	0.91	0.95	0.90	0.94	0.00	0.00
WASH WEST	6	2	38.9262	-77.1051	0.40	7.0	0.30	0.7	0.18	0.12	0.25	0.91	0.95	0.90	2.81	0.00	0.00
WASH WEST	6	3	38.9264	-77.0936	0.40	7.0	0.30	0.7	0.18	0.12	0.25	0.91	0.95	0.90	1.56	0.00	0.00
WASH WEST	6	4	38.9266	-77.0820	0.55	18.4	0.52	1.8	0.17	0.12	0.25	0.89	0.95	0.90	4.69	10.00	5.00
WASH WEST	6	5	38.9268	-77.0704	0.60	11.8	0.56	1.2	0.16	0.12	0.25	0.90	0.95	0.90	6.25	10.00	5.00
WASH WEST	6	6	38.9270	-77.0589	0.57	9.5	0.54	1.0	0.16	0.12	0.25	0.90	0.95	0.90	5.31	10.00	5.00
WASH WEST	6	7	38.9273	-77.0473	0.75	10.0	0.75	1.0	0.18	0.12	0.25	0.91	0.95	0.90	3.13	10.00	5.00
WASH WEST	6	8	38.9275	-77.0357	0.67	12.8	0.78	1.3	0.16	0.12	0.25	0.89	0.95	0.90	10.00	10.00	5.00
WASH WEST	6	9	38.9277	-77.0242	0.71	10.5	0.76	1.1	0.18	0.12	0.25	0.90	0.95	0.90	9.38	10.00	5.00
WASH WEST	6	10	38.9279	-77.0126	0.64	21.0	0.40	2.1	0.19	0.12	0.25	0.88	0.95	0.90	8.13	10.00	5.00
WAW/WAE	B6		38.9281	-77.0010	0.59	13.2	0.53	1.3	0.14	0.13	0.25	0.89	0.95	0.90	6.88	10.00	5.00
WASH EAST	6	1	38.9283	-76.9894	0.47	7.0	0.50	0.7	0.18	0.12	0.25	0.91	0.95	0.90	5.31	10.00	5.00
WASH EAST	6	2	38.9285	-76.9779	0.50	7.0	0.50	0.7	0.18	0.12	0.25	0.91	0.95	0.90	5.00	0.00	0.00
WASH EAST	6	3	38.9287	-76.9663	0.50	7.0	0.50	0.7	0.16	0.12	0.25	0.91	0.95	0.90	5.78	10.00	5.00
WASH EAST	6	4	38.9289	-76.9547	0.59	9.6	0.50	1.0	0.14	0.12	0.25	0.88	0.95	0.90	4.06	10.00	5.00
WASH EAST	6	5	38.9292	-76.9432	0.50	7.0	0.50	0.7	0.18	0.12	0.25	0.91	0.95	0.90	0.31	0.00	0.00
WASH EAST	6	6	38.9294	-76.9316	0.46	7.0	0.40	0.7	0.19	0.15	0.25	0.88	0.94	0.90	18.75	10.00	5.00
WASH EAST	6	7	38.9296	-76.9200	0.40	10.0	0.24	1.0	0.22	0.12	0.25	0.89	0.95	0.90	5.78	10.00	5.00
WASH EAST	6	8	38.9298	-76.9085	0.40	7.0	0.30	0.7	0.18	0.12	0.25	0.91	0.95	0.90	4.06	0.00	0.00
WASH EAST	6	9	38.9300	-76.8969	0.23	7.0	0.44	0.7	0.12	0.16	0.25	0.89	0.94	0.90	16.88	10.00	5.00
WASH EAST	6	10	38.9302	-76.8853	0.58	7.0	0.57	0.7	0.21	0.12	0.25	0.88	0.95	0.90	8.28	10.00	5.00
WAE/LANHAM	B6		38.9304	-76.8738	0.34	7.7	0.43	0.8	0.13	0.12	0.25	0.89	0.95	0.90	8.13	10.00	5.00
LANHAM	6	1	38.9306	-76.8622	0.39	7.4	0.34	0.7	0.19	0.12	0.25	0.91	0.95	0.90	9.22	10.00	5.00
LANHAM	6	2	38.9309	-76.8506	0.36	7.0	0.30	0.7	0.18	0.16	0.25	0.91	0.94	0.90	13.59	10.00	5.00
LANHAM	6	3	38.9311	-76.8391	0.40	7.0	0.30	0.7	0.18	0.12	0.25	0.91	0.95	0.90	0.31	0.00	0.00
LANHAM	6	4	38.9313	-76.8275	0.40	7.0	0.30	0.7	0.18	0.12	0.25	0.91	0.95	0.90	0.63	0.00	0.00
FALLS CHURCH	5	2	38.9149	-77.2322	0.35	18.5	0.37	1.9	0.19	0.12	0.25	0.89	0.95	0.90	17.34	10.00	5.00
FALLS CHURCH	5	3	38.9151	-77.2206	0.38	9.1	0.20	0.9	0.17	0.12	0.25	0.88	0.95	0.90	21.88	10.00	5.00
FALLS CHURCH	5	4	38.9153	-77.2091	0.46	10.2	0.33	1.0	0.18	0.12	0.25	0.90	0.95	0.90	5.94	10.00	5.00
FALLS CHURCH	5	5	38.9155	-77.1975	0.40	7.0	0.30	0.7	0.18	0.12	0.25	0.91	0.95	0.90	3.13	0.00	0.00
FALLS CHURCH	5	6	38.9157	-77.1860	0.38	7.0	0.30	0.7	0.18	0.12	0.25	0.91	0.95	0.90	13.13	10.00	5.00
FALLS CHURCH	5	7	38.9159	-77.1744	0.40	7.0	0.30	0.7	0.18	0.12	0.25	0.91	0.95	0.90	3.13	0.00	0.00
FALLS CHURCH	5	8	38.9161	-77.1628	0.40	7.0	0.30	0.7	0.18	0.12	0.25	0.91	0.95	0.90	2.50	0.00	0.00
FALLS CHURCH	5	9	38.9164	-77.1513	0.46	7.0	0.24	0.7	0.20	0.12	0.25	0.89	0.95	0.90	2.19	10.00	5.00
FALLS CHURCH	5	10	38.9166	-77.1397	0.41	7.4	0.31	0.7	0.19	0.12	0.25	0.91	0.95	0.90	2.97	10.00	5.00
FALLS/WAW	B5		38.9168	-77.1281	0.40	7.0	0.30	0.7	0.18	0.12	0.25	0.91	0.95	0.90	3.75	0.00	0.00
WASH WEST	5	1	38.9170	-77.1165	0.40	7.0	0.30	0.7	0.18	0.12	0.25	0.91	0.95	0.90	2.50	0.00	0.00

WASH WEST	5	2	38.9172	-77.1050	0.40	7.0	0.30	0.7	0.18	0.12	0.25	0.91	0.95	0.90	0.31	0.00	0.00
WASH WEST	5	3	38.9174	-77.0934	0.40	7.0	0.30	0.7	0.18	0.12	0.25	0.91	0.95	0.90	1.88	0.00	0.00
WASH WEST	5	4	38.9176	-77.0818	0.75	10.0	0.75	1.0	0.18	0.12	0.25	0.91	0.95	0.90	1.88	10.00	5.00
WASH WEST	5	5	38.9178	-77.0703	0.66	11.9	0.73	1.2	0.18	0.12	0.25	0.90	0.95	0.90	5.00	10.00	5.00
WASH WEST	5	6	38.9180	-77.0587	0.53	7.8	0.50	0.8	0.17	0.12	0.25	0.90	0.95	0.90	1.56	10.00	5.00
WASH WEST	5	7	38.9183	-77.0471	0.66	13.1	0.75	1.3	0.14	0.12	0.25	0.89	0.95	0.90	8.13	10.00	5.00
WASH WEST	5	8	38.9185	-77.0356	0.78	12.7	0.75	1.3	0.14	0.12	0.25	0.89	0.95	0.90	9.38	10.00	5.00
WASH WEST	5	9	38.9187	-77.0240	0.72	12.6	0.62	1.3	0.16	0.12	0.25	0.89	0.95	0.90	10.00	10.00	5.00
WASH WEST	5	10	38.9189	-77.0125	0.72	10.2	0.70	1.0	0.18	0.12	0.25	0.91	0.95	0.90	8.13	10.00	5.00
WAW/WAE	B5		38.9191	-77.0009	0.47	11.3	0.75	1.1	0.15	0.12	0.25	0.89	0.95	0.90	7.81	10.00	5.00
WASH EAST	5	1	38.9193	-76.9893	0.37	7.9	0.52	0.8	0.11	0.12	0.25	0.88	0.95	0.90	10.00	10.00	5.00
WASH EAST	5	2	38.9195	-76.9778	0.43	7.0	0.57	0.7	0.12	0.12	0.25	0.89	0.95	0.90	7.81	10.00	5.00
WASH EAST	5	3	38.9197	-76.9662	0.73	7.0	0.65	0.7	0.14	0.12	0.25	0.89	0.95	0.90	6.56	10.00	5.00
WASH EAST	5	4	38.9199	-76.9546	0.80	7.0	0.70	0.7	0.13	0.12	0.25	0.88	0.95	0.90	1.25	10.00	5.00
WASH EAST	5	5	38.9202	-76.9431	0.01	0.1	0.01	0.0	0.25	0.12	0.25	0.88	0.95	0.90	10.63	10.00	5.00
WASH EAST	5	6	38.9204	-76.9315	0.31	7.0	0.50	0.7	0.15	0.15	0.25	0.88	0.94	0.90	20.00	10.00	5.00
WASH EAST	5	7	38.9206	-76.9199	0.32	7.0	0.39	0.7	0.17	0.12	0.25	0.90	0.95	0.90	16.41	10.00	5.00
WASH EAST	5	8	38.9208	-76.9084	0.33	7.0	0.26	0.7	0.19	0.12	0.25	0.89	0.95	0.90	17.81	10.00	5.00
WASH EAST	5	9	38.9210	-76.8968	0.46	8.7	0.27	0.9	0.22	0.12	0.25	0.89	0.95	0.90	3.44	10.00	5.00
WASH EAST	5	10	38.9212	-76.8852	0.40	7.0	0.30	0.7	0.18	0.12	0.25	0.91	0.95	0.90	4.69	0.00	0.00
WAE/LANHAM	B5		38.9214	-76.8737	0.38	7.7	0.36	0.8	0.20	0.12	0.25	0.90	0.95	0.90	10.47	10.00	5.00
LANHAM	5	1	38.9216	-76.8621	0.30	9.6	0.56	1.0	0.20	0.12	0.25	0.88	0.95	0.90	10.00	10.00	5.00
LANHAM	5	2	38.9219	-76.8505	0.21	9.6	0.21	1.0	0.24	0.24	0.25	0.88	0.91	0.90	14.38	10.00	5.00
LANHAM	5	3	38.9221	-76.8390	0.00	0.0	0.00	0.0	0.00	0.00	0.00	0.00	0.00	0.00	0.00	0.00	0.00
LANHAM	5	4	38.9223	-76.8274	0.00	0.0	0.00	0.0	0.00	0.00	0.00	0.00	0.00	0.00	0.00	0.00	0.00
FALLS CHURCH	4	2	38.9059	-77.2319	0.40	7.0	0.30	0.7	0.18	0.12	0.25	0.91	0.95	0.90	1.56	0.00	0.00
FALLS CHURCH	4	3	38.9061	-77.2203	0.23	17.5	0.23	1.8	0.20	0.12	0.25	0.89	0.95	0.90	12.19	10.00	5.00
FALLS CHURCH	4	4	38.9063	-77.2088	0.43	10.5	0.35	1.1	0.19	0.12	0.25	0.90	0.95	0.90	4.38	10.00	5.00
FALLS CHURCH	4	5	38.9065	-77.1972	0.40	7.0	0.30	0.7	0.18	0.12	0.25	0.91	0.95	0.90	2.34	0.00	0.00
FALLS CHURCH	4	6	38.9067	-77.1857	0.33	7.0	0.30	0.7	0.18	0.12	0.25	0.91	0.95	0.90	12.19	10.00	5.00
FALLS CHURCH	4	7	38.9069	-77.1741	0.50	8.0	0.27	0.8	0.20	0.12	0.25	0.90	0.95	0.90	2.50	10.00	5.00
FALLS CHURCH	4	8	38.9071	-77.1625	0.40	7.0	0.30	0.7	0.18	0.12	0.25	0.91	0.95	0.90	1.56	0.00	0.00
FALLS CHURCH	4	9	38.9074	-77.1510	0.43	7.4	0.31	0.7	0.19	0.12	0.25	0.91	0.95	0.90	2.81	10.00	5.00
FALLS CHURCH	4	10	38.9076	-77.1394	0.40	7.0	0.30	0.7	0.18	0.12	0.25	0.91	0.95	0.90	2.81	0.00	0.00
FALLS/WAW	B4		38.9078	-77.1278	0.38	7.0	0.28	0.7	0.19	0.12	0.25	0.90	0.95	0.90	3.44	10.00	5.00
WASH WEST	4	1	38.9080	-77.1163	0.40	7.0	0.30	0.7	0.18	0.12	0.25	0.91	0.95	0.90	2.03	0.00	0.00
WASH WEST	4	2	38.9082	-77.1047	0.40	7.0	0.30	0.7	0.18	0.12	0.25	0.91	0.95	0.90	2.19	0.00	0.00
WASH WEST	4	3	38.9084	-77.0931	0.40	7.0	0.30	0.7	0.18	0.12	0.25	0.91	0.95	0.90	0.63	0.00	0.00
WASH WEST	4	4	38.9086	-77.0816	0.48	11.1	0.49	1.1	0.15	0.16	0.25	0.90	0.94	0.90	3.44	10.00	5.00
WASH WEST	4	5	38.9088	-77.0700	0.70	12.6	0.70	1.3	0.16	0.12	0.25	0.90	0.95	0.90	7.81	10.00	5.00
WASH WEST	4	6	38.9091	-77.0584	0.75	10.9	0.77	1.1	0.18	0.12	0.25	0.91	0.95	0.90	7.50	10.00	5.00
WASH WEST	4	7	38.9093	-77.0469	0.66	14.6	0.86	1.5	0.19	0.12	0.25	0.89	0.95	0.90	8.44	10.00	5.00
WASH WEST	4	8	38.9095	-77.0353	0.67	14.3	0.83	1.4	0.17	0.12	0.25	0.89	0.95	0.90	10.00	10.00	5.00
WASH WEST	4	9	38.9097	-77.0238	0.69	13.4	0.80	1.3	0.19	0.12	0.25	0.90	0.95	0.90	10.00	10.00	5.00
WASH WEST	4	10	38.9099	-77.0122	0.68	10.6	0.64	1.1	0.15	0.12	0.25	0.90	0.95	0.90	10.00	10.00	5.00
WAW/WAE	B4		38.9101	-77.0006	0.38	10.7	0.37	1.1	0.19	0.12	0.25	0.89	0.95	0.90	10.00	10.00	5.00
WASH EAST	4	1	38.9103	-76.9891	0.53	11.1	0.56	1.1	0.14	0.12	0.25	0.89	0.95	0.90	10.00	10.00	5.00
WASH EAST	4	2	38.9105	-76.9775	0.63	8.5	0.63	0.9	0.18	0.12	0.25	0.91	0.95	0.90	1.88	10.00	5.00
WASH EAST	4	3	38.9107	-76.9659	0.50	7.0	0.50	0.7	0.18	0.12	0.25	0.91	0.95	0.90	0.31	0.00	0.00
WASH EAST	4	4	38.9109	-76.9544	0.70	10.0	0.70	1.0	0.21	0.12	0.25	0.88	0.95	0.90	0.31	10.00	5.00
WASH EAST	4	5	38.9112	-76.9428	0.52	7.7	0.52	0.8	0.20	0.12	0.25	0.90	0.95	0.90	1.72	10.00	5.00
WASH EAST	4	6	38.9114	-76.9312	0.54	7.4	0.51	0.7	0.20	0.13	0.25	0.90	0.95	0.90	11.09	10.00	5.00
WASH EAST	4	7	38.9116	-76.9197	0.54	8.4	0.39	0.8	0.14	0.12	0.25	0.90	0.95	0.90	5.00	10.00	5.00
WASH EAST	4	8	38.9118	-76.9081	0.48	7.0	0.34	0.7	0.18	0.12	0.25	0.90	0.95	0.90	2.19	10.00	5.00
WASH EAST	4	9	38.9120	-76.8966	0.63	7.0	0.38	0.7	0.17	0.12	0.25	0.89	0.95	0.90	7.19	10.00	5.00
WASH EAST	4	10	38.9122	-76.8850	0.38	9.5	0.40	1.0	0.22	0.12	0.25	0.90	0.95	0.90	7.34	10.00	5.00
WAE/LANHAM	B4		38.9124	-76.8734	0.40	7.0	0.30	0.7	0.20	0.12	0.25	0.90	0.95	0.90	3.44	10.00	5.00
LANHAM	4	1	38.9126	-76.8619	0.40	7.0	0.26	0.7	0.21	0.12	0.25	0.90	0.95	0.90	1.09	10.00	5.00
LANHAM	4	2	38.9129	-76.8503	0.33	7.0	0.50	0.7	0.09	0.20	0.25	0.88	0.92	0.90	12.81	10.00	5.00
LANHAM	4	3	38.9131	-76.8387	0.01	0.1	0.01	0.0	0.25	0.12	0.25	0.88	0.95	0.90	5.63	10.00	5.00
LANHAM	4	4	38.9133	-76.8272	0.00	0.0	0.00	0.0	0.00	0.00	0.00	0.00	0.00	0.00	0.00	0.00	0.00
FALLS CHURCH	3	2	38.8969	-77.2316	0.41	7.0	0.31	0.7	0.19	0.12	0.25	0.91	0.95	0.90	3.44	10.00	5.00
FALLS CHURCH	3	3	38.8971	-77.2201	0.30	7.0	0.30	0.7	0.17	0.12	0.25	0.90	0.95	0.90	11.56	10.00	5.00
FALLS CHURCH	3	4	38.8973	-77.2085	0.38	7.0	0.30	0.7	0.18	0.15	0.25	0.91	0.94	0.90	13.13	10.00	5.00
FALLS CHURCH	3	5	38.8975	-77.1969	0.23	7.0	0.30	0.7	0.17	0.12	0.25	0.90	0.95	0.90	13.59	10.00	5.00
FALLS CHURCH	3	6	38.8977	-77.1854	0.26	7.0	0.30	0.7	0.17	0.12	0.25	0.90	0.95	0.90	17.97	10.00	5.00
FALLS CHURCH	3	7	38.8979	-77.1738	0.37	7.0	0.30	0.7	0.18	0.12	0.25	0.91	0.95	0.90	14.38	10.00	5.00
FALLS CHURCH	3	8	38.8981	-77.1622	0.41	7.2	0.30	0.7	0.18	0.12	0.25	0.91	0.95	0.90	4.69	10.00	5.00
FALLS CHURCH	3	9	38.8984	-77.1507	0.41	7.0	0.30	0.7	0.18	0.12	0.25	0.91	0.95	0.90	5.31	10.00	5.00
FALLS CHURCH	3	10	38.8986	-77.1391	0.41	7.3	0.31	0.7	0.17	0.12	0.25	0.90	0.95	0.90	5.63	10.00	5.00
FALLS/WAW	B3		38.8988	-77.1276	0.41	7.0	0.31	0.7	0.17	0.13	0.25	0.91	0.95	0.90	5.63	10.00	5.00
WASH WEST	3	1	38.8990	-77.1160	0.43	8.5	0.36	0.8	0.15	0.15	0.25	0.90	0.94	0.90	4.84	10.00	5.00
WASH WEST	3	2	38.8992	-77.1044	0.38	7.7	0.30	0.8	0.16	0.13	0.25	0.90	0.95	0.90	10.00	10.00	5.00
WASH WEST	3	3	38.8994	-77.0929	0.37	13.0	0.34	1.3	0.16	0.15	0.25	0.90	0.94	0.90	14.38	10.00	5.00

WASH WEST	3	4	38.8996	-77.0813	0.43	10.0	0.40	1.0	0.09	0.13	0.25	0.88	0.95	0.90	14.38	10.00	5.00
WASH WEST	3	5	38.8998	-77.0697	0.30	25.4	0.90	2.5	0.16	0.19	0.25	0.89	0.93	0.90	12.81	10.00	5.00
WASH WEST	3	6	38.9000	-77.0582	0.38	17.4	0.63	1.7	0.14	0.12	0.25	0.88	0.95	0.90	15.94	10.00	5.00
WASH WEST	3	7	38.9003	-77.0466	0.71	19.6	0.97	2.0	0.21	0.12	0.25	0.88	0.95	0.90	10.00	10.00	5.00
WASH WEST	3	8	38.9005	-77.0351	0.79	22.3	0.90	2.2	0.17	0.12	0.25	0.88	0.95	0.90	10.00	10.00	5.00
WASH WEST	3	9	38.9007	-77.0235	0.72	16.7	0.72	1.7	0.15	0.12	0.25	0.89	0.95	0.90	10.00	10.00	5.00
WASH WEST	3	10	38.9009	-77.0119	0.73	15.5	0.63	1.6	0.20	0.12	0.25	0.90	0.95	0.90	10.00	10.00	5.00
WAW/WAE	B3		38.9011	-77.0004	0.64	12.0	0.60	1.2	0.20	0.12	0.25	0.90	0.95	0.90	10.00	10.00	5.00
WASH EAST	3	1	38.9013	-76.9888	0.73	10.1	0.72	1.0	0.18	0.12	0.25	0.91	0.95	0.90	10.00	10.00	5.00
WASH EAST	3	2	38.9015	-76.9772	0.69	9.6	0.63	1.0	0.18	0.13	0.25	0.90	0.95	0.90	10.00	10.00	5.00
WASH EAST	3	3	38.9017	-76.9657	0.30	12.0	0.50	1.2	0.09	0.12	0.25	0.88	0.95	0.90	1.88	10.00	5.00
WASH EAST	3	4	38.9020	-76.9541	0.70	11.3	0.23	1.1	0.17	0.12	0.25	0.88	0.95	0.90	3.75	10.00	5.00
WASH EAST	3	5	38.9022	-76.9425	0.46	7.5	0.47	0.8	0.17	0.12	0.25	0.90	0.95	0.90	5.31	10.00	5.00
WASH EAST	3	6	38.9024	-76.9310	0.50	7.0	0.50	0.7	0.17	0.12	0.25	0.91	0.95	0.90	5.31	10.00	5.00
WASH EAST	3	7	38.9026	-76.9194	0.41	7.2	0.29	0.7	0.19	0.12	0.25	0.91	0.95	0.90	4.69	10.00	5.00
WASH EAST	3	8	38.9028	-76.9079	0.41	7.2	0.29	0.7	0.19	0.12	0.25	0.91	0.95	0.90	4.38	10.00	5.00
WASH EAST	3	9	38.9030	-76.8963	0.36	7.4	0.28	0.7	0.18	0.12	0.25	0.90	0.95	0.90	9.06	10.00	5.00
WASH EAST	3	10	38.9032	-76.8847	0.70	12.0	0.30	1.2	0.21	0.12	0.25	0.88	0.95	0.90	0.63	10.00	5.00
WAE/LANHAM	B3		38.9034	-76.8732	0.40	8.7	0.36	0.9	0.22	0.12	0.25	0.89	0.95	0.90	2.19	10.00	5.00
LANHAM	3	1	38.9036	-76.8616	0.00	0.0	0.00	0.0	0.00	0.00	0.00	0.00	0.00	0.00	0.00	0.00	0.00
LANHAM	3	2	38.9039	-76.8500	0.21	16.7	0.25	1.7	0.24	0.16	0.25	0.88	0.94	0.90	14.69	10.00	5.00
LANHAM	3	3	38.9041	-76.8385	0.00	0.0	0.00	0.0	0.00	0.00	0.00	0.00	0.00	0.00	0.00	0.00	0.00
LANHAM	3	4	38.9043	-76.8269	0.00	0.0	0.00	0.0	0.00	0.00	0.00	0.00	0.00	0.00	0.00	0.00	0.00
FALLS CHURCH	2	2	38.8879	-77.2313	0.40	7.4	0.30	0.7	0.18	0.15	0.25	0.91	0.94	0.90	9.06	10.00	5.00
FALLS CHURCH	2	3	38.8881	-77.2198	0.19	7.0	0.30	0.7	0.17	0.21	0.25	0.89	0.92	0.90	20.00	10.00	5.00
FALLS CHURCH	2	4	38.8883	-77.2082	0.34	7.0	0.30	0.7	0.18	0.16	0.25	0.91	0.94	0.90	12.50	10.00	5.00
FALLS CHURCH	2	5	38.8885	-77.1966	0.40	7.0	0.30	0.7	0.18	0.12	0.25	0.91	0.95	0.90	4.06	0.00	0.00
FALLS CHURCH	2	6	38.8887	-77.1851	0.40	7.0	0.30	0.7	0.18	0.12	0.25	0.91	0.95	0.90	2.81	0.00	0.00
FALLS CHURCH	2	7	38.8889	-77.1735	0.40	7.0	0.30	0.7	0.18	0.12	0.25	0.91	0.95	0.90	2.50	0.00	0.00
FALLS CHURCH	2	8	38.8891	-77.1620	0.34	7.0	0.33	0.7	0.16	0.12	0.25	0.90	0.95	0.90	15.94	10.00	5.00
FALLS CHURCH	2	9	38.8894	-77.1504	0.39	7.0	0.30	0.7	0.18	0.12	0.25	0.91	0.95	0.90	10.16	10.00	5.00
FALLS CHURCH	2	10	38.8896	-77.1388	0.40	7.0	0.29	0.7	0.18	0.12	0.25	0.91	0.95	0.90	5.00	10.00	5.00
FALLS/WAW	B2		38.8898	-77.1273	0.43	7.8	0.33	0.8	0.17	0.12	0.25	0.91	0.95	0.90	5.16	10.00	5.00
WASH WEST	2	1	38.8900	-77.1157	0.37	7.0	0.30	0.7	0.18	0.15	0.25	0.91	0.94	0.90	15.16	10.00	5.00
WASH WEST	2	2	38.8902	-77.1041	0.40	8.0	0.30	0.8	0.19	0.15	0.25	0.90	0.94	0.90	15.63	10.00	5.00
WASH WEST	2	3	38.8904	-77.0926	0.38	7.0	0.33	0.7	0.16	0.12	0.25	0.90	0.95	0.90	6.25	10.00	5.00
WASH WEST	2	4	38.8906	-77.0810	0.42	12.5	0.45	1.3	0.19	0.12	0.25	0.90	0.95	0.90	10.63	10.00	5.00
WASH WEST	2	5	38.8908	-77.0695	0.33	20.2	0.62	2.0	0.16	0.16	0.25	0.88	0.94	0.90	14.69	10.00	5.00
WASH WEST	2	6	38.8910	-77.0579	0.14	12.0	0.30	1.2	0.17	0.12	0.25	0.88	0.95	0.90	11.56	10.00	5.00
WASH WEST	2	7	38.8913	-77.0463	0.70	24.0	0.70	2.4	0.19	0.12	0.25	0.88	0.95	0.90	3.44	10.00	5.00
WASH WEST	2	8	38.8915	-77.0348	0.60	24.0	0.70	2.4	0.19	0.16	0.25	0.88	0.94	0.90	2.81	10.00	5.00
WASH WEST	2	9	38.8917	-77.0232	0.78	21.8	0.80	2.2	0.19	0.16	0.25	0.88	0.94	0.90	7.50	10.00	5.00
WASH WEST	2	10	38.8919	-77.0117	0.73	18.0	0.60	1.8	0.20	0.16	0.25	0.88	0.94	0.90	4.69	10.00	5.00
WAW/WAE	B2		38.8921	-77.0001	0.76	12.1	0.70	1.2	0.19	0.12	0.25	0.90	0.95	0.90	9.06	10.00	5.00
WASH EAST	2	1	38.8923	-76.9885	0.75	10.0	0.75	1.0	0.18	0.12	0.25	0.91	0.95	0.90	9.38	10.00	5.00
WASH EAST	2	2	38.8925	-76.9770	0.57	15.0	0.57	1.5	0.20	0.12	0.25	0.90	0.95	0.90	9.38	10.00	5.00
WASH EAST	2	3	38.8927	-76.9654	0.14	21.4	0.26	2.1	0.24	0.15	0.25	0.89	0.94	0.90	2.81	10.00	5.00
WASH EAST	2	4	38.8930	-76.9538	0.52	10.0	0.75	1.0	0.13	0.12	0.25	0.89	0.95	0.90	8.75	10.00	5.00
WASH EAST	2	5	38.8932	-76.9423	0.55	7.5	0.63	0.8	0.17	0.12	0.25	0.90	0.95	0.90	5.63	10.00	5.00
WASH EAST	2	6	38.8934	-76.9307	0.53	7.8	0.55	0.8	0.20	0.13	0.25	0.90	0.95	0.90	5.94	10.00	5.00
WASH EAST	2	7	38.8936	-76.9192	0.53	8.6	0.51	0.9	0.18	0.15	0.25	0.90	0.94	0.90	7.19	10.00	5.00
WASH EAST	2	8	38.8938	-76.9076	0.48	7.4	0.48	0.7	0.19	0.12	0.25	0.91	0.95	0.90	5.63	10.00	5.00
WASH EAST	2	9	38.8940	-76.8960	0.40	7.0	0.30	0.7	0.18	0.12	0.25	0.91	0.95	0.90	3.44	0.00	0.00
WASH EAST	2	10	38.8942	-76.8845	0.40	7.0	0.30	0.7	0.18	0.12	0.25	0.91	0.95	0.90	3.44	0.00	0.00
WAE/LANHAM	B2		38.8944	-76.8729	0.40	7.0	0.30	0.7	0.18	0.12	0.25	0.91	0.95	0.90	1.09	0.00	0.00
LANHAM	2	1	38.8946	-76.8614	0.40	7.0	0.30	0.7	0.18	0.12	0.25	0.91	0.95	0.90	0.63	0.00	0.00
LANHAM	2	2	38.8949	-76.8498	0.10	7.0	0.30	0.7	0.19	0.22	0.25	0.88	0.91	0.90	14.06	10.00	5.00
LANHAM	2	3	38.8951	-76.8382	0.01	0.1	0.01	0.0	0.25	0.12	0.25	0.88	0.95	0.90	5.63	10.00	5.00
LANHAM	2	4	38.8953	-76.8267	0.40	10.0	0.70	1.0	0.13	0.12	0.25	0.88	0.95	0.90	8.13	10.00	5.00
FALLS CHURCH	1	2	38.8789	-77.2310	0.50	7.0	0.61	0.7	0.14	0.20	0.25	0.89	0.92	0.90	16.41	10.00	5.00
FALLS CHURCH	1	3	38.8791	-77.2195	0.40	7.0	0.49	0.7	0.14	0.12	0.25	0.89	0.95	0.90	14.84	10.00	5.00
FALLS CHURCH	1	4	38.8793	-77.2079	0.40	7.0	0.30	0.7	0.18	0.12	0.25	0.91	0.95	0.90	1.56	0.00	0.00
FALLS CHURCH	1	5	38.8795	-77.1964	0.40	7.0	0.30	0.7	0.18	0.12	0.25	0.91	0.95	0.90	1.72	0.00	0.00
FALLS CHURCH	1	6	38.8797	-77.1848	0.40	7.0	0.30	0.7	0.18	0.12	0.25	0.91	0.95	0.90	3.13	0.00	0.00
FALLS CHURCH	1	7	38.8799	-77.1732	0.40	7.0	0.30	0.7	0.18	0.12	0.25	0.91	0.95	0.90	2.19	0.00	0.00
FALLS CHURCH	1	8	38.8801	-77.1617	0.40	7.0	0.30	0.7	0.18	0.12	0.25	0.91	0.95	0.90	4.38	0.00	0.00
FALLS CHURCH	1	9	38.8804	-77.1501	0.39	9.9	0.40	1.0	0.17	0.12	0.25	0.91	0.95	0.90	15.00	10.00	5.00
FALLS CHURCH	1	10	38.8806	-77.1386	0.42	8.7	0.32	0.9	0.16	0.13	0.25	0.90	0.95	0.90	16.09	10.00	5.00
FALLS/WAW	B1		38.8808	-77.1270	0.34	7.0	0.30	0.7	0.18	0.13	0.25	0.91	0.95	0.90	15.00	10.00	5.00
WASH WEST	1	1	38.8810	-77.1154	0.39	9.5	0.35	1.0	0.17	0.12	0.25	0.90	0.95	0.90	11.56	10.00	5.00
WASH WEST	1	2	38.8812	-77.1039	0.40	11.5	0.36	1.2	0.15	0.12	0.25	0.89	0.95	0.90	7.81	10.00	5.00
WASH WEST	1	3	38.8814	-77.0923	0.40	7.4	0.31	0.7	0.17	0.15	0.25	0.91	0.94	0.90	5.63	10.00	5.00
WASH WEST	1	4	38.8816	-77.0808	0.53	10.0	0.50	1.0	0.09	0.12	0.25	0.88	0.95	0.90	10.00	10.00	5.00
WASH WEST	1	5	38.8818	-77.0692	0.01	0.1	0.01	0.0	0.25	0.12	0.25	0.88	0.95	0.90	0.63	10.00	5.00

WASH WEST	1	6	38.8821	-77.0576	0.01	0.1	0.01	0.0	0.25	0.12	0.25	0.88	0.95	0.90	10.63	10.00	5.00
WASH WEST	1	7	38.8823	-77.0461	0.00	0.0	0.00	0.0	0.00	0.00	0.00	0.00	0.00	0.00	0.00	0.00	0.00
WASH WEST	1	8	38.8825	-77.0345	0.40	24.0	1.00	2.4	0.17	0.15	0.25	0.88	0.94	0.90	12.50	10.00	5.00
WASH WEST	1	9	38.8827	-77.0230	0.68	19.3	0.70	1.9	0.20	0.12	0.25	0.88	0.95	0.90	18.13	10.00	5.00
WASH WEST	1	10	38.8829	-77.0114	0.62	16.4	0.66	1.6	0.19	0.12	0.25	0.89	0.95	0.90	20.00	10.00	5.00
WAW/WAE	B1		38.8831	-76.9998	0.75	10.6	0.73	1.1	0.18	0.12	0.25	0.91	0.95	0.90	10.00	10.00	5.00
WASH EAST	1	1	38.8833	-76.9883	0.75	10.0	0.75	1.0	0.18	0.12	0.25	0.91	0.95	0.90	10.00	10.00	5.00
WASH EAST	1	2	38.8835	-76.9767	0.56	14.4	0.61	1.4	0.20	0.12	0.25	0.89	0.95	0.90	6.88	10.00	5.00
WASH EAST	1	3	38.8837	-76.9652	0.50	10.0	0.75	1.0	0.17	0.12	0.25	0.90	0.95	0.90	1.88	10.00	5.00
WASH EAST	1	4	38.8840	-76.9536	0.68	10.0	0.58	1.0	0.16	0.12	0.25	0.90	0.95	0.90	6.25	10.00	5.00
WASH EAST	1	5	38.8842	-76.9420	0.48	8.2	0.42	0.8	0.17	0.12	0.25	0.90	0.95	0.90	4.38	10.00	5.00
WASH EAST	1	6	38.8844	-76.9305	0.72	9.7	0.72	1.0	0.18	0.12	0.25	0.91	0.95	0.90	8.28	10.00	5.00
WASH EAST	1	7	38.8846	-76.9189	0.51	9.1	0.52	0.9	0.19	0.13	0.25	0.90	0.95	0.90	5.94	10.00	5.00
WASH EAST	1	8	38.8848	-76.9073	0.47	7.0	0.45	0.7	0.18	0.17	0.25	0.91	0.93	0.90	3.44	0.00	0.00
WASH EAST	1	9	38.8850	-76.8958	0.43	7.4	0.33	0.7	0.19	0.19	0.25	0.91	0.93	0.90	2.50	10.00	5.00
WASH EAST	1	10	38.8852	-76.8842	0.40	7.0	0.30	0.7	0.18	0.21	0.25	0.91	0.92	0.90	1.25	0.00	0.00
WAE/LANHAM	B1		38.8854	-76.8727	0.33	7.0	0.26	0.7	0.13	0.20	0.25	0.90	0.92	0.90	2.34	10.00	5.00
LANHAM	1	1	38.8857	-76.8611	0.60	7.0	0.75	0.7	0.19	0.15	0.25	0.88	0.94	0.90	5.00	10.00	5.00
LANHAM	1	2	38.8859	-76.8496	0.43	10.0	0.20	1.0	0.19	0.15	0.25	0.88	0.94	0.90	14.69	10.00	5.00
LANHAM	1	3	38.8861	-76.8380	0.42	9.3	0.53	0.9	0.13	0.16	0.25	0.89	0.94	0.90	7.19	10.00	5.00
LANHAM	1	4	38.8863	-76.8264	0.50	10.6	0.64	1.1	0.15	0.12	0.25	0.88	0.95	0.90	2.19	10.00	5.00
FALLS/ANNAN		B2	38.8699	-77.2309	0.53	8.6	0.38	0.9	0.16	0.12	0.25	0.88	0.95	0.90	7.81	10.00	5.00
FALLS/ANNAN		B3	38.8701	-77.2193	0.24	21.7	0.39	2.2	0.19	0.20	0.25	0.88	0.92	0.90	16.41	10.00	5.00
FALLS/ANNAN		B4	38.8703	-77.2078	0.44	7.6	0.30	0.8	0.19	0.15	0.25	0.90	0.94	0.90	3.75	10.00	5.00
FALLS/ANNAN		B5	38.8705	-77.1962	0.37	7.0	0.30	0.7	0.18	0.16	0.25	0.91	0.94	0.90	4.06	10.00	5.00
FALLS/ANNAN		B6	38.8707	-77.1847	0.37	7.0	0.30	0.7	0.18	0.16	0.25	0.91	0.94	0.90	4.06	10.00	5.00
FALLS/ANNAN		B7	38.8709	-77.1731	0.35	7.0	0.30	0.7	0.18	0.16	0.25	0.91	0.94	0.90	2.81	10.00	5.00
FALLS/ANNAN		B8	38.8711	-77.1615	0.37	7.0	0.30	0.7	0.18	0.16	0.25	0.91	0.94	0.90	4.06	10.00	5.00
FALLS/ANNAN		B9	38.8714	-77.1500	0.37	9.1	0.33	0.9	0.12	0.15	0.25	0.88	0.94	0.90	7.50	10.00	5.00
FALLS/ANNAN		B10	38.8716	-77.1384	0.36	7.0	0.26	0.7	0.15	0.15	0.25	0.90	0.94	0.90	4.06	10.00	5.00
FA/AN/WW/ALEX	B1		38.8718	-77.1269	0.40	7.0	0.30	0.7	0.18	0.12	0.25	0.91	0.95	0.90	2.66	0.00	0.00
WAW/ALEX		B1	38.8720	-77.1153	0.47	8.9	0.35	0.9	0.15	0.12	0.25	0.90	0.95	0.90	5.31	10.00	5.00
WAW/ALEX		B2	38.8722	-77.1037	0.41	8.4	0.36	0.8	0.15	0.15	0.25	0.90	0.94	0.90	10.94	10.00	5.00
WAW/ALEX		B3	38.8724	-77.0922	0.40	8.0	0.32	0.8	0.19	0.12	0.25	0.90	0.95	0.90	5.63	10.00	5.00
WAW/ALEX		B4	38.8726	-77.0806	0.35	8.5	0.35	0.9	0.17	0.12	0.25	0.90	0.95	0.90	4.69	10.00	5.00
WAW/ALEX		B5	38.8728	-77.0691	0.70	15.0	0.60	1.5	0.17	0.12	0.25	0.88	0.95	0.90	1.88	10.00	5.00
WAW/ALEX		B6	38.8731	-77.0575	0.35	15.0	2.00	1.5	0.11	0.12	0.25	0.88	0.95	0.90	16.25	10.00	5.00
WAW/ALEX		B7	38.8733	-77.0460	0.01	0.1	0.01	0.0	0.25	0.13	0.25	0.88	0.95	0.90	12.81	10.00	5.00
WAW/ALEX		B8	38.8735	-77.0344	0.20	4.0	0.20	0.4	0.25	0.12	0.25	0.88	0.95	0.90	0.94	10.00	5.00
WAW/ALEX		B9	38.8737	-77.0228	0.50	24.0	0.75	2.4	0.15	0.12	0.25	0.88	0.95	0.90	3.75	10.00	5.00
WAW/ALEX		B10	38.8739	-77.0113	0.58	13.2	0.47	1.3	0.15	0.12	0.25	0.88	0.95	0.90	9.69	10.00	5.00
WW/WE/ALEX/AN	B1		38.8741	-76.9997	0.65	16.4	0.72	1.6	0.16	0.12	0.25	0.89	0.95	0.90	6.88	10.00	5.00
WAE/ANACOSTIA		B1	38.8743	-76.9882	0.59	18.1	0.62	1.8	0.15	0.12	0.25	0.89	0.95	0.90	15.31	10.00	5.00
WAE/ANACOSTIA		B2	38.8745	-76.9766	0.35	7.0	0.44	0.7	0.17	0.15	0.25	0.90	0.94	0.90	7.66	10.00	5.00
WAE/ANACOSTIA		B3	38.8747	-76.9650	0.43	7.0	0.39	0.7	0.18	0.12	0.25	0.91	0.95	0.90	8.91	10.00	5.00
WAE/ANACOSTIA		B4	38.8750	-76.9535	0.40	7.0	0.30	0.7	0.18	0.12	0.25	0.91	0.95	0.90	1.72	0.00	0.00
WAE/ANACOSTIA		B5	38.8752	-76.9419	0.40	7.0	0.30	0.7	0.18	0.12	0.25	0.91	0.95	0.90	1.88	0.00	0.00
WAE/ANACOSTIA		B6	38.8754	-76.9304	0.40	7.0	0.30	0.7	0.17	0.12	0.25	0.91	0.95	0.90	4.84	10.00	5.00
WAE/ANACOSTIA		B7	38.8756	-76.9188	0.40	7.0	0.30	0.7	0.18	0.12	0.25	0.91	0.95	0.90	3.59	0.00	0.00
WAE/ANACOSTIA		B8	38.8758	-76.9072	0.40	7.0	0.30	0.7	0.18	0.12	0.25	0.91	0.95	0.90	0.47	0.00	0.00
WAE/ANACOSTIA		B9	38.8760	-76.8957	0.47	9.0	0.37	0.9	0.13	0.12	0.25	0.89	0.95	0.90	1.56	10.00	5.00
WAE/ANACOSTIA		B10	38.8762	-76.8841	0.43	7.9	0.33	0.8	0.16	0.12	0.25	0.90	0.95	0.90	2.66	10.00	5.00
WE/LANH/AN+A1144/UM	B1		38.8764	-76.8726	0.40	7.0	0.30	0.7	0.18	0.12	0.25	0.91	0.95	0.90	1.09	0.00	0.00
LANHAM/UMARL		B1	38.8766	-76.8610	0.40	7.0	0.37	0.7	0.15	0.12	0.25	0.89	0.95	0.90	1.56	10.00	5.00
LANHAM/UMARL		B2	38.8769	-76.8495	0.40	7.0	0.30	0.7	0.21	0.12	0.25	0.88	0.95	0.90	2.50	10.00	5.00
LANHAM/UMARL		B3	38.8771	-76.8379	0.34	7.0	0.30	0.7	0.18	0.19	0.25	0.91	0.93	0.90	12.50	10.00	5.00
LANHAM/UMARL		B4	38.8773	-76.8263	0.40	7.0	0.30	0.7	0.18	0.12	0.25	0.91	0.95	0.90	1.56	0.00	0.00
ANNANDLE, VA	13	2	38.8609	-77.2305	0.46	15.7	0.37	1.6	0.15	0.12	0.25	0.88	0.95	0.90	4.38	10.00	5.00
ANNANDLE, VA	13	3	38.8611	-77.2189	0.26	28.1	0.24	2.8	0.22	0.17	0.25	0.89	0.93	0.90	12.19	10.00	5.00
ANNANDLE, VA	13	4	38.8613	-77.2073	0.46	12.1	0.30	1.2	0.20	0.12	0.25	0.90	0.95	0.90	4.06	10.00	5.00
ANNANDLE, VA	13	5	38.8615	-77.1958	0.40	7.0	0.30	0.7	0.18	0.12	0.25	0.91	0.95	0.90	3.91	0.00	0.00
ANNANDLE, VA	13	6	38.8617	-77.1842	0.40	7.0	0.30	0.7	0.18	0.12	0.25	0.91	0.95	0.90	4.06	0.00	0.00
ANNANDLE, VA	13	7	38.8619	-77.1727	0.40	7.0	0.30	0.7	0.18	0.12	0.25	0.91	0.95	0.90	2.34	0.00	0.00
ANNANDLE, VA	13	8	38.8621	-77.1611	0.40	7.0	0.30	0.7	0.18	0.12	0.25	0.91	0.95	0.90	2.19	0.00	0.00
ANNANDLE, VA	13	9	38.8624	-77.1496	0.40	7.0	0.30	0.7	0.18	0.12	0.25	0.91	0.95	0.90	2.81	0.00	0.00
ANNANDLE, VA	13	10	38.8626	-77.1380	0.38	7.0	0.30	0.7	0.18	0.15	0.25	0.91	0.94	0.90	2.66	10.00	5.00
ANNAN/ALEX	B13		38.8628	-77.1264	0.39	7.7	0.32	0.8	0.20	0.15	0.25	0.90	0.94	0.90	3.44	10.00	5.00
ALEXANDRIA, VA	13	1	38.8630	-77.1149	0.40	7.0	0.30	0.7	0.18	0.12	0.25	0.91	0.95	0.90	2.81	0.00	0.00
ALEXANDRIA, VA	13	2	38.8632	-77.1033	0.40	7.0	0.30	0.7	0.18	0.12	0.25	0.91	0.95	0.90	1.56	0.00	0.00
ALEXANDRIA, VA	13	3	38.8634	-77.0918	0.40	7.0	0.30	0.7	0.18	0.12	0.25	0.91	0.95	0.90	4.06	0.00	0.00
ALEXANDRIA, VA	13	4	38.8636	-77.0802	0.40	7.0	0.30	0.7	0.18	0.12	0.25	0.91	0.95	0.90	3.13	0.00	0.00
ALEXANDRIA, VA	13	5	38.8638	-77.0687	0.33	7.0	0.43	0.7	0.23	0.12	0.25	0.89	0.95	0.90	14.69	10.00	5.00
ALEXANDRIA, VA	13	6	38.8641	-77.0571	0.12	7.0	0.30	0.7	0.16	0.12	0.25	0.89	0.95	0.90	13.44	10.00	5.00
ALEXANDRIA, VA	13	7	38.8643	-77.0455	0.24	27.0	0.80	2.7	0.21	0.12	0.25	0.88	0.95	0.90	8.13	10.00	5.00

ALEXANDRIA, VA	13	8	38.8645	-77.0340	0.00	0.0	0.00	0.0	0.00	0.00	0.00	0.00	0.00	0.00	0.00	0.00	0.00
ALEXANDRIA, VA	13	9	38.8647	-77.0224	0.70	8.0	0.50	0.8	0.15	0.12	0.25	0.88	0.95	0.90	1.25	10.00	5.00
ALEXANDRIA, VA	13	10	38.8649	-77.0109	0.50	9.0	0.40	0.9	0.15	0.12	0.25	0.88	0.95	0.90	4.06	10.00	5.00
ALEX/ANAC	B13		38.8651	-76.9993	0.35	8.4	0.47	0.8	0.19	0.13	0.25	0.89	0.95	0.90	14.69	10.00	5.00
ANACOSTIA, MD	13	1	38.8653	-76.9878	0.68	10.0	0.69	1.0	0.19	0.12	0.25	0.90	0.95	0.90	18.44	10.00	5.00
ANACOSTIA, MD	13	2	38.8655	-76.9762	0.62	8.6	0.61	0.9	0.18	0.12	0.25	0.91	0.95	0.90	4.53	10.00	5.00
ANACOSTIA, MD	13	3	38.8658	-76.9646	0.54	8.4	0.45	0.8	0.19	0.12	0.25	0.91	0.95	0.90	4.53	10.00	5.00
ANACOSTIA, MD	13	4	38.8660	-76.9531	0.42	7.5	0.34	0.8	0.17	0.12	0.25	0.90	0.95	0.90	4.38	10.00	5.00
ANACOSTIA, MD	13	5	38.8662	-76.9415	0.38	7.5	0.30	0.7	0.17	0.16	0.25	0.91	0.94	0.90	9.69	10.00	5.00
ANACOSTIA, MD	13	6	38.8664	-76.9300	0.38	8.0	0.36	0.8	0.18	0.12	0.25	0.90	0.95	0.90	8.75	10.00	5.00
ANACOSTIA, MD	13	7	38.8666	-76.9184	0.44	9.1	0.31	0.9	0.19	0.17	0.25	0.89	0.93	0.90	4.06	10.00	5.00
ANACOSTIA, MD	13	8	38.8668	-76.9069	0.44	7.6	0.32	0.8	0.19	0.12	0.25	0.90	0.95	0.90	0.94	10.00	5.00
ANACOSTIA, MD	13	9	38.8670	-76.8953	0.50	10.0	0.40	1.0	0.21	0.12	0.25	0.88	0.95	0.90	1.56	10.00	5.00
ANACOSTIA, MD	13	10	38.8672	-76.8837	0.50	8.5	0.35	0.9	0.18	0.12	0.25	0.90	0.95	0.90	1.88	10.00	5.00
ANAC/UMARL	B13		38.8674	-76.8722	0.40	7.0	0.30	0.7	0.18	0.12	0.25	0.91	0.95	0.90	0.94	0.00	0.00
UPPER MARLBORO	13	1	38.8677	-76.8606	0.43	7.0	0.30	0.7	0.16	0.12	0.25	0.90	0.95	0.90	1.56	10.00	5.00
UPPER MARLBORO	13	2	38.8679	-76.8491	0.01	0.1	0.01	0.0	0.25	0.25	0.25	0.88	0.90	0.90	10.31	10.00	5.00
UPPER MARLBORO	13	3	38.8681	-76.8375	0.40	4.0	0.50	0.4	0.25	0.21	0.25	0.88	0.92	0.90	5.94	10.00	5.00
UPPER MARLBORO	13	4	38.8683	-76.8260	0.00	0.0	0.00	0.0	0.00	0.00	0.00	0.00	0.00	0.00	0.00	0.00	0.00
ANNANDLE, VA	12	2	38.8519	-77.2303	0.44	7.7	0.32	0.8	0.15	0.12	0.25	0.90	0.95	0.90	3.44	10.00	5.00
ANNANDLE, VA	12	3	38.8521	-77.2187	0.36	7.0	0.30	0.7	0.18	0.13	0.25	0.91	0.95	0.90	13.13	10.00	5.00
ANNANDLE, VA	12	4	38.8523	-77.2072	0.40	7.0	0.30	0.7	0.18	0.12	0.25	0.91	0.95	0.90	1.72	0.00	0.00
ANNANDLE, VA	12	5	38.8525	-77.1956	0.40	7.0	0.30	0.7	0.18	0.12	0.25	0.91	0.95	0.90	1.25	0.00	0.00
ANNANDLE, VA	12	6	38.8527	-77.1841	0.40	7.0	0.30	0.7	0.18	0.12	0.25	0.91	0.95	0.90	2.50	0.00	0.00
ANNANDLE, VA	12	7	38.8529	-77.1725	0.40	7.0	0.30	0.7	0.18	0.12	0.25	0.91	0.95	0.90	1.88	0.00	0.00
ANNANDLE, VA	12	8	38.8532	-77.1610	0.40	7.0	0.30	0.7	0.18	0.12	0.25	0.91	0.95	0.90	2.81	0.00	0.00
ANNANDLE, VA	12	9	38.8534	-77.1494	0.40	7.0	0.30	0.7	0.18	0.12	0.25	0.91	0.95	0.90	1.56	0.00	0.00
ANNANDLE, VA	12	10	38.8536	-77.1379	0.40	7.0	0.30	0.7	0.18	0.12	0.25	0.91	0.95	0.90	2.50	0.00	0.00
ANNAN/ALEX	B12		38.8538	-77.1263	0.34	7.0	0.30	0.7	0.18	0.12	0.25	0.91	0.95	0.90	7.50	10.00	5.00
ALEXANDRIA, VA	12	1	38.8540	-77.1147	0.40	7.0	0.30	0.7	0.18	0.12	0.25	0.91	0.95	0.90	2.81	0.00	0.00
ALEXANDRIA, VA	12	2	38.8542	-77.1032	0.40	7.0	0.30	0.7	0.18	0.12	0.25	0.91	0.95	0.90	2.50	0.00	0.00
ALEXANDRIA, VA	12	3	38.8544	-77.0916	0.40	7.0	0.30	0.7	0.18	0.12	0.25	0.91	0.95	0.90	4.38	0.00	0.00
ALEXANDRIA, VA	12	4	38.8546	-77.0801	0.40	7.0	0.30	0.7	0.18	0.12	0.25	0.91	0.95	0.90	1.25	0.00	0.00
ALEXANDRIA, VA	12	5	38.8548	-77.0685	0.36	7.0	0.30	0.7	0.18	0.12	0.25	0.91	0.95	0.90	13.44	10.00	5.00
ALEXANDRIA, VA	12	6	38.8551	-77.0570	0.45	7.0	0.50	0.7	0.18	0.12	0.25	0.91	0.95	0.90	8.44	10.00	5.00
ALEXANDRIA, VA	12	7	38.8553	-77.0454	0.29	17.0	0.47	1.7	0.18	0.15	0.25	0.88	0.94	0.90	8.75	10.00	5.00
ALEXANDRIA, VA	12	8	38.8555	-77.0339	0.01	0.1	0.01	0.0	0.25	0.13	0.25	0.88	0.95	0.90	2.19	10.00	5.00
ALEXANDRIA, VA	12	9	38.8557	-77.0223	0.00	0.0	0.00	0.0	0.00	0.00	0.00	0.00	0.00	0.00	0.00	0.00	0.00
ALEXANDRIA, VA	12	10	38.8559	-77.0107	0.44	8.0	0.40	0.8	0.21	0.12	0.25	0.88	0.95	0.90	15.31	10.00	5.00
ALEX/ANAC	B12		38.8561	-76.9992	0.54	8.7	0.60	0.9	0.17	0.12	0.25	0.90	0.95	0.90	4.38	10.00	5.00
ANACOSTIA, MD	12	1	38.8563	-76.9876	0.59	9.7	0.56	1.0	0.18	0.12	0.25	0.89	0.95	0.90	11.88	10.00	5.00
ANACOSTIA, MD	12	2	38.8565	-76.9761	0.50	7.0	0.59	0.7	0.18	0.12	0.25	0.90	0.95	0.90	3.59	10.00	5.00
ANACOSTIA, MD	12	3	38.8568	-76.9645	0.55	8.4	0.54	0.8	0.17	0.12	0.25	0.90	0.95	0.90	5.31	10.00	5.00
ANACOSTIA, MD	12	4	38.8570	-76.9530	0.43	7.5	0.33	0.8	0.18	0.12	0.25	0.91	0.95	0.90	2.19	10.00	5.00
ANACOSTIA, MD	12	5	38.8572	-76.9414	0.50	10.0	0.40	1.0	0.07	0.12	0.25	0.88	0.95	0.90	0.63	10.00	5.00
ANACOSTIA, MD	12	6	38.8574	-76.9299	0.44	7.5	0.35	0.8	0.19	0.12	0.25	0.90	0.95	0.90	4.06	10.00	5.00
ANACOSTIA, MD	12	7	38.8576	-76.9183	0.45	9.1	0.41	0.9	0.19	0.17	0.25	0.89	0.93	0.90	10.31	10.00	5.00
ANACOSTIA, MD	12	8	38.8578	-76.9067	0.38	7.3	0.27	0.7	0.20	0.15	0.25	0.90	0.94	0.90	4.69	10.00	5.00
ANACOSTIA, MD	12	9	38.8580	-76.8952	0.40	7.6	0.30	0.8	0.17	0.12	0.25	0.90	0.95	0.90	4.84	10.00	5.00
ANACOSTIA, MD	12	10	38.8582	-76.8836	0.40	7.0	0.30	0.7	0.18	0.12	0.25	0.91	0.95	0.90	5.00	0.00	0.00
ANAC/UMARL	B12		38.8584	-76.8721	0.40	7.0	0.30	0.7	0.18	0.12	0.25	0.91	0.95	0.90	3.75	0.00	0.00
UPPER MARLBORO	12	1	38.8587	-76.8605	0.38	6.5	0.28	0.7	0.19	0.13	0.25	0.90	0.95	0.90	1.56	10.00	5.00
UPPER MARLBORO	12	2	38.8589	-76.8490	0.23	5.0	0.43	0.5	0.23	0.22	0.25	0.89	0.91	0.90	11.56	10.00	5.00
UPPER MARLBORO	12	3	38.8591	-76.8374	0.60	4.0	0.50	0.4	0.25	0.12	0.25	0.88	0.95	0.90	0.63	10.00	5.00
UPPER MARLBORO	12	4	38.8593	-76.8259	0.00	0.0	0.00	0.0	0.00	0.00	0.00	0.00	0.00	0.00	0.00	0.00	0.00
ANNANDLE, VA	11	2	38.8429	-77.2299	0.40	7.0	0.30	0.7	0.18	0.12	0.25	0.91	0.95	0.90	2.81	0.00	0.00
ANNANDLE, VA	11	3	38.8431	-77.2183	0.40	7.0	0.30	0.7	0.18	0.12	0.25	0.91	0.95	0.90	1.88	0.00	0.00
ANNANDLE, VA	11	4	38.8433	-77.2068	0.40	7.0	0.30	0.7	0.18	0.12	0.25	0.91	0.95	0.90	1.88	0.00	0.00
ANNANDLE, VA	11	5	38.8435	-77.1952	0.40	7.0	0.30	0.7	0.18	0.12	0.25	0.91	0.95	0.90	3.44	0.00	0.00
ANNANDLE, VA	11	6	38.8437	-77.1836	0.40	7.0	0.30	0.7	0.18	0.12	0.25	0.91	0.95	0.90	3.75	0.00	0.00
ANNANDLE, VA	11	7	38.8439	-77.1721	0.40	7.0	0.30	0.7	0.18	0.12	0.25	0.91	0.95	0.90	1.56	0.00	0.00
ANNANDLE, VA	11	8	38.8441	-77.1605	0.40	7.0	0.30	0.7	0.18	0.12	0.25	0.91	0.95	0.90	1.88	0.00	0.00
ANNANDLE, VA	11	9	38.8444	-77.1490	0.40	7.0	0.30	0.7	0.18	0.12	0.25	0.91	0.95	0.90	0.94	0.00	0.00
ANNANDLE, VA	11	10	38.8446	-77.1374	0.40	7.0	0.30	0.7	0.18	0.12	0.25	0.91	0.95	0.90	2.50	0.00	0.00
ANNAN/ALEX	B11		38.8448	-77.1259	0.40	7.0	0.30	0.7	0.18	0.12	0.25	0.91	0.95	0.90	1.56	0.00	0.00
ALEXANDRIA, VA	11	1	38.8450	-77.1143	0.40	7.0	0.30	0.7	0.18	0.12	0.25	0.91	0.95	0.90	1.88	0.00	0.00
ALEXANDRIA, VA	11	2	38.8452	-77.1028	0.40	7.0	0.30	0.7	0.18	0.12	0.25	0.91	0.95	0.90	2.19	0.00	0.00
ALEXANDRIA, VA	11	3	38.8454	-77.0912	0.44	7.0	0.37	0.7	0.21	0.12	0.25	0.90	0.95	0.90	4.69	10.00	5.00
ALEXANDRIA, VA	11	4	38.8456	-77.0797	0.28	17.2	0.24	1.7	0.20	0.12	0.25	0.89	0.95	0.90	15.00	10.00	5.00
ALEXANDRIA, VA	11	5	38.8458	-77.0681	0.40	7.0	0.30	0.7	0.18	0.12	0.25	0.91	0.95	0.90	1.88	0.00	0.00
ALEXANDRIA, VA	11	6	38.8461	-77.0566	0.40	7.0	0.27	0.7	0.20	0.12	0.25	0.90	0.95	0.90	2.50	10.00	5.00
ALEXANDRIA, VA	11	7	38.8463	-77.0450	0.18	9.1	0.30	0.9	0.22	0.16	0.25	0.88	0.94	0.90	7.19	10.00	5.00
ALEXANDRIA, VA	11	8	38.8465	-77.0334	0.01	0.1	0.01	0.0	0.25	0.12	0.25	0.88	0.95	0.90	2.19	10.00	5.00
ALEXANDRIA, VA	11	9	38.8467	-77.0219	0.60	7.0	0.40	0.7	0.17	0.12	0.25	0.88	0.95	0.90	1.56	10.00	5.00

ALEXANDRIA, VA	11	10	38.8469	-77.0103	0.15	7.0	0.30	0.7	0.19	0.12	0.25	0.88	0.95	0.90	12.50	10.00	5.00
ALEX/ANAC	B11		38.8471	-76.9988	0.50	8.2	0.42	0.8	0.16	0.12	0.25	0.90	0.95	0.90	4.38	10.00	5.00
ANACOSTIA, MD	11	1	38.8473	-76.9872	0.50	8.3	0.36	0.8	0.13	0.12	0.25	0.88	0.95	0.90	3.75	10.00	5.00
ANACOSTIA, MD	11	2	38.8475	-76.9757	0.50	7.0	0.50	0.7	0.13	0.12	0.25	0.88	0.95	0.90	8.13	10.00	5.00
ANACOSTIA, MD	11	3	38.8478	-76.9641	0.47	7.4	0.38	0.7	0.18	0.12	0.25	0.91	0.95	0.90	2.81	10.00	5.00
ANACOSTIA, MD	11	4	38.8480	-76.9526	0.45	7.0	0.35	0.7	0.18	0.12	0.25	0.90	0.95	0.90	3.75	10.00	5.00
ANACOSTIA, MD	11	5	38.8482	-76.9410	0.60	9.2	0.38	0.9	0.22	0.12	0.25	0.88	0.95	0.90	1.56	10.00	5.00
ANACOSTIA, MD	11	6	38.8484	-76.9295	0.38	9.8	0.47	1.0	0.15	0.13	0.25	0.89	0.95	0.90	5.47	10.00	5.00
ANACOSTIA, MD	11	7	38.8486	-76.9179	0.53	7.0	0.43	0.7	0.17	0.12	0.25	0.89	0.95	0.90	4.69	10.00	5.00
ANACOSTIA, MD	11	8	38.8488	-76.9063	0.35	7.8	0.35	0.8	0.15	0.17	0.25	0.90	0.93	0.90	7.97	10.00	5.00
ANACOSTIA, MD	11	9	38.8490	-76.8948	0.40	7.7	0.35	0.8	0.16	0.12	0.25	0.90	0.95	0.90	10.00	10.00	5.00
ANACOSTIA, MD	11	10	38.8492	-76.8832	0.34	7.5	0.26	0.8	0.19	0.12	0.25	0.89	0.95	0.90	5.78	10.00	5.00
ANAC/UMARL	B11		38.8494	-76.8717	0.40	7.0	0.33	0.7	0.18	0.12	0.25	0.90	0.95	0.90	4.84	10.00	5.00
UPPER MARLBORO	11	1	38.8497	-76.8601	0.23	7.0	0.30	0.7	0.17	0.21	0.25	0.90	0.92	0.90	11.56	10.00	5.00
UPPER MARLBORO	11	2	38.8499	-76.8486	0.40	7.0	0.30	0.7	0.18	0.12	0.25	0.91	0.95	0.90	0.94	0.00	0.00
UPPER MARLBORO	11	3	38.8501	-76.8370	0.00	0.0	0.00	0.0	0.00	0.00	0.00	0.00	0.00	0.00	0.00	0.00	0.00
UPPER MARLBORO	11	4	38.8503	-76.8255	0.00	0.0	0.00	0.0	0.00	0.00	0.00	0.00	0.00	0.00	0.00	0.00	0.00
ANNANDLE, VA	10	2	38.8339	-77.2560	0.40	7.0	0.30	0.7	0.18	0.12	0.25	0.91	0.95	0.90	1.88	0.00	0.00
ANNANDLE, VA	10	3	38.8341	-77.2445	0.21	9.3	0.30	0.9	0.23	0.12	0.25	0.89	0.95	0.90	14.38	10.00	5.00
ANNANDLE, VA	10	4	38.8343	-77.2329	0.35	7.0	0.30	0.7	0.18	0.12	0.25	0.91	0.95	0.90	7.81	10.00	5.00
ANNANDLE, VA	10	5	38.8345	-77.2214	0.40	7.0	0.30	0.7	0.18	0.12	0.25	0.91	0.95	0.90	3.13	0.00	0.00
ANNANDLE, VA	10	6	38.8347	-77.2098	0.40	7.0	0.30	0.7	0.18	0.12	0.25	0.91	0.95	0.90	3.13	0.00	0.00
ANNANDLE, VA	10	7	38.8349	-77.1983	0.40	7.0	0.30	0.7	0.18	0.12	0.25	0.91	0.95	0.90	1.09	0.00	0.00
ANNANDLE, VA	10	8	38.8352	-77.1867	0.40	7.0	0.30	0.7	0.18	0.12	0.25	0.91	0.95	0.90	2.81	0.00	0.00
ANNANDLE, VA	10	9	38.8354	-77.1752	0.40	7.0	0.30	0.7	0.18	0.12	0.25	0.91	0.95	0.90	4.69	0.00	0.00
ANNANDLE, VA	10	10	38.8356	-77.1636	0.42	7.3	0.31	0.7	0.19	0.12	0.25	0.91	0.95	0.90	3.13	10.00	5.00
ANNAN/ALEX	B10		38.8358	-77.1521	0.45	7.7	0.32	0.8	0.18	0.12	0.25	0.90	0.95	0.90	5.00	10.00	5.00
ALEXANDRIA, VA	10	1	38.8360	-77.1405	0.47	13.3	0.38	1.3	0.15	0.12	0.25	0.89	0.95	0.90	6.41	10.00	5.00
ALEXANDRIA, VA	10	2	38.8362	-77.1290	0.37	11.2	0.34	1.1	0.13	0.15	0.25	0.89	0.94	0.90	15.94	10.00	5.00
ALEXANDRIA, VA	10	3	38.8364	-77.1174	0.44	9.3	0.38	0.9	0.11	0.13	0.25	0.89	0.95	0.90	18.75	10.00	5.00
ALEXANDRIA, VA	10	4	38.8366	-77.1059	0.40	7.0	0.30	0.7	0.18	0.12	0.25	0.91	0.95	0.90	5.00	0.00	0.00
ALEXANDRIA, VA	10	5	38.8368	-77.0943	0.40	7.0	0.30	0.7	0.18	0.12	0.25	0.91	0.95	0.90	4.53	0.00	0.00
ALEXANDRIA, VA	10	6	38.8371	-77.0828	0.55	9.4	0.52	0.9	0.13	0.12	0.25	0.89	0.95	0.90	4.69	10.00	5.00
ALEXANDRIA, VA	10	7	38.8373	-77.0712	0.01	0.1	0.01	0.0	0.25	0.12	0.25	0.88	0.95	0.90	3.75	10.00	5.00
ALEXANDRIA, VA	10	8	38.8375	-77.0597	0.00	0.0	0.00	0.0	0.00	0.00	0.00	0.00	0.00	0.00	0.00	0.00	0.00
ALEXANDRIA, VA	10	9	38.8377	-77.0481	0.40	7.5	0.30	0.8	0.14	0.12	0.25	0.88	0.95	0.90	6.25	10.00	5.00
ALEXANDRIA, VA	10	10	38.8379	-77.0365	0.33	7.6	0.41	0.8	0.17	0.12	0.25	0.89	0.95	0.90	15.63	10.00	5.00
ALEX/ANAC	B10		38.8381	-77.0250	0.50	8.5	0.44	0.9	0.17	0.12	0.25	0.90	0.95	0.90	4.69	10.00	5.00
ANACOSTIA, MD	10	1	38.8383	-77.0134	0.49	8.2	0.48	0.8	0.15	0.12	0.25	0.90	0.95	0.90	3.75	10.00	5.00
ANACOSTIA, MD	10	2	38.8385	-77.0019	0.00	0.0	0.00	0.0	0.00	0.00	0.00	0.00	0.00	0.00	0.00	0.00	0.00
ANACOSTIA, MD	10	3	38.8388	-76.9903	0.43	8.0	0.37	0.8	0.16	0.12	0.25	0.90	0.95	0.90	4.84	10.00	5.00
ANACOSTIA, MD	10	4	38.8390	-76.9788	0.43	7.2	0.31	0.7	0.18	0.12	0.25	0.90	0.95	0.90	5.94	10.00	5.00
ANACOSTIA, MD	10	5	38.8392	-76.9672	0.46	7.4	0.43	0.7	0.22	0.12	0.25	0.88	0.95	0.90	4.06	10.00	5.00
ANACOSTIA, MD	10	6	38.8394	-76.9557	0.34	9.4	0.38	0.9	0.11	0.15	0.25	0.89	0.94	0.90	8.91	10.00	5.00
ANACOSTIA, MD	10	7	38.8396	-76.9441	0.43	7.3	0.33	0.7	0.16	0.12	0.25	0.90	0.95	0.90	2.50	10.00	5.00
ANACOSTIA, MD	10	8	38.8398	-76.9326	0.48	9.4	0.38	0.9	0.14	0.12	0.25	0.89	0.95	0.90	1.41	10.00	5.00
ANACOSTIA, MD	10	9	38.8400	-76.9210	0.50	10.0	0.40	1.0	0.15	0.12	0.25	0.88	0.95	0.90	3.75	10.00	5.00
ANACOSTIA, MD	10	10	38.8402	-76.9095	0.42	8.5	0.32	0.9	0.19	0.12	0.25	0.90	0.95	0.90	9.22	10.00	5.00
ANAC/UMARL	B10		38.8404	-76.8979	0.24	7.0	0.23	0.7	0.20	0.16	0.25	0.89	0.94	0.90	20.63	10.00	5.00
UPPER MARLBORO	10	1	38.8407	-76.8864	0.27	7.0	0.43	0.7	0.23	0.17	0.25	0.89	0.93	0.90	18.59	10.00	5.00
UPPER MARLBORO	10	2	38.8409	-76.8748	0.00	0.0	0.00	0.0	0.00	0.00	0.00	0.00	0.00	0.00	0.00	0.00	0.00
UPPER MARLBORO	10	3	38.8411	-76.8633	0.40	7.0	0.30	0.7	0.18	0.12	0.25	0.91	0.95	0.90	0.63	0.00	0.00
UPPER MARLBORO	10	4	38.8413	-76.8517	0.00	0.0	0.00	0.0	0.00	0.00	0.00	0.00	0.00	0.00	0.00	0.00	0.00
ANNANDLE, VA	9	2	38.8249	-77.2293	0.40	7.0	0.30	0.7	0.18	0.12	0.25	0.91	0.95	0.90	1.88	0.00	0.00
ANNANDLE, VA	9	3	38.8251	-77.2177	0.50	9.6	0.48	1.0	0.13	0.12	0.25	0.88	0.95	0.90	15.63	10.00	5.00
ANNANDLE, VA	9	4	38.8253	-77.2062	0.40	7.0	0.30	0.7	0.18	0.12	0.25	0.91	0.95	0.90	2.19	0.00	0.00
ANNANDLE, VA	9	5	38.8255	-77.1946	0.40	7.0	0.30	0.7	0.18	0.12	0.25	0.91	0.95	0.90	2.50	0.00	0.00
ANNANDLE, VA	9	6	38.8257	-77.1831	0.40	7.0	0.30	0.7	0.18	0.12	0.25	0.91	0.95	0.90	1.56	0.00	0.00
ANNANDLE, VA	9	7	38.8259	-77.1715	0.40	7.0	0.30	0.7	0.18	0.12	0.25	0.91	0.95	0.90	1.88	0.00	0.00
ANNANDLE, VA	9	8	38.8262	-77.1600	0.36	8.2	0.26	0.8	0.15	0.15	0.25	0.90	0.94	0.90	4.38	10.00	5.00
ANNANDLE, VA	9	9	38.8264	-77.1484	0.41	7.4	0.33	0.7	0.17	0.12	0.25	0.91	0.95	0.90	3.75	10.00	5.00
ANNANDLE, VA	9	10	38.8266	-77.1369	0.42	7.2	0.31	0.7	0.18	0.12	0.25	0.91	0.95	0.90	4.38	10.00	5.00
ANNAN/ALEX	B9		38.8268	-77.1253	0.53	10.0	0.40	1.0	0.21	0.12	0.25	0.88	0.95	0.90	15.00	10.00	5.00
ALEXANDRIA, VA	9	1	38.8270	-77.1138	0.32	10.4	0.44	1.0	0.18	0.12	0.25	0.89	0.95	0.90	15.63	10.00	5.00
ALEXANDRIA, VA	9	2	38.8272	-77.1022	0.35	7.8	0.30	0.8	0.17	0.12	0.25	0.90	0.95	0.90	1.56	10.00	5.00
ALEXANDRIA, VA	9	3	38.8274	-77.0907	0.56	7.9	0.39	0.8	0.11	0.12	0.25	0.88	0.95	0.90	5.78	10.00	5.00
ALEXANDRIA, VA	9	4	38.8276	-77.0791	0.40	7.0	0.30	0.7	0.17	0.12	0.25	0.90	0.95	0.90	5.31	10.00	5.00
ALEXANDRIA, VA	9	5	38.8278	-77.0676	0.43	7.0	0.35	0.7	0.18	0.12	0.25	0.91	0.95	0.90	2.97	0.00	0.00
ALEXANDRIA, VA	9	6	38.8281	-77.0560	0.51	7.2	0.48	0.7	0.17	0.12	0.25	0.91	0.95	0.90	5.78	10.00	5.00
ALEXANDRIA, VA	9	7	38.8283	-77.0445	0.01	0.1	0.01	0.0	0.25	0.12	0.25	0.88	0.95	0.90	3.13	10.00	5.00
ALEXANDRIA, VA	9	8	38.8285	-77.0329	0.00	0.0	0.00	0.0	0.00	0.00	0.00	0.00	0.00	0.00	0.00	0.00	0.00
ALEXANDRIA, VA	9	9	38.8287	-77.0214	0.42	10.4	0.30	1.0	0.17	0.12	0.25	0.89	0.95	0.90	17.03	10.00	5.00
ALEXANDRIA, VA	9	10	38.8289	-77.0098	0.64	9.3	0.64	0.9	0.18	0.12	0.25	0.91	0.95	0.90	11.09	10.00	5.00
ALEX/ANAC	B9		38.8291	-76.9983	0.52	9.4	0.47	0.9	0.13	0.12	0.25	0.89	0.95	0.90	6.88	10.00	5.00

ANACOSTIA, MD	9	1	38.8293	-76.9867	0.44	10.0	0.41	1.0	0.12	0.12	0.25	0.88	0.95	0.90	5.00	10.00	5.00
ANACOSTIA, MD	9	2	38.8295	-76.9752	0.40	7.0	0.30	0.7	0.18	0.12	0.25	0.91	0.95	0.90	1.25	0.00	0.00
ANACOSTIA, MD	9	3	38.8298	-76.9636	0.40	8.4	0.33	0.8	0.17	0.12	0.25	0.90	0.95	0.90	4.22	10.00	5.00
ANACOSTIA, MD	9	4	38.8300	-76.9521	0.44	7.6	0.32	0.8	0.19	0.12	0.25	0.90	0.95	0.90	5.00	10.00	5.00
ANACOSTIA, MD	9	5	38.8302	-76.9405	0.32	7.0	0.34	0.7	0.16	0.12	0.25	0.89	0.95	0.90	10.63	10.00	5.00
ANACOSTIA, MD	9	6	38.8304	-76.9290	0.27	7.0	0.23	0.7	0.23	0.12	0.25	0.89	0.95	0.90	7.66	10.00	5.00
ANACOSTIA, MD	9	7	38.8306	-76.9174	0.27	7.0	0.23	0.7	0.20	0.12	0.25	0.89	0.95	0.90	0.78	10.00	5.00
ANACOSTIA, MD	9	8	38.8308	-76.9059	0.40	7.0	0.30	0.7	0.18	0.12	0.25	0.91	0.95	0.90	0.94	0.00	0.00
ANACOSTIA, MD	9	9	38.8310	-76.8943	0.40	7.0	0.30	0.7	0.18	0.12	0.25	0.91	0.95	0.90	3.59	0.00	0.00
ANACOSTIA, MD	9	10	38.8312	-76.8827	0.50	8.0	0.30	0.8	0.21	0.16	0.25	0.88	0.94	0.90	2.19	10.00	5.00
ANAC/UMARL	B9		38.8314	-76.8712	0.29	7.0	0.38	0.7	0.12	0.16	0.25	0.89	0.94	0.90	13.13	10.00	5.00
UPPER MARLBORO	9	1	38.8317	-76.8596	0.34	7.0	0.40	0.7	0.23	0.16	0.25	0.88	0.94	0.90	12.19	10.00	5.00
UPPER MARLBORO	9	2	38.8319	-76.8481	0.00	0.0	0.00	0.0	0.00	0.00	0.00	0.00	0.00	0.00	0.00	0.00	0.00
UPPER MARLBORO	9	3	38.8321	-76.8365	0.00	0.0	0.00	0.0	0.00	0.00	0.00	0.00	0.00	0.00	0.00	0.00	0.00
UPPER MARLBORO	9	4	38.8323	-76.8250	0.00	0.0	0.00	0.0	0.00	0.00	0.00	0.00	0.00	0.00	0.00	0.00	0.00
ANNANDLE, VA	8	2	38.8159	-77.2290	0.40	7.6	0.28	0.8	0.19	0.12	0.25	0.90	0.95	0.90	0.94	10.00	5.00
ANNANDLE, VA	8	3	38.8161	-77.2174	0.43	8.3	0.34	0.8	0.18	0.16	0.25	0.90	0.94	0.90	15.16	10.00	5.00
ANNANDLE, VA	8	4	38.8163	-77.2059	0.40	7.0	0.30	0.7	0.18	0.12	0.25	0.91	0.95	0.90	2.19	0.00	0.00
ANNANDLE, VA	8	5	38.8165	-77.1943	0.40	7.0	0.30	0.7	0.18	0.12	0.25	0.91	0.95	0.90	1.56	0.00	0.00
ANNANDLE, VA	8	6	38.8167	-77.1828	0.40	7.0	0.30	0.7	0.18	0.12	0.25	0.91	0.95	0.90	1.56	0.00	0.00
ANNANDLE, VA	8	7	38.8169	-77.1712	0.44	7.4	0.33	0.7	0.19	0.12	0.25	0.91	0.95	0.90	2.81	10.00	5.00
ANNANDLE, VA	8	8	38.8172	-77.1597	0.42	7.3	0.29	0.7	0.18	0.12	0.25	0.91	0.95	0.90	4.06	10.00	5.00
ANNANDLE, VA	8	9	38.8174	-77.1482	0.44	8.6	0.35	0.9	0.13	0.12	0.25	0.89	0.95	0.90	5.47	10.00	5.00
ANNANDLE, VA	8	10	38.8176	-77.1366	0.36	19.9	0.25	2.0	0.16	0.12	0.25	0.88	0.95	0.90	18.91	10.00	5.00
ANNAN/ALEX	B8		38.8178	-77.1250	0.40	21.7	0.31	2.2	0.17	0.12	0.25	0.89	0.95	0.90	17.03	10.00	5.00
ALEXANDRIA, VA	8	1	38.8180	-77.1135	0.48	8.2	0.34	0.8	0.17	0.12	0.25	0.90	0.95	0.90	3.91	10.00	5.00
ALEXANDRIA, VA	8	2	38.8182	-77.1019	0.45	7.2	0.29	0.7	0.18	0.12	0.25	0.90	0.95	0.90	3.75	10.00	5.00
ALEXANDRIA, VA	8	3	38.8184	-77.0904	0.40	7.0	0.30	0.7	0.18	0.12	0.25	0.91	0.95	0.90	1.88	0.00	0.00
ALEXANDRIA, VA	8	4	38.8186	-77.0789	0.40	7.0	0.30	0.7	0.18	0.12	0.25	0.91	0.95	0.90	2.50	0.00	0.00
ALEXANDRIA, VA	8	5	38.8188	-77.0673	0.46	7.0	0.42	0.7	0.18	0.12	0.25	0.91	0.95	0.90	3.75	0.00	0.00
ALEXANDRIA, VA	8	6	38.8191	-77.0558	0.46	9.5	0.56	1.0	0.19	0.12	0.25	0.90	0.95	0.90	6.56	10.00	5.00
ALEXANDRIA, VA	8	7	38.8193	-77.0442	0.50	11.2	0.57	1.1	0.13	0.12	0.25	0.88	0.95	0.90	8.44	10.00	5.00
ALEXANDRIA, VA	8	8	38.8195	-77.0326	0.00	0.0	0.00	0.0	0.00	0.00	0.00	0.00	0.00	0.00	0.00	0.00	0.00
ALEXANDRIA, VA	8	9	38.8197	-77.0211	0.54	8.0	0.50	0.8	0.21	0.12	0.25	0.88	0.95	0.90	16.25	10.00	5.00
ALEXANDRIA, VA	8	10	38.8199	-77.0095	0.68	9.4	0.64	0.9	0.18	0.12	0.25	0.90	0.95	0.90	3.13	10.00	5.00
ALEX/ANAC	B8		38.8201	-76.9980	0.44	8.2	0.36	0.8	0.14	0.13	0.25	0.89	0.95	0.90	11.88	10.00	5.00
ANACOSTIA, MD	8	1	38.8203	-76.9865	0.47	9.1	0.37	0.9	0.19	0.12	0.25	0.89	0.95	0.90	4.22	10.00	5.00
ANACOSTIA, MD	8	2	38.8205	-76.9749	0.45	7.5	0.35	0.7	0.19	0.12	0.25	0.91	0.95	0.90	2.34	10.00	5.00
ANACOSTIA, MD	8	3	38.8208	-76.9634	0.40	7.0	0.30	0.7	0.18	0.12	0.25	0.91	0.95	0.90	0.94	0.00	0.00
ANACOSTIA, MD	8	4	38.8210	-76.9518	0.38	7.3	0.32	0.7	0.19	0.12	0.25	0.90	0.95	0.90	3.75	10.00	5.00
ANACOSTIA, MD	8	5	38.8212	-76.9402	0.38	7.3	0.40	0.7	0.16	0.17	0.25	0.88	0.93	0.90	13.75	10.00	5.00
ANACOSTIA, MD	8	6	38.8214	-76.9287	0.23	7.0	0.30	0.7	0.17	0.22	0.25	0.90	0.91	0.90	11.56	10.00	5.00
ANACOSTIA, MD	8	7	38.8216	-76.9171	0.19	9.4	0.22	0.9	0.16	0.20	0.25	0.89	0.92	0.90	20.94	10.00	5.00
ANACOSTIA, MD	8	8	38.8218	-76.9056	0.34	7.6	0.32	0.8	0.19	0.17	0.25	0.90	0.93	0.90	13.59	10.00	5.00
ANACOSTIA, MD	8	9	38.8220	-76.8941	0.37	7.0	0.30	0.7	0.16	0.16	0.25	0.89	0.94	0.90	13.13	10.00	5.00
ANACOSTIA, MD	8	10	38.8222	-76.8825	0.31	7.8	0.22	0.8	0.17	0.22	0.25	0.89	0.91	0.90	12.50	10.00	5.00
ANAC/UMARL	B8		38.8224	-76.8710	0.01	0.1	0.01	0.0	0.25	0.13	0.25	0.88	0.95	0.90	1.25	10.00	5.00
UPPER MARLBORO	8	1	38.8227	-76.8594	0.30	10.5	0.33	1.1	0.16	0.19	0.25	0.88	0.93	0.90	4.53	10.00	5.00
UPPER MARLBORO	8	2	38.8229	-76.8478	0.24	4.0	0.50	0.4	0.25	0.12	0.25	0.88	0.95	0.90	11.56	10.00	5.00
UPPER MARLBORO	8	3	38.8231	-76.8363	0.00	0.0	0.00	0.0	0.00	0.00	0.00	0.00	0.00	0.00	0.00	0.00	0.00
UPPER MARLBORO	8	4	38.8233	-76.8247	0.00	0.0	0.00	0.0	0.00	0.00	0.00	0.00	0.00	0.00	0.00	0.00	0.00
ANNANDLE, VA	7	2	38.8069	-77.2288	0.40	7.0	0.30	0.7	0.18	0.12	0.25	0.91	0.95	0.90	1.88	0.00	0.00
ANNANDLE, VA	7	3	38.8071	-77.2173	0.34	15.0	0.52	1.5	0.17	0.16	0.25	0.89	0.94	0.90	17.03	10.00	5.00
ANNANDLE, VA	7	4	38.8073	-77.2058	0.40	7.0	0.30	0.7	0.18	0.12	0.25	0.91	0.95	0.90	4.38	0.00	0.00
ANNANDLE, VA	7	5	38.8075	-77.1942	0.40	7.0	0.30	0.7	0.18	0.12	0.25	0.91	0.95	0.90	1.88	0.00	0.00
ANNANDLE, VA	7	6	38.8077	-77.1826	0.40	7.0	0.30	0.7	0.18	0.12	0.25	0.91	0.95	0.90	1.56	0.00	0.00
ANNANDLE, VA	7	7	38.8079	-77.1711	0.35	7.0	0.30	0.7	0.18	0.12	0.25	0.90	0.95	0.90	3.13	10.00	5.00
ANNANDLE, VA	7	8	38.8082	-77.1596	0.33	7.4	0.34	0.7	0.19	0.12	0.25	0.90	0.95	0.90	13.59	10.00	5.00
ANNANDLE, VA	7	9	38.8084	-77.1480	0.25	48.2	0.46	4.8	0.17	0.12	0.25	0.89	0.95	0.90	12.50	10.00	5.00
ANNANDLE, VA	7	10	38.8086	-77.1365	0.49	21.3	0.51	2.1	0.18	0.12	0.25	0.88	0.95	0.90	8.75	10.00	5.00
ANNAN/ALEX	B7		38.8088	-77.1249	0.57	8.3	0.63	0.8	0.15	0.12	0.25	0.88	0.95	0.90	7.50	10.00	5.00
ALEXANDRIA, VA	7	1	38.8090	-77.1134	0.38	7.0	0.70	0.7	0.14	0.12	0.25	0.89	0.95	0.90	5.00	10.00	5.00
ALEXANDRIA, VA	7	2	38.8092	-77.1018	0.41	7.0	0.53	0.7	0.16	0.12	0.25	0.90	0.95	0.90	5.00	10.00	5.00
ALEXANDRIA, VA	7	3	38.8094	-77.0903	0.34	7.5	0.35	0.7	0.18	0.12	0.25	0.90	0.95	0.90	5.47	10.00	5.00
ALEXANDRIA, VA	7	4	38.8096	-77.0787	0.42	7.4	0.33	0.7	0.21	0.12	0.25	0.90	0.95	0.90	5.63	10.00	5.00
ALEXANDRIA, VA	7	5	38.8099	-77.0672	0.45	7.0	0.50	0.7	0.18	0.12	0.25	0.91	0.95	0.90	3.28	10.00	5.00
ALEXANDRIA, VA	7	6	38.8101	-77.0556	0.54	10.8	0.65	1.1	0.16	0.12	0.25	0.89	0.95	0.90	8.75	10.00	5.00
ALEXANDRIA, VA	7	7	38.8103	-77.0441	0.67	14.0	0.66	1.4	0.15	0.12	0.25	0.88	0.95	0.90	9.69	10.00	5.00
ALEXANDRIA, VA	7	8	38.8105	-77.0325	0.00	0.0	0.00	0.0	0.00	0.00	0.00	0.00	0.00	0.00	0.00	0.00	0.00
ALEXANDRIA, VA	7	9	38.8107	-77.0210	0.24	7.0	0.25	0.7	0.13	0.12	0.25	0.88	0.95	0.90	13.13	10.00	5.00
ALEXANDRIA, VA	7	10	38.8109	-77.0094	0.40	7.0	0.34	0.7	0.14	0.12	0.25	0.90	0.95	0.90	2.03	10.00	5.00
ALEX/ANAC	B7		38.8111	-76.9979	0.38	7.4	0.32	0.7	0.19	0.16	0.25	0.91	0.94	0.90	14.38	10.00	5.00
ANACOSTIA, MD	7	1	38.8113	-76.9863	0.40	7.0	0.30	0.7	0.18	0.12	0.25	0.91	0.95	0.90	2.50	0.00	0.00
ANACOSTIA, MD	7	2	38.8115	-76.9748	0.31	7.0	0.35	0.7	0.16	0.19	0.25	0.90	0.93	0.90	14.38	10.00	5.00

ANACOSTIA, MD	7	3	38.8118	-76.9632	0.35	10.8	0.38	1.1	0.22	0.20	0.25	0.89	0.92	0.90	14.38	10.00	5.00
ANACOSTIA, MD	7	4	38.8120	-76.9517	0.37	7.7	0.32	0.8	0.20	0.17	0.25	0.90	0.93	0.90	12.50	10.00	5.00
ANACOSTIA, MD	7	5	38.8122	-76.9401	0.40	7.0	0.30	0.7	0.18	0.12	0.25	0.91	0.95	0.90	2.66	0.00	0.00
ANACOSTIA, MD	7	6	38.8124	-76.9286	0.40	7.0	0.30	0.7	0.18	0.12	0.25	0.91	0.95	0.90	3.59	0.00	0.00
ANACOSTIA, MD	7	7	38.8126	-76.9170	0.38	7.0	0.30	0.7	0.18	0.16	0.25	0.91	0.94	0.90	12.81	10.00	5.00
ANACOSTIA, MD	7	8	38.8128	-76.9055	0.32	7.0	0.30	0.7	0.18	0.20	0.25	0.90	0.92	0.90	5.94	10.00	5.00
ANACOSTIA, MD	7	9	38.8130	-76.8939	0.45	7.9	0.38	0.8	0.19	0.12	0.25	0.89	0.95	0.90	6.41	10.00	5.00
ANACOSTIA, MD	7	10	38.8132	-76.8824	0.43	11.4	0.40	1.1	0.19	0.17	0.25	0.88	0.93	0.90	10.00	10.00	5.00
ANAC/UMARL	B7		38.8134	-76.8709	0.01	0.1	0.01	0.0	0.25	0.25	0.25	0.88	0.90	0.90	3.13	10.00	5.00
UPPER MARLBORO	7	1	38.8137	-76.8593	0.19	7.0	0.30	0.7	0.25	0.21	0.25	0.88	0.92	0.90	6.88	10.00	5.00
UPPER MARLBORO	7	2	38.8139	-76.8477	0.50	6.3	0.48	0.6	0.22	0.15	0.25	0.88	0.94	0.90	2.50	10.00	5.00
UPPER MARLBORO	7	3	38.8141	-76.8362	0.01	0.1	0.01	0.0	0.25	0.12	0.25	0.88	0.95	0.90	10.63	10.00	5.00
UPPER MARLBORO	7	4	38.8143	-76.8247	0.01	0.1	0.01	0.0	0.25	0.12	0.25	0.88	0.95	0.90	11.25	10.00	5.00
ANNANDLE, VA	6	2	38.7979	-77.2286	0.40	7.0	0.30	0.7	0.18	0.12	0.25	0.91	0.95	0.90	1.09	0.00	0.00
ANNANDLE, VA	6	3	38.7981	-77.2170	0.40	7.0	0.30	0.7	0.18	0.12	0.25	0.91	0.95	0.90	1.25	0.00	0.00
ANNANDLE, VA	6	4	38.7983	-77.2055	0.34	7.0	0.30	0.7	0.18	0.15	0.25	0.91	0.94	0.90	12.50	10.00	5.00
ANNANDLE, VA	6	5	38.7985	-77.1939	0.34	7.0	0.30	0.7	0.18	0.15	0.25	0.91	0.94	0.90	13.44	10.00	5.00
ANNANDLE, VA	6	6	38.7987	-77.1824	0.55	7.0	0.38	0.7	0.23	0.13	0.25	0.89	0.95	0.90	4.38	10.00	5.00
ANNANDLE, VA	6	7	38.7989	-77.1708	0.51	7.0	0.70	0.7	0.09	0.12	0.25	0.88	0.95	0.90	16.88	10.00	5.00
ANNANDLE, VA	6	8	38.7992	-77.1593	0.43	7.5	0.40	0.7	0.15	0.12	0.25	0.89	0.95	0.90	14.69	10.00	5.00
ANNANDLE, VA	6	9	38.7994	-77.1477	0.40	7.6	0.32	0.8	0.16	0.12	0.25	0.90	0.95	0.90	13.13	10.00	5.00
ANNANDLE, VA	6	10	38.7996	-77.1362	0.47	7.0	0.80	0.7	0.19	0.12	0.25	0.88	0.95	0.90	15.63	10.00	5.00
ANNAN/ALEX	B6		38.7998	-77.1246	0.38	11.5	0.51	1.2	0.16	0.12	0.25	0.89	0.95	0.90	15.31	10.00	5.00
ALEXANDRIA, VA	6	1	38.8000	-77.1131	0.31	7.0	0.38	0.7	0.16	0.12	0.25	0.90	0.95	0.90	13.75	10.00	5.00
ALEXANDRIA, VA	6	2	38.8002	-77.1015	0.27	7.0	0.30	0.7	0.17	0.12	0.25	0.90	0.95	0.90	11.25	10.00	5.00
ALEXANDRIA, VA	6	3	38.8004	-77.0900	0.29	7.0	0.30	0.7	0.17	0.12	0.25	0.90	0.95	0.90	12.97	10.00	5.00
ALEXANDRIA, VA	6	4	38.8006	-77.0784	0.23	9.1	0.30	0.9	0.19	0.12	0.25	0.89	0.95	0.90	13.75	10.00	5.00
ALEXANDRIA, VA	6	5	38.8008	-77.0669	0.34	15.2	0.26	1.5	0.16	0.12	0.25	0.89	0.95	0.90	13.75	10.00	5.00
ALEXANDRIA, VA	6	6	38.8011	-77.0554	0.47	9.9	0.57	1.0	0.18	0.12	0.25	0.88	0.95	0.90	7.19	10.00	5.00
ALEXANDRIA, VA	6	7	38.8013	-77.0438	0.70	11.6	0.67	1.2	0.16	0.12	0.25	0.88	0.95	0.90	8.44	10.00	5.00
ALEXANDRIA, VA	6	8	38.8015	-77.0323	0.00	0.0	0.00	0.0	0.00	0.00	0.00	0.00	0.00	0.00	0.00	0.00	0.00
ALEXANDRIA, VA	6	9	38.8017	-77.0207	0.01	0.1	0.01	0.0	0.25	0.25	0.25	0.88	0.90	0.90	10.94	10.00	5.00
ALEXANDRIA, VA	6	10	38.8019	-77.0092	0.01	0.1	0.01	0.0	0.25	0.25	0.25	0.88	0.90	0.90	10.31	10.00	5.00
ALEX/ANAC	B6		38.8021	-76.9976	0.22	7.0	0.38	0.7	0.11	0.22	0.25	0.89	0.91	0.90	18.59	10.00	5.00
ANACOSTIA, MD	6	1	38.8023	-76.9861	0.34	8.6	0.38	0.9	0.17	0.16	0.25	0.89	0.94	0.90	15.63	10.00	5.00
ANACOSTIA, MD	6	2	38.8025	-76.9745	0.33	8.6	0.34	0.9	0.21	0.12	0.25	0.89	0.95	0.90	3.91	10.00	5.00
ANACOSTIA, MD	6	3	38.8028	-76.9630	0.00	0.0	0.00	0.0	0.00	0.00	0.00	0.00	0.00	0.00	0.00	0.00	0.00
ANACOSTIA, MD	6	4	38.8030	-76.9514	0.40	7.9	0.46	0.8	0.16	0.12	0.25	0.88	0.95	0.90	3.91	10.00	5.00
ANACOSTIA, MD	6	5	38.8032	-76.9399	0.40	7.0	0.30	0.7	0.18	0.12	0.25	0.91	0.95	0.90	1.88	0.00	0.00
ANACOSTIA, MD	6	6	38.8034	-76.9283	0.40	7.0	0.30	0.7	0.18	0.12	0.25	0.91	0.95	0.90	3.44	0.00	0.00
ANACOSTIA, MD	6	7	38.8036	-76.9168	0.41	7.2	0.32	0.7	0.19	0.12	0.25	0.91	0.95	0.90	4.53	10.00	5.00
ANACOSTIA, MD	6	8	38.8038	-76.9052	0.41	7.8	0.46	0.8	0.20	0.16	0.25	0.89	0.94	0.90	15.63	10.00	5.00
ANACOSTIA, MD	6	9	38.8040	-76.8937	0.56	7.0	0.57	0.7	0.18	0.12	0.25	0.88	0.95	0.90	8.75	10.00	5.00
ANACOSTIA, MD	6	10	38.8042	-76.8821	0.40	7.5	0.40	0.8	0.17	0.21	0.25	0.88	0.92	0.90	3.75	10.00	5.00
ANAC/UMARL	B6		38.8045	-76.8706	0.01	0.1	0.01	0.0	0.25	0.25	0.25	0.88	0.90	0.90	1.88	10.00	5.00
UPPER MARLBORO	6	1	38.8047	-76.8591	0.24	7.0	0.30	0.7	0.23	0.22	0.25	0.88	0.91	0.90	3.13	10.00	5.00
UPPER MARLBORO	6	2	38.8049	-76.8475	0.55	4.8	0.45	0.5	0.24	0.16	0.25	0.89	0.94	0.90	3.44	10.00	5.00
UPPER MARLBORO	6	3	38.8051	-76.8360	0.40	7.0	0.30	0.7	0.18	0.12	0.25	0.91	0.95	0.90	0.63	0.00	0.00
UPPER MARLBORO	6	4	38.8053	-76.8244	0.00	0.0	0.00	0.0	0.00	0.00	0.00	0.00	0.00	0.00	0.00	0.00	0.00
ANNANDLE, VA	5	2	38.7889	-77.2283	0.40	7.0	0.30	0.7	0.18	0.12	0.25	0.91	0.95	0.90	2.19	0.00	0.00
ANNANDLE, VA	5	3	38.7891	-77.2167	0.40	7.0	0.30	0.7	0.18	0.12	0.25	0.91	0.95	0.90	1.41	0.00	0.00
ANNANDLE, VA	5	4	38.7893	-77.2052	0.46	7.0	0.34	0.7	0.19	0.12	0.25	0.90	0.95	0.90	2.81	10.00	5.00
ANNANDLE, VA	5	5	38.7895	-77.1936	0.40	7.0	0.30	0.7	0.18	0.12	0.25	0.91	0.95	0.90	4.38	0.00	0.00
ANNANDLE, VA	5	6	38.7897	-77.1821	0.27	7.0	0.30	0.7	0.17	0.19	0.25	0.90	0.93	0.90	20.00	10.00	5.00
ANNANDLE, VA	5	7	38.7899	-77.1705	0.26	7.0	0.30	0.7	0.17	0.13	0.25	0.90	0.95	0.90	18.59	10.00	5.00
ANNANDLE, VA	5	8	38.7902	-77.1590	0.16	7.0	0.30	0.7	0.17	0.12	0.25	0.89	0.95	0.90	11.25	10.00	5.00
ANNANDLE, VA	5	9	38.7904	-77.1474	0.32	7.0	0.30	0.7	0.18	0.12	0.25	0.90	0.95	0.90	10.94	10.00	5.00
ANNANDLE, VA	5	10	38.7906	-77.1359	0.40	7.0	0.30	0.7	0.18	0.12	0.25	0.91	0.95	0.90	2.03	0.00	0.00
ANNAN/ALEX	B5		38.7908	-77.1243	0.40	7.0	0.30	0.7	0.18	0.12	0.25	0.91	0.95	0.90	2.50	0.00	0.00
ALEXANDRIA, VA	5	1	38.7910	-77.1128	0.40	7.0	0.30	0.7	0.18	0.12	0.25	0.91	0.95	0.90	3.13	0.00	0.00
ALEXANDRIA, VA	5	2	38.7912	-77.1013	0.40	7.0	0.30	0.7	0.18	0.12	0.25	0.91	0.95	0.90	2.50	0.00	0.00
ALEXANDRIA, VA	5	3	38.7914	-77.0897	0.40	7.0	0.30	0.7	0.18	0.12	0.25	0.91	0.95	0.90	1.41	0.00	0.00
ALEXANDRIA, VA	5	4	38.7916	-77.0782	0.44	7.4	0.31	0.7	0.18	0.13	0.25	0.90	0.95	0.90	3.13	10.00	5.00
ALEXANDRIA, VA	5	5	38.7918	-77.0666	0.32	24.9	0.30	2.5	0.18	0.12	0.25	0.90	0.95	0.90	3.91	10.00	5.00
ALEXANDRIA, VA	5	6	38.7921	-77.0551	0.35	10.7	0.63	1.1	0.15	0.15	0.25	0.88	0.94	0.90	13.44	10.00	5.00
ALEXANDRIA, VA	5	7	38.7923	-77.0435	0.54	15.4	0.67	1.5	0.18	0.12	0.25	0.88	0.95	0.90	12.19	10.00	5.00
ALEXANDRIA, VA	5	8	38.7925	-77.0320	0.01	0.1	0.01	0.0	0.25	0.25	0.25	0.88	0.90	0.90	10.63	10.00	5.00
ALEXANDRIA, VA	5	9	38.7927	-77.0204	0.01	0.1	0.01	0.0	0.25	0.25	0.25	0.88	0.90	0.90	17.19	10.00	5.00
ALEXANDRIA, VA	5	10	38.7929	-77.0089	0.29	7.0	0.30	0.7	0.17	0.19	0.25	0.90	0.93	0.90	11.41	10.00	5.00
ALEX/ANAC	B5		38.7931	-76.9973	0.40	7.5	0.33	0.8	0.18	0.12	0.25	0.90	0.95	0.90	13.75	10.00	5.00
ANACOSTIA, MD	5	1	38.7933	-76.9858	0.40	7.0	0.30	0.7	0.18	0.12	0.25	0.91	0.95	0.90	1.88	0.00	0.00
ANACOSTIA, MD	5	2	38.7935	-76.9743	0.40	7.0	0.30	0.7	0.18	0.12	0.25	0.91	0.95	0.90	2.03	0.00	0.00
ANACOSTIA, MD	5	3	38.7938	-76.9627	0.40	7.7	0.30	0.8	0.21	0.12	0.25	0.89	0.95	0.90	3.13	10.00	5.00
ANACOSTIA, MD	5	4	38.7940	-76.9512	0.60	7.0	0.40	0.7	0.15	0.12	0.25	0.88	0.95	0.90	1.56	10.00	5.00

ANACOSTIA, MD	5	5	38.7942	-76.9396	0.40	7.0	0.30	0.7	0.18	0.12	0.25	0.91	0.95	0.90	0.31	0.00	0.00
ANACOSTIA, MD	5	6	38.7944	-76.9281	0.40	7.0	0.30	0.7	0.20	0.12	0.25	0.90	0.95	0.90	3.91	10.00	5.00
ANACOSTIA, MD	5	7	38.7946	-76.9165	0.40	7.0	0.30	0.7	0.18	0.25	0.25	0.91	0.90	0.90	4.38	0.00	0.00
ANACOSTIA, MD	5	8	38.7948	-76.9050	0.38	7.0	0.30	0.7	0.18	0.15	0.25	0.91	0.94	0.90	7.81	10.00	5.00
ANACOSTIA, MD	5	9	38.7950	-76.8934	0.46	7.0	0.50	0.7	0.15	0.16	0.25	0.88	0.94	0.90	9.38	10.00	5.00
ANACOSTIA, MD	5	10	38.7952	-76.8819	0.60	4.0	0.30	0.4	0.17	0.12	0.25	0.88	0.95	0.90	1.25	10.00	5.00
ANAC/UMARL	B5		38.7955	-76.8704	0.01	0.1	0.01	0.0	0.25	0.25	0.25	0.88	0.90	0.90	0.63	10.00	5.00
UPPER MARLBORO	5	1	38.7957	-76.8588	0.01	0.1	0.01	0.0	0.25	0.25	0.25	0.88	0.90	0.90	0.31	10.00	5.00
UPPER MARLBORO	5	2	38.7959	-76.8473	0.40	7.0	0.30	0.7	0.18	0.12	0.25	0.91	0.95	0.90	0.63	0.00	0.00
UPPER MARLBORO	5	3	38.7961	-76.8357	0.40	7.0	0.30	0.7	0.18	0.25	0.25	0.91	0.90	0.90	0.94	0.00	0.00
UPPER MARLBORO	5	4	38.7963	-76.8242	0.00	0.0	0.00	0.0	0.00	0.00	0.00	0.00	0.00	0.00	0.00	0.00	0.00
ANNANDLE, VA	4	2	38.7799	-77.2280	0.40	7.0	0.30	0.7	0.18	0.12	0.25	0.91	0.95	0.90	0.63	0.00	0.00
ANNANDLE, VA	4	3	38.7801	-77.2164	0.40	7.0	0.30	0.7	0.18	0.12	0.25	0.91	0.95	0.90	2.81	0.00	0.00
ANNANDLE, VA	4	4	38.7803	-77.2049	0.40	7.0	0.30	0.7	0.18	0.12	0.25	0.91	0.95	0.90	1.09	0.00	0.00
ANNANDLE, VA	4	5	38.7805	-77.1933	0.40	7.0	0.30	0.7	0.18	0.12	0.25	0.91	0.95	0.90	3.13	0.00	0.00
ANNANDLE, VA	4	6	38.7807	-77.1818	0.26	7.0	0.24	0.7	0.22	0.15	0.25	0.89	0.94	0.90	14.22	10.00	5.00
ANNANDLE, VA	4	7	38.7809	-77.1702	0.42	7.3	0.30	0.7	0.16	0.19	0.25	0.90	0.93	0.90	3.75	10.00	5.00
ANNANDLE, VA	4	8	38.7812	-77.1587	0.38	7.0	0.27	0.7	0.20	0.15	0.25	0.90	0.94	0.90	2.50	10.00	5.00
ANNANDLE, VA	4	9	38.7814	-77.1472	0.40	7.0	0.29	0.7	0.18	0.12	0.25	0.91	0.95	0.90	2.97	10.00	5.00
ANNANDLE, VA	4	10	38.7816	-77.1356	0.47	7.7	0.32	0.8	0.15	0.12	0.25	0.90	0.95	0.90	2.50	10.00	5.00
ANNAN/ALEX	B4		38.7818	-77.1241	0.42	7.6	0.32	0.8	0.19	0.12	0.25	0.90	0.95	0.90	3.44	10.00	5.00
ALEXANDRIA, VA	4	1	38.7820	-77.1125	0.40	7.0	0.30	0.7	0.18	0.12	0.25	0.91	0.95	0.90	3.75	0.00	0.00
ALEXANDRIA, VA	4	2	38.7822	-77.1010	0.40	7.0	0.30	0.7	0.18	0.12	0.25	0.91	0.95	0.90	3.44	0.00	0.00
ALEXANDRIA, VA	4	3	38.7824	-77.0894	0.40	7.0	0.30	0.7	0.18	0.12	0.25	0.91	0.95	0.90	1.56	0.00	0.00
ALEXANDRIA, VA	4	4	38.7826	-77.0779	0.35	7.0	0.30	0.7	0.14	0.12	0.25	0.89	0.95	0.90	5.31	10.00	5.00
ALEXANDRIA, VA	4	5	38.7829	-77.0663	0.38	9.4	0.30	0.9	0.17	0.12	0.25	0.91	0.95	0.90	3.28	10.00	5.00
ALEXANDRIA, VA	4	6	38.7831	-77.0548	0.40	7.0	0.30	0.7	0.18	0.12	0.25	0.91	0.95	0.90	0.63	0.00	0.00
ALEXANDRIA, VA	4	7	38.7833	-77.0433	0.00	0.0	0.00	0.0	0.00	0.00	0.00	0.00	0.00	0.00	0.00	0.00	0.00
ALEXANDRIA, VA	4	8	38.7835	-77.0317	0.00	0.0	0.00	0.0	0.00	0.00	0.00	0.00	0.00	0.00	0.00	0.00	0.00
ALEXANDRIA, VA	4	9	38.7837	-77.0202	0.00	0.0	0.00	0.0	0.00	0.00	0.00	0.00	0.00	0.00	0.00	0.00	0.00
ALEXANDRIA, VA	4	10	38.7839	-77.0086	0.40	7.0	0.30	0.7	0.18	0.12	0.25	0.91	0.95	0.90	1.56	0.00	0.00
ALEX/ANAC	B4		38.7841	-76.9971	0.40	7.5	0.33	0.7	0.18	0.12	0.25	0.90	0.95	0.90	14.06	10.00	5.00
ANACOSTIA, MD	4	1	38.7843	-76.9855	0.40	7.0	0.33	0.7	0.17	0.12	0.25	0.90	0.95	0.90	1.56	10.00	5.00
ANACOSTIA, MD	4	2	38.7845	-76.9740	0.40	7.0	0.30	0.7	0.18	0.12	0.25	0.91	0.95	0.90	0.31	0.00	0.00
ANACOSTIA, MD	4	3	38.7848	-76.9624	0.40	7.0	0.30	0.7	0.18	0.12	0.25	0.91	0.95	0.90	3.13	0.00	0.00
ANACOSTIA, MD	4	4	38.7850	-76.9509	0.40	7.0	0.30	0.7	0.18	0.12	0.25	0.91	0.95	0.90	2.50	0.00	0.00
ANACOSTIA, MD	4	5	38.7852	-76.9394	0.40	7.0	0.30	0.7	0.18	0.12	0.25	0.91	0.95	0.90	2.50	0.00	0.00
ANACOSTIA, MD	4	6	38.7854	-76.9278	0.40	7.0	0.30	0.7	0.18	0.12	0.25	0.91	0.95	0.90	1.09	0.00	0.00
ANACOSTIA, MD	4	7	38.7856	-76.9163	0.40	7.0	0.30	0.7	0.18	0.12	0.25	0.91	0.95	0.90	1.41	0.00	0.00
ANACOSTIA, MD	4	8	38.7858	-76.9047	0.45	7.0	0.32	0.7	0.18	0.12	0.25	0.90	0.95	0.90	3.28	10.00	5.00
ANACOSTIA, MD	4	9	38.7860	-76.8932	0.38	8.1	0.41	0.8	0.23	0.15	0.25	0.88	0.94	0.90	15.00	10.00	5.00
ANACOSTIA, MD	4	10	38.7862	-76.8816	0.40	7.0	0.30	0.7	0.18	0.12	0.25	0.91	0.95	0.90	0.31	0.00	0.00
ANAC/UMARL	B4		38.7865	-76.8701	0.00	0.0	0.00	0.0	0.00	0.00	0.00	0.00	0.00	0.00	0.00	0.00	0.00
UPPER MARLBORO	4	1	38.7867	-76.8586	0.40	7.0	0.30	0.7	0.18	0.12	0.25	0.91	0.95	0.90	0.16	0.00	0.00
UPPER MARLBORO	4	2	38.7869	-76.8470	0.40	7.0	0.30	0.7	0.18	0.12	0.25	0.91	0.95	0.90	0.78	0.00	0.00
UPPER MARLBORO	4	3	38.7871	-76.8355	0.50	7.0	0.40	0.7	0.20	0.12	0.25	0.90	0.95	0.90	2.50	10.00	5.00
UPPER MARLBORO	4	4	38.7873	-76.8239	0.00	0.0	0.00	0.0	0.00	0.00	0.00	0.00	0.00	0.00	0.00	0.00	0.00
ANNANDLE, VA	3	2	38.7709	-77.2277	0.40	7.0	0.30	0.7	0.18	0.12	0.25	0.91	0.95	0.90	2.50	0.00	0.00
ANNANDLE, VA	3	3	38.7711	-77.2161	0.40	7.0	0.30	0.7	0.18	0.12	0.25	0.91	0.95	0.90	1.56	0.00	0.00
ANNANDLE, VA	3	4	38.7713	-77.2046	0.40	7.0	0.30	0.7	0.18	0.12	0.25	0.91	0.95	0.90	0.31	0.00	0.00
ANNANDLE, VA	3	5	38.7715	-77.1931	0.40	7.0	0.30	0.7	0.18	0.12	0.25	0.91	0.95	0.90	1.88	0.00	0.00
ANNANDLE, VA	3	6	38.7717	-77.1815	0.35	7.0	0.30	0.7	0.11	0.12	0.25	0.89	0.95	0.90	16.41	10.00	5.00
ANNANDLE, VA	3	7	38.7719	-77.1700	0.36	7.0	0.27	0.7	0.19	0.22	0.25	0.90	0.91	0.90	2.81	10.00	5.00
ANNANDLE, VA	3	8	38.7722	-77.1584	0.70	8.5	0.65	0.9	0.09	0.12	0.25	0.88	0.95	0.90	3.75	10.00	5.00
ANNANDLE, VA	3	9	38.7724	-77.1469	0.40	7.0	0.30	0.7	0.18	0.12	0.25	0.91	0.95	0.90	0.94	0.00	0.00
ANNANDLE, VA	3	10	38.7726	-77.1353	0.00	0.0	0.00	0.0	0.00	0.00	0.00	0.00	0.00	0.00	0.00	0.00	0.00
ANNAN/ALEX	B3		38.7728	-77.1238	0.00	0.0	0.00	0.0	0.00	0.00	0.00	0.00	0.00	0.00	0.00	0.00	0.00
ALEXANDRIA, VA	3	1	38.7730	-77.1123	0.40	7.0	0.30	0.7	0.18	0.12	0.25	0.91	0.95	0.90	1.56	0.00	0.00
ALEXANDRIA, VA	3	2	38.7732	-77.1007	0.40	7.0	0.30	0.7	0.18	0.12	0.25	0.91	0.95	0.90	2.34	0.00	0.00
ALEXANDRIA, VA	3	3	38.7734	-77.0892	0.43	7.8	0.33	0.8	0.19	0.12	0.25	0.90	0.95	0.90	4.53	10.00	5.00
ALEXANDRIA, VA	3	4	38.7736	-77.0776	0.37	7.0	0.30	0.7	0.18	0.12	0.25	0.90	0.95	0.90	5.47	10.00	5.00
ALEXANDRIA, VA	3	5	38.7739	-77.0661	0.36	7.2	0.28	0.7	0.19	0.12	0.25	0.90	0.95	0.90	3.44	10.00	5.00
ALEXANDRIA, VA	3	6	38.7741	-77.0545	0.45	11.2	0.35	1.1	0.19	0.12	0.25	0.89	0.95	0.90	5.00	10.00	5.00
ALEXANDRIA, VA	3	7	38.7743	-77.0430	0.00	0.0	0.00	0.0	0.00	0.00	0.00	0.00	0.00	0.00	0.00	0.00	0.00
ALEXANDRIA, VA	3	8	38.7745	-77.0314	0.00	0.0	0.00	0.0	0.00	0.00	0.00	0.00	0.00	0.00	0.00	0.00	0.00
ALEXANDRIA, VA	3	9	38.7747	-77.0199	0.40	7.0	0.30	0.7	0.18	0.12	0.25	0.91	0.95	0.90	1.09	0.00	0.00
ALEXANDRIA, VA	3	10	38.7749	-77.0084	0.43	7.7	0.31	0.8	0.19	0.12	0.25	0.91	0.95	0.90	1.25	10.00	5.00
ALEX/ANAC	B3		38.7751	-76.9968	0.31	6.6	0.29	0.7	0.20	0.15	0.25	0.90	0.94	0.90	12.97	10.00	5.00
ANACOSTIA, MD	3	1	38.7753	-76.9853	0.40	7.0	0.30	0.7	0.18	0.12	0.25	0.91	0.95	0.90	0.31	0.00	0.00
ANACOSTIA, MD	3	2	38.7756	-76.9737	0.00	0.0	0.00	0.0	0.00	0.00	0.00	0.00	0.00	0.00	0.00	0.00	0.00
ANACOSTIA, MD	3	3	38.7758	-76.9622	0.40	7.0	0.30	0.7	0.18	0.12	0.25	0.91	0.95	0.90	0.63	0.00	0.00
ANACOSTIA, MD	3	4	38.7760	-76.9506	0.40	7.0	0.30	0.7	0.18	0.12	0.25	0.91	0.95	0.90	2.19	0.00	0.00
ANACOSTIA, MD	3	5	38.7762	-76.9391	0.40	7.0	0.30	0.7	0.18	0.12	0.25	0.91	0.95	0.90	1.09	0.00	0.00
ANACOSTIA, MD	3	6	38.7764	-76.9276	0.00	0.0	0.00	0.0	0.00	0.00	0.00	0.00	0.00	0.00	0.00	0.00	0.00

ANACOSTIA, MD	3	7	38.7766	-76.9160	0.40	7.0	0.30	0.7	0.18	0.12	0.25	0.91	0.95	0.90	0.31	0.00	0.00
ANACOSTIA, MD	3	8	38.7768	-76.9045	0.35	6.5	0.27	0.7	0.19	0.16	0.25	0.91	0.94	0.90	2.19	10.00	5.00
ANACOSTIA, MD	3	9	38.7770	-76.8929	0.39	7.0	0.38	0.7	0.18	0.16	0.25	0.90	0.94	0.90	7.19	10.00	5.00
ANACOSTIA, MD	3	10	38.7772	-76.8814	0.29	7.0	0.30	0.7	0.23	0.15	0.25	0.89	0.94	0.90	6.56	10.00	5.00
ANAC/UMARL	B3		38.7775	-76.8698	0.48	7.0	0.46	0.7	0.20	0.12	0.25	0.90	0.95	0.90	3.28	10.00	5.00
UPPER MARLBORO	3	1	38.7777	-76.8583	0.40	7.0	0.30	0.7	0.18	0.12	0.25	0.91	0.95	0.90	0.78	0.00	0.00
UPPER MARLBORO	3	2	38.7779	-76.8468	0.00	0.0	0.00	0.0	0.00	0.00	0.00	0.00	0.00	0.00	0.00	0.00	0.00
UPPER MARLBORO	3	3	38.7781	-76.8352	0.40	7.0	0.30	0.7	0.18	0.12	0.25	0.91	0.95	0.90	0.94	0.00	0.00
UPPER MARLBORO	3	4	38.7783	-76.8237	0.00	0.0	0.00	0.0	0.00	0.00	0.00	0.00	0.00	0.00	0.00	0.00	0.00
ANNANDLE, VA	2	2	38.7619	-77.2274	0.40	7.0	0.30	0.7	0.18	0.12	0.25	0.91	0.95	0.90	2.19	0.00	0.00
ANNANDLE, VA	2	3	38.7621	-77.2158	0.33	7.0	0.30	0.7	0.18	0.12	0.25	0.90	0.95	0.90	8.13	10.00	5.00
ANNANDLE, VA	2	4	38.7623	-77.2043	0.40	7.0	0.30	0.7	0.18	0.12	0.25	0.91	0.95	0.90	0.31	0.00	0.00
ANNANDLE, VA	2	5	38.7625	-77.1928	0.40	7.0	0.30	0.7	0.18	0.12	0.25	0.91	0.95	0.90	0.94	0.00	0.00
ANNANDLE, VA	2	6	38.7627	-77.1812	0.38	7.0	0.30	0.7	0.13	0.15	0.25	0.89	0.94	0.90	14.38	10.00	5.00
ANNANDLE, VA	2	7	38.7629	-77.1697	0.39	8.5	0.30	0.9	0.13	0.20	0.25	0.90	0.92	0.90	2.81	10.00	5.00
ANNANDLE, VA	2	8	38.7632	-77.1581	0.40	7.0	0.30	0.7	0.18	0.12	0.25	0.91	0.95	0.90	1.09	0.00	0.00
ANNANDLE, VA	2	9	38.7634	-77.1466	0.40	7.0	0.30	0.7	0.18	0.12	0.25	0.91	0.95	0.90	0.31	0.00	0.00
ANNANDLE, VA	2	10	38.7636	-77.1351	0.40	7.0	0.30	0.7	0.18	0.12	0.25	0.91	0.95	0.90	0.63	0.00	0.00
ANNAN/ALEX	B2		38.7638	-77.1235	0.48	8.2	0.34	0.8	0.14	0.12	0.25	0.90	0.95	0.90	1.09	10.00	5.00
ALEXANDRIA, VA	2	1	38.7640	-77.1120	0.40	7.0	0.30	0.7	0.18	0.12	0.25	0.91	0.95	0.90	1.88	0.00	0.00
ALEXANDRIA, VA	2	2	38.7642	-77.1004	0.40	7.0	0.30	0.7	0.18	0.12	0.25	0.91	0.95	0.90	1.09	0.00	0.00
ALEXANDRIA, VA	2	3	38.7644	-77.0889	0.50	7.0	0.44	0.7	0.16	0.12	0.25	0.90	0.95	0.90	4.84	10.00	5.00
ALEXANDRIA, VA	2	4	38.7646	-77.0774	0.42	7.7	0.30	0.8	0.15	0.12	0.25	0.90	0.95	0.90	5.00	10.00	5.00
ALEXANDRIA, VA	2	5	38.7648	-77.0658	0.40	7.0	0.30	0.7	0.18	0.12	0.25	0.91	0.95	0.90	2.81	0.00	0.00
ALEXANDRIA, VA	2	6	38.7651	-77.0543	0.40	7.0	0.30	0.7	0.18	0.12	0.25	0.91	0.95	0.90	1.88	0.00	0.00
ALEXANDRIA, VA	2	7	38.7653	-77.0427	0.00	0.0	0.00	0.0	0.00	0.00	0.00	0.00	0.00	0.00	0.00	0.00	0.00
ALEXANDRIA, VA	2	8	38.7655	-77.0312	0.00	0.0	0.00	0.0	0.00	0.00	0.00	0.00	0.00	0.00	0.00	0.00	0.00
ALEXANDRIA, VA	2	9	38.7657	-77.0197	0.40	7.0	0.30	0.7	0.18	0.12	0.25	0.91	0.95	0.90	4.22	0.00	0.00
ALEXANDRIA, VA	2	10	38.7659	-77.0081	0.46	8.0	0.32	0.8	0.19	0.12	0.25	0.90	0.95	0.90	0.94	10.00	5.00
ALEX/ANAC	B2		38.7661	-76.9966	0.33	8.5	0.40	0.9	0.22	0.12	0.25	0.90	0.95	0.90	11.88	10.00	5.00
ANACOSTIA, MD	2	1	38.7663	-76.9850	0.45	8.5	0.40	0.9	0.22	0.12	0.25	0.90	0.95	0.90	2.81	10.00	5.00
ANACOSTIA, MD	2	2	38.7666	-76.9735	0.00	0.0	0.00	0.0	0.00	0.00	0.00	0.00	0.00	0.00	0.00	0.00	0.00
ANACOSTIA, MD	2	3	38.7668	-76.9619	0.40	7.0	0.30	0.7	0.18	0.12	0.25	0.91	0.95	0.90	1.25	0.00	0.00
ANACOSTIA, MD	2	4	38.7670	-76.9504	0.42	7.3	0.31	0.7	0.19	0.12	0.25	0.91	0.95	0.90	1.56	10.00	5.00
ANACOSTIA, MD	2	5	38.7672	-76.9389	0.40	7.0	0.30	0.7	0.18	0.12	0.25	0.91	0.95	0.90	1.25	0.00	0.00
ANACOSTIA, MD	2	6	38.7674	-76.9273	0.45	5.5	0.40	0.6	0.22	0.12	0.25	0.90	0.95	0.90	1.41	10.00	5.00
ANACOSTIA, MD	2	7	38.7676	-76.9158	0.40	7.0	0.30	0.7	0.18	0.12	0.25	0.91	0.95	0.90	2.66	0.00	0.00
ANACOSTIA, MD	2	8	38.7678	-76.9042	0.35	10.3	0.28	1.0	0.18	0.12	0.25	0.90	0.95	0.90	1.56	10.00	5.00
ANACOSTIA, MD	2	9	38.7680	-76.8927	0.45	8.5	0.45	0.9	0.20	0.12	0.25	0.90	0.95	0.90	3.75	10.00	5.00
ANACOSTIA, MD	2	10	38.7682	-76.8812	0.31	7.0	0.30	0.7	0.22	0.16	0.25	0.90	0.94	0.90	13.28	10.00	5.00
ANAC/UMARL	B2		38.7685	-76.8696	0.40	7.0	0.30	0.7	0.18	0.12	0.25	0.91	0.95	0.90	2.03	0.00	0.00
UPPER MARLBORO	2	1	38.7687	-76.8581	0.40	7.0	0.30	0.7	0.18	0.12	0.25	0.91	0.95	0.90	0.94	0.00	0.00
UPPER MARLBORO	2	2	38.7689	-76.8465	0.00	0.0	0.00	0.0	0.00	0.00	0.00	0.00	0.00	0.00	0.00	0.00	0.00
UPPER MARLBORO	2	3	38.7691	-76.8350	0.40	7.0	0.30	0.7	0.18	0.12	0.25	0.91	0.95	0.90	0.78	0.00	0.00
UPPER MARLBORO	2	4	38.7693	-76.8234	0.40	7.0	0.30	0.7	0.18	0.12	0.25	0.91	0.95	0.90	0.31	0.00	0.00
ANNANDLE, VA	1	2	38.7529	-77.2271	0.40	7.0	0.30	0.7	0.18	0.12	0.25	0.91	0.95	0.90	1.88	0.00	0.00
ANNANDLE, VA	1	3	38.7531	-77.2156	0.40	7.0	0.30	0.7	0.18	0.12	0.25	0.91	0.95	0.90	0.94	0.00	0.00
ANNANDLE, VA	1	4	38.7533	-77.2040	0.00	0.0	0.00	0.0	0.00	0.00	0.00	0.00	0.00	0.00	0.00	0.00	0.00
ANNANDLE, VA	1	5	38.7535	-77.1925	0.17	7.0	0.20	0.7	0.15	0.12	0.25	0.88	0.95	0.90	2.19	10.00	5.00
ANNANDLE, VA	1	6	38.7537	-77.1809	0.11	7.0	0.30	0.7	0.16	0.12	0.25	0.89	0.95	0.90	11.88	10.00	5.00
ANNANDLE, VA	1	7	38.7539	-77.1694	0.47	8.0	0.53	0.8	0.18	0.12	0.25	0.90	0.95	0.90	1.25	10.00	5.00
ANNANDLE, VA	1	8	38.7542	-77.1579	0.40	7.0	0.30	0.7	0.18	0.12	0.25	0.91	0.95	0.90	0.94	0.00	0.00
ANNANDLE, VA	1	9	38.7544	-77.1463	0.60	10.0	0.60	1.0	0.15	0.12	0.25	0.88	0.95	0.90	1.25	10.00	5.00
ANNANDLE, VA	1	10	38.7546	-77.1348	0.40	7.0	0.30	0.7	0.18	0.12	0.25	0.91	0.95	0.90	2.50	0.00	0.00
ANNAN/ALEX	B1		38.7548	-77.1232	0.00	0.0	0.00	0.0	0.00	0.00	0.00	0.00	0.00	0.00	0.00	0.00	0.00
ALEXANDRIA, VA	1	1	38.7550	-77.1117	0.00	0.0	0.00	0.0	0.00	0.00	0.00	0.00	0.00	0.00	0.00	0.00	0.00
ALEXANDRIA, VA	1	2	38.7552	-77.1002	0.00	0.0	0.00	0.0	0.00	0.00	0.00	0.00	0.00	0.00	0.00	0.00	0.00
ALEXANDRIA, VA	1	3	38.7554	-77.0886	0.40	7.0	0.35	0.7	0.15	0.12	0.25	0.89	0.95	0.90	3.13	10.00	5.00
ALEXANDRIA, VA	1	4	38.7556	-77.0771	0.40	8.4	0.30	0.8	0.15	0.12	0.25	0.90	0.95	0.90	4.84	10.00	5.00
ALEXANDRIA, VA	1	5	38.7559	-77.0655	0.40	7.0	0.30	0.7	0.18	0.12	0.25	0.91	0.95	0.90	3.75	0.00	0.00
ALEXANDRIA, VA	1	6	38.7561	-77.0540	0.40	7.0	0.30	0.7	0.18	0.12	0.25	0.91	0.95	0.90	2.34	0.00	0.00
ALEXANDRIA, VA	1	7	38.7563	-77.0425	0.00	0.0	0.00	0.0	0.00	0.00	0.00	0.00	0.00	0.00	0.00	0.00	0.00
ALEXANDRIA, VA	1	8	38.7565	-77.0309	0.40	7.0	0.30	0.7	0.18	0.12	0.25	0.91	0.95	0.90	0.31	0.00	0.00
ALEXANDRIA, VA	1	9	38.7567	-77.0194	0.42	7.2	0.30	0.7	0.18	0.12	0.25	0.91	0.95	0.90	3.13	10.00	5.00
ALEXANDRIA, VA	1	10	38.7569	-77.0078	0.40	7.0	0.30	0.7	0.18	0.12	0.25	0.91	0.95	0.90	0.31	0.00	0.00
ALEX/ANAC	B1		38.7571	-76.9963	0.33	8.0	0.20	0.8	0.21	0.12	0.25	0.88	0.95	0.90	11.88	10.00	5.00
ANACOSTIA, MD	1	1	38.7573	-76.9848	0.40	7.0	0.30	0.7	0.18	0.12	0.25	0.91	0.95	0.90	0.47	0.00	0.00
ANACOSTIA, MD	1	2	38.7576	-76.9732	0.40	7.0	0.30	0.7	0.18	0.12	0.25	0.91	0.95	0.90	1.09	0.00	0.00
ANACOSTIA, MD	1	3	38.7578	-76.9617	0.40	7.0	0.30	0.7	0.18	0.12	0.25	0.91	0.95	0.90	1.56	0.00	0.00
ANACOSTIA, MD	1	4	38.7580	-76.9501	0.40	7.0	0.30	0.7	0.18	0.12	0.25	0.91	0.95	0.90	0.16	0.00	0.00
ANACOSTIA, MD	1	5	38.7582	-76.9386	0.00	0.0	0.00	0.0	0.00	0.00	0.00	0.00	0.00	0.00	0.00	0.00	0.00
ANACOSTIA, MD	1	6	38.7584	-76.9271	0.40	7.0	0.30	0.7	0.18	0.12	0.25	0.91	0.95	0.90	0.16	0.00	0.00
ANACOSTIA, MD	1	7	38.7586	-76.9155	0.40	7.3	0.29	0.7	0.19	0.12	0.25	0.91	0.95	0.90	1.56	10.00	5.00
ANACOSTIA, MD	1	8	38.7588	-76.9040	0.43	7.3	0.34	0.7	0.17	0.12	0.25	0.91	0.95	0.90	1.88	10.00	5.00

ANACOSTIA, MD	1	9	38.7590	-76.8924	0.43	7.5	0.33	0.7	0.19	0.12	0.25	0.91	0.95	0.90	2.34	10.00	5.00
ANACOSTIA, MD	1	10	38.7592	-76.8809	0.27	7.0	0.30	0.7	0.17	0.12	0.25	0.90	0.95	0.90	11.25	10.00	5.00
ANAC/UMARL	B1		38.7595	-76.8694	0.40	7.0	0.30	0.7	0.18	0.12	0.25	0.91	0.95	0.90	1.25	0.00	0.00
UPPER MARLBORO	1	1	38.7597	-76.8578	0.40	7.0	0.30	0.7	0.18	0.12	0.25	0.91	0.95	0.90	0.63	0.00	0.00
UPPER MARLBORO	1	2	38.7599	-76.8463	0.00	0.0	0.00	0.0	0.00	0.00	0.00	0.00	0.00	0.00	0.00	0.00	0.00
UPPER MARLBORO	1	3	38.7601	-76.8347	0.40	7.0	0.30	0.7	0.18	0.12	0.25	0.91	0.95	0.90	0.63	0.00	0.00
UPPER MARLBORO	1	4	38.7603	-76.8232	0.40	7.0	0.30	0.7	0.18	0.12	0.25	0.91	0.95	0.90	2.19	0.00	0.00
Average					0.41	8.3	0.36	0.8	0.18	0.13	0.25	0.90	0.95	0.90	5.97	6.91	3.46

REFERENCES

Al-Jiboori, M. H., Y. Xu, and Y. Qian, 2002: Local similarity relationships in the urban boundary layer. *Bound.-Layer Meteor.*, **102**, 63-82.

Alonso, M. S., J. L. Labajo, and M. R. Fidalgo, 2003: Characteristics of the urban heat island in the city of Salamanca, Spain. *Atmósfera*, **16**, 137-148.

Angevine, Wayne M., and K. Mitchell, 2001: Evaluation of the NCEP mesoscale Eta model convective boundary layer for air quality applications. *Mon. Wea. Rev*., **129**, 2761-2775.

Arnfield, A. J., 2003: Two decades of urban climate research: A review of turbulence, exchanges of energy and water, and the urban heat island. *Int. J. Climatol*., **23**, 1-26.

Atkinson, B. W., 2003: Numerical modeling of urban heat-island intensity. *Bound.-Layer Meteor*., **109**, 285-310.

Avissar, R., and Pielke, R. A., Sr., 1989: A Parameterization of heterogeneous land surfaces for atmospheric numerical models and its impact on regional meteorology. *Mon. Wea. Rev.,* **117**, 2113-2136.

Avissar, R., 1996: Potential effects of vegetation on the urban thermal environment. *Atmos. Environ.,* **30**, 437-448.

Baik, J. J., and Kim, J. J., 1999: A numerical study of flow and pollutant dispersion characteristics in urban street canyons. *J. Appl. Meteor.*, **38**, 1576-1589.

Baik, J. J., Kim, Y. H., and Chun, H. Y., 2001: Dry and moist convection forced by an urban heat island. *J. Appl. Meteor*., **40,** 1462-1475.

Baik, J. J., Park, S.B., and Kim, J. J., 2009: Urban flow and dispersion simulation using a CFD model coupled to a mesoscale model. *J. Appl. Meteor. Climatol.,* **48**, 1667-1681

Balling, R., and R. S. Cerveny, 1987: Long-term associations between wind speeds and the urban heat islands of Phoenix, Arizona. *J. Climatol. Appl. Meteor.,* **26**, 712-716.

Banta, R. M., C. J. Senff, J. Nelsen-Gammon, L. S. Darby, T. B. Ryerson, J. R. Alvarez, S. P. Sandberg, E. J. Williams, and M. Trainer, 2005: A bad air day in Houston.

Bull. Amer. Met. Soc., **86**, 657-669.

Barlow, J. F., and Belcher, S. E., 2002: A wind tunnel model for quantifying fluxes in the urban boundary layer. *Bound.-Layer Meteor.*, **104**, 131-150.

Barron, E. J., 2003: Tracking and predicting the atmospheric dispersion of hazardous material releases: Implication for homeland security. Testimony provided to the 1st session of the 108th Congress Jun 2, 2003.

Basara, J.B., Hall, P.K. Jr., Schroeder, A.J., Illston, B.G., and Nemunaitis, K.L., 2008: Diurnal cycle of the Oklahoma City urban heat island. *J. Geophys. Rev*. **113**, D20109. DOI:10.1029/2008JD010311.

Belcher, S.E., and O. Coceal, 2001: Scaling the urban boundary layer. *Proc. COST 715 Workshop on Urban Boundary Layer Parameterisations*, Zurich, Switzerland.

Best, M. J., 2006: Progress towards better weather forecasts for city dwellers: From short range to climate change. *Theor. Appl. Climatol*. **84**, 47-55.

Bornstein, Robert, and Lin, Qinglu, 2000: Urban heat islands and summertime convective thunderstorms in Atlanta: Three case studies. *Atmos. Environ.*, **34,** 507-516.

Bounoua, L., Safia, A, Masek, J., Peters-Lidard, C., and M. Imhoff, 2009: Impact of urban growth on surface climate: A case study in Oran, Algeria. *J. Appl. Meteor Climatol*., **48**, 217-231.

Brandsma, T., Konnen, G. P., and Wessels, H. R. A., 2003: Empirical estimation of the effect of urban heat advection on the temperature series of De Bilt (The Netherlands). *Int. J. Climatol*., **23**, 829-845.

Brazel, A. J., H. J. S. Fernando, J. C. R. Hunt, N. Selover, B. C. Hedquist, and E. Pardyjak, 2005: Evening transition observations in Phoenix, Arizona. *J Appl. Meteor*., **44**, 99-112.

Brown, M. and Williams, M.: 1998, 'An urban canopy parameterization for mesoscale meteorological models'. *Proc. 2nd AMS Urban Environmental Symposium*, Albuquerque, NM, U.S.A, American Meteorological Society.

Burian, S.J., Maddula, S.R.K., Velugubantla, S.P., and Brown, M.J. (2005): Morphological analyses using 3D urban databases: Seattle, W. Los Alamos National Laboratory Tech. LA-UR-05-1822.

Byun, D., and K. Schere, 2006: Review of the Governing Equations, Computational Algorithms, and other Components of the Models-3 Community Multiscale Air Quality modeling system. *Appl. Mech. Rev.,* **59**, 51-77.

Cameron, R., 2000: *Above Washington*. Cameron and Company, 159pp.

Carlson, T. N., and Boland, F. E., 1978: Analysis of urban-rural canopy using a surface heat flux/temperature model. *J. Appl. Meteor.*, **17**, 998-1013.

Carrió G. G., W. R. Cotton, and W.Y.Y. Cheng, 2010: Urban growth and aerosol effects on convection over Houston Part I: The August 2000 case. *Atmos. Res.,* **96**, 560-574.

Chan, S. T., and M. J. Leach, 2007: A validation of FEM3MP with Joint Urban 2003 data. *J. Appl. Meteor. Climotol.,* **46**, 2127-2146.

Chan, T. L., Dong, G., Leung, C. W., Cheung, C. S., and Hung W. T., 2002: Validation of a two-dimensional pollutant dispersion model in an isolated street canyon. *Atmos. Environ.*, **36,** 861-872.

Changnon, Stanley A., 2003: Urban modification of freezing-rain events. *J. Appl. Meteor.*, **42**, 863-870.

Chen, T-C., S-Y. Wang, and M-C. Yen, 2007: Enhancement of afternoon thunderstorm activity by urbanization in a valley: Taipei. *J. Appl. Meteor.*, **46**, 1324-1340.

Ching, Jason, M. Brown, S. Burian, F. Chen, R. Cionco, A. Hanna, T. Hultgren, T. McPherson, D. Sailor, H. Taha, and D. Williams, 2009: National urban database and access portal tool, *Bull. Amer. Meteor. Soc*., **90**,1157-1168.

Chou, M. D., P. H. Lin, P. L. Ma, and H. J. Lin, 2006: Effects of aerosols on the surface solar radiation in a tropical urban area. *J. Geophys. Res.,* **111**, D15207. Doi: 10.1029/2005JD006910.

Cleugh, H. A., and Oke, T. R., 1986: Suburban-rural energy balance comparisons in summer for Vancouver, B.C. *Bound.-Layer Meteor.,* **36**, 351-369.

Cohen, J. E., 2003: Human population: The next half century. *Science*, **302**, 1172-1175.

Collier, C. G., F. Davies, K. E. Bozier, A. R. Holt, D. R. Middleton, G. N. Pearson, S. Siemen, D. V. Willetts, G. J. G. Upton, R. I. Young, 2005: Dual-doppler lidar measurements for improving dispersion models. *Bull. Amer. Meteor. Soc*., **86**, 825-838.

Cotton, W.R., Pielke Sr., R. A., Walko R. L., Liston, G. E., Tremback, C., Jiang, H., McAnelly, R. L., Harrington, J. Y., Nicholls M. E., G. G. Carrio, and J. P. McFadden, 2003: RAMS 2001: Current status and future directions. *Meteor. Atmos. Phys*., **82**, 5-29.

Coutts, A. M., J. Beringer, and N. J. Tapper, 2007: Impact of increasing urban density on local climate: Spatial and temporal variations in the surface energy balance in Melbourne, Australia. *J. Appl. Meteor. Climatol.*, **46**, 477-493.

Craig, K. J. and R. D. Bornstein, 2001: Urbanisation of numerical mesoscale models. *Proc. COST 715 Workshop on Urban Boundary Layer Parameterisations*, Zurich, Switzerland.

.

Craig, Kenneth, J., 2002: MM5 Simulations of urban induced convective precipitation over Atlanta, GA. M.S. Thesis, Department of Meteorology, San Jose State University. 62pp.

Dabberdt, W. F., and Hoydysh, W. G., 1991: Street canyon dispersion: Sensitivity to block shape and entrainment. *Atmos. Enviorn.*, **25A**, 1143-1153.

Dabberdt, Walter F., A. Crook, C. Mueller, J. Hales, S. Zubrick, W. Krajewski, J. C. Doran, C. King, R. N. Keener, R. Bornstein, D. Rodenhuis, P. Kocin, M. A. Rossetti, F. Sharrocks, E. M. Stanley Sr., 2000: Forecast issues in the urban zone: Report of the 10th prospectus development team of the U.S. weather research program. *Bull. Amer. Meteor. Soc.*, **81**, 2047-2064.

Dandou, A., M. Tombrou, E. Akylas, N. Soulakellis, E. Bossioli, 2005: Development and evaluation of an urban parameterization scheme in the Penn State/NCAR Mesoscale Model (MM5). *J. Geophys. Res.*, **110**, D10102. doi: 10.1029/2004JD005192.

DeMarrais, G. A., 1975: Nocturnal heat island intensities and relevance to forecasts of mixing heights. *Mon. Wea. Rev.*, **103**, 235-245.

DePaul, F. T., and Sheih, C. M., 1985: A tracer study of dispersion in an urban street canyon., *Atmos. Environ.*, **19**, 555-559.

Dickinson, A., A. Henderson-Sellers, P.J. Kennedy, and M. F. Wilson, 1986: Biosphere-Atmosphere Transfer Scheme (BATS) for the NCAR Community Climate Model (CCM). NCAR Tech. Rep. NCAR/TN-275+STR, 69pp.

Dixon, P. Grady, and Thomas L. Mote, 2003: Patterns and causes of Atlanta's urban heat island-initiated precipitation. *J Appl. Meteor.*, **42**, 1273-1284.

Draxler, R. R., 1985: Metropolitan Tracer Experiment (METREX). NOAA Tech Mem., ERL-ARL-140, 102pp.

Dupont, S. and P. G. Mestayer, 2006: Parameterization of the urban energy budget with the submesoscale soil model. *J Appl. Meteor.*, **45**, 1744-1765.

Ek M. B., K. E. Mitchell, Y. Lin, E. Rogers, P. Grunmann, V. Koren, G. Gayno, and J. D. Tarpley, 2003: Implementation of NOAH land surface model advances in the National

Centers for Environmental Prediction operational mesoscale Eta model. *J Geophys. Res.,* **108(D22),** 8851. Doi: 10.1029/2002JD003296.

Fan H., and D. J. Sailor, 2005: Modeling the impacts of anthropogenic heating on the urban climate of Philadelphia: A comparison of implementation schemes. *Atmos. Environ*., **39**, 73-84.

Farias, W.R.G., O. Pinto Jr., K.P. Naccarato, and I.R.C.A. Pinto, 2009: Anomalous lightning activity over the metropolitan region of São Paulo due to urban effects. *Atmos. Res.,* **91**, 485-490.

Gaffen, D. and Bornstein, R., 1988: Case study of urban interactions with a synoptic scale cold front. *Meteor Atmos. Phys.,* **38**, 185-194.

Ganguly, D., A. Jayaraman, and H. Gadhavi, 2006a: Physical and optical properties of aerosols over an urban location in western India: Seasonal variabilities. *J. Geophys. Res.,* **111**: D24206. Doi:10.1029/2006JD007392.

Ganguly, D., and Al Jayaraman, 2006b: Physical and optical properties of aerosols over an urban location in western India: Implications for shortwave radiative forcing. *J. Geophys. Res.*, **111**, D24207. Doi:10.1029/2006JD007393.

Ganguly, D., A. Jayaraman, T. A. Rajesh, and H. Gadhavi, 2006c: Wintertime aerosol properties during foggy and nonfoggy days over urban center Delhi and their implications for shortwave radiative forcing. *J. Geophys. Res.,* **111**, D15217. Doi: 10.1029/2005JD007029.

Gauthier, M. L., W. A. Petersen, and L. D. Carey, 2010: Cell mergers and their impact on cloud-to-ground lightning over the Houston area. *Atmos. Res*., **96**, 626-632.

Georgescu, M., Miguez-Macho, G., Steyaert, L.T., and C.P. Weaver, 2008: Sensitivity of summer climate to anthropogenic land-cover change over the greater Phoenix, AZ, region. *J. Arid Environ*., **72**, 1538-1373.

Goetz, S., and P. Jantz, 2006: Satellite maps show Chesapeake Bay urban development. *EOS*: **87**, 150-153.

Grimmond, C.S.B., and Oke, T.R., 1995: Comparison of heat fluxes from summertime observations in the suburbs of four North American cities. *J Appl. Meteor.,* **34**, 873-889.

Grimmond, C. S. B., and Oke, T. R., 1999a: Heat storage in urban areas: Local-scale observations and evaluation of a simple model. *J. Appl. Meteor.*, **38**, 922-940.

Grimmond, C. S. B., and Oke, T. R., 1999b: Aerodynamic properties of urban areas derived from analysis of surface form. *J. Appl. Meteor.*, **38**, 1262-1292.

Grimmond, C. S. B., and Oke, T. R., 2002: Turbulent heat fluxes in urban areas: Observations and a local-scale urban meteorological parameterization scheme (LUMPS). *J. Appl. Meteor.*, **41**, 792-810.

Grimmond, C.S.B., J. A. Salmond, T.R. Oke, B. Offerle, and A. Lemonsu, 2004: Flux and turbulence measurements at a densely built-up site in Marseille: Heat, mass (water and carbon dioxide), and momentum. *J. Geophys. Res.,* **109**, D24101, doi:10.1029/2004JD004936.

Grossman-Clarke, S., J. A. Zehnder, W. L. Stefanov, Y. Liu, and M. A. Zoldak, 2005: Urban modifications in a mesoscale meteorological model and the effects on near-surface variables in an arid metropolitan region. *J Appl. Meteor.*, **44**, 1281-1297.

Grossman-Clarke, S., Y. Liu, J. Zehnder, J. Fast, 2008: Simulations of the urban planetary boundary layer in an arid metropolitan area. *J. Appl. Meteor. Climatol.,* **47**, 752-768.

Haeger-Eugensson, Marie, and Holmer, Bjorn, 1999: Advection caused by the urban heat island circulation as a regulating factor on the nocturnal urban heat island. *Int. J. Climatatol.*, **19**, 975-988.

Hamdi, R., Deckmyn A., Termonia, P., Demaree, G.R., Baguis, P., Vanhuysse, S., and Wolff, E., 2009: Effects of historical urbanization in the Brussels Capital Region on surface air temperature time series: A model study, *J. Appl. Meteor. Climatol*., **48**, 2181-2196.

Han J-Y, and J. J. Baik, 2008: A theoretical and numerical study of urban heat island-induced circulation and convection. *J. Atmos. Science*, **65**, 1859-1877.

Hand, L., and J. M. Shepherd, 2009: An investigation of warm-season spatial rainfall variability in Oklahoma City: Possible linkages to urbanization and prevailing wind. *J. Appl. Meteor. Climatol*., **48**, 251-269.

Hanna, S. R., and Y. Zhou, 2009: Space and time variations in turbulence during the Manhattan Midtown 2005 field experiment. *J. Appl. Meteor. Climatol.*, **48**, 2295-2304.

Hawkins, Timothy, W., A. J. Brazel, W. L. Stefanov, W. Bigler, and E. M. Saffell, 2004: The role of rural variability in urban heat island determination for Phoenix, Arizona. *J. Appl. Meteor.,* **43**, 476-486.

Henderson-Sellers, A., Z-L. Yang, and R. E. Dickinson 1993: The Project for Intercomparison of Land Surface Parameterization Schemes (PILPS). *Bull. Amer. Meteor. Soc*., **74**, 1335-1349.

Henderson-Sellers, A., A. J. Pitman, P. K. Love, P. Irannejad, and T. H. Chen, 1995: The Project for Intercomparison of Land Surface Parameterization Schemes (PILPS): Phases 2 and 3. *Bull. Amer. Meteor. Soc*., **76**, 489-503.

Hicks, B. B., Callahan, W. J., and M. A. Hoekzema, 2010: On the heat islands of Washington, DC and New York City, NY. *Bound.-Layer Met*., **135**, 291-300.

Hildebrand, P. H., and Ackerman, B., 1984: Urban effects on the convective boundary layer. *J. Atmos. Sci.*, **41**, 76-91.

Holmer, Bjorn, and Eliasson, Ingegard, 1999: Urban-rural vapour pressure differences and their role in the development of urban heat islands. *Int. J. Climatol*., **19**, 989-1009.

Holt, T., and J. Pullen, 2007: Urban canopy modeling of the New York City metropolitan area: A comparison and validation of single and multilayer parameterizations. *Mon. Wea. Rev.*, **135**, 1906-1930.

Hoydysh, W. G., and Dabberdt, W. F., 1988: Kinematics and dispersion characteristics of flows in asymmetric street canyons. *Atmos. Environ.*, **22**, 2677-2689.

Huff, F. A. and S. A. Changnon, Jr., 1973: Precipitation modification by major urban areas. *Bull. Amer. Meteor. Soc.*, **54**, 1220-1232.

Huff, F. A., 1986: Urban hydrometeorology review. *Bull. Amer. Meteor. Soc.*, **67**,703-711.

Hunter, L. J., Watson, I. D., and Johnson, G. T., 1990/1991: Modeling air flow regimes in urban canyons. *Energy and Buildings*, **15-16**, 315-324.

Jauregui, E. and A. Tejeda, 1997: Urban-rural humidity contrasts in Mexico City. *Int. J. Climatol*., **17**, 187-196.

Jeong, S.J., and Andrews, M. J., 2002: Application of the k-e turbulence model to the high reynolds number skimming flow field of an urban street canyon. *Atmos. Environ.*, **36**, 1137-1145.

Jin, M., J. M. Shepherd, and C. Peters-Lidard, 2007: Development of a parameterization for simulating the urban temperature hazard using satellite observations in climate model. *Nat. Hazards*, **43**: 257-271. doi:10.1007/s11069-007-9117-2.

Jin, M., J. M. Shepherd, and M. D. King, 2005a: Urban aerosols and their variation with clouds and rainfall: A case study for New York and Houston. *J. Geophys Res*, **110**, doi:10.1029/2004JD005081.

Jin, M., R. E. Dickinson, and D. Zhang, 2005b: The footprint of urban areas on global

climate as characterized by MODIS. *J. Climate*, **18**, 1551-1565.

Johnston, A. K., and T. R. Watters, 1996: Assessing spatial growth of the Washington metropolitan area using thematic mapper data. *Proc. ASPRS/ACSM Annual Convention*, Baltimore, MD P.3, 74–76,

Kalnay, E., M. Kanamitsu, R. Kistler, W. Collins, D. Deaven, L. Gandin, M. Iredell, S. Saha, G. White, J. Woollen, Y. Zhu, A. Leetmaa, R. Reynolds, M. Chelliah, W. Ebisuzaki, W. Higgens, J. Janowiak, K.C. Mo, C. Ropelewski, J. Wang, Roy Jenne, and Dennis Joseph, 1996: The NCEP/NCAR 40-year reanalysis project. *Bull. Amer. Meteor. Soc.*, **77**, 431-437.

Kim, J. J., and Baik, J. J., 1999: A numerical study of thermal effects on flow and pollutant dispersion in urban street canyons. *J. Appl. Meteor.*, **38**, 1249-1261.

Kim, Y. H. and J. j. Baik, 2005: Spatial and temporal structure of the urban heat island in Seoul. *J. Appl. Meteor*., **44**, 591-605.

Klein, P. and J. V. Clark, 2007: Flow variability in a North American downtown street canyon. *J. Appl. Meteor. Climatol*., **46**, 851-877.

Klipp, C., 2007: Wind direction dependence of atmospheric boundary layer turbulence parameters in the urban roughness sublayer. *J. Appl. Meteor*., **46**, 2086-2097.

Kusaka, H., Kondo, Y. K., and F. Kimura, 2001: A simple single-layer urban canopy model for atmospheric models: Comparison with multi-layer and slab models. *Bound.-Layer Meteor*., **101**, 329-258.

Kusaka, Hiroyuki, 2002: Formation mechanism of urban heat island, numerical study on flow and heat budget. PhD Dissertation, University of Tsukuba, Japan. 153pp.

Kusaka, H. and F. Kimura, 2004: Thermal effects of urban canyon structure on the nocturnal heat island: Numerical experiment using a mesoscale model coupled with an urban canopy model. *J. Appl. Meteor.*, **43**, 1899-1910.

Lee, I. Y., and Park, H. M., 1994: Parameterization of the pollutant transport and dispersion in urban street canyons. *Atmos. Environ.*, **28**, 2343-2349.

Lee, T. J., 1992: The impact of vegetation on the atmospheric boundary layer and convective storms. PhD dissertation, Colorado State University, Ft Collins, CO. pp 137.

Lee, Tsengdar J., R. A. Pielke, and P. W. Mielke, 1995: Modeling the clear-sky surface energy budget during FIFE 1987. *J Geophys. Res.*, **100**, 25,585-25,593.

Lei, Ming, D. Niyogi, C. Kishtawal, R. Pielke, Sr., A. Beltran-Przekurat, T. Nobis, and S.S. Vaidya, 2008: Effect of explicit urban land surface representation on the simulation of the 26 July 2005 heavy rain event over Mumbai, India. *Atmos. Chem. Phys. Discussions*, **8**, 8773–8816

Lemonsu, A. and Masson, V., 2002: Simulation of a summer urban breeze over Paris. *Bound.-Layer Meteor.*, **104**: 463-490.

Lemonsu, A., Grimmond, C.S.B., and Masson, V., 2004: Modeling the surface energy balance of the core of an old Mediterranean city: Marseille. *J. Appl. Meteor*., **43**, 312-327.

Lemonsu A., Belair S., and Mailhot, J., 2009: The new Canadian urban modelling system: Evaluation for two cases from the Joint Urban 2003 Oklahoma City Experiment. *Bound.-Layer Met.,* **133**, 47-70.

Liu, C. H., and Barth, M. C., 2002: Large-eddy simulation of flow and scalar transport in a modeled street canyon. *J. Appl. Meteor.*, **41**, 660-673.

Lo, J. C. F., A. K. H. Lau, F. Chen, J. C. H. Fung, K. K. M. Leung, 2007: Urban modification in a mesoscale model and the effects on the local circulation in the Pearl River Delta region. *J. Appl. Meteor. Climatol.,* **46**, 457-476.

Loose, T. and Bornstein, R., 1977: Observations of mesoscale effects on frontal movement through an urban area. *Mon. Wea. Rev.*, **105**, 567-571.

Lynn, B., Carlson, T., Rosenzweig, C., Goldberg, R., Druyan, L., Cox, J., Gaffin, S., Parshall, L., and K. Civerolo, 2009: A modification to the NOAH LSM to simulate heat mitigation strategies in the New York City metropolitan area. *J. Appl. Meteor. Climatol.,*., 48: 199-216.

Manley, G., 1958: On the frequency of snowfall in metropolitan England. *Quart. J. Roy. Meteor. Soc*., **84**, 70-72.

Martilli, Alberto, Clappier, Alain, and Rotach, Mathias W., 2002: An urban surface exchange parameterisation for mesoscale models. *Bound.-Layer Meteor.*, **104**, 261-304.

Martilli, Alberto, 2003: A two-dimensional numerical study of the impact of a city on atmospheric circulation and pollutant dispersion in a coastal environment. *Bound.-Layer Meteor.* **108**, 91-119.

Martilli, Alberto, Y. A. Roulet, M. Junier, F. Kirchner, M. W. Rotach and A. Clappier, 2003: On the impact of urban surface exchange parameterisations on air quality simulations: The Athens case. *Atmos. Environ.,* **37**, 4217-4231.

Martilli, A., 2007: Current research and future challenges in urban mesoscale modeling. *Int. J. Climatol*., **27**, 1909-1918.

Masson, V., 2000: A physically-based scheme for the urban energy budget in atmospheric models. *Bound.-Layer Meteor.*, **94**, 357-397.

Masson, V., Grimmond, C.S.B., and Oke, T.R., 2002: Evaluation of the Town Energy Balance (TEB) scheme with direct measurement from dry districts in two cities. *J. Appl. Meteor.*, **41**, 1011-1026.

Masson, V., 2006: Urban surface modeling and the meso-scale impact of cities. *Theor. Appl. Climatol*., **84**, 35-45.

Memon, R. A., Lenung, D. Y.C., and Liu, C. H., 2009: An investigation of urban heat island intensity (UHII) as an indicator of urban heating. *Atmos. Res*., **94**, 491-500.

Meroney, R. N., Pavageau, M., Rafailidis, S., and Schatzmann, M., 1996: Study of line source characteristics for 2-D physical modeling of pollutant dispersion in street canyons. *J Wind Eng*., **62**: 37-56.

Mestayer, P. G. and M. Bottema, 2001: Parameterizations for roughness parameters in urban areas. *Proc. COST 715 Workshop on Urban Boundary Layer Parameterisations*, Zurich, Switzerland, P5-m.

Miao, S., Chen, F., LeMone, M., Tewari, M., Li, Q., and Y. Wang, 2009: An observational and modeling study of characteristics of urban heat island and boundary layer structures in Beijing. *J. Appl. Meteor. Climatol.,* **48**, 484-501.

Mihailovic, D.T., Lee, T. J., Pielke, R. A., Lalic, B., Arsenic, I. D., Rajkovic, B., and Vidale, P. L., 2000: Comparison of different boundary layer surface schemes using single point micrometeorological field data. *Theor. Appl. Climatol.*, **67**, 135-151.

Mills, G. M., 1993: Simulation of the energy budget of an urban canyon - I. model structure and sensitivity test. *Atmos. Environ*., **27B**, 157-170.

Mills, G. M., and Arnfield, A. J., 1993: Simulation of the energy budget of an urban canyon - II. Comparison of the model results with measurments. *Atmos. Environ.*, **27B**, 171-181.

Molders, Nicole, and Olson, Mark A., 2004: Impact of urban effects on precipitation in high latitudes. *J. Hydrometeor*. **5**, 409-429.

Montavez, Juan P., Rodrigues, A. and Jimenez, J. I., 2000: A study of the urban heat island of Granada. *Int. J. Climatol.*, **20**, 899-911.

Mote, T. L., M. C. Lacke, and J. M. Shepherd, 2007: Radar signatures of the urban

effect on precipitation distribution: A case study for Atlanta, Georgia. *Geophys. Res. Lett.*, **34** doi: 10.1029/2007GL031903.

Nichol, J. E., Fung, W. Y., Lam, K., and Wong, M. S., 2009: Urban heat island diagnosis using ASTER satellite images and 'in-situ' air temperature. *Atmos. Res.* **94**, 276-284.

Niyogi, D., T. Holt, S. Zhong, P. C. Pyle, and J. Basara, 2006: Urban and land surface effects on the 30 July 2003 mesoscale convective system event observed in the southern Great Plains. *J. Geophys. Res*., **111**, D19107, doi:10.1029/2005JD006746.

Ntelekos, A. A., J. A. Smith, and W. F. Krajewski, 2007: Climatological analyses of thunderstorms and flash floods in the Baltimore metropolitan region. *J. Hydrometeor.,* **8**, 88-101.

Offerle, B., P. Jonsson, I. Eliasson, and C.S.B. Grimmond, 2005: Urban modification of the surface energy balance in the West African Sahel: Ouagadougou, Burkina Faso. *J. Climate.,* **18**, 3983-3995.

Offerle, B., C. S. B. Grimmond, K. Fortuniak and W. Pawlak, 2006: Intraurban differences of surface energy fluxes in a central European city. *J. Appl. Meteor.*, **45**, 125-136.

Ohashi, Y., and Kida, H., 2002: Local circulations developed in the vicinity of both coastal and inland urban areas: A numerical study with a mesoscale model. *J. Appl. Meteor.*, **41**, 30-45.

Ohashi, Y., and Kida, H., 2004: Local circulations developed in the vicinity of both coastal and inland urban areas. Part II: Effects of urban and mountain areas on moisture transport. *J. Appl. Meteor*., **43**, 119-133.

Ohashi, Y., Y. Genchi, H. Kondo, Y. Kikegawa, H. Yoshikado, and Y. Hirano., 2007: Influence of air-conditioning waste heat on air temperature in Tokyo during summer: Numerical experiments using an urban canopy model coupled with a building energy model. *J. Appl. Meteor.*, **46**, 66-81

Oke, T. R., 1979: Advectively-assisted evapotranspiration from irrigated urban vegetation. *Bound.-Layer Meteor.* **17**, 167-173.

Oke, T. R., 1987: *Boundary Layer Climates*, 2nd ed. Routledge Press, 435pp.

Oke, T. R., 1988: The urban energy balance. *Prog. Phys. Geogr.*, **12**, 471-508.

Oke, T. R., Johnson, G. T., Steyn, D. G., and Watson, I. D., 1991: Simulation of surface urban heat islands under 'ideal` conditions at night part 2: Diagnosis of causation. *Bound.-Layer Meteor.*, **56**, 339-358.

Otte, T. L., A. Lacser, S. Dupont, and J. K. S. Ching, 2004: Implementation of an urban canopy parameterization in a mesoscale meteorological model. *J. Appl. Meteor.*, **43**, 1648-1665.

Otte, T. L., and Coauthors, 2005: Linking the Eta model with the Community Multiscale Air Quality (CMAQ) modeling system to build a national air quality forecasting system. *Weather and Forecasting*, **20**, 367-384.

Parker, D. S., J. E. R. McIlvaine, S. F. Barkaszi, D. J. Beal and M. T. Anello, 2000: *Laboratory Testing of the Reflectance Properties of Roofing Material*. Florida Solar Energy Center Report, FSEC-CR670-00.

Pearlmutter, D., P. Berliner, and E. Shaviv, 2005: Evaluation of urban surface energy fluxes using an open-air scale model. *J. Appl. Meteor.*, **44**, 532-545.

Pielke, R. A., G. A. Dalu, J. S. Snook, T. J. Lee, and T. G. F. Kittel, 1991: Nonlinear influence of mesoscale land use on weather and climate. *J. Climate*, **4**, 1053-1069.

Pielke, R. A., R. L. Walko, L. Steyaert, P. L. Vidale, G. E. Liston, and W. A. Lyons, 1999: The influence of anthropogenic landscape changes on weather in south Florida. *Mon. Wea. Rev.*, **127**, 1663-1673.

Pielke, R. A., 2001: Influence of the spatial distribution of vegetation and soils on the rediction of cumulus convective rainfall. *Rev. Geophys.*, **39**, 151-177.

Pielke, R. A., J. Adegoke, A. Beltran-Przeukurat, C. A. Hiemstra, J. Y. Lin, U. S. Nair, D. Niyogu, and T. E. Nobis, 2007: An overview of regional land-use and land-cover impacts on rainfall. *Tellus*, **59B**, 587-601.

Pomerantz, M. and H. Akbari, 1998: *Cooler paving materials for heat island mitigation*. In 1998 ACEEE Summer Study on Energy Efficiency in Buildings, Asilomar, CA, City: American Council for an Energy-Efficient Economy.

Pullen, J., Ching, J., Sailor, D., Thompson, W., Bornstein, B., and Koracin, D., 2008: Progress toward meeting the challenges of our coastal urban future. *Bull. Amer. Meteor. Soc.*, **89**, 1727-1731.

Robba, S. M., 2003: Urban-suburban / rural differences over greater Cairo, Egypt. *Atmósfera*, **16**, 157-171.

Roberts, S. M., and T. R. Oke, 2006: Comparison of four methods to estimate urban heat storage. *J. Appl. Meteor.*, **45**, 1766-1781.

Rosenfeld, D., Jin Dai, Xing Yu, Zhanyu Yao, Xiaohong Xu, Xing Yang, Chuanli Du, 2007: Inverse relations between amounts of air pollution and orographic

precipitation. *Science*, **315**, 1396-1398.

Rosenzweig, C. Solecki, W.D., Parshall, L., Lynn, B., Cox, J., Goldberg, R., Hodges, S., Gaffin, S., Slosberg, R.B., Savio, P., Dunstan, F., and Watson, M., 2009: Mitigating New York City's heat island: Integrating stakeholder perspectives and scientific evaluation. *Bull. Amer. Meteor. Soc*., **90**, 1297-1312.

Rotach, M. W., B. Fisher, and M. Piringer, 2001: COST 715 Workshop on Urban Boundary Layer Parameterizations: Overview and Discussion Summary. *Proc. COST 715 Workshop on Urban Boundary Layer Parameterisations*, Zurich, Switzerland, P1.0

Rotach, M. W., Fisher, B., and Piringer, M., 2002: COST 715 Workshop on urban boundary layer parameterizations. *Bull. Amer. Meteor. Soc.,* **83**, 1501-1504.

Roth, M., 2000: Review of atmospheric turbulence over cities. *Quart. J. Roy. Meteor. Soc.*, **126**, 941-990.

Roth, M., 2007: Review of urban climate research in (sub)tropical regions. *Int. J. Climatol.*, **27**, 1859-1873.

Roulet, Y. A., A. Martilli, M. W. Rotach, and A. Clappier, 2005: Validation of an urban surface exchange parameterization for mesoscale models-1D case in a street canyon. *J. Appl. Meteor.,* **44**, 1484-1498.

Roy, S., and F. Yuan, 2009: Trends in extreme temperatures in relation to urbanization in the Twin Cities Metropolitan Area, Minnesota. *J. Appl. Meteor. Climatol.*, **48**, 669-679.

Rozoff, C. M., 2002: Simulation of the St. Louis, MO land-use impacts on thunderstorms. M.S. thesis, Colorado State University, Atm Science paper No. 724.

Rozoff, C.M., W. R. Cotton, and J. O. Adegoke, 2003: Simulation of St. Louis Missouri, land use impacts on thunderstorms. *J. Appl. Meteor.*, **42**, 716-738.

Sailor, D. J. and H. Fan, 2004: The importance of including anthropogenic heating in mesoscale modeling of the urban heat island. *Symposium on Planning, Nowcasting, and Forecasting in Urban Zone,* Seattle, WA, Amer. Meteor. Soc., P3.5.

Sailor, D. J., and L. Lu, 2004: A top-down methodology for developing diurnal and seasonal anthropogenic heating profiles for urban areas. *Atmos Environ.*, **38**, 2737-2748.

Salmond, J. A., T. R. Oke, C. S. B. Grimmond, S. Roberts, and B. Offerle, 2005: Venting of heat and carbon dioxide from urban canyons at night. *J Appl. Meteor.*, **86**,

1180-1194.

Seaman, N. L., F. L. Ludwig, E. G. Donall, T. T. Warner, and C. M. Bhumralkar, 1989: Numerical studies of urban planetary boundary-layer structure under realistic synoptic conditions. *J. Appl. Meteor.*, **28**, 760-781.

Serafin, and Coauthors, 2003: *Tracking and Predicting the Atmospheric Dispersion of Hazardous Marterial Releases.* National Research Council, National Academies Press. 114pp.

Shem, W., and M. Shepherd, 2009: On the impact of urbanization on summertime thunderstorms in Atlanta: Two numerical model case studies. *Atmos. Res*., **92**, 172-189.

Shepherd, J.M., and S.J. Burian, 2003: Detection of urban-induced rainfall anomalies in a major coastal city. *Earth Interactions*, **7**: paper 4, 17pp.

Shepherd, J. M., 2006: Evidence of urban-induced precipitation variability in arid climate regimes. *J. Arid Environ*., **67**, 607-628.

Shepherd, J. M., M. Manyin, D. Messen, and S. Burian, 2010: The impact of urbanization on current and future coastal precipitation: A case study for Huston. *Environ. Planning B: Planning and Design*, **37**(2) 284 – 304.

Silva, H., Bhardwaj, R., Phelan, P., Golden, J. and S. Grossman-Clarke, 2009: Development of a zero-dimensional mesoscale thermal model for urban climate. *J. Appl. Meteor. Climatol*., **48**: 657-668.

Soriano, C., E. Batchvarova, R. Berkowicz, J. Brechler, Z. Janour, P. Kastner-Klein, D. Middleton, V. Prior, M. W. Rotach, C. Sacré, and J. M. Baldasano, 2001: Comparison of urban and rural wind speeds. *Proc. COST 715 Workshop on Urban Boundary Layer Parameterisations*, Zurich, Switerzland, P4-s.

Steinecke, K., 1999. Urban climatological studies in the Reykjav´ık sub-arctic environment, Iceland. *Atmos. Environ.* **33**, 4157–4162.

Stull, R. B. 1998: *An Introduction to boundary layer meteorology*. Kluwer Academic Press. 670pp.

Taha, H., 1999: Modifying a Mesoscale Meteorological Model to Better Incorporate Urban Heat Storage: A Bulk-Parameterization Approach. *J. Appl. Meteor.*, **38**, 466-473.

Taylor, C. M., R. J. Harding, R. A. Pielke, Sr., P. L. Vidale and R. L. Walko, 1998: Snow breezes in the boreal forest. *J. Geophys. Res*., **103**, 23,087-23,101.

Tomita, T., H. Kusaka, R. Akiyoshi, and Y. Imasato, 2007: Thermal and Geometric Controls on the Rate of Surface Air Temperature Changes in a Medium-Sized, Midlatitude City. *J. Appl. Meteor. Climatol.,* **46**, 241-247.

Tonkaz, T., and M. Cetin, 2007: Effects of Urbanization and Land-use Type on Monthly Extreme Temperatures in a Developing Semi-arid Region, Turkey. *J. Arid Environ.*, **68**, 143-158.

Torok, Simon J., Morris, Christopher J. G., Skinner, Carol, and Plummer, Neil, 2001: Urban Heat Island Features of Southeast Australian Towns. *Aust. Meteor. Mag*. **50**, 1-15.

Trusilova, K., Jung, M., and G. Churkina, 2009: On climate impacts of a potential expansion of urban land in Europe. *J. Appl. Meteor. Climatol.,* **48**, 1971-1980.

Unger, Janos, 1999: Urban-rural air humidity differences in Szeged, Hungary. *Int. J. Climatol.,* **19**, 1509-1515.

Van Den Heever, S. C. and W. R. Cotton, 2007: Urban aerosol impacts on downwind convective storms. *J. Appl. Meteor. Climatol.* **46**, 828-850.

Vardoulakis, S., Gonzalez-Flesca, N., and Fisher, B. E. A., 2002: Assessment of traffic-related air pollution in two street canyons in Paris: Implications for exposure studies. *Atmos. Environ.*, **36**, 1025-1039.

Vardoulakis, S., Fisher, B. E. A., Pericleous, K., and Gonzales-Flesca, N., 2003: Modeling air quality in street canyons: A review. *Atmos. Environ*., **37**: 155-182.

Vidale, P.L., Pielke, R. A., Barr, A., Steyaert, L. T., 1997: Case study modeling of turbulent and mesoscale fluxes over the BOREAS region. *J. Geophys. Res.*, **102**, 29167-29188.

Walko, Robert L., L. E. Band, J. Baron, T. G. F. Kittel, R. Lammers, T. J. Lee, D. Ojima, R. A. Pielke Sr., C. Taylor, C. Tague, C. J. Tremback, P. L. Vidale, 2000: Coupled atmosphere-biophysics-hydrology models for environmental modeling. *J. Appl. Meteor.*, **39**, 931-944.

Wang, K., J. Wang, P. Wang, M. Sparrow, J. Yang, and H. Chen, 2007: Influences of urbanization on surface characteristics as derived from the Moderate-Resolution Imaging Spectroradiometer: A case study for the Beijing metropolitan area. *J. Geophys. Res.,* **112**, D22S06 doi:10.1029/2006JD007997.

Xia, X., H. Chen, P. Goloub, W. Zhang, B. Chatenet, and P. Wang, 2007: A compilation of aerosol optical properties and calculation of direct radiative forcing over an urban region in northern China. *J. Geophys. Res.,* **112**, D12203, doi:10.1029/2006DJ008119.

Yoshikado, H., 1992: Numerical study of the daytime urban effect and its interaction with the sea breeze. *J. Appl. Meteor.*, **31**, 1146-1164.

Zehnder, J., 2002: Simple modifications to improve fifth-generation Pennsylvania State University – National Center for Atmospheric Research mesoscale model performance for the Phoenix, Arizona, metropolitan area. *J. Appl. Meteor*., **41**, 971-979.

Zhang, F., N. Bei, J. W. Nielsen-Gammon, G. Li, R. Zhang, A. Stuart, and A. Aksoy, 2007: Impacts of meteorological uncertainties on ozone pollution predictability estimated through meteorological and photochemical ensemble forecasts. *J. Geophys. Res*., **112**:D04302. Doi:10.1029/2006JD007429.

Zhang, H., Sato, N., Izumi, T., Hanaki, K., and T. Aramaki, 2008: Modified RAMS-urban canopy model for heat island simulation in Chongqing, China. *J. Appl. Meteor. Climatol.*, **47**, 509-524.